

The charge expansion in quantum field theory

Bersini, Jahmall Matteo

Doctoral thesis / Disertacija

2021

*Degree Grantor / Ustanova koja je dodijelila akademski / stručni stupanj: **University of Zagreb, Faculty of Science / Sveučilište u Zagrebu, Prirodoslovno-matematički fakultet***

Permanent link / Trajna poveznica: <https://urn.nsk.hr/um:nbn:hr:217:352600>

Rights / Prava: [In copyright](#)

*Download date / Datum preuzimanja: **2021-12-04***



Repository / Repozitorij:

[Repository of Faculty of Science - University of Zagreb](#)





University of Zagreb

FACULTY OF SCIENCE
DEPARTMENT OF PHYSICS

Jahmall Matteo Bersini

**THE CHARGE EXPANSION IN
QUANTUM FIELD THEORY**

DOCTORAL DISSERTATION

Zagreb, 2021



University of Zagreb

FACULTY OF SCIENCE
DEPARTMENT OF PHYSICS

Jahmall Matteo Bersini

THE CHARGE EXPANSION IN QUANTUM FIELD THEORY

DOCTORAL DISSERTATION

Supervisor:
Dr. sc. Oleg Antipin

Zagreb, 2021



University of Zagreb

PRIRODOSLOVNO - MATEMATIČKI FAKULTET
FIZIČKI ODSJEK

Jahmall Matteo Bersini

**RAZVOJ PO NABOJU U KVANTNOJ
TEORIJI POLJA**

DOKTORSKI RAD

Mentor:
Dr. sc. Oleg Antipin

Zagreb, 2021

On the supervisor

Oleg Antipin is currently employed as a Research Associate at the Institute Ruđer Bošković, Zagreb. He started to work there since November 2015 and in March 2017 became a principal investigator of the 4-year HRZZ project “Terascale Physics for the LHC and Cosmos” within which this thesis was completed. His major research interests are in semiclassical and large- N methods in QFT, ADS/CFT correspondence, phases of strongly interacting theories, and dark matter. He is an author/co-author of 40 published papers and contributed to several scientific and popular journal articles/reviews.

Acknowledgements

Meeting Oleg two and a half years ago, I found a true master who taught me how to surf over the physics sea and a formidable person who truly enriched my life. His down-to-earth and straight-to-the-point attitude in science will always be a benchmark for me. Moreover, he taught me that physics without physical intuition is *just* math. All his support is priceless, so thank you, Oleg.

I would also like to thank all my collaborators Francesco, Zhi-Wei, Chen, Alessio, and Juan Carlos, for patiently teaching me the tools of the trade and for supporting my growth as an apprentice scientist. Moreover, I wish to acknowledge my colleagues at the Ruder, especially Georgios, Luca, and Kenji, for all the good time together in Zagreb. Finally, I thank Vanja for many interesting discussions and for helping me with the parts of the thesis in Croatian, and Thanasis for his valuable comments on the manuscript.

Un grazie di cuore va a Skarto, Ino, Rus, Fau, Lore, Tara, 3V, Ste, Fra Paura, Ary, Armo, Papilla Bronx, Papilla Virgi e tutta la ballotta che ne sa, per tutto il bene e per rendere il giro di giostra migliore. Un abbraccione sbralli!

Ringrazio i miei zii per il supporto e l'affetto. Soprattutto, grazie nonna per essere così hard-ecore. Un grazie speciale è per miei genitori, per tutto l'amore e per avermi reso chi sono. Qualunque ringraziamento io possa scrivere non gli renderebbe giustizia.

Infine, voglio ringraziare Giorgia per essere la mia compagna d'avventura. Tutto quello di buono che ho combinato negli ultimi tre anni è anche, in buona parte, merito suo.

Ciao Tobi!

Abstract

We study the spectrum of operators carrying large values of the conserved charges in conformal field theories (CFTs) with global symmetries. In particular, we explore the computation of the related CFT data within the recently-developed large charge expansion framework.

In the first three chapters, we review the basics of CFT at large charge, focusing on the general phenomenon of *classicalization* of quantum physics in the presence of large quantum numbers and on the physical implications of the spontaneous breaking of conformal invariance induced by the charge-fixing.

In chapter four, we show how to set up the large charge expansion in weakly-coupled non-abelian theories. To this end, we focus on the $O(N)$ critical model in $d = 4 - \varepsilon$ dimensions, which is relevant for the description of the critical behaviour of a variety of real-world systems. Using semiclassical methods, we compute the scaling dimensions of traceless symmetric composite operators to the next-to-leading order in the large charge expansion and all-orders in the ε -expansion. Furthermore, we derive new results for the spectrum of anomalous dimensions in the $O(N)$ model with cubic anisotropy.

In $4 < d < 6$, the $O(N)$ theory flows to an asymptotically safe UV fixed point that is believed to play a relevant role in (higher-spin) AdS/CFT. Recently, it has been conjectured a dual description of this critical theory in terms of the IR fixed point of an $O(N)$ -invariant theory with $N + 1$ fields and cubic interactions. In chapter five, we probe this conjecture by means of the large charge expansion, arguing in favor of the equality of the large charge sectors of the two models in $d = 6 - \varepsilon$ dimensions.

Chapter six concerns large charge operators in the $U(N) \times U(M)$ model in $d = 4 - \varepsilon$ dimensions. The role of the charge configuration is investigated in detail via both group-theoretical and semiclassical analyses. In particular, we show how, varying the charge assignment, we can access the anomalous dimension of different operators transforming according to a variety of irreducible representations. To this end, we introduce a novel general strategy apt at determining the correspondence between the charge configuration and the related large charge operators in generic non-abelian CFTs. As a byproduct of our investigation, we obtain many new results for the $U(N) \times U(M)$ model.

Hrvatski produljeni sažetak

Konformne teorije polja (CFT, *od engl. conformal field theory*) bez sumnje vrlo su važne za opis prirode. One imaju bitnu ulogu u teoriji kontinuiranih faznih prijelaza, te su ključne za naše razumijevanje kvantne teorije polja. Štoviše, CFT-ovi imaju veliku važnost u teoriji struna i predstavljaju jednu stranu proslavljenе AdS/CFT korespondencije. Nadalje, CFT alati često se koriste za istraživanje dinamike kvantnih teorija polja u režimima u kojima se uobičajene metode pokažu neučinkovitim.

Za danu grupu simetrija, za rješavanje CFT-a potrebno je izračunati njezine *CFT podatke*, tj. dimenziju skaliranja svih primarnih operatora i potpun skup OPE koeficijenata teorije. CFT-ovi se obično proučavaju putem perturbativnog računa [1], razvoja po epsilonu [2, 3], te neperturbativno putem konformne bootstrap metode [4–6] te AdS/CFT korespondencije [7, 8]. Nadalje, u posebnom slučaju dvodimenzionalnog prostor-vremena, postoji mnogo primjera CFT-ova koji su egzaktno rješivi [9].

Nedavno je pokazano da se CFT podaci s obzirom na operatore koji nose veliku vrijednost određenog očuvanog naboja mogu izračunati i putem *razvoja po naboju* u inverznim potencijama Noetheričinog naboja, pri čemu su se prvi radovi fokusirali na limes velikog naboja [10–12]. U tom limesu, CFT stanje i njegova pobuđenja ulaze u “fazu kondenzirane materije sličnu supratekućini” konačne gustoće. Takve su faze karakterizirane spontanim lomljenjem prostorno-vremenskih i unutarnjih simetrija te ih se može opisati efektivnom teorijom polja (EFT, *od engl. effective field theory*) za Goldstoneove bozone simetrije.

Spomenuti EFT pristup pogodan je za bavljenje jako vezanim teorijama, parametariziranjem nepoznate fizike konačnim brojem neperturbativnih koeficijenata u svakom redu razvoja po naboju. Nadalje, razvoj po naboju sadrži *univerzalne* koeficijente koje je moguće izračunati i koji ne ovise o mikroskopskom opisu CFT-a, već isključivo o simetriji i broju prostorno-vremenskih dimenzija. Zapravo, ti pojmovi proizlaze iz univerzalnih značajki fononskog spektra u generaliziranoj supratekućoj fazi. Pomoću EFT-a s velikim nabojem istraženo je nekoliko teorija, poput $O(N)$ vektorskog modela u tri dimenzije [11], trodimenzionalnog $SU(N)$ matričnog modela [13, 14], i Chern-Simonsove teorije [15, 16]. Supersimetrične teorije u limesu velikog R-naboja ispitane su u [17–19].

U slučaju kad je CFT perturbativno dostupan zahvaljujući prisutnosti malog parametra ε , može se zaobići EFT konstrukciju i raditi izravno u potpunoj teoriji. Tada razvoj po velikom naboju ima oblik 't Hooft-ovog razvoja [20], gdje se definira 't Hooft-ova konstanta vezanja $\mathcal{A} = \varepsilon Q$, s nabojem Q , i uzima limes $\varepsilon \rightarrow 0$ i $Q \rightarrow \infty$ uz držanje \mathcal{A} fiksni. To omogućuje dobivanje rezultata svakog reda u terminima A konstanti vezanja, resumirajući odjednom beskonačni niz Feynmanovih dijagrama u svakom redu razvoja po velikom naboju. Nadalje, sada možemo postaviti čvrst temelj za EFT konstrukciju, povezujući perturbativnu i neperturbativnu fiziku.

Ovdje važnu ulogu igra općeniti fenomen „klasikalizacije“ kvantnih sustava u prisutnosti velikih vrijednosti nekog kvantnog broja. Ustvari, Feynmanovim integralima koji opisuju korelatore operatora velikih naboja dominiraju netrivijalne klasične putanje karakterizirane specifičnim obrascem lomljenja simetrije. Kao posljedica, razvoj po naboju svodi se na poluklasični razvoj oko tih klasičnih rješenja.

Prva istraživanja razvoja po naboju u slabo vezanim teorijama pojavila su se u [21–24], gdje su se autori usredotočili na abelovu $\varphi^4 U(1)$ teoriju.

Ova doktorska disertacija fokusira se na razvoj, poopćenje i primjenu razvoja po naboju u CFT-u, kao moćnog pristupa u otkrivanju strukture kvantne teorije polja s posebnim naglaskom na slabo vezane neabelove CFT-ove.

U drugom poglavlju uvodimo osnove konformne teorije polja usredotočujući se na aspekte relevantne za proučavanje sektora velikih naboja CFT-ova, kao što su radikalna kvantizacija, korespondencija operator-stanje te Weylove transformacije.

Međuigra klasikalizacije CFT-ova s velikim nabojem i spontanog lomljenja relativističke invarijantnosti, što dovodi do netrivijalnog brojanja i svojstava Goldstoneovih bozona, čini proučavanje CFT-a s velikim nabojem složenom i fascinantnom temom koju ćemo pregledati u trećem poglavlju. Tamo također uvodimo poluklasični pristup razvoju po naboju i pokazujemo njegovu povezanost s konvencionalnim razvojem po Feynmanovim dijagramima. Nadalje, pregledavamo poopćenje Goldstoneovog teorema relevantno za QFT s velikim nabojem. (Djelomični) dokaz ovog teorema dan je u dodatku.

U četvrtom poglavlju proučavamo razvoj po naboju u $O(N)$ kritičnoj teoriji u $4-\varepsilon$ dimenzije, što je relevantno za opis kritičnog ponašanja različitih sustava iz stvarnog svijeta. Nakon opće rasprave

o neabelovim modelima s velikim nabojem, proučavamo postupak fiksiranja naboja i inducirano spontano lomljenje simetrije u $O(N)$ vektorskom modelu.

Konkretno, otkrivamo da ako je osnovno stanje prostorno homogeno, onda su sve moguće konfiguracije naboja s istim ukupnim nabojem povezane $O(N)$ transformacijama. Zapanjujuća posljedica je da u ovom modelu zbroj naboja djeluje kao jedinstveni naboj, dok konfiguracija naboja uopće nema ulogu. Za homogeno osnovno stanje s ukupnim nabojem Q zatim identificiramo odgovarajuću familiju operatora fiksnih naboja kao Q -indekse simetričnih $O(N)$ tenzora traga nula s klasičnom dimenzijom Q te računamo njihovu dimenziju skaliranja do prvog reda iznad vodećeg u razvoju po naboju i u svim redovima u konstanti vezanja. Te anomalne dimenzije definiraju skup (kritičnih) eksponenata križanja koji mijere nestabilnost sustava (npr. kritičnih magneta) protiv anizotropnih perturbacija [25–27].

Izračun je napravljen koristeći Weylove transformacije za preslikavanje teorije na cilindar i korespondencije stanje-operator kako bi se dimenzije skaliranja povezale s energetskim spektrom na cilindru. Potonje se izračunava semiklasično rješavanjem odgovarajućeg klasičnog sustava i određivanjem spektra fluktuacija oko vodeće putanje. Akcija dobivena iz klasičnog rješenja daje vodeći red anomalne dimenzije u razvoju po naboju, dok je slijedeći red određen funkcionalnom determinantom fluktuacija koja se može izraziti u terminima njihovih disperzijskih odnosa. Potvrđujemo naš pristup testiranjem rezultata do najvišeg poznatog reda u perturbacijskoj teoriji (2 petlje u razvoju po epsilon) i iskorištavamo ih za "boost" same teorije perturbacije, dobivajući potpun skup eksponenata križanja u 4 petlje u razvoju po epsilonu.

Nadalje, predviđamo članove proizvoljno visokog reda u razvoju po epsilonu, koji se mogu koristiti za provjeru budućih dijagramskih izračuna. Poglavlje zaključujemo raspravom o nastanku faze nalik supratekućini u limesu velikog naboja i povezane pojave univerzalnih doprinosa u razvoju po velikog naboju. Konačno, raspravljamo o ograničenjima metoda velikih naboja, s naglaskom na njihovu relevantnost za eksperiment. Konkretno, provodimo heurističku analizu kako bismo odredili raspon vrijednosti naboja takve da je razvoj po naboju pod nadzorom.

Zatim idemo između četiri i šest dimenzija, gdje $O(N)$ kvartični model teče u *asimptotski sigurne* [28,29] UV fiksne točke pri negativnim vrijednostima konstanti vezanja [30], za što se vjeruje da igra relevantnu ulogu u AdS / CFT-u (višeg spina) [31,32]. Zanimljivo je da se odnedavno nađa dualan opis te kritične teorije u terminima IR fiksne točke u $O(N)$ -invarijantnoj teoriji s $N + 1$

polja i kubičnim potencijalom [33, 34].

U petom poglavlju istražujemo ova nagađanja pomoću razvoja po naboju, argumentirajući u prilog jednakosti velikih sektora naboja dvaju modela u $6 - \epsilon$ dimenzija.

Konkretno, uspoređujemo dimenzije skaliranja operatora velikih naboja do prvog reda nakon vodećeg u razvoju po naboju i pronalazimo slaganje. Izračun dimenzija skaliranja u kubnom modelu srođan je onom izvedenom u četvrtom poglavlju. Budući da naši rezultati resumiraju beskončni red Feynmanovih dijagrama, te uključuju beskonačnu familiju kompozitnih operatora, značajno proširujemo prethodne testove ekvivalencije dvaju modela. To pokazuje kako metode velikih naboja mogu biti korisne u ispitivanju dualnosti u kvantnoj teoriji polja.

Nadalje, analiziramo pojavu kompleksnih dimenzija skaliranja iznad kritične vrijednosti naboja. Takva kritična vrijednost netrivijalno je određena parametrom N i brojem prostorno-vremenskih dimenzija. Raspravlja se o odnosu doprinosa instantona slobodnoj energiji modela.

U šestom poglavlju koristimo razvoj po naboju da bismo proučili dinamiku $U(N) \times U(M)$ modela, relevantnih za fiziku elementarnih čestica i kozmologiju [35–37]. Konkretno, kada imamo $N = M = 2$, ovaj model opisuje standardni Higgsov model, a u općenitom slučaju $N = M$ opisuje kiralan fazni prijelaz na konačnoj temperaturi u kvantnoj kromodinamici (QCD) [36, 38].

Uz fenomenološke primjene, imamo dvije različite motivacije za razmatranje ovog modela. Prvo, u ovoj je teoriji moguće analizirati utjecaj konfiguracije naboja na razvoj po naboju za CFT podatke. Štoviše, u velikom dijelu svog prostora parametara, i u $4 - \epsilon$ dimenzije, ova teorija ne teče ni u jednu fiksnu točku za realne vrijednosti njezinih dviju konstanti vezanja nego sadrži dvije kompleksno konjugirane fiksne točke. Odgovarajući *kompleksni CFT* nije unitaran i povezan je s pojavom blizu konformnog ponašanja tzv. *walking* tipa u teoriji [39, 40].

Uspješnom primjenom metoda velikih naboja ilustriramo, stoga, kako koristiti ove alate temeljene na CFT-u u računanju funkcija renormalizacijske grupe čak i u teorijama bez fiksnih točaka. Nadalje, raspravljamo o uvjetima pod kojima korespondencija stanje-operator i Weylovo preslikavanje vrijede u neunitarnim CFT-ovima. U istom poglavlju pokazujemo kako mijenjajući konfiguraciju naboja možemo bez pomoći dijagramske proračuna pristupiti anomalnoj dimenziji različitih operatora koji se transformiraju u skladu s različitim ireducibilnim reprezentacijama globalne grupe simetrije. To ilustrira posebnu učinkovitost metoda velikih naboja s obzirom na konvencionalni razvoj po Feynmanovim dijagramima kada se radi o teorijama s uključenim neabelovim grupama

simetrije, kao što je $U(N) \times U(M)$.

U tu svrhu upotpunjujemo semiklasični pristup razvijanjem opće strategije koja je sposobna identificirati, za danu konfiguraciju naboja, operator fiksnog naboja s minimalnom dimenzijom skaliranja, koja, putem korespondencije stanje-operator, odgovara osnovnom stanju teorije na cilindru. Zapravo, kao što ćemo vidjeti u tom poglavlju, energija osnovnog stanja (a time i pripadajuća dimenzija skaliranja) može se tada lako izračunati semiklasično kao funkcija konfiguracije naboja. Naša je strategija ukorijenjena u teoriji reprezentacije Liejevih grupa, a poduprta je eksplisitnom konstrukcijom relevantnih operatora.

Kao nus produkt naših analiza dobivamo mnogo novih rezultata o spektru anomalnih dimenzija u modelu $U(N) \times U(M)$. Rezultate testiramo uspoređujući ih s literaturom, izvodeći dijagramske izračune te uzimajući određene limese u prostoru parametara gdje model se pojednostavljuje.

Ključne riječi: konformna teorija polja, razvoj po naboju, semiklasične metode

Contents

1	INTRODUCTION	1
2	BASICS OF CONFORMAL FIELD THEORY	8
2.1	The conformal algebra	8
2.2	Radial quantization and state-operator correspondence	11
2.3	Correlation functions	13
2.4	The operator product expansion	14
2.5	Weyl maps	15
2.6	Complex CFT	17
3	QFT AT LARGE CHARGE	20
3.1	Invitation I: the semiclassical Hydrogen atom	20
3.2	Invitation II: the spinning rigid rotor	22
3.3	Fixing the charge	25
3.4	Goldstone bosons at large charge	28
3.5	The RG flow at large charge	30
3.6	Feynman diagrams at large charge	37
3.7	Path integrals at large charge	45
4	CHARGING THE $O(N)$ MODEL	48
4.1	Charging non-abelian theories	48
4.2	The critical $O(N)$ model in $d = 4 - \varepsilon$ dimensions	52
4.3	Charging the system	55
4.4	Fixed-charge operators	60
4.5	The large charge expansion in the $O(N)$ model: LO	62
4.6	The large charge expansion in the $O(N)$ model: NLO	63
4.7	Regularization and renormalization	66
4.8	Results	68
4.9	How large is the charge?	73

4.10	Cubic anisotropy	74
5	CHARGING A QUARTIC/CUBIC DUALITY	86
5.1	The $O(N)$ model in $4 < d < 6$	86
5.2	Large charge expansion in the cubic model: LO	92
5.3	Large charge expansion in the cubic model: NLO	95
5.4	Complex anomalous dimensions	100
6	CHARGING NON-ABELIAN HIGGS THEORIES	104
6.1	Charging the system	108
6.2	Fixed-charge operators in the $U(N) \times U(M)$ model	111
6.3	Semiclassical expansion and results	121
6.4	On how to identify the fixed-charge operators	130
7	CONCLUSIONS	139
Bibliography		142
Appendix A Proof of the <i>charged Goldstone theorem</i>		164
Appendix B One-loop computation in the $U(N) \times U(N)$ Higgs model		169
Appendix C The functions $\rho(\mathcal{A}_h^*, \mathcal{A}_v^*)$ and $\sigma(\ell, \mathcal{A}_h^*, \mathcal{A}_v^*)$		172

1 INTRODUCTION

If you ask a high-energy physicist “*How things happen in nature?*”, (s)he may answer “*In all the possible ways..., together*”. Indeed, the path integral formulation of quantum field theory (QFT) tells us that, to determine the probability of a certain event, we have to sum over all the *paths, processes, stories* which may lead to that event. Unfortunately, when it comes to QFT, apart from a few “lucky” cases, we actually do not know how to sum over all the paths.

Strikingly, in many cases, we can sum solely over *some* paths and still obtain precise results. This is the case of classical physics, where a single classical trajectory (the least-action one) is so predominant that we can completely forget about all the other possible (quantum) paths.

Another example is provided by low energy quantum electrodynamics (QED), where the smallness of the interaction strength allows us to efficiently organize the paths according to their relevance, setting up a perturbative expansion so efficient that it led to some of the most precise predictions of history of physics [41].

However, often nature is not so nice to us, and perturbative methods are not feasible. This happens in strongly-coupled QFTs, such as low-energy quantum chromodynamics (QCD). A common strategy roughly consists in discretizing the spacetime in order to consider only a finite (although huge) number of paths, computing the discretized path integral on a supercomputer, and finally extrapolating the continuum limit. This non-perturbative first-principle approach takes the name of *lattice field theory*. Another possibility is to adhere to the effective field theory (EFT) philosophy: *if you can't beat 'em parametrize 'em*, which, albeit often leaving a sense of bitterness, can be very efficient in capturing the phenomenological aspects.

Leaving aside for a moment strongly-coupled systems, it is well-known that, in perturbative theories, the conventional diagrammatic method becomes soon unpractical as we go beyond the first few perturbative orders due to the fast growth of the number of Feynman diagrams with the loop order.

Another case when perturbation theory can break down and become ineffective even in weakly-coupled theories is when describing multi-particle production processes with a large number of final states [42, 43] and, more broadly, processes involving multi-legged amplitudes. This phenomenon has important applications for future collider physics since perturbative unitarity may be violated

in multi-Higgs (or W , Z) boson production processes at energy scales as high as $\mathcal{O}(100)$ TeV¹ [44, 45], which are expected to be accessible at the next generation of colliders such as the Future Circular Collider (FCC) at CERN [46, 47]. The renormalization of composite operators with a large number of legs is, in itself, a notoriously tough task when tackled with conventional techniques. The underlying reason is the rapid growth of the number of diagrams, not only with the number of loops but also with the number of legs.

In the light of the above, every method able to give an insight into the structure of QFT should be retained of great value².

In this thesis, we focus on that subset of quantum field theories which are invariant under conformal transformations. Conformal field theories are of general interest since they generally occur at the extrema of the renormalization group (RG) flow. For this reason, every continuum QFT can be seen as a (relevant) deformation of a CFT. The Standard Model itself, in many respects, can be seen as a slight deformation of a CFT [49, 50]. Furthermore, whenever in an arbitrary theory we have a large hierarchy between two energy/length scales, the physics at intermediate scales is, in first approximation, conformal.

In nature, CFTs appear in the description of continuous phase transitions [51, 52], such as the ferromagnetic, superconducting, and superfluid transitions. In this case, the scaling dimensions of the operators define the *critical exponents* describing the behavior of a physical system as it approaches the critical point.

CFT plays a fundamental role in string theory too, where physical properties are encoded in two-dimensional conformal theories living on the strings' worldsheets [53]. Moreover, they may provide a non-perturbative UV completion of quantum gravity via the AdS/CFT correspondence [7, 8].

For a given symmetry group, to solve a CFT amounts to compute its CFT data, i.e. the scaling dimensions of all the primary operators and the full set of three-point function coefficients (OPE coefficients) of the theory. CFTs are usually investigated via perturbation theory [1], the epsilon

¹ An obvious question is: *how many Higgs does it take?* A recent analysis concluded that, at energies $\sim \mathcal{O}(100)$ TeV, the number of Higgs bosons needed to have unitarity violation at the perturbative level is 130 [44].

² "The underlying physical laws necessary for the mathematical theory of a large part of physics and the whole of chemistry are thus completely known, and the difficulty is only that the exact application of these laws leads to equations much too complicated to be soluble. It therefore becomes desirable that approximate practical methods of applying quantum mechanics should be developed." P. Dirac (1929) [48].

expansion [2, 3], and non-perturbatively by means of the conformal bootstrap method [4–6], Monte Carlo simulations [54–56], and AdS/CFT [57, 58].

In this work, we study the spectrum of operators carrying a large value of one or more conserved charges in CFTs with internal global symmetries. According to the state-operator correspondence, this can be also viewed as the study of CFT in states with a large charge density. In general, a conformal theory at large charge can be associated with a finite density “superfluid-like condensed matter phase” characterized by a specific pattern of spontaneous symmetry breaking, which mixes spacetime and internal symmetries and leads to a new form of Goldstone’s theorem. Moreover, observables with large quantum numbers are generally controlled by classical physics. In other words, the sum over paths is dominated by a leading classical trajectory around which we can set up a semiclassical expansion. This is a general fact observed in a variety of systems, ranging from the Hydrogen atom at large values of the magnetic quantum number to meson resonances with large spin [59, 60].

Recently, this phenomenon has been further elucidated in [10], where, studying the three-dimensional $U(1)$ scalar CFT, the authors show that the scaling dimensions of operators carrying large values of the $U(1)$ charge Q can be computed via a semiclassical *large charge expansion* in inverse powers of Q . To this end, they developed a powerful EFT approach suited to deal with strongly-coupled theories, encapsulating the unknown non-perturbative physics in a *finite* number of coefficients at every order of the $1/Q$ expansion.

After this first pioneering work, several theories have been investigated by means of the large charge EFT, such as non-abelian scalar models [11, 13, 61–63], Chern-Simons theories [15, 16], and non-relativistic systems with Schrödinger symmetry [64, 65]. Supersymmetric theories at large R-charge have been examined in [17–19]. The first review on the topic appeared in [66].

The above works show that a general (and intriguing) feature of the large charge expansion for CFT data is the presence of calculable *universal* terms that do not depend on the microscopic description of the CFT but solely on the symmetry of the theory and the number of spacetime dimensions. In fact, these terms stem from the universal features of the phonon-like spectrum in the generalized superfluid phase.

When the CFT is perturbatively accessible thanks to the presence of a small parameter ε , one can bypass the EFT construction and work directly in the full theory. In this case, the large charge

expansion becomes a 't Hooft-like expansion [20], where one defines a 't Hooft coupling $\mathcal{A} = \varepsilon Q$, and takes the limit $\varepsilon \rightarrow 0$ and $Q \rightarrow \infty$ while maintaining \mathcal{A} fixed. As a result, the scaling dimension³ Δ_Q of (large) charge Q operators takes the form

$$\Delta_Q = \sum_{k=-1} \frac{1}{Q^k} \Delta_k(\mathcal{A}) , \quad (1.1)$$

where Δ_k is the $k + 1$ -loop correction in the large- Q semiclassical expansion. In the above form, the large charge expansion shares many similarities with the *large number of flavors* [67–70] and the *large number of colors* [20, 71, 72] expansions in gauge theories.

The exploration of the large charge expansion in weakly-coupled theories begun in [21–24], where the authors focused on the $U(1)$ -invariant φ^4 scalar CFTs in $d = 4 - \varepsilon$ dimensions. Noticeably, every Δ_k in (1.1) resums at once an infinite series of Feynman diagrams of the conventional perturbative expansion. This opens the intriguing possibility of accessing the large-order behavior of perturbation theory, which is known to encode non-perturbative information [73–75], as well as performing all-order tests of conjectured dualities in QFT.

Moreover, by studying weakly-coupled theories at large charge, we can put on firm ground and "UV complete" the large charge EFT discussed above, bridging perturbative and non-perturbative physics. This has been done in [76] for the three-dimensional $U(1)$ -symmetric scalar CFT.

As we will argue in this thesis, large charge methods allow to efficiently compute the scaling dimension of composite operators with a large number of legs, being effective in realms (many loops, many legs) where diagrammatic methods are not, providing then a *complementary* approach to the latter. Indeed, large charge operators are naturally connected with the multi-legged amplitudes that, as discussed above, are problematic within perturbation theory.

Ultimately, a shared hope is to be able, one day, to transfer the techniques and knowledge matured by exploring CFT at large charge to the study of Standard Model processes involving a large number of Higgs, W , and Z bosons.

³ In this thesis, we will mainly focus on the computation of the anomalous dimension spectrum of large charge operators. However, the approach discussed here can also be extended to the computation of general correlators (and in particular to the three-point functions) of large charge operators, as discussed in [77, 78] and [23] for strongly- and weakly-coupled theories, respectively.

This thesis concerns the development and applications of the large charge expansion in CFT⁴ with a particular emphasis on weakly-coupled non-abelian scalar CFTs. The work is organized as follows:

- In Chap.2, we introduce the well-known basics of conformal field theory, focusing on the aspects relevant to the study of the large charge sectors of CFTs, such as radial quantization, operator-state correspondence, and Weyl transformations.

- In Chap.3, we review the main ideas underlying the study of CFT at large charge. There, we also introduce the semiclassical approach to the large charge expansion and show its connection to the conventional diagrammatic expansion.

- In Chap.4, we study the large charge expansion in the $O(N)$ critical theory in $4-\varepsilon$ dimensions. In particular, we show how to apply (non-EFT) large charge methods to non-abelian theories and use them to compute the anomalous dimensions of the spin-0 operators transforming as traceless symmetric $O(N)$ tensors to the next-to-leading order (NLO) in the large charge expansion. These anomalous dimensions define a set of *crossover (critical) exponents* which measure the instability of the system against anisotropic perturbations [25–27]. We validate the approach by testing our results to the maximum known order in perturbation theory (2-loops in the ε -expansion) and use them to “boost” perturbation theory itself, obtaining the 4-loop crossover exponents in the ε -expansion. Furthermore, we predict an infinite number of higher-order terms that can be used to check future diagrammatic calculations.

The emergence of a superfluid phase and the related EFT description is discussed. Finally, we focus on the $O(N)$ model with cubic anisotropy and perform a 1-loop study of the spectrum of anomalous dimensions.

- In Chap.5, we study the $O(N)$ theory in $4 < d < 6$ dimensions. In this range of dimensions, this model exhibits, at least for large N , a UV fixed point (FP) [30], which provides an example of an interacting, strongly-coupled, non-supersymmetric CFT in $d = 5$, as well as a realization of the *asymptotic safety* (or *non-perturbative renormalizability*) scenario [28], which may be realized

⁴ Notice that the large charge expansion considered here, where the charge is some *internal* quantum number, is a particular case of a more general *large quantum number expansion* that includes, for example, also the large-spin expansion in CFT [79] and QCD [80].

in nature by quantum gravity [29, 81, 82] and UV completions of the Standard Model [35, 83]. Moreover, it is believed that, in $d = 5$, this model has an AdS_6 holographic dual in terms of higher-spin theories [31, 32].

Interestingly, it has been conjectured a dual description of this UV fixed point (FP) in terms of the IR Wilson-Fisher (WF) FP of an $O(N)$ -invariant theory with $N + 1$ fields and cubic potential [33, 34]. We will test this conjecture using large charge methods and argue in favor of the equality of the large charge sectors of the two models in $6 - \varepsilon$ dimensions. Specifically, we will compare the scaling dimensions of large charge operators to the NLO in the large charge expansion finding agreement. Since our results resum an infinite series of Feynman diagrams and involve an infinite family of composite operators, we substantially extend previous tests of the equivalence between the two theories.

- In Chap.6, we use the charge expansion to study the dynamics of the $U(N) \times U(M)$ Higgs model in $d = 4 - \varepsilon$ dimensions. As we shall see, this model is suited to the investigation of the role of the charge configuration in theories with multiple conserved charges. Specifically, we show how large charge semiclassical methods can be efficiently employed to compute the scaling dimension of a variety of different operators identified by the charge configuration they carry. This will illustrate the effectiveness of the approach when dealing with theories invariant under involved non-abelian symmetry groups such as $U(N) \times U(M)$.

In a large region of its parameter space, the $U(N) \times U(M)$ theory does not flow to any FP. Instead, the zeros of the beta functions occur at complex values of the two couplings of the theory. The corresponding *complex CFT* is non-unitary and related to an emerging near-conformal behaviour of the *walking* type [39, 40]. We illustrate how to study the non-conformal theory by considering the associated complex CFTs and applying large charge methods.

- In Chap.7, we offer our conclusions and discuss the future challenges in the field.

Finally, the thesis includes three appendices containing additional details on some of the computations presented.

The original material starts from chapter 4 on, while previous chapters review the known literature. In particular, Chap.4 is based on our work [84], except for Sec.4.10, which presents material

from our publication [85], and Sec.4.9 that contains a (so far) unpublished novel analysis. Chap.6 is based on our publication [86] and our preprint [87]. Results from Chap.5 will appear in a paper that is currently in preparation. Chaps.4 and 6, and related appendices, contain many unpublished details absent in the original papers.

Keywords: *conformal field theory, large charge expansion, semiclassical methods*

2 BASICS OF CONFORMAL FIELD THEORY

In this section, we will introduce the basics of conformal field theory. Since this subject is well-documented, we will just present the main results relevant to the study of the large charge sectors of CFTs. The reader interested in a pedagogical introduction to CFT can refer to [88–90] (see also chapter 2 of [53] for a more string-oriented introduction to 2D CFT) and references therein.

In general, a physical system looks different when examined at different energy/length scales. In QFT and statistical physics the change of a system when probed at different scales is encoded in the *renormalization group* (RG) flow in the space of the theories i.e. the space of the Lagrangians/Hamiltonians. *Fixed points* (FPs) of the RG flow are given by theories invariant under RG transformation i.e. by scale invariant theories. At the quantum level, fixed points are defined by the zeros of the beta functions for the couplings of the theory.

Amazingly, most scale invariant QFTs show an enhanced *conformal symmetry*, defined as invariance under general angle-preserving changes of coordinates. This is an intriguing fact of nature that still asks for a full theoretical explanation⁵. Then CFTs represent useful oases in the space of quantum field theories. Furthermore, conformal symmetry highly constrains the dynamics of QFTs. In fact, it allows us to non-perturbatively define CFTs as well as obtain many important results on their structure without making reference to any Lagrangian/Hamiltonian description. We will illustrate this last point in the rest of this introductory section.

2.1 The conformal algebra

Conformal Transformations on a d -dimensional flat space with signature (p, q) , $p + q = d$ are diffeomorphisms that locally preserve the angle between lines. This is realized if under the change of coordinates $x^\mu \rightarrow x'^\mu(x)$, the metric changes only by an overall factor, that is

$$\eta_{\mu\nu} \rightarrow \Lambda(x)\eta_{\mu\nu} . \quad (2.1)$$

⁵ See [91] for a comprehensive review on the relation between scale and conformal invariance and [92] for a discussion in the four-dimensional case.

A local rescaling of the metric tensor as the one above is called *Weyl transformation*. An infinitesimal transformation

$$x'^\mu = x^\mu + \varepsilon^\mu(x) + \mathcal{O}(\varepsilon^2) , \quad \Lambda(x) = e^{w(x)} \sim 1 + w(x) , \quad (2.2)$$

is conformal if

$$\partial_\mu \varepsilon_\nu + \partial_\nu \varepsilon_\mu = w(x) \eta_{\mu\nu} . \quad (2.3)$$

The above condition can be rewritten as

$$\begin{aligned} w(x) &= \frac{2}{d} \partial \cdot \varepsilon , \\ (\eta_{\mu\nu} \partial^2 + (d-2) \partial_\mu \partial_\nu) w(x) &= 0 , \\ (d-1) \partial^2 w(x) &= 0 . \end{aligned} \quad (2.4)$$

For $d = 2$ the second and third equations coincide, leading to deep differences between the cases $d = 2$ and $d \geq 3$. We start from the case $d \geq 3$, where (2.4) has only four types of solution which we give below together with the corresponding transformations and their generators

Solution	Transformation	Generator
$\varepsilon^\mu = a^\mu = \text{const.}$	Translations: $x'^\mu = x^\mu + a^\mu$	$P_\mu = -i\partial_\mu$
$\varepsilon^\mu = x^\nu \omega_{\nu\mu}$	Rotations: $x'^\mu = x^\mu + \omega_\nu^\mu x^\nu$	$M_{\mu\nu} = i(x_\mu \partial_\nu - x_\nu \partial_\mu)$
$\varepsilon^\mu = \lambda x^\mu$	Dilatations: $x'^\mu = (1 + \lambda) x^\mu$	$D = -ix^\mu \partial_\mu$
$\varepsilon^\mu = 2(b \cdot x) x^\mu - x^2 b^\mu$	SCT: $x'^\mu = x^\mu + 2(b \cdot x) x^\mu - x^2 b^\mu$	$K_\mu = -i(2x_\mu x^\nu \partial_\nu - x^2 \partial_\mu)$

where $\omega_{\nu\mu} = -\omega_{\mu\nu}$ and SCT stands for *special conformal transformations*. The global form of the SCT reads

$$x'^\mu = \frac{x^\mu - b^\mu x^2}{1 - 2(b \cdot x) + b^2 x^2} , \quad (2.6)$$

and diverges when the denominator vanishes. Thus, in order to globally define the SCT, we need to perform a so-called *conformal compactification*, which adds the point at ∞ .

With the explicit expression for the generators given above, we can compute the commutation

relations defining the *conformal algebra*

$$\begin{aligned}
[M_{\mu\nu}, M_{\rho\sigma}] &= i(\delta_{\mu\rho}M_{\nu\sigma} \pm \text{permutations}) , \\
[M_{\mu\nu}, P_\rho] &= i(\delta_{\nu\rho}P_\mu - \delta_{\mu\rho}P_\nu) , \\
[M_{\mu\nu}, K_\rho] &= i(\delta_{\nu\rho}K_\mu - \delta_{\mu\rho}K_\nu) , \\
[D, P_\mu] &= iP_\mu , \\
[D, K_\mu] &= -iK_\mu , \\
[P_\mu, K_\nu] &= -2i(\delta_{\mu\nu}D - M_{\mu\nu}) ,
\end{aligned} \tag{2.7}$$

where the first two relations define the Poincare algebra. The overall number of generators is $\frac{1}{2}(d+1)(d+2)$. In fact, the conformal group acting on $\mathcal{R}^{p,q} \cup \infty$ is isomorphic to $SO(p+1, q+1)$. This can be easily proven by using the so-called "projective light cone" formalism [93, 94] where one embeds $\mathcal{R}^{p,q}$ into $\mathcal{R}^{p+1,q+1}$ by considering a section of the light cone in the latter spacetime to eliminate the additional coordinates. Since the conformal group acts linearly on $\mathcal{R}^{p+1,q+1}$, this formalism is very useful for studying the implications of conformal invariance.

To study the conformal algebra in $d = 2$ dimensions, we consider the Euclidean signature and introduce complex coordinates $z = x^0 + ix^1$, $\bar{z} = x^1 - ix^2$. Hence, Eqs.(2.4) reduce to

$$\partial_z \bar{\epsilon} = \partial_{\bar{z}} \epsilon = 0 , \tag{2.8}$$

where

$$\epsilon = \epsilon^0 + i\epsilon^1 , \quad \bar{\epsilon} = \bar{\epsilon}^0 - i\bar{\epsilon}^1 , \quad \partial_z = \frac{1}{2}(\partial^0 - i\partial^1) , \quad \bar{\partial}_{\bar{z}} = \frac{1}{2}(\partial^0 + i\partial^1) . \tag{2.9}$$

Thus the group of infinitesimal conformal transformations in two dimensions is generated by all the meromorphic functions $\epsilon = \epsilon(z)$ and $\bar{\epsilon} = \bar{\epsilon}(\bar{z})$, which can be Laurent-expanded as

$$\epsilon(z) = \sum_{n \in \mathbb{Z}} \epsilon_n z^{n+1} , \quad \bar{\epsilon}(\bar{z}) = \sum_{n \in \mathbb{Z}} \bar{\epsilon}_n \bar{z}^{n+1} . \tag{2.10}$$

Then a basis of generators is given by

$$l_n = -z^{n+1} \partial_z, \quad \bar{l}_n = -\bar{z}^{n+1} \partial_{\bar{z}}, \quad n \in \mathbb{Z}, \quad (2.11)$$

and generates the Witt algebra

$$\begin{aligned} [l_m, l_n] &= (m - n)l_{m+n}, \\ [\bar{l}_m, \bar{l}_n] &= (m - n)\bar{l}_{m+n}, \\ [\bar{l}_m, l_n] &= 0. \end{aligned} \quad (2.12)$$

The Witt algebra is infinite-dimensional, and this highly constrains the CFT dynamics, sometimes allowing a complete solution of the theory [9]. On the other hand, the group of globally defined conformal transformations depends on the topology of the considered space. For instance, it is easy to prove that the group of conformal transformations on the two-sphere $S^2 \cong \mathbb{C} \cup \infty$, is the Möbius group $PSL(2, \mathbb{C}) = SL(2, \mathbb{C})/\mathbb{Z}_2$, which is generated by l_{-1}, l_0, l_1 and $\bar{l}_{-1}, \bar{l}_0, \bar{l}_1$. In particular, l_{-1} generates translations, l_0 generates complex dilatations (which can be seen as real dilatations plus rotations), while l_1 generates the SCT.

2.2 Radial quantization and state-operator correspondence

We move to analyze the Hilbert space of a CFT and the action of the conformal group on operators. From now on, we will focus uniquely on case $d \geq 3$, to which is devoted the content of this dissertation.

In general, we construct the space of states of a quantum theory by foliating the spacetime into $d - 1$ dimensional surfaces. States defined on the same surface belong to the same Hilbert space. Moreover, if the surfaces are related by a symmetry transformation, then the Hilbert space is the same on each surface. It is, therefore, convenient to choose a foliation according to the symmetries of the theory.

A prototypical example is a foliation into equal-time surfaces in theories with Poincare symmetry. In that case, we create states on a given surface $t = t'$ by inserting operators in its past $t < t'$ and computing the path integral over the field configuration in the past. States on different equal-time

surfaces $t = t'$ and $t = t''$ are hence related by the time evolution unitary operator $U = e^{iH(t'' - t')}$, where the Hamiltonian H corresponds to the operator generating time translations.

In theories with conformal symmetry, it is convenient to foliate the space into spherical surfaces centered in the origin $x = 0$. Then we can move from one surface to another by acting with the dilatation operator D , which takes the role of the Hamiltonian. For obvious reasons, this approach takes the name of *radial quantization*.

Since the angular momentum operator $M_{\mu\nu}$ commutes with D , we can label the states with the eigenvalues of D and their spin l . We naturally choose the vacuum $|0\rangle$ to be conformal invariant and thus annihilated by all the conformal generators. The action of the conformal generators on the operators is [95]

$$\begin{aligned} [P_\mu, \mathcal{O}(x)] &= -i\partial_\mu \mathcal{O}(x) , \\ [D, \mathcal{O}(x)] &= i(\Delta + x^\mu \partial_\mu) \mathcal{O}(x) , \\ [M_{\mu\nu}, \mathcal{O}(x)] &= -i(\Sigma_{\mu\nu} + x_\mu \partial_\nu - x_\nu \partial_\mu) \mathcal{O}(x) , \\ [K_\mu, \mathcal{O}(x)] &= -i(2x_\mu \Delta + 2x^\lambda \Sigma_{\lambda\mu} + 2x_\mu (x^\rho \partial_\rho) - x^2 \partial_\mu) \mathcal{O}(x) , \end{aligned} \tag{2.13}$$

where Δ is the scaling dimension of $\mathcal{O}(x)$ and $\Sigma_{\mu\nu}$ acts on the spin indices according to the $SO(p, q)$ irreducible representation (or *irrep*) of $\mathcal{O}(x)$.

Eigenstates of D are created by inserting operators with scaling dimension Δ in the origin

$$D|\Delta\rangle = D\mathcal{O}_\Delta(0)|0\rangle = [D, \mathcal{O}_\Delta(0)]|0\rangle + \mathcal{O}_\Delta(0)D|0\rangle = i\Delta\mathcal{O}_\Delta(0)|0\rangle = i\Delta|\Delta\rangle . \tag{2.14}$$

Since dilatation moves the insertion point, when $x \neq 0$ the insertion of operators inside a sphere does not generate eigenstates of D , but a superposition of them.

From the commutators (2.7), we have that the action of P_μ increases the scaling dimensions by 1, whereas K_μ decreases them by 1

$$P_\mu |\Delta\rangle \propto |\Delta + 1\rangle , \quad K_\mu |\Delta\rangle \propto |\Delta - 1\rangle . \tag{2.15}$$

Therefore, P_μ and K_μ act, respectively, as raising and lowering operators of the conformal algebra. A classic result [96] is that, in unitary theories, the scaling dimensions of primary operators are

bounded from below as⁶

$$\begin{aligned}\Delta_{\min}(l) &= l + D - 2, \quad l > 0 \text{ (Spin-}l\text{ traceless symmetric representations of } SO(p, q)) \\ \Delta_{\min}(0) &= \frac{D}{2} - 1, \quad l = 0 \text{ (Scalar representations).}\end{aligned}\tag{2.16}$$

Then, by repeatedly acting with K_μ on an arbitrary state at some point we will encounter a state $|\Delta\rangle$ such that $K_\mu|\Delta\rangle = 0$. The operators creating such states are called *primary operators* and satisfy the following defining property

$$[K_\mu, \mathcal{O}(0)] = 0.\tag{2.17}$$

Starting from a primary operator \mathcal{O} and acting with the raising operator P_μ , we can build a *conformal multiplet* of \mathcal{O} , $\{\mathcal{O}, P_\mu \mathcal{O}, P_\mu P_\nu \mathcal{O}, \dots\}$. The members of the multiplet are obtained by differentiating \mathcal{O} (remember that $[P_\mu, \mathcal{O}(x)] = -i\partial_\mu \mathcal{O}(x)$) and are called *descendants operators*. In this way, we can obtain all the operators with a definite scaling dimension and use them to construct the entire Hilbert space.

To sum up, the insertion of local primary operators at the origin produce the highest weight states, which have a definite scaling dimension and are annihilated by K_μ . Vice versa, from an eigenstate of D satisfying $K_\mu|\Delta\rangle = 0$, we can build a local primary operator with scaling dimension Δ . This one-to-one correspondence between states and local operators is called *state-operator correspondence* [98, 99] and plays a fundamental role in CFT⁷.

2.3 Correlation functions

In CFT, the interesting physical quantities are the scaling dimensions and the correlation functions of the scaling operators of the theory. Given two scalar primaries \mathcal{O}_i and \mathcal{O}_j ⁸, the requirement of conformal invariance fixes entirely the two-point function as

$$\langle \mathcal{O}_i(x) \mathcal{O}_j(y) \rangle = c \frac{\delta_{ij}}{|x - y|^{2\Delta}},\tag{2.18}$$

⁶ See [88, 89, 97] for a detailed derivation of the so-called *unitarity bounds* (2.16).

⁷ In non-conformal field theories, states and local operators are not equivalent since the former carry non-local information about the entire field configuration. On the other hand, in a CFT, we can map the entire space to the origin and we can think at the Hilbert space of the theory as living in a single point.

⁸ The indices of the operators represent the complete set of their quantum numbers and uniquely identify them.

where Δ is the scaling dimension of $\mathcal{O}_i(x)$ and c is a normalization factor which is fixed by the normalization of the operators⁹. This can be easily proven by acting with the conformal generators on the two-point function and using Eq.(2.13). Analogously, the three-point functions are fixed by conformal symmetry up to a constant C_{ijk} [100]

$$\langle \mathcal{O}_i(x)\mathcal{O}_j(y)\mathcal{O}_k(z) \rangle = \frac{C_{ijk}}{|x-y|^{\Delta_i+\Delta_j-\Delta_k}|y-z|^{\Delta_j+\Delta_k-\Delta_i}|z-x|^{\Delta_k+\Delta_i-\Delta_j}}. \quad (2.19)$$

The constants C_{ijk} are called *3pt function coefficients*, *OPE coefficients*, or *structure constants* and play a fundamental role in CFT. Higher-point functions are less constrained than the two and three-point function but are, of course, more constrained than in absence of conformal symmetry. For instance, in CFT, the four-point function of 4 identical scalars takes the form

$$\langle \mathcal{O}(x_1)\mathcal{O}(x_2)\mathcal{O}(x_3)\mathcal{O}(x_4) \rangle = \frac{1}{x_{12}^{2\Delta}x_{34}^{2\Delta}} f(u, v), \quad u = \frac{x_{12}^2 x_{34}^2}{x_{13}^2 x_{24}^2}, \quad v = u|_{2 \leftrightarrow 4}, \quad x_{ij} = x_i - x_j. \quad (2.20)$$

Analogous considerations apply to correlators involving composite operators with non-zero spin.

2.4 The operator product expansion

The operator product expansion (OPE) in QFT is a formal expansion of the product of two local operators as a series of other local operators

$$\mathcal{O}_i(x)\mathcal{O}_j(y) = \sum_k \lambda_{ijk}(|x_i - x_j|) \mathcal{O}_k(z), \quad (2.21)$$

where the sum goes over all the local operators in accord with any requirements of conserved quantum numbers. In general QFT the OPE is an asymptotic series formally valid in the limit $x \rightarrow y$. On the other hand, the conformal OPE is, when viewed as an operator equation, an exact expression with a radius of convergence equal to the distance to the next field insertion, as proved long ago by G. Mack in [101]. In fact, via the state-operator correspondence, the CFT OPE can be simply viewed as an expansion of the state created by the insertions of $\mathcal{O}_i(x)$ and $\mathcal{O}_j(y)$ in eigenstates of the dilatation operator.

Furthermore, the contribution of descendants fields can be adsorbed in a differential operator

⁹ In particular, we can always set $c = 1$.

$\mathcal{A}_{ijk}(|x_i - x_j|, \partial_z)$ which is fixed by conformal invariance up to a constant C_{ijk} . We then have

$$\mathcal{O}_i(x)\mathcal{O}_j(y) = \sum_k \mathcal{A}_{ijk}(|x_i - x_j|, \partial_z)\mathcal{O}_k(z) , \quad (2.22)$$

where the sum now involves only the primaries of the theory. The constants C_{ijk} are the same appearing in the expression for the three-point functions (2.19). In fact, by using the OPE, we can reduce any n -point function to a $n - 1$ -point function¹⁰. As a consequence, a CFT is fully characterized by the spectrum of local primary operators \mathcal{O}_i , their scaling dimensions $\Delta_{\mathcal{O}_i}$, and the set of OPE coefficients C_{ijk} . This information is collectively denoted as *CFT data*. The goal of CFT is to compute CFT data and use them to make predictions for experiments and understand the structure of the quantum world. CFT data can be computed perturbatively or by means of non-perturbative techniques such as *functional RG* methods, *conformal bootstrap*, and *lattice*.

2.5 Weyl maps

Weyl invariance is the invariance of the theory under Weyl transformations of the metric, which, in curved spacetimes, read

$$g_{\mu\nu} \longrightarrow \Lambda(x)g_{\mu\nu} \sim g_{\mu\nu} + w(x)g_{\mu\nu} . \quad (2.23)$$

General Weyl transformations can change the spacetime geometry while those considered in the definition of the conformal transformations map the flat spacetime into itself. This subclass of Weyl maps can be realized by diffeomorphisms i.e. they are induced by conformal changes of coordinates.

Clearly, Weyl invariance implies conformal symmetry, but the opposite is not generally true. By definition, the theory is Weyl invariant if the change of the action δS under a Weyl rescaling vanishes

$$\delta S = \int d^d x \sqrt{g} T^{\mu\nu} \delta g_{\mu\nu} = \int d^d x \sqrt{g} T^\mu_\mu w(x) = 0 , \quad (2.24)$$

where we have used the infinitesimal form of the Weyl transformation (2.23) and $T^{\mu\nu}$ is by definition the energy-momentum tensor of theory. Since $w(x)$ is arbitrary, the condition for infinitesimal

¹⁰ Asking consistency between the different ways we can reduce a four-point function to three-point functions by means of the OPE, it is possible to derive the *crossing symmetry constraints* at the heart of the conformal bootstrap method [5, 102, 103].

Weyl invariance is

$$T_\mu^\mu = 0 , \quad (2.25)$$

i.e. the energy-momentum tensor has to be traceless¹¹. It can be proven that this happens in all local unitary CFTs [88, 105]. This allows us to exploit Weyl invariance in order to simplify computations. In particular, to apply large charge methods we will often map our CFTs from \mathbb{R}^d to a cylinder $\mathbb{R} \times S^{d-1}$ ¹².

Considering polar coordinates (r, Ω_{d-1}) for \mathbb{R}^d , the map reads

$$\mathbb{R}^d \rightarrow \mathbb{R} \times S^{d-1} , \quad (r, \Omega_{d-1}) \rightarrow (\tau, \Omega_{d-1}) , \quad r = R e^{\tau/R} , \quad (2.26)$$

and corresponds to a Weyl rescaling of the metric

$$ds_{\text{cyl}}^2 = d\tau^2 + R^2 d\Omega_{d-1}^2 = \frac{R^2}{r^2} ds_{\text{flat}}^2 , \quad (2.27)$$

with R the radius of the sphere and τ the time coordinate on the cylinder. Under this map, dilatations D become time translations on the cylinder, and thus the radial quantization in flat space reduces to the usual equal-time quantization on the cylinder; states are classified according to their energy and live on spheres connected by time evolution. The latter is generated by the dilatation operator D , which plays the role of the Hamiltonian.

Under a Weyl transformation (2.23), correlation functions change according to

$$\frac{1}{\langle 1 \rangle_g} \langle \mathcal{O}_1(x_1) \dots \mathcal{O}_n(x_n) \rangle_g = \left(\prod_i \Lambda(x_i)^{\frac{\Delta_{\mathcal{O}_i}}{2}} \right) \frac{1}{\langle 1 \rangle_{\Lambda(x)g}} \langle \mathcal{O}_1(x_1) \dots \mathcal{O}_n(x_n) \rangle_{\Lambda(x)g} . \quad (2.28)$$

Under the map to the cylinder (2.26), the two-point function of a scalar primary operator \mathcal{O} and

¹¹ Since T_μ^μ gets a non-vanishing vacuum expectation value (vev) on curved even-dimensional spacetimes, to prove invariance under finite Weyl transformations is more complicated. This is known as the *Weyl anomaly*. In what follows, we will not consider theories living in an even number of dimensions, and thus we will not face this issue. We refer the reader to Refs. [104–106] for detailed discussions and recent progress on the relation between conformal and Weyl invariance, including the implication for correlation functions.

¹² Notice that the Weyl map on the cylinder is not conformal for $d > 2$.

its conjugate \mathcal{O}^\dagger transforms as [89, 90]

$$\langle \mathcal{O}^\dagger(x_f) \mathcal{O}(x_i) \rangle_{\text{cyl}} = |x_f|^{\Delta_{\mathcal{O}}} |x_i|^{\Delta_{\mathcal{O}}} \langle \mathcal{O}^\dagger(x_f) \mathcal{O}(x_i) \rangle_{\text{flat}} \equiv \frac{|x_f|^{\Delta_{\mathcal{O}}} |x_i|^{\Delta_{\mathcal{O}}}}{|x_f - x_i|^{2\Delta_{\mathcal{O}}}}, \quad (2.29)$$

where $x_{f,i}$ are the Cartesian coordinates on the plane, and the operators are canonically normalized. Notice that the limit $x_i \rightarrow 0$ corresponds to $\tau_i \rightarrow -\infty$ on the cylinder. In view of the state-operator correspondence discussed in Sec.2.2, the action of an operator \mathcal{O} at $\tau = -\infty$ creates a state on the cylinder with the same quantum numbers and with energy given by

$$E_{\mathcal{O}} = \frac{\Delta_{\mathcal{O}}}{R}. \quad (2.30)$$

Due to the above relation, our goal of computing scaling dimensions of fixed charge operators will often turn to the computation of the energy spectrum on the cylinder.

Finally, consider a conformal theory of massless scalar fields living on \mathcal{R}^d . When we map the theory to the cylinder, the scalar fields will couple to the Ricci scalar \mathcal{R} of S^{d-1} , generating a mass term with $m^2 = \xi \mathcal{R}$ in the Lagrangian. Naively, we might think to preserve conformality by taking the renormalized ξ to vanish, but it can be shown that if we fix $\xi = 0$ at some energy scale it will be generated anyway during the RG flow. Instead, it can be proven that the *conformal coupling* is dictated by conformal invariance to be $\frac{1}{4} \frac{d-2}{d-1}$ [107]. On a $d-1$ -dimensional sphere of radius R , we have $\mathcal{R} = \frac{(d-1)(d-2)}{R^2}$, and thus the mass of a conformal scalar on the cylinder is

$$m = \frac{d-2}{2R}. \quad (2.31)$$

2.6 Complex CFT

It can happen that fixed points of the RG flow occur at *complex* values of the couplings. Even if the theory will not actually flow to the FP, considering the associated *complex CFT*, which is, in general, non-unitary, can be a useful tool to explore the associated non-conformal theory. This can be achieved, for instance, using the so-called *conformal perturbation theory* [40, 108–110], where one perturbs the CFT by adding an operator \mathcal{O} with some (in general complex) coupling g , or with the aid of large charge methods, as we will show in Chap.6.

Furthermore, complex CFTs are strictly related to a RG behaviour of the *walking* type which, being a general natural mechanism for generating hierarchies in QFT, has been invoked in the literature for models of dynamical electroweak symmetry breaking [111–114] and for describing weak first order phase transitions (i.e. first order phase transitions near the critical point) in condensed matter systems [40, 110, 115, 116].

To illustrate the general connection between complex CFT, walking and hierarchies, consider a theory with only one coupling g . Then walking dynamics is realized when the beta function of g is very small but there is no FP. Then, there is a, eventually long, range of energies where the coupling is close to a constant value and the system shows near-conformal dynamics i.e. the coupling does not *run* but *walks*. To see this, consider a toy beta function given by¹³

$$\beta(g) = \mu \frac{\partial g}{\partial \mu} = (\alpha - \alpha_*) - (g - g^*)^2, \quad (2.32)$$

with μ the RG scale and α an external parameter¹⁴. For $\alpha > \alpha_*$, there are real FPs

$$g_{\pm} = g^* \pm \sqrt{\alpha - \alpha_*}, \quad (2.33)$$

where the plus and minus signs correspond, respectively, to ultraviolet (UV) and infrared (IR) FPs. Consider now decreasing the value of α . Then the two FPs will approach each other till they merge and disappear to the complex plane giving rise to two complex CFTs. For $\alpha < \alpha_*$, there are no FPs at real value of the coupling.

This behaviour of the beta function is shown in Fig. 1 together with the corresponding "walking" of the coupling as a function of the RG time $t = \log(\mu)$ for α slightly smaller than α_* . In fact, this case clearly illustrates how a hierarchy of scale arises: if one takes the coupling at a UV scale Λ_{UV} to have the value $g_{UV} < g^*$, flowing towards the IR, g grows, lingers near $g = g^*$, and finally blows up quickly. This defines an intrinsic IR scale Λ_{IR} , which is insensitive to the UV part of the flow and to the precise initial value g_{UV} . In particular, assuming $|g_{UV,IR} - g^*| \gg |\alpha - \alpha_*|$ to integrate

¹³This simple example has been first presented in the classical paper [39].

¹⁴In concrete cases, the role of α could be played by (a function of) the number of spacetime dimensions, colors, flavors, etc.

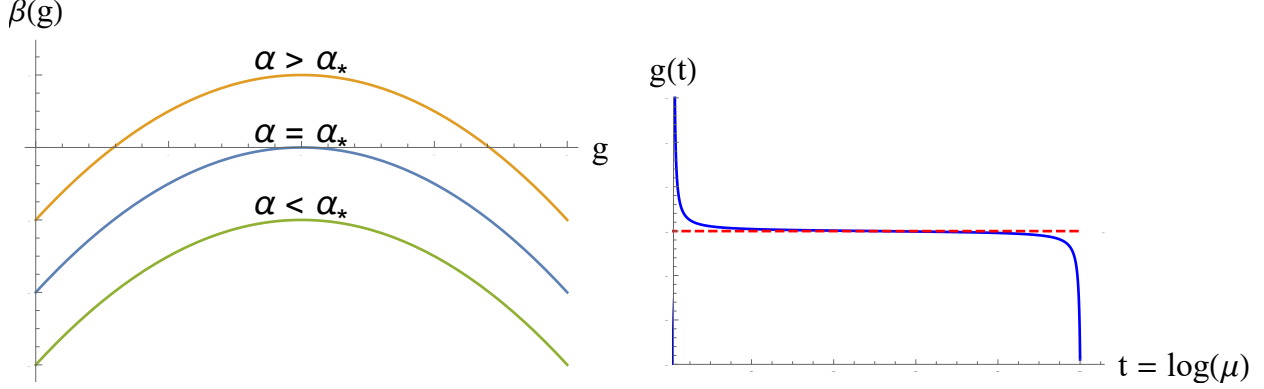


Figure 1: *Left:* The toy beta function $\beta(g)$, Eq.(2.32), for various values of the parameter α . For $\alpha > \alpha_*$, there are two FPs which merge when $\alpha = \alpha_*$. For $\alpha < \alpha_*$ there are no real FPs and the beta function has a "bump" centered in g^* . *Right:* The running of the g coupling for $\alpha < \alpha_*$ and $|\alpha - \alpha_*| \ll 1$ (blue solid line). The dashed red line indicates the value of g^* .

Eq.(2.32), we obtain Λ_{IR} as

$$\frac{\Lambda_{IR}}{\Lambda_{UV}} = e^{\int_{\Lambda_{UV}}^{g_{IR}} \frac{dg}{\beta(g)}} \sim e^{\frac{-\pi}{\sqrt{\alpha_* - \alpha}}} . \quad (2.34)$$

We have just generated a hierarchy: the theory contains two energy scales and the physics in the intermediate range between them is approximately scale invariant.

This concludes our general introduction to CFT. In the next section, we will explore what happens in CFTs with continuous internal global symmetries when we fix the value of the conserved charges.

3 QFT AT LARGE CHARGE

In the previous section, we introduced the CFT fundamentals. In particular, we saw that solving a CFT amounts to the computation of its CFT data. This thesis concerns CFT data relative to operators carrying a large value of some (internal) quantum number in theories with global symmetries. Via the state-operator correspondence, this can be also seen as the study of CFT in states of fixed charge density. In this section, we will introduce the main ideas behind CFT at large charge.

Given a Noether current j^μ ($\partial_\mu j^\mu = 0$), the associated conserved charge is

$$Q = \int d^{d-1}x j_0 , \quad \partial_0 Q = 0 . \quad (3.1)$$

Then, we say that an operator \mathcal{O} carries a value \bar{Q} of the charge Q if

$$[Q, \mathcal{O}] = \bar{Q}\mathcal{O} , \quad (3.2)$$

with $\bar{Q} \neq 0$.

In what follows, we will argue that the spectrum of operators carrying a large charge *classicalizes* and can thus be studied via a semiclassical expansion corresponding to a *large charge expansion* in inverse powers of the charge. To provide the reader with physical intuition on how classical physics emerges from a large value of some conserved quantum number, we start by examining two simple quantum mechanical examples, namely the hydrogen atom and the free particle on S^2 .

3.1 Invitation I: the semiclassical Hydrogen atom

Our first example of quantum systems at large charge is the quantum mechanical Hydrogen atom in the limit of infinite mass of the proton and at large values of the magnetic quantum number. The electron Hamiltonian is given by

$$H = \frac{\vec{p}^2}{2M} - \frac{\alpha}{r} , \quad (3.3)$$

where \vec{p} and M are, respectively, the momentum and mass of the electron. The second term in the RHS is the usual Coulomb potential with α the fine structure constant. The eigenvalues of the

Hamiltonian are found by solving the Schrödinger equation and read

$$E_n = -\frac{M\alpha^2}{2n^2}, \quad (3.4)$$

where n is an integer quantum number which labels the energy levels. The corresponding eigenstates of the Hamiltonian are labelled by n and other two quantum numbers: l , that labels the eigenvalues of the angular momentum $L^2 = l(l+1)$, and m , labelling its projection on the z -axis $L_z = m$. n , l , and m are known, respectively, as the *principal*, *azimuthal* and *magnetic* quantum numbers and are bounded as $n \geq 1$, $1 \leq l \leq n-1$, and $-l \leq m \leq l$. At fixed m , the ground state saturates these bounds as $m = l = n-1$ and has energy given by

$$E_0(m) = -\frac{M\alpha^2}{2(m+1)^2}. \quad (3.5)$$

Consider now the corresponding classical system at fixed angular momentum $l = m$. The effective potential $V_{eff} = \frac{m^2}{2Mr^2} - \frac{\alpha}{r}$ contains a centrifugal and a Coulomb term. By minimizing V_{eff} we have the minimal energy solution as a circular motion with radius $r^* = \frac{m^2}{M\alpha}$. Evaluating the Hamiltonian on this solution gives the ground state energy

$$E_0^{class}(m) = -\frac{M\alpha^2}{2m^2}. \quad (3.6)$$

By comparing the classical result for E_0 above with the quantum one (3.5), we see that the difference goes to zero for $m \rightarrow \infty$. In fact, for $m \gg 1$, $m+1 \sim m$, and we have

$$\frac{E_0 - E_0^{class}}{E_0} \simeq \frac{2}{m}. \quad (3.7)$$

Consistently, the semiclassical WKB approximation [117] can be used when the de Broglie wavelength $\lambda_{DB} = \frac{2\pi}{|\vec{p}|} \sim \frac{m}{r}$ is slowly varying, i.e. $\frac{d\lambda_{DB}}{dr} \ll 1$, which in turn implies $m \gg 1$. The qualitative behaviour of the classical effective potential is shown in Fig.2; the centrifugal barrier keeps the electron localized on the classical trajectory $r = r^*$ and at large m we can study the corresponding quantum mechanical path-integral via a saddle point expansion around it.

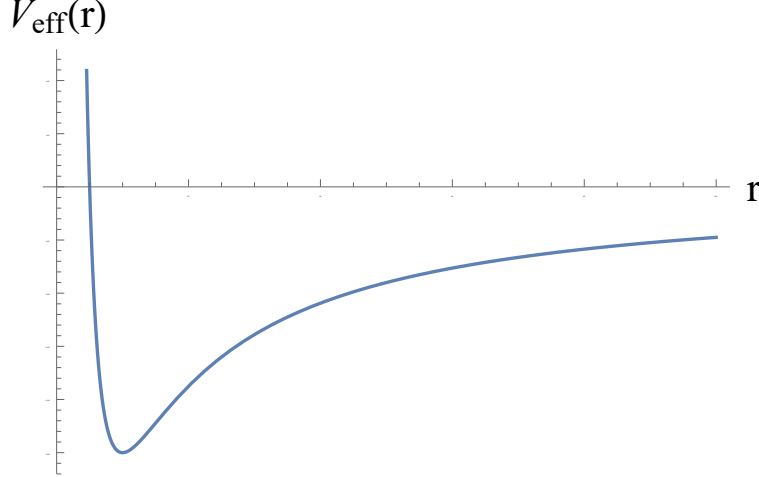


Figure 2: The qualitative behaviour of the effective potential V_{eff} as a function of r .

3.2 Invitation II: the spinning rigid rotor

As our second example of a quantum system at large charge, we consider a free quantum mechanical particle living on a 2-sphere. This example has been already presented in [77]. The Lagrangian of the model reads

$$\mathcal{L} = \frac{I}{2} (\dot{\theta}^2 + \sin^2 \theta \dot{\phi}^2) , \quad (3.8)$$

with I the moment of inertia while the dot denotes the time derivative. By solving the Schrödinger equation, one finds that the states are organized in $SO(3)$ multiplets $|L^2 = l, L_z = m\rangle$, and have energy $E_l = l(l+1)/2I$.¹⁵ As in the previous example, the ground state with fixed m satisfies $l = m$ and has energy

$$E_0(m) = \frac{m(m+1)}{2I} . \quad (3.9)$$

Our goal is to reproduce this result semiclassically as an expansion in $1/m$. To this end, consider the transition amplitude between states with fixed $L_z = m$ which, since L_z and φ are canonically conjugate, we can write as

$$\langle \theta_f, m | e^{-H(\tau_f - \tau_i)} | \theta_i, m \rangle = \frac{1}{2\pi} \int_{\theta, \varphi(\tau_i) = \theta_i, \varphi_i}^{\theta, \varphi(\tau_f) = \theta_f, \varphi_f} \mathcal{D}\theta \mathcal{D}\varphi e^{-\int d\tau \mathcal{L}} e^{-im(\varphi_f - \varphi_i)} d\varphi_i d\varphi_f . \quad (3.10)$$

¹⁵ The energy eigenfunctions are given, as usual, by the spherical harmonics $Y_{lm}(\theta, \varphi)$.

where H is the Hamiltonian and τ the time coordinate. In fact, if we fix L_z to be an integer m , then its wave function is $e^{im\phi}$, while the operator L_z acts as $-i\frac{\partial}{\partial\phi}$.

We can bring the second exponential term in the RHS into the Lagrangian by noting that $\varphi_f - \varphi_i = \int_{\tau_i}^{\tau_f} d\tau \dot{\varphi}$. Then the above amplitude can be computed by means of the modified fixed-charge Lagrangian

$$\mathcal{L}_m = \mathcal{L} + im\dot{\varphi}. \quad (3.11)$$

Taking the limit $T \equiv \tau_f - \tau_i \rightarrow \infty$ amounts to project this matrix element onto the ground state with fixed $L_z = m$, $|m\rangle$.

$$\lim_{T \rightarrow \infty} \langle \theta_f, m | e^{-HT} | \theta_i, m \rangle = \langle \theta_f, m | m \rangle \langle m | \theta_i, m \rangle e^{-E_0(m)T} \left[1 + O(e^{-\Delta E(m)T}) \right], \quad (3.12)$$

where $\Delta E(m)$ is the energy gap of the first excited state with fixed m .

Inspired by the previous example, let us compute the above via a saddle-point expansion around the solution of the corresponding classical system. The equations of motion (EOM) are

$$\ddot{\theta} = \sin \theta \cos \theta \dot{\varphi}^2, \quad I \sin^2 \theta \dot{\varphi} = -im. \quad (3.13)$$

We are free to choose the in and out states as long as they have $L_z = m$ and overlap with the ground state. A convenient choice is given by $\theta_i = \theta_f = \pi/2$, and leads to the following classical solution

$$\theta_s = \frac{\pi}{2}, \quad \varphi_s = -i\frac{m}{I}\tau + \varphi_0, \quad (3.14)$$

where φ_0 is an integration constant. Plugging this solution into the modified Lagrangian \mathcal{L}_m (3.11), we obtain

$$E_0^{(0)}(m) = \frac{1}{T} \int \mathcal{L}_m d\tau = \frac{m^2}{2I}. \quad (3.15)$$

This is the leading order (LO) of the semiclassical expansion. As for the Hydrogen atom, by comparing the above with (3.9), we see that the difference between classical and quantum results vanishes in the limit $m \rightarrow \infty$.

Notice that the integration over φ_0 in the path integral does not affect the computation of the energy levels. On the other hand, it enforces L_z invariance when computing correlators involving

φ [77].

The classical variable conjugate to m is $i\dot{\phi}_s = \frac{m}{I} = \mu$, which can be identified as a chemical potential measuring the response of the system with respect to a change of m . In fact,

$$\frac{\partial E_0^{(0)}(m)}{\partial m} = \frac{m}{I} = \mu . \quad (3.16)$$

To compute the leading quantum correction to the classical result, we parametrize the quantum fluctuations as $\theta = \theta_s + \xi$, $\varphi = \varphi_s + \chi$. Rescaling the time as $\tau \rightarrow \tau/m$ we have

$$\langle \pi/2, m | e^{-HT} | \pi/2, m \rangle = e^{-\frac{m^2}{2I} T} \int \mathcal{D}\xi \mathcal{D}\chi e^{-m \int d\tau (\mathcal{L}^{(2)} + \mathcal{L}^{(\text{int})})} , \quad (3.17)$$

where

$$\mathcal{L}^{(2)} = \frac{I}{2} \left(\dot{\xi}^2 + \dot{\chi}^2 + \frac{1}{I^2} \xi^2 \right) , \quad (3.18)$$

$$\mathcal{L}^{(\text{int})} = \frac{1}{2I} (\sin^2 \xi - \xi^2) - \left(\frac{I}{2} \dot{\chi}^2 - im\dot{\chi} \right) \sin^2 \xi . \quad (3.19)$$

From Eq.(3.17) we see that $1/m$ plays the role of the loop counting parameter. Hence our semiclassical expansion is actually a *large quantum number expansion* in $1/m$, as anticipated. Therefore, we have

$$E_0 = \sum_{n=0}^{n=\infty} E_0^{(n)} = \frac{m^2}{2I} \left(1 + \sum_{n=1}^{n=\infty} a_m m^{-n} \right) . \quad (3.20)$$

We proceed by computing a_1 . This 1-loop contribution arises from the quadratic Lagrangian $\mathcal{L}^{(2)}$ and is given by the corresponding fluctuation functional determinant as

$$\Delta^{(1)} E_0 = \frac{1}{2} \int \frac{d\omega}{2\pi} (\ln(\omega^2 + m^2/I^2) + \ln \omega^2) = \Lambda_{UV} + \frac{m}{2I} . \quad (3.21)$$

We have a regularization scheme-dependent divergent term plus a finite part corresponding to the zero-point energy of the harmonic oscillator ξ . After adding this contribution to the classical result (3.15) we obtain the exact result (3.9). In fact, it can be proved that higher-loops contribution vanishes [77].

3.3 Fixing the charge

The idea suggested in the previous examples is that physical systems with large quantum numbers are amenable to semiclassical treatment. As we will see, this conclusion applies also to relativistic scalar QFTs with global symmetries at large (internal) charge. In general, as most non-trivial classical solutions, the leading trajectory around which we will set up the semiclassical expansion will break both spacetime and internal symmetries.

Consider a conserved Noether current j_μ . The charge fixing constraint is

$$Q = \int d^{d-1}x j_0 = \bar{Q}, \quad (3.22)$$

with \bar{Q} a certain constant. Fixing the time component of the conserved current, which transforms as a d-vector, induces an asymmetry between time and space breaking relativistic invariance.

Consider a relativistic theory with Hamiltonian H and fix the charge Q . The ground state $|0\rangle$ can be found via the standard method of Lagrange multipliers to implement the charge fixing constraint (3.22). We, therefore, consider the modified Hamiltonian

$$\hat{H} = H - \mu Q, \quad (3.23)$$

where the Lagrangian multiplier μ is a non-zero chemical potential. The ground state minimize \hat{H} , i.e.

$$\hat{H}|0\rangle = 0. \quad (3.24)$$

If the symmetry generated by \bar{Q} is also spontaneously broken (for instance, by a non-zero vev generated by the charge fixing), then $|0\rangle$ cannot be an eigenstate of \bar{Q} . Hence (3.23) says that $|0\rangle$ cannot be an eigenstate of H too, implying that we cannot classify the states with the eigenvalues of H but we have to diagonalize \hat{H} . However, to describe the system by using the non-relativistic Hamiltonian \hat{H} is just a, usually convenient, mathematical choice. The underlying system is relativistic and it is H that generates the microscopic time evolution of the operators. On the other hand, the ground state of its fixed charge sectors spontaneously breaks Lorentz invariance via the coupling of the charge to μ , which can be seen as the zeroth-component of an external gauge field.

This point of view can be applied to more general cases. In fact, since the fundamental laws of physics are relativistic, real-world non-relativistic systems can always be seen as states of a relativistic theory that spontaneously break Lorentz invariance. Actually, this can be taken as a *definition* of condensed matter itself, and we can classify condensed matter systems according to the spacetime symmetries they break [118].

Which is the condensed matter phase of a relativistic QFT at large charge?

Consider for simplicity a system with an internal $U(1)$ symmetry generated by Q , i.e. $[Q, H] = 0$. The symmetry breaking pattern which field-theoretically defines the *superfluid phase* is realized when Q is broken and the Poincare group generated by $\{P_0, P_i, J_i, K_i\}$ breaks to $\{\hat{P}_0, P_i, J_i\}$ [77, 118, 119] with

$$\hat{P}_0 = P_0 - \mu Q. \quad (3.25)$$

Here $P_0 = H$ generates time translations, P_i generates space translations, J_i generates rotations, and K_i generates boost. By comparing with Eq.(3.23), we see that a superfluid-like phase arises as a natural situation in QFTs at large charge.

Consider a classical $U(1)$ -invariant scalar theory with Lagrangian

$$\mathcal{L} = \partial_\mu \varphi^* \partial^\mu \varphi - V(\varphi^* \varphi), \quad (3.26)$$

The $U(1)$ charge is given by Eq.(3.1) with

$$j^\mu = i(\varphi^* \partial^\mu \varphi - \varphi \partial^\mu \varphi^*), \quad \partial_\mu j^\mu = 0. \quad (3.27)$$

The canonical Hamiltonian density is

$$\mathcal{H} = \Pi^* \Pi + \nabla \varphi^* \cdot \nabla \varphi + V(\varphi^* \varphi), \quad (3.28)$$

with $\Pi = \partial_0 \varphi$ the momentum canonically conjugate to φ . We can rewrite the charge density in terms of Π as

$$\mathcal{Q} = i(\Pi^* \varphi^* - \Pi \varphi). \quad (3.29)$$

As discussed above, the ground state minimizes the fixed-charge Hamiltonian $\hat{\mathcal{H}}$ of Eq.(3.23),

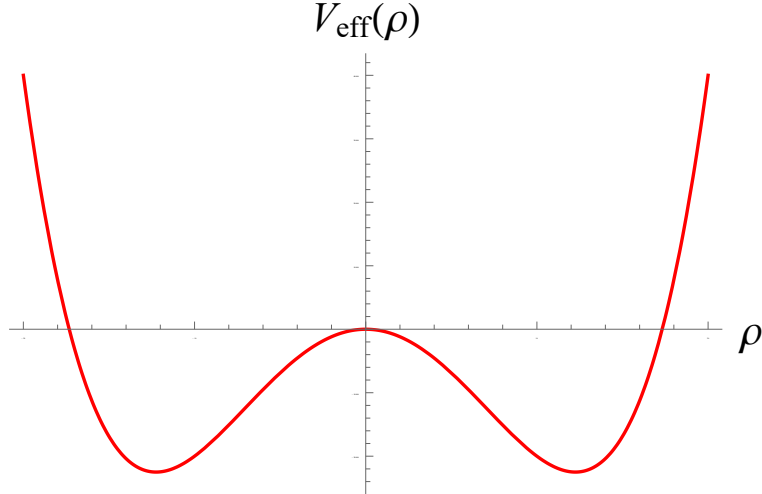


Figure 3: The effective potential $V_{eff}(\rho)$ for the radial mode of the complex field in the broken phase.

which we can rewrite as

$$\hat{\mathcal{H}} = |\Pi - i\mu\varphi^*|^2 + \nabla\varphi^* \cdot \nabla\varphi + V_{eff}(\varphi^*\varphi) . \quad (3.30)$$

We can minimize separately the first two terms and the effective potential $V_{eff} = V - \mu^2\varphi^*\varphi$. As a consequence, the ground state is a spatially homogeneous field configuration minimizing $V_{eff}(\varphi^*\varphi)$. Also, the time dependence is fixed by the first term in the effective Hamiltonian. This is minimized by $\Pi = i\mu\varphi^*$, yielding

$$\varphi(t) = \varphi(0)e^{-i\mu t} . \quad (3.31)$$

For any V bounded from below and that asymptotically grows faster than $\varphi^*\varphi$, the minimum of V_{eff} is not at $\varphi = 0$ for enough large μ , i.e. we have a broken phase. In the broken phase, the radial mode of the φ field, $\varphi^*\varphi = \rho^2$, acquires a non-zero vev which spontaneously breaks the $U(1)$ symmetry. For example, for a quartic potential $V = m^2\rho^2 + \lambda\rho^4$ the qualitative behaviour of the effective potential for ρ is shown in Fig.3. The broken phase realizes the superfluid pattern (3.25).

From the above discussion, it is clear that SSB plays a fundamental role in studying QFTs at large charge. In the next section, we will revisit the Goldstone theorem identifying the generalization relevant for large charge systems.

3.4 Goldstone bosons at large charge

In relativistic theories, SSB is described by the *Goldstone theorem* [120], stating that the spectrum of a theory with spontaneously broken internal symmetries contains as many massless relativistic modes (Goldstone bosons) as the number of broken generators. Furthermore, given that the group \mathcal{G} breaks down to \mathcal{H} , the Goldstone excitations live in the *coset space* \mathcal{G}/\mathcal{H} .

The Goldstone theorem does no longer apply in non-relativistic theories and this leads to a much more variegated connection between SSB and the low-energy spectrum of the theory. QFTs at large charge lies between the relativistic and non-relativistic cases. In fact, according to the discussion in the previous section, we are still dealing with a relativistic QFT, but its fixed charge sector breaks both spacetime and internal symmetries. We will call the relevant generalization of the Goldstone theorem, the *Charged Goldstone theorem*.

Charged Goldstone theorem

Consider a relativistic theory with a global (internal and continuous) symmetry group \mathcal{G} generated by Q_a , $a = 1, \dots, \text{rank}(\mathcal{G})$. Fix a charge $Q_1 = Q$ and introduce the effective Hamiltonian $\hat{H} = H + \mu Q$. We denote as $\hat{\mathcal{G}}$ the subgroup of \mathcal{G} commuting with \hat{H} .

Assume that

1. n generators of \mathcal{G} are spontaneously broken, i.e. there exist n fields (order parameters) ϕ_i such that

$$\det \langle 0[\phi_i(0), Q_a(t)]0 \rangle \neq 0, \quad (3.32)$$

where $|0\rangle$ is the \hat{H} -vacuum. Denote the number of spontaneously broken generators of $\hat{\mathcal{G}}$ as m .

2. Translational invariance is not completely broken.
3. The currents j_a^μ evolve in time according to H , i.e.

$$j_a^\mu(t, \vec{x}) = e^{i(Ht - \vec{P} \cdot \vec{x})} j_a^\mu(0) e^{-i(Ht - \vec{P} \cdot \vec{x})}, \quad (3.33)$$

where \vec{P} generates the spatial translations.

4. \mathcal{G} is a direct product of simple compact Lie groups.

Then

In the spectrum of the theory, there are three types of "generalized" Goldstone bosons:

1. Type I ("relativistic") Goldstone bosons with low-energy dispersion relation $E_k \sim k^{2s+1}$ with s an integer.
2. Type II ("non-relativistic") Goldstone bosons with low-energy dispersion relation $E_k \sim k^{2s}$ with s an integer.
3. Type III ("gapped") Goldstone bosons with gapped dispersion relation and gap fixed non-perturbatively as $E_{k \rightarrow 0} = q_a \mu$ with q_a a group-theoretical calculable factor.

The number of Type-I and type-II Goldstone bosons equals the number of broken generators of $\widehat{\mathcal{G}}$, i.e.

$$n_I + 2n_{II} = m . \quad (3.34)$$

The number of type II modes is

$$n_{II} = \frac{1}{2}p , \quad p = \text{rank}(\widehat{\rho}) , \quad (\widehat{\rho})_{ab} = \langle 0 | \widehat{Q}_a, \widehat{Q}_b | 0 \rangle , \quad (3.35)$$

where $\{\widehat{Q}_a\}$ is the subset of $\{Q_a\}$ which generates $\widehat{\mathcal{G}}$.

The number of type III modes is

$$n_{III} = \frac{1}{2}(\text{rank}(\rho) - p) , \quad (\rho)_{ab} = \langle 0 | Q_a, Q_b | 0 \rangle . \quad (3.36)$$

Part of this result, i.e. $n_I + 2n_{II} \geq m$, has been proved by H. B. Nielsen and S. Chadha in their classical paper [121]. This result has been later improved in [122–124] till the equality sign has been finally proven years later by H. Watanabe and H. Murayama in [125] following Leutwyler's works [126, 127]. These works implicitly assumed that the Hamiltonian governing the time evolution was \widehat{H} and not H . Then the existence of gapped modes with symmetry-controlled dynamics

in theories with SSB, i.e. Type III Goldstone bosons, has been not pointed out till the work of A. Nicolis and F. Piazza [128], which explained the necessary condition for their presence in the spectrum. The final result about the counting of Type III modes has been given in [129].

Type I modes are the usual Goldstone bosons appearing in the relativistic Goldstone theorem at zero charge. According to the charged Goldstone theorem, Type II bosons appear when two broken generators Q_a, Q_b satisfy $\langle 0[Q_a, Q_b]0 \rangle \neq 0$. In such a case, the corresponding Goldstone bosons become canonically conjugate variables effectively reducing the number of degrees of freedom. This is the reason why they count double with respect to the number of broken generators of $\widehat{\mathcal{G}}$. [123]. Finally, Type III modes appear when the broken generators do not commute with the modified Hamiltonian \widehat{H} . From the point of view of the latter, the chemical potential acts as an explicitly symmetry breaking term that leads to a mass proportional to μ . A partial proof of the theorem is given in App. A.

3.5 The RG flow at large charge

In this section, we illustrate how fixing the charge affects the RG flow by a toy-model analysis. To this end, we consider a $U(1)$ massless scalar theory in $d < 4$ dimensions. In particular, following [10], we will show how fixing the charge introduces a scale in the CFT and how the infrared physics of the fixed charge sectors of the theory is described by an approximately scale-invariant action.

We take the UV Lagrangian of the theory to be

$$\mathcal{L}_{UV} = \partial \bar{\varphi} \partial \varphi - \frac{\lambda}{4} (\bar{\varphi} \varphi)^2. \quad (3.37)$$

For $d < 4$, this model flows to an infrared Wilson Fisher (WF) fixed point which, in $d = 3$, is strongly-coupled and defines the XY universality class. By virtue of the Noether theorem, the $U(1)$ symmetry implies the existence of a conserved charge Q given by (3.1) with the Noether current given by Eq.(3.27). We consider this theory as living on $\mathbb{R} \times \Sigma$, where Σ is an arbitrary compact homogeneous two-dimensional manifold with volume V . One can derive the commutation relation

$$[Q, \varphi] = \varphi, \quad (3.38)$$

from canonical commutation relations for the field operator φ . This equation says that the $U(1)$ charge of φ is $+1$. Then the operator $\varphi^{\bar{Q}}$ (\bar{Q} is a positive integer) has $U(1)$ charge \bar{Q} . Besides the normalization of the $U(1)$ charge, which can be changed by multiplication by a nonzero real number the charge of the operators of the theory will be an integer multiple of the charge of φ , as long as we can write them as a linear combination of products of φ and its derivatives (non-integer powers of fields and their derivatives are ill-defined). This illustrates the important feature that the charge is discretized for well-defined local operators of the theory, regardless of the normalization convention.

We consider polar coordinates for the field:

$$\varphi = \frac{\rho}{\sqrt{2}} e^{i\chi} , \quad \bar{\varphi} = \frac{\rho}{\sqrt{2}} e^{-i\chi} . \quad (3.39)$$

and the Lagrangian becomes

$$\mathcal{L}_{UV} = \frac{1}{2}(\partial\rho)^2 + \frac{1}{2}\rho^2(\partial\chi)^2 - \frac{\lambda}{16}\rho^4 . \quad (3.40)$$

Following [10], we consider a toy-model RG evolution where we truncate the exact Wilsonian RG flow to the flow for the quartic coupling λ , neglecting all other operators. By integrating out modes and lowering the cutoff Λ we generate the RG evolution of the quartic coupling $\lambda(\Lambda)$. Furthermore, we *assume* that the theory flows to an attractive FP in the infrared. We can define a dimensionless coupling $\hat{\lambda}$ as $\lambda = \Lambda^{4-d}\hat{\lambda}(\Lambda)$. Essentially, the coupling defines the characteristic scale of the system. Then when we start flowing towards the infrared, the first scale we meet is fixed by λ as

$$\Lambda_{UV} = \lambda^{\frac{1}{4-d}} , \quad (3.41)$$

and the quantum corrections to the free theory for processes at energy Λ are suppressed as $\frac{\Lambda}{\Lambda_{UV}}$. Then at $\Lambda = \Lambda_{UV}$, the quantum corrections to the coupling are of the same order of the coupling itself, and λ is quickly attracted by the FP. Then, below Λ_{UV} , λ takes its fixed point value $\hat{\lambda} = \lambda^*$ and we have

$$\frac{\lambda(\Lambda)}{\Lambda^{4-d}} = \lambda^* , \quad \Lambda \ll \Lambda_{UV} . \quad (3.42)$$

We now fix the charge as $Q = \bar{Q}$ where \bar{Q} is a certain fixed number. Alike the Hydrogen atom studied in Sec.3.1, this operation produces a centrifugal barrier in the effective potential for the radial mode. This is the effective potential depicted in Fig.3 and results in a non-zero vev for ρ .

Furthermore, by considering the classical EOM and the charge-fixing constraint, it can be easily shown that the field $\partial\chi$ gets a vev too. The latter can be identified with the chemical potential μ canonically conjugate to Q , in full analogy with the rigid spinning rotor of Sec.3.2. Then, we have

$$\rho(x) = v + r(x) , \quad \langle \rho(x) \rangle = v , \quad \langle \partial\chi(x) \rangle = \mu . \quad (3.43)$$

Let us have a look at the symmetry breaking pattern induced by the charge fixing. The starting theory possesses conformal symmetry plus a global $U(1)$ symmetry. However, the ground state spontaneously breaks boosts, time-translations, and the global symmetry, resulting in

$$SO(d, 2) \times U(1) \rightarrow SO(d) \times D \times U(1) \sim SO(d) \times D' , \quad (3.44)$$

where $D' = D + \mu Q$. As expected, the large charge sector of the theory is in a superfluid phase. The charged Goldstone theorem predicts the existence of a single type I Goldstone mode which can be identified with the angular mode. In condensed matter language this mode is called the *superfluid phonon*. In other words, the Goldstone theorem implies that the field $\partial\chi$ remains free and massless in the infrared.

On the other hand, since there is a potential term for ρ , we expect its fluctuations $r(x)$ to be gapped, and thus we can decouple them from the RG flow below their gap. In fact, by expanding the potential term $\frac{\lambda}{16}(v + r)^4$, we can immediately read off the squared mass of the r field as

$$m_r^2 = \frac{3}{8}\lambda v^2 . \quad (3.45)$$

This is the next scale we encounter as we flow to the IR. Below m_r , r decouples from the RG flow and its contributions to the running of the quartic coupling are suppressed by positive powers

of Λ/m_r . As a consequence, the coupling $\lambda(\Lambda)$ freezes and takes the value

$$\lambda(m_r) = \lambda^* m_r^{4-d} = \left(\left(\frac{3}{8} v^2 \right)^{4-d} \lambda^{*2} \right)^{1/(d-2)}. \quad (3.46)$$

implying

$$m_r = \left(\frac{3}{8} \lambda^* v^2 \right)^{1/(d-2)}. \quad (3.47)$$

Plugging the above results into the effective Lagrangian \mathcal{L}_Λ , we obtain

$$\mathcal{L}_\Lambda = \frac{v^2}{2} \partial_\mu \chi \partial^\mu \chi - \left(\frac{3}{8} \lambda^{*2} \right)^{1/(d-2)} v^{\frac{2d}{d-2}} + \mathcal{O} \left(\frac{\Lambda}{v^{\frac{2}{d-2}}} \right). \quad (3.48)$$

Then, the infrared effective action is approximately (classically) scale-invariant up to (quantum) corrections suppressed by $\Lambda/v^{2/(d-1)}$. Of course, the full theory is still conformally invariant, but in its charged sectors conformal invariance is spontaneously broken by the vev of the radial mode $\langle \rho \rangle = v$.

Since the χ field is shifted by a constant under $U(1)$ transformation only its derivative is physical. Then, to analyze the IR dynamics of the χ field, it is useful to introduce a new scalar d.o.f. as $B = (\partial_\mu \chi \partial^\mu \chi)^{1/2}$ which satisfies $\langle B \rangle = \mu$. In the IR μ is related to v by

$$\mu^2 = \frac{2d}{d-2} \left(\frac{3}{8} \lambda^{*2} \right)^{\frac{1}{d-2}} v^{\frac{4}{d-2}}, \quad (3.49)$$

while they are both related to the charge density $\frac{Q}{V}$ by¹⁶

$$v = 6^{\frac{d-4}{4(d-1)}} \left(\frac{d-2}{d} \right)^{\frac{d-2}{4(d-1)}} (2\lambda^*)^{-\frac{1}{2(d-1)}} \left(\frac{Q}{V} \right)^{\frac{d-2}{2(d-1)}}, \quad (3.50)$$

$$\mu = 6^{\frac{4-d}{2(d-1)}} \left(\frac{d}{d-2} \right)^{\frac{d-2}{2(d-1)}} \left(2\lambda^* \frac{Q}{V} \right)^{\frac{1}{d-1}}. \quad (3.51)$$

In the spirit of effective field theory, we can integrate out the radial mode ρ which does not participate in the IR dynamics. In practice, this is too cumbersome to be done without resorting to

¹⁶ Since the underlying theory is conformal, Eq.(3.50) follows directly from dimensional analysis alone by noting that ρ , μ , and v have mass dimension $[\rho] = d-1$, $[\mu] = 1$, and $[v] = (d-2)/2$, respectively.

approximations. However, to leading order in the saddle-point approximation, we can simply eliminate it via its EOM, obtaining

$$\mathcal{L}_{\text{EFT}}(\chi) = c_1 B^d + \dots = c_1 (\partial_\mu \chi \partial^\mu \chi)^{\frac{d}{2}} + \dots , \quad (3.52)$$

with c_1 a dimensionless constant. This Lagrangian is both scale and Weyl invariant. Analogously, higher-order terms can be obtained in the usual EFT spirit via dimensional analysis and symmetry constraints. However, the novelty is that we can now organize the terms appearing in the EFT action for the B field by analyzing their \bar{Q} -scaling which acts as a useful organizing principle. In fact, in the large charge regime, we can consistently truncate the effective action retaining only terms with a positive \bar{Q} -scaling.

Independently from the details of the construction of the EFT, it will have the same structure of Eq.(3.48) i.e. it will contain a scale-invariant part, plus quantum corrections which are controlled by $\Lambda/m_r \approx \Lambda/\langle B \rangle = \Lambda/\mu$

$$\mathcal{L}_\Lambda(B) = \mathcal{L}_{cl}(B) + \sum_{\Delta < d} \Lambda^{d-\Delta} \mathcal{L}_q^{(\Delta)}(B) , \quad \Lambda \ll \mu , \quad (3.53)$$

where Δ is the dimension of the corresponding operators. Notice that the upper limit $\Delta < d$ in the above sum does not imply a finite number of terms in the effective action since in general B can appear at the denominator.

Fixing the charge we introduced a new scale in the theory, which controls the low-energy physics when the following hierarchy is realized

$$\begin{array}{ccccccc} \Lambda & \ll & m_r \sim \nu^{\frac{2}{d-2}} \sim \mu \sim \rho^{\frac{1}{d-1}} & \ll & \Lambda_{UV} = \lambda^{1/(4-d)} \\ \downarrow & & \downarrow & & \downarrow \\ \text{Scale-invariant EFT} & & \rho\text{-fluctuations are frozen} & & \lambda \text{ is frozen} \\ \text{for } B & & & & & & \end{array}$$

Furthermore, if we work on a compact curved manifold with a characteristic length scale R as we will do later, the EFT is well-defined only on length scales that are $\ll R$, with R acting as an IR

cutoff. Then the above hierarchy becomes

$$\frac{1}{R} \ll \Lambda \ll \frac{\bar{Q}^{\frac{1}{d-1}}}{R} \ll \Lambda_{UV} , \quad (3.54)$$

and can be satisfied only if the charge is large i.e. $\bar{Q} \gg 1$. The condition of being at the fixed point fixes entirely the terms appearing in the quantum part of the effective Lagrangian $\mathcal{L}_q^{(\Delta)}(B)$ in terms of the ones in $\mathcal{L}_{cl}(B)$ as

$$\Lambda \frac{\delta \mathcal{L}_\Lambda}{\delta \Lambda} = \sum_{\Delta < d} (\Delta - d - 2) \Lambda^{d-\Delta} \mathcal{L}_q^{(\Delta)} , \quad (3.55)$$

where the LHS has to be interpreted as the result of integrating out an infinitesimal shell of momenta. Besides being calculable, the cutoff-dependent terms are, in general, scheme-dependent and their physical role in the present context is solely to enforce conformal invariance at the quantum level.

In the EFT (and CFT) spirit, we now forget about the microscopic Lagrangian description (3.37) and consider a generic d -dimensional $U(1)$ -invariant scalar CFT in its superfluid large charge phase. It is convenient to work on a cylinder of unit radius $\mathcal{R} \times S^{d-1}$ and switch to Euclidean signature. The key observation is that the modified metric $\hat{g}_{\mu\nu} = g_{\mu\nu} B^2$, where $g_{\mu\nu}$ is the cylinder metric and B is now defined as $B = (-\partial_\nu \chi g^{\mu\nu} \partial_\mu \chi)^{1/2}$, is invariant under Weyl transformations. The invariant operators entering the EFT action can, therefore, be built out of B , $\hat{g}_{\mu\nu}$ and the covariant derivative \widehat{D}_μ consistent with $\hat{g}_{\mu\nu}$. The first terms of the effective action read

$$\begin{aligned} S_{EFT}(\chi) &= c_1 \int d^d x \sqrt{g} B^d + c_2 \int d^d x \sqrt{g} B^d \left\{ \frac{\mathcal{R}}{B^2} + (d-1)(d-2) \frac{\widehat{(D_\mu B)^2}}{B^4} \right\} \\ &+ c_3 \int d^d x \sqrt{g} B^d \left\{ \mathcal{R}_{\mu\nu} \frac{\partial^\mu \chi \partial^\nu \chi}{B^4} + \dots \right\} + \mathcal{O}\left(\bar{Q}^{\frac{d-4}{d-1}}\right) . \end{aligned} \quad (3.56)$$

where \mathcal{R} and $\mathcal{R}_{\mu\nu}$ are, respectively, the Ricci scalar and Ricci tensor of S^{d-1} .

The leading term of the effective action is given by Eq.(3.52) and scales as $\bar{Q}^{\frac{d}{d-1}}$, while the remaining term scales as $\bar{Q}^{\frac{d-2}{d-1}}$. By organizing the EFT operators according to their \bar{Q} -scaling as done above, we can use the action (3.56) to compute CFT data in a well-defined $\frac{1}{\bar{Q}}$ expansion. At every order in the large charge expansion, we have only a finite number of terms in the effective

action, and the predictions are, therefore, given in terms of a *finite* number of unknown coefficients c_i . The latter can be fixed by experiments or computed with Monte Carlo methods.

A quantity which is particularly easy to obtain in this framework is the ground state energy on the unit-cylinder $E_{\bar{Q}}$ which, according to Eq.(2.30), delivers the scaling dimension $\Delta_{\bar{Q}}$ of the charge \bar{Q} -operator with the *minimal scaling dimension* (MSD). This is the part of the CFT data in which we will be mainly interested in the rest of this thesis, and that is usually computed in the large charge literature.

$E_{\bar{Q}}$ can be calculated by considering the expectation value of the evolution operator e^{HT} (with H the Hamiltonian and $T = \tau_f - \tau_i$) in an arbitrary state $|\bar{Q}\rangle$ with fixed charge \bar{Q} and then taking the limit $T \rightarrow \infty$ to project out the ground state from it. That is

$$\langle \bar{Q} | e^{-HT} | \bar{Q} \rangle_{T \rightarrow \infty} = \tilde{\mathcal{N}} e^{-E_{\bar{Q}} T} = \tilde{\mathcal{N}} e^{-\Delta_{\bar{Q}} T}. \quad (3.57)$$

Notice that we only require $|\bar{Q}\rangle$ to have a non-zero overlap with the lowest-lying state in the fixed charge sector. Then once we insert a complete set of energy eigenstates in the left-hand side (LHS) of the above equation, only the contribution of the lowest energy state survives, with a prefactor $\tilde{\mathcal{N}}$ that is independent of T but depends on the overlap between the states. Therefore, we may always extract the ground state energy from the T -dependent part of the expectation value. Eq.(3.57) is the CFT analogous of Eq.(3.12) for the rigid rotor and can be computed semiclassically by using the effective action Eq.(3.56). The result reads [10, 66]

$$\Delta_{\bar{Q}} = \bar{Q}^{\frac{d}{d-1}} \left[\alpha_1 + \alpha_2 \bar{Q}^{\frac{-2}{d-1}} + \alpha_3 \bar{Q}^{\frac{-4}{d-1}} + \dots \right] + \bar{Q}^0 \left[\beta_0 + \beta_1 \bar{Q}^{\frac{-2}{d-1}} + \dots \right] + \dots. \quad (3.58)$$

The terms in the first square bracket come from the leading (classical) order in the semiclassical expansion. The α coefficients are combinations of the c_i in (3.56). For instance

$$\alpha_1 = -\frac{c_1(d-1)\Omega_{d-1}}{(-c_1 d \Omega_{d-1})^{\frac{d}{d-1}}}, \quad \alpha_2 = \frac{c_2(d-1)(d-2)\Omega_{d-1}}{(-c_1 d \Omega_{d-1})^{\frac{d-2}{d-1}}}, \quad (3.59)$$

with Ω_{d-1} the solid angle in d dimensions.

The terms in the second square bracket in (3.58) represent instead the 1-loop quantum correction

to the classical result. It can be shown that it is given by the sum of zero-point phonon energies as

$$\frac{1}{2} \sum_{\ell} n_{\ell} \omega_{\ell} = \beta_0 + \beta_1 \bar{Q}^{-\frac{2}{d-1}} + \dots . \quad (3.60)$$

where

$$n_{\ell} = \frac{(2\ell+d-2)\Gamma(\ell+d-2)}{\Gamma(\ell+1)\Gamma(d-1)} , \quad (3.61)$$

is the multiplicity of the eigenvalues of the Laplacian on S^{d-1} , J_{ℓ} , and

$$\omega_{\ell} = c_s J_{\ell} + \mathcal{O}\left(\frac{1}{\bar{Q}^{\frac{2}{d-1}}}\right) , \quad (3.62)$$

is the dispersion relation of the phonon mode. The speed of sound is $c_s = \frac{1}{\sqrt{d-1}}$ and is dictated by tracelessness of the energy-momentum tensor [119]. As a consequence, when d is odd, the order $\mathcal{O}(\bar{Q}^0)$ term in the large charge expansion is calculable and *universal*, in the sense that it does not depend on the microscopic description of the CFT but only on symmetry and d . Two-loop corrections to $\Delta_{\bar{Q}}$ start at order $\mathcal{O}(\bar{Q}^{-\frac{d}{d-1}})$.

For instance, in $d = 3$ we have

$$\Delta_{\bar{Q}}|_{d=3} = \alpha_1 \bar{Q}^{\frac{3}{2}} + \alpha_2 \bar{Q}^{\frac{1}{2}} - 0.0937255 + \mathcal{O}\left(\bar{Q}^{-\frac{1}{2}}\right) . \quad (3.63)$$

The value of the universal coefficient $\beta_0|_{d=3} = -0.0937255$ has been later confirmed via lattice studies [12, 130] and first-principle computations [76]. In an even number of dimensions the large charge EFT predicts instead the existence of a universal $Q^0 \ln Q$ term with calculable coefficient δ_0 , e.g. $\delta_0|_{d=4} = -\frac{1}{48\sqrt{3}}$ [131]. This term arises in the renormalization of β_0 , which features a pole in even dimensions.

More details on the EFT construction in $U(1)$ -invariant CFTs can be found in [10, 66, 77].

3.6 Feynman diagrams at large charge

The EFT approach discussed in the previous section is suited to deal with strongly-coupled systems where there are no small parameters other than $\frac{1}{\bar{Q}}$. On the other hand, when the theory has a perturbative parameter λ , one can bypass the EFT construction and work in the full theory. The

large charge expansion takes the form of a '*t Hooft-like* expansion, where one introduces a '*t Hooft* coupling $\mathcal{A} = \lambda \bar{Q}$, and consider the limit $\lambda \rightarrow 0$ and $\bar{Q} \rightarrow \infty$ with \mathcal{A} fixed. In this and the next section, we focus on the large charge expansion in perturbative theories.

The scaling dimensions can be computed in perturbation theory via the usual diagrammatic loop-expansion. Here, we will show how this expansion can be reorganized when dealing with large charge operators. We will mainly follow the analyses originally presented in [21, 22]. Let's keep considering the scalar $\frac{\lambda}{4}\varphi^4$ theory studied in the previous section. We take the number of spacetime dimensions to be $d = 4 - \varepsilon$, with $\varepsilon > 0$ and consider Euclidean signature. The Lagrangian reads

$$\mathcal{L} = \partial \bar{\varphi}_0 \partial \varphi_0 + \frac{\lambda_0}{4} (\bar{\varphi}_0 \varphi_0)^2. \quad (3.64)$$

In $d = 4$ this theory has trivial (free) infrared physics, whereas, as shown in the previous section, in $2 < d < 4$ this model exhibits an infrared Wilson-Fisher (WF) FP that, when $\varepsilon \ll 1$, is weakly interacting and can be investigated by means of the so-called ε -expansion in powers of ε .

As we saw before, the composite operators $\varphi^{\bar{Q}}$ and $\bar{\varphi}^{\bar{Q}}$ have, respectively, charge $+\bar{Q}$ and $-\bar{Q}$. We work in the minimal subtraction (MS) scheme and renormalize the coupling and the fields according to

$$\lambda_0 = M^\varepsilon \lambda Z_\lambda, \quad \varphi_0^{\bar{Q}} = Z_{\bar{Q}} \varphi^{\bar{Q}}, \quad (3.65)$$

where M is the RG scale. The two-loop beta function of the model reads

$$\frac{\partial \lambda}{\partial \ln M} \equiv \beta(\lambda) = -\varepsilon \lambda + 5 \frac{\lambda^2}{(4\pi)^2} - 15 \frac{\lambda^3}{(4\pi)^4} + \mathcal{O}\left(\frac{\lambda^4}{(4\pi)^6}\right). \quad (3.66)$$

The condition $\beta(\lambda) = 0$ determines the value of the FP coupling as

$$\frac{\lambda^*}{(4\pi)^2} = \frac{1}{5}\varepsilon + \frac{3}{25}\varepsilon^2 + \mathcal{O}(\varepsilon^3). \quad (3.67)$$

In general, the scaling dimensions are scheme-dependent and, therefore, unphysical quantities. However, they become physical at the FP. We write the scaling dimension of $\varphi^{\bar{Q}}$ at the FP as

$$\Delta_{\bar{Q}} = \bar{Q} \left(\frac{d}{2} - 1 \right) + \gamma_{\bar{Q}}(\lambda^*), \quad (3.68)$$

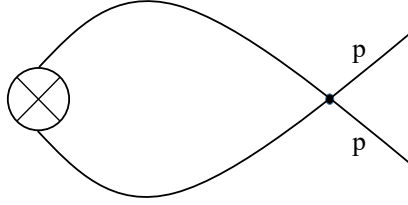


Figure 4: The only Feynman diagram contributing at 1-loop. The crossed vertex represents the operator insertion.

with $\gamma_{\bar{Q}}$ the anomalous dimension of $\varphi^{\bar{Q}}$. $\gamma_{\bar{Q}}$ is related to the renormalization factor $Z_{\bar{Q}}$ by

$$\gamma_{\bar{Q}}(\lambda) = \frac{\partial \ln Z_{\bar{Q}}}{\partial \lambda} \beta(\lambda) . \quad (3.69)$$

We proceed by diagrammatically computing the 1-loop anomalous dimensions. Working in momentum space, we consider the insertion of the $\varphi^{\bar{Q}}$ operator with \bar{Q} incoming momenta p . The relevant correlator is

$$\langle \varphi_0^{\bar{Q}} \bar{\varphi}_0(p) \bar{\varphi}_0(p) \dots \bar{\varphi}_0(p) \rangle = Z_{\bar{Q}} Z_{\varphi}^{\bar{Q}} \langle \varphi^{\bar{Q}} \bar{\varphi}(p) \bar{\varphi}(p) \dots \bar{\varphi}(p) \rangle . \quad (3.70)$$

As usual, we fix $Z_{\bar{Q}}$ and Z_{φ} such that the renormalized correlator $\langle \varphi^{\bar{Q}} \bar{\varphi}(p) \bar{\varphi}(p) \dots \bar{\varphi}(p) \rangle$ is finite. The Feynman rule for the propagator and the quartic vertex are, respectively, $\frac{1}{p^2}$ and $-\lambda$. At one-loop we simply have $Z_{\varphi} = 1$, while the coupling counterterm is $\delta_{\lambda} = \frac{5\lambda^2}{16\pi^2 \epsilon}$ [132]. Furthermore, there is only one diagram to calculate, which is shown in Fig.4, where the crossed vertex represents the insertion of the $\varphi^{\bar{Q}}$ operator. This diagram evaluates to

$$-\frac{\bar{Q}(\bar{Q}-1)}{2} \frac{1}{2} \lambda \int \frac{d^d k}{(2\pi)^d} \frac{1}{k^2} \frac{1}{(k+2p)^2} = -\frac{\lambda}{16\pi^2} \frac{\bar{Q}(\bar{Q}-1)}{4} \left(\frac{2}{\epsilon} + 2 - \gamma + \ln \left(\frac{\pi M^2}{p^2} \right) \right) + \mathcal{O}(\epsilon) . \quad (3.71)$$

The $\frac{\bar{Q}(\bar{Q}-1)}{2}$ factor arises from the combinatorics, being the number of ways we can connect the external momenta to form the diagram by choosing legs among \bar{Q} . Then, from Eq.(3.69), we have

the 1-loop anomalous dimension of $\varphi^{\bar{Q}}$

$$\gamma_{\bar{Q}} = \frac{\lambda}{16\pi^2} \frac{\bar{Q}(\bar{Q}-1)}{2} + \mathcal{O}(\lambda^2) . \quad (3.72)$$

We would like to reorganize our perturbative expansion in powers of \bar{Q} . To this end, we classify the diagrams according to their leading \bar{Q} -scaling and loop order. As for the 1-loop diagram of Fig.4, which scales as $\sim \bar{Q}^2$, the \bar{Q} -scaling of a given diagram arises from the combinatorics. In particular, the combinatorial factor is proportional to $\frac{\bar{Q}!}{(\bar{Q}-k)!}$ with k the number of legs of the inserted $\varphi^{\bar{Q}}$ operator which do undergo interaction, i.e. the number of external legs. At large \bar{Q} , we can use the de Moivre-Stirling formula to obtain

$$\frac{\bar{Q}!}{(\bar{Q}-k)!} \approx \bar{Q}^k . \quad (3.73)$$

Then the leading \bar{Q} -scaling of a diagram is given by k while its loop order is determined by the number of vertices.

At loop order $\ell \ll \bar{Q}$, the diagrams contributing to $Z_{\bar{Q}}$ goes from $\lambda^\ell \bar{Q}^{2\ell}$ to $\lambda^\ell \bar{Q}$. However, it can be shown that, at any loop order, the terms with the highest powers of \bar{Q} exponentiate terms from lower loops [21, 22]. As a consequence, the leading contribution at order k scales like as, $\lambda^\ell \bar{Q}^{\ell+1}$. Hence the perturbative expansion takes the following form

$$\Delta_{\bar{Q}} = \bar{Q} \left(\frac{d}{2} - 1 \right) + \gamma_{\bar{Q}}(\lambda^*) = \bar{Q} \left(\frac{d}{2} - 1 + \sum_{\ell=1} \lambda^{*\ell} P_\ell(\bar{Q}) \right) , \quad (3.74)$$

where we have considered the expression at the fixed point and P_ℓ is a polynomial of degree ℓ . We can reorganize the above as a *large charge expansion* in terms of powers of \bar{Q}

$$\Delta_{\bar{Q}} = \sum_{k=-1} \frac{1}{\bar{Q}^k} \Delta_k(\mathcal{A}^*) , \quad \mathcal{A}^* \equiv \lambda^* \bar{Q} ,$$

(3.75)

where we introduced the (renormalized) 't Hooft coupling \mathcal{A} in order to take consistently the limit $\lambda \rightarrow 0, \bar{Q} \rightarrow \infty$ by keeping \mathcal{A} fixed. In fact, like the original perturbative expansion, the large charge expansion is an asymptotic series formally valid in the limit $\bar{Q} \rightarrow \infty$. Notice that all the functions Δ_k receive contributions from arbitrarily high loop orders of the conventional diagrammatic expansion.

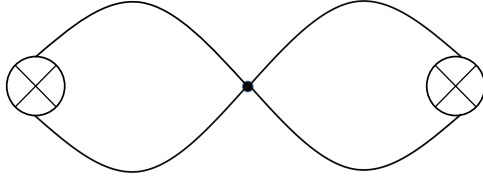


Figure 5: The only diagram which contribute to the two-point function (3.76) at order $\mathcal{O}(\lambda)$.

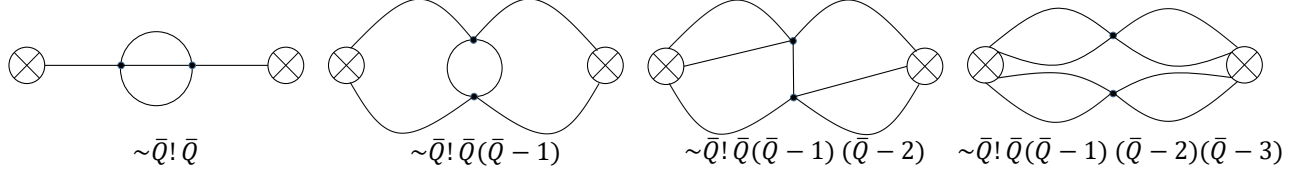


Figure 6: The four topologies contributing at order $O(\lambda^2)$ and their \bar{Q} scaling.

At criticality, $\Delta_{\bar{Q}}$ can also be computed by considering the following two-point function

$$\langle \bar{\varphi}^{\bar{Q}}(x) \varphi^{\bar{Q}}(0) \rangle = \frac{\bar{Q}!}{(4\pi)^{\bar{Q}} |x|^{2\Delta_{\bar{Q}}}}. \quad (3.76)$$

Following the analysis originally presented in [22], we now re-obtain the 1-loop result (3.72) by studying the loop expansion for $\langle \bar{\varphi}^{\bar{Q}}(x) \varphi^{\bar{Q}}(0) \rangle$ in order to make contact with the semiclassical analysis of the next section. Furthermore, we will explicitly show the exponentiation of the diagrams discussed above.

At order $\mathcal{O}(\lambda)$, there is only one diagram to compute, which is displayed in Fig.5.

The authors of [22] dubbed this diagram the 1-loop *Kermit the frog diagram*. We are going to prove that the leading diagrams at every loop order are obvious generalizations of this diagram.

As before, the \bar{Q} dependence is of combinatorial origin and it is given by $\bar{Q}! \frac{\bar{Q}!}{(\bar{Q}-k)!}$ ¹⁷, with k the number of legs of the $\varphi_{\bar{Q}}$ operator which enter in a vertex. For instance, consider the 4 topologies contributing at two-loop, which are shown in Fig.6 together with their \bar{Q} scaling. At large \bar{Q} , the fourth diagram scales as $\bar{Q}! \bar{Q}^4$ and is the dominant 2-loop diagram in this limit.

At the ℓ -loop order, the diagram with the lowest number of legs that do not enter in a vertex is realized when two legs of each vertex come from the insertion of the composite operator $\varphi^{\bar{Q}}$ and the other two legs come from the insertion of $\bar{\varphi}^{\bar{Q}}$, i.e. we have an iteration of the Kermit diagram.

¹⁷ These diagrams have an additional $\bar{Q}!$ factor with respect to those contributing to $Z_{\bar{Q}}$. It comes from the insertion of $\bar{\varphi}^{\bar{Q}}$.

At any loop order, these diagrams are leading in \bar{Q} . In fact, they have combinatorial factor $\bar{Q}!^2/(\bar{Q}-2\ell)!$, and then scale as $\bar{Q}! \lambda^\ell \bar{Q}^{2\ell}$. The correlation function reads

$$\langle \bar{\varphi}^{\bar{Q}}(x) \varphi^{\bar{Q}}(0) \rangle = \bar{Q}! \sum_{\ell=0} (-i\lambda)^\ell K_\ell \frac{1}{4^\ell} \frac{\bar{Q}!}{(\bar{Q}-2\ell)!} \frac{1}{\ell!}, \quad (3.77)$$

where K_ℓ denotes the ℓ -loop Kermit diagram. Let us have a closer look at the various factors appearing in (3.77): we have \bar{Q} legs for every operator insertion and the permutations of the legs give a factor $(\bar{Q}!)^2$. Next, we have to divide over the number of permutations that produces an equivalent diagram. Clearly, we do not change the diagram if we exchange the $(\bar{Q}-2\ell)!$ legs which do not participate the interaction and this gives the factor $\frac{1}{(\bar{Q}-2\ell)!}$. We can also permute pairs of legs inside every loop and this produces the $1/2^\ell$. Finally we have the usual $1/\ell!$ from the Taylor series of the exponential of the interaction term.

In the large \bar{Q} limit the two-point function becomes

$$\langle \bar{\varphi}^{\bar{Q}}(x) \varphi^{\bar{Q}}(0) \rangle = \bar{Q}! \sum_{\ell=0} K_\ell \left(\frac{-i\bar{Q}\mathcal{A}}{4} \right)^\ell \frac{1}{\ell!}, \quad (3.78)$$

where \mathcal{A} is the 't Hooft coupling introduced in Eq.(3.75). To evaluate the Kermit diagram we write it in position space

$$K_\ell = G(0, x)^{n-2\ell} \prod_{i=1}^{\ell} \int d^4 z_i G(0, z_i)^2 G(z_i, x)^2 = G(0, x)^{\bar{Q}} \mathcal{K}^\ell, \quad (3.79)$$

where

$$\mathcal{K} = \frac{1}{G(0, x)^2} \int d^4 z G(0, z)^2 G(z, x)^2. \quad (3.80)$$

with $G(x, y)$ the propagator of φ

$$G(x, y) = \frac{1}{4\pi^2} \frac{1}{(x-y)^2}. \quad (3.81)$$

Then

$$\langle \bar{\varphi}^{\bar{Q}}(x) \varphi^{\bar{Q}}(0) \rangle = \bar{Q}! G(0, x)^{\bar{Q}} \sum_{\ell=0} \left(\frac{-i\bar{Q}\mathcal{A}\mathcal{K}}{4} \right)^\ell \frac{1}{\ell!} = \bar{Q}! G(0, x)^{\bar{Q}} e^{-i\frac{\bar{Q}\mathcal{A}\mathcal{K}}{4}}, \quad (3.82)$$

i.e. the Kermit diagrams exponentiate. Furthermore, we have

$$\bar{Q}! G(0, x)^{\bar{Q}} = \langle \bar{\varphi}^{\bar{Q}}(x) \varphi^{\bar{Q}}(0) \rangle_0 , \quad (3.83)$$

where $\langle \bar{\varphi}^{\bar{Q}}(x) \varphi^{\bar{Q}}(0) \rangle_0$ is the correlation function in the free theory (3.76). Thus

$$\langle \bar{\varphi}^{\bar{Q}}(x) \varphi^{\bar{Q}}(0) \rangle = \frac{\bar{Q}!}{(4\pi)^{\bar{Q}} |x|^{2\Delta_{\bar{Q}}}} e^{-i \frac{\bar{Q}\mathcal{A}\mathcal{K}}{4}} . \quad (3.84)$$

To compute \mathcal{K} we use the propagator (3.81) and obtain

$$G(0, x)^2 \mathcal{K} = -\frac{i}{(4\pi^2)^4} \int d^4 z \frac{1}{z^4 (x-z)^4} . \quad (3.85)$$

To regularize this integral we introduce a cutoff Λ and we use that in $d = 4$ the following identity holds [133]

$$\frac{1}{z^4} = -\frac{1}{4} \partial^2 \left(\frac{\ln z^2 \Lambda^2}{z^2} \right) . \quad (3.86)$$

Using (3.86) into Eq.(3.85), we arrive at

$$\mathcal{K} = -\frac{i}{8\pi^2} \ln(\Lambda^2 x^2) . \quad (3.87)$$

Then

$$\langle \bar{\varphi}^{\bar{Q}}(x) \varphi^{\bar{Q}}(0) \rangle = \frac{\bar{Q}!}{(4\pi)^{\bar{Q}} |x|^{2\Delta_{\bar{Q}}}} \frac{1}{|x|^{\frac{\bar{Q}\mathcal{A}}{16\pi^2}}} = \frac{\bar{Q}!}{(4\pi^2)^{\bar{Q}} |x|^{2(\bar{Q} + \frac{\bar{Q}\mathcal{A}}{32\pi^2})}} . \quad (3.88)$$

Comparing with Eq.(3.76), we have the scaling dimension of $\varphi_{\bar{Q}}$, i.e. we re-obtain Eq.(3.72)

$$\Delta_{\bar{Q}} = \bar{Q} + \lambda \left(\frac{\bar{Q}^2}{32\pi^2} + \mathcal{O}(\bar{Q}) \right) + \mathcal{O}(\lambda^2) . \quad (3.89)$$

Our large charge expansion formula (3.75) shares various similarities with other types of 't Hooft expansion, such as the *large number of flavor* N_f [67–70] and the *large number of color* N_C [20, 71, 72] expansions in gauge theories. The main similarity is that we rewrite perturbation

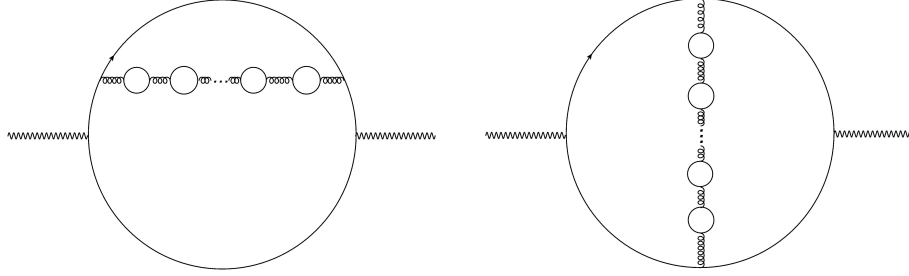


Figure 7: The dominant topology of Feynman diagrams in the large number of flavors limit. *Note: reprinted from [70].*

theory to expand the observables (or other important quantities such as the beta function) as

$$\text{observable} \sim \sum_{\ell=\text{loops}} \lambda^\ell P_\ell(N) = N^j \sum_k \frac{1}{N^k} F_k(\mathcal{A}) , \quad (3.90)$$

where, for simplicity, we have considered a theory with just one coupling λ and j is some number that depends on the particular case under consideration. $N = \{N_c, N_f, \bar{Q}, \dots\}$ is a large parameter. A crucial difference of the large charge expansion is that, while N_c and N_f are parameters of the theory, the charge \bar{Q} is a property of the operators, or equivalently of the states, of a given theory.

In both the large N_f and N_C expansion the Feynman diagrams can be organized according to their N_f (N_C)-scaling. In the large N_f case, since every fermion loop comes along with a N_f factor, the dominant diagrams at every fixed loop order ℓ , are those which maximise the number of fermion loops. These are the diagrams contributing to the function F_1 in Eq.(3.90) and are known in the literature as *bubble diagrams*. An example of how they look is shown in Fig.7. Amazingly, in some interesting cases, such as the MS beta functions in Standard model-like theories, it is possible to completely resum the bubble diagrams and obtain the function F_1 in closed form.

In the large N_C limit, the dominant topology is given by the so-called *planar diagrams*, i.e. diagrams which can be drawn on a plane without superposing the lines. What about the large charge expansion?

Consider the general form of the large charge expansion for $\Delta_{\bar{Q}}$ (3.75). Our previous analysis says that the leading order Δ_{-1} , among the diagrams contributing to $Z_{\bar{Q}}$, resums all the diagrams that at the ℓ -th loop order scale as $\lambda^\ell \bar{Q}^{\ell+1}$. These are the diagrams where the number of external legs minus one is equal to the number of interaction vertices and are shown in Fig.8

To be more precise, Δ_{-1} does not resum all these Feynman diagrams but only the leading

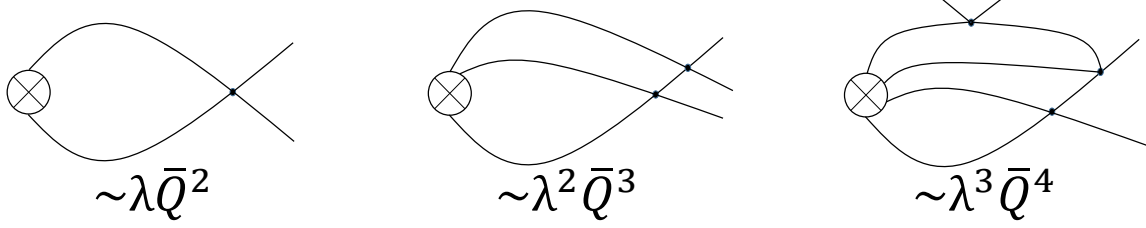


Figure 8: The dominant topology of diagrams in the large charge expansion.

\bar{Q} contribution coming from each of them, i.e. it resums the highest powers of \bar{Q} up to arbitrarily high-loop orders. Computing the full Δ_{-1} directly from the relevant diagrams is likely to be a tough task and has never been performed so far. However, the examples analyzed until now strongly invite us to perform the computation by exploiting the *classicalization* of the physics at large charge to set up a semiclassical approach. This strategy is the content of the next section.

3.7 Path integrals at large charge

In this section, we will show how the scaling dimensions of large charge operators can be calculated via a semiclassical expansion which coincides with the large charge expansion in Eq.(3.75).

To this end, we continue our investigation of the $U(1)$ model in $4 - \varepsilon$ dimension defined in Eq.(3.64). As shown in the previous section, we can extract the scaling dimension of $\varphi^{\bar{Q}}$ from the following two-point function

$$\langle \bar{\varphi}_0^{\bar{Q}}(x_f) \varphi_0^{\bar{Q}}(x_i) \rangle = Z_{\bar{Q}}^2 \langle \bar{\varphi}^{\bar{Q}}(x_f) \varphi^{\bar{Q}}(x_i) \rangle \equiv \frac{\int \mathcal{D}\varphi_0 \mathcal{D}\bar{\varphi}_0 \bar{\varphi}_0^{\bar{Q}}(x_f) \varphi_0^{\bar{Q}}(x_i) \exp[-\int \mathcal{L}]}{\int \mathcal{D}\varphi_0 \mathcal{D}\bar{\varphi}_0 \exp[-\int \mathcal{L}]} . \quad (3.91)$$

The key observation made in [21, 22] is that we can rewrite this path integral as

$$Z_{\bar{Q}}^2 \langle \bar{\varphi}^{\bar{Q}}(x_f) \varphi^{\bar{Q}}(x_i) \rangle = \bar{Q}^{\bar{Q}} \frac{\int \mathcal{D}\varphi_0 \mathcal{D}\bar{\varphi}_0 e^{-\bar{Q}[\int \partial\bar{\varphi}_0 \partial\varphi_0 + \frac{\mathcal{A}_0}{4}(\bar{\varphi}_0 \varphi_0)^2 - (\ln \bar{\varphi}_0(x_f) + \ln \varphi_0(x_i))]} }{\int \mathcal{D}\varphi_0 \mathcal{D}\bar{\varphi}_0 e^{-\bar{Q}[\int \partial\bar{\varphi}_0 \partial\varphi_0 + \frac{\mathcal{A}_0}{4}(\bar{\varphi}_0 \varphi_0)^2]} } , \quad (3.92)$$

where we have rescaled the field as $\varphi \rightarrow \varphi \sqrt{\bar{Q}}$, brought the field insertions into the exponent, and introduced the (bare) 't Hooft coupling $\mathcal{A}_0 \equiv \bar{Q}\lambda_0$. From Eq.(3.92), we see that the charge \bar{Q} takes the role of the loop counting parameter. For large values of the charge, the path integral will

be, therefore, dominated by the extrema of the effective action

$$S_{eff} = \int \partial \bar{\varphi}_0 \partial \varphi_0 + \frac{\mathcal{A}_0}{4} (\bar{\varphi}_0 \varphi_0)^2 - (\ln \bar{\varphi}_0(x_f) + \ln \varphi_0(x_i)) . \quad (3.93)$$

When \bar{Q} is large, we can compute this path integral via a saddle point expansion in $\frac{1}{\bar{Q}}$ which, independently from the details of the classical trajectory, can be written as

$$Z_{\bar{Q}}^2 \langle \bar{\varphi}^{\bar{Q}}(x_f) \varphi^{\bar{Q}}(x_i) \rangle = \bar{Q}! e^{\bar{Q} \Gamma_{-1}(\mathcal{A}_0, x_{fi}) + \Gamma_0(\mathcal{A}_0, x_{fi}) + \frac{1}{\bar{Q}} \Gamma_1(\mathcal{A}_0, x_{fi}) + \dots} , \quad x_{fi} = x_f - x_i . \quad (3.94)$$

where in the exponent on the right hand side, \bar{Q} counts the loop order while the coefficient functions Γ_k depends only on the 't Hooft coupling \mathcal{A}_0 and x_{fi} . We can renormalize Eq.(3.94) by isolating the UV divergence in each term in the exponent

$$\frac{1}{\bar{Q}^k} \Gamma_k(\mathcal{A}_0, x_{fi}) = \frac{1}{\bar{Q}^k} \Gamma_k^{\text{div}}(\mathcal{A}) + \frac{1}{\bar{Q}^k} \Gamma_k^{\text{ren}}(\mathcal{A}, x_{fi}, M) , \quad (3.95)$$

where $\mathcal{A} = \mathcal{A}(M)$ is the renormalized coupling. Thus we can factorize Eq.(3.94) as

$$Z_{\bar{Q}}^2 = \exp \left[\sum_{k=-1}^{\infty} \lambda^k \Gamma_k^{\text{div}}(\mathcal{A}) \right] , \quad (3.96)$$

$$\langle \bar{\varphi}^{\bar{Q}}(x_f) \varphi^{\bar{Q}}(x_i) \rangle = \bar{Q}! \exp \left[\sum_{k=-1}^{\infty} \lambda^k \Gamma_k^{\text{ren}}(\mathcal{A}, x_{fi}, M) \right] . \quad (3.97)$$

Hence the anomalous dimension of the $\varphi^{\bar{Q}}$ operator takes the form (3.75)

$$\gamma_{\bar{Q}} = \bar{Q} \sum_{k=0} \frac{1}{\bar{Q}^k} F_k(\mathcal{A}) , \quad (3.98)$$

and we re-obtain Eq.(3.75)

$$\Delta_{\bar{Q}} = \sum_{k=-1} \frac{1}{\bar{Q}^k} \Delta_k(\mathcal{A}^*) , \quad \mathcal{A}^* \equiv \lambda^* \bar{Q} . \quad (3.99)$$

Now we can identify the coefficients Δ_k of the large charge expansion as the $k+1$ loop correction to the saddle point expansion.

The above analysis is based on general considerations on the form of the semiclassical expansion. To actually compute the coefficients Δ_k , one needs to solve the EOM stemming from the effective action (3.93). This step is, in general, not easy, and different strategies can be considered. For instance, one may solve the EOM perturbatively for small \mathcal{A} . However, beyond the first few orders, the computations become quickly cumbersome and unpractical ¹⁸. Another possibility is to work directly at the fixed point and use the CFT constraints to simplify our task. This is the strategy we will follow in the rest of this thesis in order to compute the scaling dimensions of large charge operators in the $O(N)$ and $U(N) \times U(M)$ scalar CFTs.

¹⁸This approach has been considered in [21–23].

4 CHARGING THE $O(N)$ MODEL

Until now, the discussion has been restricted to quantum mechanical models and abelian CFTs. Here, we start our exploration of the large charge expansion in non-abelian theories. As we shall see, the presence of multiple large quantum numbers leads to interesting new challenges related to the role of the charge configuration in the expansion.

In this chapter, we focus on the time-honoured critical $O(N)$ model in $d = 4 - \varepsilon$ dimensions, which is relevant for the description of phase transitions in many real-worlds three-dimensional condensed matter systems, such as dilute polymer solutions ($N = 0$), Ising magnets ($N = 1$), superfluid helium and easy plan magnets ($N = 2$), isotropic (Heisenberg) magnets ($N = 3$), strongly-correlated electronic systems at half-filling ($N = 4$) [?], and superconductors ($N = 5$) [134], to name a few. Moreover, for $\varepsilon = 0$ and $N = 4$, we recover the Higgs sector of the Standard Model up to gauge and Yukawa interactions. Finally, the $O(4)$ model appears also in the description of the finite-temperature chiral phase transitions in two-flavor QCD [135, 136].

The large charge sector of the three-dimensional $O(N)$ model has been first investigated in [11, 130], by means of the EFT approach discussed in Sec.3.5. Here, we instead conduct a first-principle analysis, based on the microscopic description of the model in $4 - \varepsilon$ dimensions. At the end of this chapter, we will connect the two approaches by computing the Wilson coefficients of the $3d$ large charge EFT in the ε -expansion and comparing with Monte Carlo simulations. A similar approach, directly in $d = 3$ and at LO in the large N expansion, has been previously considered in [137].

Before going into a detailed analysis of the large charge sector of the $O(N)$ model, we start our analysis with some general considerations on the large charge expansion in non-abelian models.

4.1 Charging non-abelian theories

Consider a general scalar d -dimensional CFT with a global symmetry group \mathcal{G} of rank M . The general goal is to efficiently determine correlators involving primary operators carrying large values of the charges $\vec{Q} = (\bar{Q}_1, \dots, \bar{Q}_M)$ associated with the Cartan generators Q_i . On the other hand, in this thesis, we will mainly focus on the more modest task of computing the ground state energy of the CFT on the unit cylinder that, as we saw in Sec.3.5, is equal to the scaling dimension of the

MSD operator with charge \vec{Q} .

The ground state energy $E_{\vec{Q}}$ (at fixed charge \vec{Q}) on the cylinder is given by the non-abelian counterpart of Eq.(3.57). That is

$$\langle \vec{Q} | e^{-HT} | \vec{Q} \rangle \underset{T \rightarrow \infty}{=} \tilde{\mathcal{N}} e^{-E_{\vec{Q}} T} = \tilde{\mathcal{N}} e^{-\Delta_{\vec{Q}} T}. \quad (4.1)$$

where $|\vec{Q}\rangle$ is an arbitrary state with fixed charge \vec{Q} .

As discussed in the previous section, in the large charge limit the path-integral expression for the above matrix element will be dominated by semiclassical trajectories. In particular, in weakly-coupled theories, the semiclassical large charge expansion is a 't Hooft like expansion which in the abelian case takes the form Eq.(3.75), i.e

$$\Delta_{\vec{Q}} = \sum_{k=-1} \frac{1}{\vec{Q}^k} \Delta_k(\mathcal{A}^*), \quad \mathcal{A}^* \equiv \lambda^* \vec{Q}. \quad (4.2)$$

How the non-abelian counterpart of the above equation looks?

First, consider fixing only one of the M charges, e.g. $\vec{Q} = (\bar{Q}_1 = \bar{Q}, 0, 0, \dots, 0)$, in theories with multiple (small) couplings $\lambda_1, \lambda_2, \dots$. In this case, the most natural procedure consists in defining multiple 't Hooft coupling $\mathcal{A}_1 = \bar{Q}\lambda_1, \mathcal{A}_2 = \bar{Q}\lambda_2, \dots$, and thus the large charge expansion for the scaling dimension of the MSD operator with charge \vec{Q} takes the form

$$\Delta_{\vec{Q}} = \sum_{k=-1} \frac{1}{\bar{Q}^k} \Delta_k(\{\mathcal{A}_i^*\}), \quad \mathcal{A}_i^* \equiv \lambda_i^* \bar{Q}. \quad (4.3)$$

When we fix multiple charges, and we take all of them to be large, we can rescale them by the same large parameter \bar{Q} , i.e. $\vec{Q} = \bar{Q}(q_1, q_2, q_3, \dots)$, where the $\{q_i\}$ are order $\mathcal{O}(1)$ parameters which define the *charge configuration*, i.e. the specific quantum number assignment of the MSD operator. Then the large charge expansion takes the following form

$$\Delta_{\vec{Q}} = \sum_{k=-1} \frac{1}{\bar{Q}^k} \Delta_k(\{\mathcal{A}_i^*\}, \{q_i\}), \quad \mathcal{A}_i^* \equiv \lambda_i^* \bar{Q}. \quad (4.4)$$

Similar considerations apply when not all the charges are large, with the order $\mathcal{O}(1)$ charges playing the role of additional quantum numbers. The role of the charge configuration in the large

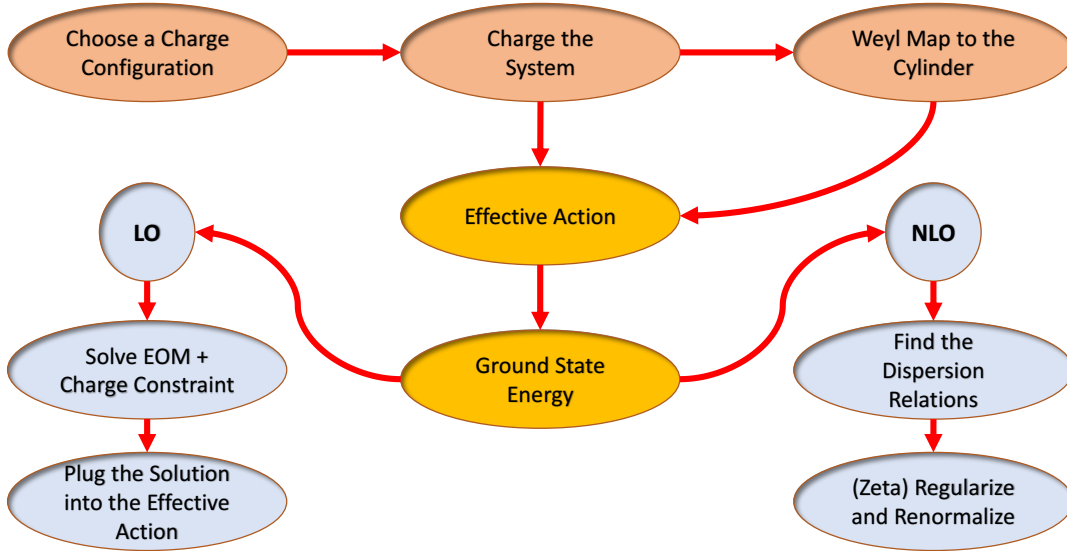


Figure 9: The procedure we will follow to compute the scaling dimensions of large charge MSD operators to NLO in the large charge expansion in non-abelian theories.

charge expansion will be explored in detail in Chap.6.

The practical way to compute the scaling dimension of the MSD operator is through Eq.(4.1). A flowchart of the computational strategy that we will follow in the next chapters is shown in Fig.(9). For a given charge configuration, we will map the theory to the cylinder and impose the charge fixing constraints, after which we are left with an "effective" cylinder action. The latter will be used to semiclassically compute the ground state energy from Eq.(4.1). The leading order of the large charge expansion is obtained by solving the classical system, while the NLO is determined by the dispersion relations of the fluctuation spectrum around the leading trajectory.

An important feature of this approach is that we do *not* fix the full symmetry properties of the MSD operator corresponding to the ground state on the cylinder¹⁹. In fact, in choosing the state \vec{Q} in Eq.(4.1), we fix only the eigenvalues corresponding to a set of Cartan charges. Put it simpler, we fix only the group-theoretical weights (the charge configuration) but not the irreducible representation the MSD operator belongs to. Multiple irreducible representations can share the same weight,

¹⁹This is very different from conventional perturbative methods, where the explicit form of the composite operator is needed as input for the computation of its scaling dimension.

and a given irreducible representation can be realized by different sets of local operators. This is where the Lie algebraic theory cannot tell us more, and we need some dynamical information. This information is contained in the MSD condition. The problem is thus to identify, among all the operators with fixed charge \bar{Q} , the one with the lowest scaling dimension. This is in general not an easy task and, for this reason, the explicit form of the considered MSD operator is often left unspecified in the literature. In weakly-coupled theory, where the anomalous dimensions are small, we can make progress by assuming that the minimal scaling dimension operator has also the minimal classical scaling dimension (MCSD or minimal-CSD). This will be called the *MCSD assumption* and can be taken as our definition of perturbativity. For instance, in the $U(1)$ theory discussed in the previous chapter, the MCSD operator with $U(1)$ -charge \bar{Q} is obviously $\varphi^{\bar{Q}}$. In fact, any additional $(\bar{\varphi}\varphi)$ factor or derivative would necessarily increase the classical scaling dimension. Therefore, at small values of the coupling λ we expect the ground state energy on the cylinder to deliver the scaling dimension of $\varphi^{\bar{Q}}$.

On the other hand, in the strongly-coupled regime, *level crossing* between operators with different MCSD can occur, and the MSD operator might no longer be $\varphi^{\bar{Q}}$. In general, the identification of the MSD operator in strongly-coupled theory is an extremely hard task which implies having already (at least partially) solved the theory.

In the $U(1)$ case, the identification in the weakly-coupled regime is relatively easy since there is only one charge with the charge configuration playing no role. In non-abelian weakly-coupled theories, the situation is more involved. Given a charge configuration, a brute force strategy may consist of listing all the candidates using the MCSD assumption and then compute their scaling dimension in perturbation theory. In absence of particular degeneracies in the 1-loop spectrum of anomalous dimensions, the 1-loop scaling dimensions are enough to identify the MSD operator. However, after all, we are interested in the large charge expansion because we do not want to compute Feynman diagrams. This approach can be improved if employing group-theoretical considerations one can narrow down the list of candidate operators.

As we will show in Chap.6, there are cases when group theory alone uniquely selects the MSD operator. Furthermore, in the same section, we will propose an alternative identification procedure that does not require diagrammatic computations. Notice that, even if the precise form of the MSD operator does not affect the calculation of its scaling dimension, it, however, enters in the

computation of the normalization of the correlator $\tilde{\mathcal{N}}$, and thus of higher-point functions.

We conclude this section with some general considerations about the symmetry breaking pattern induced by the charge-fixing. As discussed before, abelian theories at large charge realize the superfluid pattern (3.25). For non-abelian theories at large charge, a natural situation corresponds to a *generalized superfluid phase* whose definition generalizes Eq.(3.25). This phase occurs when both dilatations D and \mathcal{G} are broken, but at least one linear combination of the generators $D' = D + \mu_i Q_i$ remains unbroken. That is

$$SO(d+1,1) \otimes \mathcal{G} \longrightarrow SO(d) \otimes D' \otimes \mathcal{G}' , \quad (4.5)$$

where \mathcal{G}' is the unbroken subgroup of \mathcal{G} , and the μ_i have the role of i chemical potentials. Since D is the cylinder Hamiltonian H , the generalized superfluid condition can be read also as $\hat{H} = H + \mu_i Q_i$.

4.2 The critical $O(N)$ model in $d = 4 - \varepsilon$ dimensions

In this section, we use the large charge expansion to investigate the critical $O(N)$ vector model in $d = 4 - \varepsilon$ dimensions described below

$$\mathcal{S} = \int d^d x \left(\frac{(\partial \phi_a)^2}{2} + \frac{(4\pi)^2 g_0}{4!} (\phi_a \phi_a)^2 \right) . \quad (4.6)$$

The renormalized coupling g is related to the bare coupling g_0 as

$$g_0 = M^\varepsilon g Z_g , \quad (4.7)$$

with M the RG scale. In dimensional regularization and MS scheme, Z_g can be expanded as a Laurent series in ε poles

$$Z_g(g, \varepsilon) = 1 + \sum_{k=1}^{\infty} \frac{Z_{g,k}(g)}{\varepsilon^k} , \quad (4.8)$$

where every $Z_{g,k}(g)$ is a formal power series in g . The beta function of the coupling g is related to Z_g by

$$\beta(g, \varepsilon) \equiv \mu \frac{\partial g}{\partial \mu} = -\varepsilon g + g^2 \frac{\partial Z_{g,1}(g)}{\partial g} . \quad (4.9)$$

where

$$Z_{g,1}(g) = \frac{g(8+N)}{3} + \mathcal{O}(g^2) . \quad (4.10)$$

In $d = 4 - \varepsilon$ this theory features an infrared WF fixed point at $g^* = g^*(\varepsilon)$. The fixed point value has been computed to 6-loop in [138]. For our analyses, we will make use of the 4-loop result reported below

$$\begin{aligned} g^*(\varepsilon) = & \frac{3\varepsilon}{8+N} + \frac{9(3N+14)\varepsilon^2}{(8+N)^3} + \frac{\varepsilon^3}{(8+N)^5} \left[\frac{3}{8} (4544 + 1760N + 110N^2 - 33N^3) \right. \\ & \left. - 36 \zeta(3)(N+8)(5N+22) \right] + \frac{\varepsilon^4}{(N+8)^7} \left[120 (2N^2 + 55N + 186) (N+8)^2 \zeta(5) \right. \\ & + 6 (63N^3 - 82N^2 - 3796N - 9064) (N+8) \zeta(3) + \frac{1}{16} \left(-5N^5 - 2670N^4 - 5584N^3 \right. \\ & \left. + 52784N^2 + 309312M + 529792 \right) - \frac{1}{5} \pi^4 (5N+22)(N+8)^3 \right] + \mathcal{O}(\varepsilon^5) . \end{aligned} \quad (4.11)$$

In what follows, we will be interested in composite operators with no derivatives and transforming according to the traceless symmetric $O(N)$ representations with $O(N)$ -spin \bar{Q} . These representations can be depicted as Young tableaux with \bar{Q} boxes in a single row

$$\underbrace{\square \square \square \square \dots \square}_{\bar{Q}} , \quad (4.12)$$

while the operators can be written as

$$T_{p,\bar{Q}} = (\phi^2)^p t_{\bar{Q}}^{a_1 \dots a_{\bar{Q}}}(\phi_a) , \quad (4.13)$$

where $t_{\bar{Q}}^{a_1 \dots a_{\bar{Q}}}$ is a homogeneous polynomial of degree \bar{Q} in the ϕ_a that is traceless and symmetric in the indices while p counts the ϕ^2 factors. The CSD of $T_{p,\bar{Q}}$ is $\bar{Q} + 2p$. The explicit form of the first four $t_{\bar{Q}}^{a_1 \dots a_{\bar{Q}}}$ polynomials reads

$$t_1^a(\phi) = \phi^a , \quad (4.14)$$

$$t_2^{ab}(\phi) = \phi^a \phi^b - \frac{1}{N} \delta^{ab} \phi^2 , \quad (4.15)$$

$$t_3^{abc}(\phi) = \phi^a \phi^b \phi^c - \frac{\phi^2}{N+2} \left(\phi^a \delta^{bc} + \phi^b \delta^{ac} + \phi^c \delta^{ab} \right), \quad (4.16)$$

$$\begin{aligned} t_4^{abcd}(\phi) = & \phi^a \phi^b \phi^c \phi^d - \frac{1}{N+4} \phi^2 \left(\delta^{ab} \phi^c \phi^d + \delta^{ac} \phi^b \phi^d + \delta^{ad} \phi^b \phi^c + \delta^{bc} \phi^a \phi^d + \delta^{bd} \phi^a \phi^c + \delta^{cd} \phi^a \phi^b \right) \\ & + \frac{1}{(N+2)(N+4)} (\phi^2)^2 \left(\delta^{ab} \delta^{cd} + \delta^{ac} \delta^{bd} + \delta^{ad} \delta^{bc} \right). \end{aligned} \quad (4.17)$$

Physically, the $T_{p,\bar{Q}}$ operators represent anisotropic perturbations in $O(N)$ -invariant critical systems. Their scaling dimensions define a family of *crossover (critical) exponents* controlling the capacity of the perturbations to influence and change the critical behavior. Crossover exponents are relevant for a variety of condensed matter systems, such as density-wave systems [139, 140] and magnets with a cubic crystal structure [85, 141]. These crossover exponents determine also the behavior near bicritical points at the intersection of two transition lines with different $O(N)$ symmetries [142, 143]. This multicritical behavior appears in the $SO(5)$ theory of superconductivity [134, 144].

Below, we report the known results for $T_{0,1}$ [138, 145], $T_{0,2}$ [146], and $T_{0,4}$ [144]²⁰ up to 4-loops

$$\begin{aligned} \Delta_{T_{0,1}} = \Delta_\phi = & 1 - \frac{\epsilon}{2} + \frac{(N+2)\epsilon^2}{4(N+8)^2} \left(1 + \frac{\epsilon}{4(N+8)^2} [-N^2 + 56N + 272] - \frac{\epsilon^2}{16(N+8)^4} \right. \\ & \times [5N^4 + 230N^3 - 1124N^2 - 17920N - 46144 + 384\zeta(3)(N+8)(5N+22)] \left. \right) + \mathcal{O}(\epsilon^5), \end{aligned} \quad (4.18)$$

$$\begin{aligned} \Delta_{T_{0,2}} = & 2 - \epsilon + \frac{2}{N+8} \epsilon + \frac{(-N^2 + 18N + 88)}{2(N+8)^3} \epsilon^2 + \frac{1}{8(N+8)^5} \\ & \times [-5N^4 - 134N^3 - 960N^2\zeta(3) + 56N^2 - 11904N\zeta(3) + 4192N - 33792\zeta(3) + 10624] \epsilon^3 \\ & + \frac{1}{160(N+8)^7} \left[80N^6\zeta(3) - 65N^6 + 1920N^5\zeta(3) - 4100N^5 + 25600N^4\zeta(5) + 65280N^4\zeta(3) \right. \\ & - 160\pi^4N^4 - 79720N^4 + 1113600N^3\zeta(5) + 592000N^3\zeta(3) - 4544\pi^4N^3 - 403960N^3 \\ & + 15283200N^2\zeta(5) + 138240N^2\zeta(3) - 47616\pi^4N^2 - 533920N^2 + 83148800N\zeta(5) \\ & \left. - 11719680N\zeta(3) - 217088\pi^4N + 1275520N + 152371200\zeta(5) - 24944640\zeta(3) \right] \end{aligned}$$

²⁰There is a misprint in equation (3.14) of [144]: the sign of the first term in $c_{4,4}$ is wrong.

$$-360448\pi^4 + 3571200] \varepsilon^4 + \mathcal{O}(\varepsilon^5) , \quad (4.19)$$

$$\begin{aligned} \Delta_{T_{0,4}} = & 4 - 2\varepsilon + \frac{(N+20)}{N+8}\varepsilon + \frac{(-5N^2 - 14N - 152)}{(N+8)^3}\varepsilon^2 - \frac{1}{4(N+8)^5} \\ & \times [13N^4 + 398N^3 + 1464N^2 - 192(N+8)(N(N+7) + 46)\zeta(3) + 1568N - 17024]\varepsilon^3 \\ & + \left(-\frac{120(13N^2 + 130N + 712)\zeta(5)}{(N+8)^5} + \frac{2\pi^4(N^2 + 7N + 46)}{5(N+8)^4} \right. \\ & \left. - \frac{29N^6 + 1516N^5 + 27272N^4 + 112856N^3 + 223328N^2 + 402304N + 2995712}{16(N+8)^7} \right. \\ & \left. + \frac{3(N^5 - 8N^4 + 256N^3 + 1592N^2 + 1664N - 21568)\zeta(3)}{(N+8)^6} \right) \varepsilon^4 + \mathcal{O}(\varepsilon^5) . \end{aligned} \quad (4.20)$$

The scaling dimension of $T_{0,\bar{Q}}$ with arbitrary \bar{Q} is known to order $\mathcal{O}(\varepsilon^2)$ [147]

$$\begin{aligned} \Delta_{T_{0,\bar{Q}}} \equiv \Delta_{\bar{Q}} = & \bar{Q} + \left(-\frac{\bar{Q}}{2} + \frac{\bar{Q}(\bar{Q}-1)}{8+N} \right) \varepsilon - \left[\frac{184 + N(14 - 3N)}{4(8+N)^3} \bar{Q} \right. \\ & \left. + \frac{(N-22)(N+6)}{2(8+N)^3} \bar{Q}^2 + \frac{2}{(8+N)^2} \bar{Q}^3 \right] \varepsilon^2 + \mathcal{O}(\varepsilon^3) . \end{aligned} \quad (4.21)$$

There is also an old $\mathcal{O}(\varepsilon^3)$ result [148], but we found out that it disagrees with the known literature for the cases $\bar{Q} = 2, 3, 4$ considered above. In the next section, we will compute $\Delta_{\bar{Q}}$ to NLO in the large charge expansion. Moreover, we will use our results to obtain $\Delta_{\bar{Q}}$ to order $\mathcal{O}(\varepsilon^4)$.

4.3 Charging the system

The conserved Noether current associated with the global $O(N)$ symmetry transforms in the adjoint representation of $O(N)$, and it is given by

$$(j^\mu)_{ab} = (\phi_a \partial^\mu \phi_b - \phi_b \partial^\mu \phi_a) . \quad (4.22)$$

The corresponding conserved charge is matrix-valued and can be decomposed in terms of the generators of the $O(N)$ algebra T^A

$$\mathcal{Q}_{ab} = \int d^{d-1}x \ (j^0)_{ab} = \sum_A Q_A \left(T^A \right)_{ab} . \quad (4.23)$$

The $O(N)$ group with even (odd) N has rank (i.e. the number of mutually commuting Cartan generators \mathcal{H}_i) $N/2$ ($\frac{N-1}{2}$), which corresponds to the number of "charges" Q_A we can fix. Without loss of generality, we focus on the even- N case, and we fix $k \leq N/2$ charges via k constraints $Q_i = \bar{Q}_i$, where $\{\bar{Q}_i\}$ is a set of fixed constants and $i = 1, \dots, k$. According to the discussion at the beginning of this chapter, we write the charge configuration as

$$\vec{Q} = \bar{Q}(q_1, \dots, q_k) , \quad (4.24)$$

where $\bar{Q} \equiv \sum_{i=1}^k \bar{Q}_i$ is the sum of the charges and $\sum_{i=1}^k \bar{q}_i = 1$. To make explicit the relation between fields and charges, we consider the $SU(N/2) \times U(1)$ subalgebra of $O(N)$ and introduce $N/2$ complex field variables as

$$\varphi_1 = \frac{1}{\sqrt{2}} (\phi_1 + i\phi_2) = \frac{1}{\sqrt{2}} \sigma_1 e^{i\chi_1} , \quad (4.25)$$

$$\varphi_2 = \frac{1}{\sqrt{2}} (\phi_3 + i\phi_4) = \frac{1}{\sqrt{2}} \sigma_2 e^{i\chi_2} , \quad (4.26)$$

$$\varphi_3 = \dots . \quad (4.27)$$

Then φ_i has charge $Q_i = +1$, while $\bar{\varphi}_i$ has Q_i charge -1 . In fact, we can use an $O(N)$ rotation to write

$$\sum_{i=1}^k Q_i \mathcal{H}^i = \begin{pmatrix} 0 & Q_1 & & & \\ -Q_1 & 0 & & & \\ & & 0 & Q_2 & \\ & & -Q_2 & 0 & \\ & & & & \ddots \end{pmatrix} . \quad (4.28)$$

Then

$$\mathcal{Q}_{2i,2i-1} = \int dx (\bar{\varphi}_i \partial^0 \varphi_i - \varphi_i \partial^0 \bar{\varphi}_i) = \int dx (\sigma_i)^2 \partial^0 \chi_i = Q_i , \quad i = 1, \dots, k , \quad (4.29)$$

and the charges Q_i are canonically conjugated to the angular modes χ_i .

Having fixed the charge, we now focus on the computation of the scaling dimension of the MSD operators with charge \vec{Q} . As we will see in the next section, these operators can be identified as the $T_{0,\vec{Q}}$ anisotropic perturbations.

As anticipated, we work at the Wilson Fisher FP g^* , and we map the theory onto the cylinder, $\mathbb{R}^d \rightarrow \mathbb{R} \times S^{d-1}$. The cylinder action reads

$$\mathcal{S}_{cyl} = \int d^d x \sqrt{g} \left(g_{\mu\nu} \partial^\mu \bar{\varphi}_i \partial^\nu \varphi_i + m^2 \bar{\varphi}_i \varphi_i + \frac{(4\pi)^2 g_0}{6} (\bar{\varphi}_i \varphi_i)^2 \right) . \quad (4.30)$$

As discussed in Sec.2.5, the cylinder action contains an effective mass term with $m = \frac{d-2}{2R}$, where R is the radius of S^{d-1} . We are interested in the computation of the scaling dimension of the MSD $O(N)$ operator with charge \vec{Q} , i.e. of the ground state energy on the cylinder. According to Eq.(4.1), the latter can be obtained from the matrix element $\langle \vec{Q} | e^{-HT} | \vec{Q} \rangle$ with $|\vec{Q}\rangle$ an arbitrary state with charge \vec{Q} .

Stemming from the considerations made in the previous chapter, we expect this matrix element to be controlled by a modified Hamiltonian $\hat{H} = H + \vec{Q} \cdot \vec{\mu}$, where $\vec{\mu} = (\mu_1, \dots, \mu_k)$ is a set of k (a priori) independent chemical potentials. On the other hand, in the ground state, simplifications occur. This can be seen by solving the classical EOM, which read

$$\left(-\partial^2 + [(\partial \chi_j)^2 + m^2] + \frac{(4\pi)^2}{6} g_0 \sigma_i \sigma_i \right) \sigma_j = 0 , \quad i \partial_\mu (\sigma_i \sigma_i g^{\mu\nu} \partial_\nu \chi_i) = 0 , \quad (4.31)$$

and have to be solved together with the k charge-fixing constraints $Q_i = \bar{Q}_i$. The solution with minimal energy is spatially homogeneous, and it is given by

$$\begin{cases} \sigma_i = A_i , \quad \chi_i = -i\mu t \quad i = 1, \dots, k , \\ \varphi_{k+j} = 0 , \quad j = 1, \dots, N/2 - k . \end{cases} \quad (4.32)$$

The striking consequence of this homogeneous solution is that all the chemical potentials are equal, $\mu_i = \mu$, even if the charges \bar{Q}_i are different. This solution describes k circular motions in the planes spanned by the real and imaginary parts of the φ_i . These motions are synchronous with the same angular velocity μ but different radii of the circles A_i . μ and the A_i are fixed by the EOM and the charge constraints as

$$\mu^2 - m^2 = \frac{(4\pi)^2}{6} g_0 v^2, \quad \frac{\bar{Q}}{\Omega_{d-1} R^{d-1}} = \mu v^2, \quad (4.33)$$

where $\Omega_{d-1} = \frac{2\pi^{d/2}}{\Gamma(d/2)}$ is the solid angle in d dimensions, and we have defined the sum of the square vevs as

$$v^2 \equiv \sum_{i=1}^k A_i^2. \quad (4.34)$$

The presence of a single chemical potential implies that the non-relativistic effective Hamiltonian reads

$$\hat{H} = H + \vec{Q} \cdot \vec{\mu} = H + \bar{Q} \mu, \quad (4.35)$$

i.e. μ couples to the sum of the charges. In fact, a convenient choice for $|\bar{Q}\rangle$ in (4.1) is given by

$$|\bar{Q}\rangle = \int \mathcal{D}\alpha(\vec{n}) \left\{ \prod_i^k \exp \left[\frac{i\bar{Q}_i}{R^{d-1} \Omega_{d-1}} \int d\Omega_{d-1} \alpha_i(\vec{n}) \right] \right\} |\vec{A}, \vec{\alpha}(\vec{n})\rangle, \quad (4.36)$$

where \vec{n} identify points on S^{d-1} and $|\vec{A}, \vec{\alpha}(\vec{n})\rangle$ is the state with fixed values of the fields $\sigma_i(\vec{n}) = A_i$ and $\chi_i = \alpha_i(\vec{n})$. The term in the brace can be thought of as a wave-functional for the state in radial quantization which fixes its charge to \bar{Q} . Now consider fixing all the charges, i.e. $k = N/2$. Then Eq.(4.36) leads to

$$\langle \bar{Q} | e^{-HT} | \bar{Q} \rangle = \frac{1}{\mathcal{Z}} \int_{\sigma_i = A_i}^{\sigma_i = A_i} D^n \sigma D^n \chi e^{-\hat{\mathcal{S}}}, \quad (4.37)$$

with

$$\begin{aligned} \hat{\mathcal{S}} &= \int_{-T/2}^{T/2} dt \int d\Omega_{d-1} \left(\frac{1}{2} \partial \sigma_i \partial \sigma_i + \frac{1}{2} \sigma_i^2 \partial \chi_i \partial \chi_i + \frac{m^2}{2} \sigma_i^2 + \frac{(4\pi)^2}{24} g_0 (\sigma_i \sigma_i)^2 + \frac{i\bar{Q}}{\Omega_{d-1} R^{d-1}} q_i \dot{\chi}_i \right) \\ &\simeq \int_{-T/2}^{T/2} dt \int d\Omega_{d-1} \left(\frac{1}{2} \partial \sigma_i \partial \sigma_i + \frac{1}{2} \sigma_i^2 \partial \chi_i \partial \chi_i + \frac{m^2}{2} \sigma_i^2 + \frac{(4\pi)^2}{24} g_0 (\sigma_i \sigma_i)^2 + \frac{\mu \bar{Q}}{\Omega_{d-1} R^{d-1}} \right). \end{aligned} \quad (4.38)$$

where the sum over i runs from 1 to $N/2$ and the \simeq has to be understood as equivalence up to a term which is linear in the fluctuations of the χ_i fields, and does not affect the computation of the ground state energy. In the last line, we made explicit that the physics is controlled by the modified Hamiltonian \hat{H} given by Eq.(4.35). Notice the analogy with the rigid rotor of Sec.(3.2); specifically, Eq.(4.37) corresponds to Eq.(3.10), while Eq.(4.38) is the counterpart of Eq.(3.11).

In short, in presence of a homogeneous background, the sum of the charges acts as a single $U(1)$ charge while the charge configuration plays no role. This fact can be made explicit by using an $O(N)$ transformation to rotate the ground state as

$$\frac{1}{\sqrt{2}}(A_1, \dots, A_{N/2}) \longrightarrow (\underbrace{0, \dots, 0}_{N/2-1}, \frac{v}{\sqrt{2}}) . \quad (4.39)$$

This operation assigns "all the vevs" to a single radial field $\sigma_{N/2}$ and all the charge to one Cartan generator $\mathcal{H}_{N/2}$, i.e.

$$\vec{Q} = \bar{Q}(\underbrace{0, \dots, 0}_{N/2-1}, 1) . \quad (4.40)$$

At large values of \bar{Q} , Eq.(4.37) can be computed via a semiclassical expansion resulting in

$$\Delta_{\bar{Q}} = E_{\bar{Q}} R = \sum_{j=-1}^{\infty} g^{*j} \tilde{\Delta}_j(\mathcal{A}^*) = \sum_{j=-1}^{\infty} \frac{1}{\bar{Q}^j} \Delta_j(\mathcal{A}^*) , \quad (4.41)$$

where the $*$ denotes the quantities evaluated at the FP.

This can be easily seen by rescaling the radial fields as $\sigma_i \rightarrow \sqrt{\bar{Q}} \sigma_i$ as done in Sec.(3.7), in order to exhibit \bar{Q} as the loop counting parameter. This analysis shows that we can organize our large charge expansion as a semiclassical expansion in $1/\bar{Q}$ with fixed 't Hooft coupling $\mathcal{A}_0 = g_0 \bar{Q}$, in full analogy with the abelian case (3.75). To access more general charge configurations, it is necessary to consider non-homogeneous ground states, as done for the $O(4)$ case in [130, 149, 150].

Let us analyze the symmetry breaking pattern produced by the classical solution. In general, the breaking is a direct consequence of the fact that the ground state is an eigenstate of the non-relativistic Hamiltonian \hat{H} and not of H . This breaking can also be viewed as an explicit breaking induced by the charge-fixing followed by an SSB due to the ground state (4.39). In fact, according

to the *charged Goldstone theorem* discussed in Sec.3.4, we will have both massive (type III) and massless (type I and type II) Goldstone bosons. Specifically, the ones commuting with \hat{H} are massless, while the others have a mass gap proportional to μ . Then we can think of the chemical potential as an explicit symmetry-breaking term setting the mass scale for the type III Goldstones²¹.

Consider the "explicit" breaking due to the charge fixing, i.e. by the $\sum_i^{N/2} \mu Q_i$ term in \hat{H} . Since all the charges couple to the same chemical potential, an $U(N/2)$ subgroup of the original $O(N)$ symmetry remains unbroken. In fact, the term

$$\sum_i \mu Q_i = \mu \sum_i \int dx (\bar{\varphi}_i \partial^0 \varphi_i - \varphi_i \partial^0 \bar{\varphi}_i) = \mu \int dx (\vec{\bar{\varphi}} \partial^0 \vec{\varphi} - \vec{\varphi} \partial^0 \vec{\bar{\varphi}}) , \quad (4.42)$$

is clearly invariant under $U(N/2)$ rotations of the vector $\vec{\bar{\varphi}} = (\varphi_1, \dots, \varphi_{N/2})$.

Then the vacuum Eq.(4.39), in turn, spontaneously breaks the $U(N/2)$ symmetry of $\vec{\bar{\varphi}}$ to $U(N/2 - 1)$, leading to massless Goldstone modes. Altogether, the symmetry breaking pattern is

$$SO(d+1, 1) \times O(N) \rightarrow SO(d) \times D' \times U(N/2 - 1) , \quad (4.43)$$

where $D = H$ is the generator of time translations and $D' = D + \mu Q_{N/2}$.

Then, according to the charged Goldstone theorem, we expect $\dim(U(N/2)/U(N/2 - 1)) = N - 1$ massless Goldstone bosons, once type II states are double-counted. This can be realized with one type I scalar and one type II $U(N/2 - 1)$ -vector. In fact, counting twice the type II modes we have

$$1 + 2 \times (N/2 - 1) = N - 1 . \quad (4.44)$$

4.4 Fixed-charge operators

The goal of this section is to determine the MSD operator with total charge \bar{Q} . In particular, we will identify it as the anisotropic perturbations $T_{0, \bar{Q}}$ introduced in Eq.(4.13).

In CFT with global symmetries, we can organize the operators into multiplets transforming

²¹ In fact, we might as well have introduced the chemical potential as the zero component of a gauge field through the usual covariant derivative. In such a case, the Lagrangian would have contained a mass term $\mu^2 \sigma_j \sigma_j$ for the radial modes, which would explicitly break the symmetry. On the other hand, as can be seen from the fact that we can always eliminate the chemical potential from the Lagrangian by a simple field redefinition, the charge-fixing symmetry breaking should be retained purely spontaneous.

according to irreducible representations of the symmetry group. Within any multiplet, component operators are further distinguished by their charge configuration, i.e. the value of the charges associated with the Cartan generators. Operators with different symmetry properties (i.e. belonging to nonequivalent irreducible representations) do not mix under renormalization. Moreover, by virtue of the Wigner-Eckart theorem, they necessarily have the same scaling dimension. We restrict ourselves to the case when ε is small, and the theory is perturbative. We can, therefore, consider the MCSD assumption introduced in Sec.4.1 and look for operators with the minimal classical dimension for a given charge configuration.

Let us start with a *top-down* approach. First, the MCSD assumption implies that the MSD operator does not contain derivatives, since the latter increase the classical dimension. Furthermore, since scalar fields commute, operators without derivatives live in the fully symmetric $O(N)$ space. The latter is composed by the $T_{p,\bar{Q}}$ operators defined in Eq.(4.13) which have total charge \bar{Q} and CSD $\bar{Q} + 2p$. At fixed \bar{Q} , the MSD operator is clearly obtained when $p = 0$ and, as anticipated, we are left with the $T_{0,\bar{Q}}$ operators.

For later convenience, we consider also a *bottom-up* approach performing the explicit construction of the MSD operators. The charge configuration is given by Eq.(4.24) and is parametrized by a set of numbers $\{q_i\}$ such that $\sum_i^k q_i = 1$. Without loss of generality, we assume all q_i 's to be positive. Hence, according to the MCSD assumption, the fixed-charge operator with the MCSD can be written as²²

$$\mathcal{O}_{q_i} \equiv \prod_{i=1}^k (\varphi_i)^{\bar{Q}q_i}. \quad (4.45)$$

On the other hand, we know that we can use an $O(N)$ transformation to set $q_k = 1$ and $q_{i \neq k} = 0$. Then the MSD operator becomes $\mathcal{O}_{q_i} = (\varphi_k)^{\bar{Q}}$. Clearly, this operator transforms according to the traceless symmetric $O(N)$ representations, has total charge \bar{Q} and CSD \bar{Q} . Then, we can again identify the MSD operators as the $T_{0,\bar{Q}}$ anisotropic perturbations. Note that for $N = 2$ we have the $\varphi^{\bar{Q}} U(1)$ operator we considered in Secs.3.6 and 3.7.

²²If some q_i were negative, they would correspond to replace φ_i with $\bar{\varphi}_i$.

4.5 The large charge expansion in the $O(N)$ model: LO

We now have all the instruments to proceed with the semiclassical computation of $\Delta_{T_{0,\bar{Q}}} \equiv \Delta_{\bar{Q}}$, i.e. of the Δ_j coefficients in Eq.(4.41).

The leading term of the large charge expansion, Δ_{-1} , is given by the effective action (4.38) evaluated on the classical trajectory (4.32) at the fixed point

$$\Delta_{-1}(\mathcal{A}^*) = \frac{R}{4} \left(3\mu + \frac{m^2}{\mu} \right) . \quad (4.46)$$

Notice that, since this contribution is purely classical, bare and renormalized couplings coincide at the LO.

By inserting the second equation in (4.33) into the first one and setting $d = 4$, we obtain

$$R^3 \mu^3 - R\mu = \frac{4}{3} \mathcal{A}^* , \quad (4.47)$$

with solution

$$R\mu = \frac{3^{\frac{1}{3}} + \left(6\mathcal{A}^* + \sqrt{-3 + 36\mathcal{A}^{*2}} \right)^{\frac{2}{3}}}{3^{\frac{2}{3}} \left(6\mathcal{A}^* + \sqrt{-3 + 36\mathcal{A}^{*2}} \right)^{\frac{1}{3}}} . \quad (4.48)$$

Then the leading order of the semiclassical large charge expansion reads

$$4\Delta_{-1} = \frac{3^{\frac{2}{3}} \left(6\mathcal{A}^* + \sqrt{-3 + 36\mathcal{A}^{*2}} \right)^{\frac{1}{3}}}{3^{\frac{1}{3}} + \left(6\mathcal{A}^* + \sqrt{-3 + 36\mathcal{A}^{*2}} \right)^{\frac{2}{3}}} + \frac{3^{\frac{1}{3}} \left(3^{\frac{1}{3}} + \left(6\mathcal{A}^* + \sqrt{-3 + 36\mathcal{A}^{*2}} \right)^{\frac{2}{3}} \right)}{\left(6\mathcal{A}^* + \sqrt{-3 + 36\mathcal{A}^{*2}} \right)^{\frac{1}{3}}} . \quad (4.49)$$

We would like to stress again that this classical result resums an infinite series of Feynman diagrams in the usual perturbative expansion. These are the diagrams shown in Fig.8. In particular, Eq.(4.49) resums the leading power of \bar{Q} at every perturbative order. The expansion for small \mathcal{A}^* reads

$$\bar{Q}\Delta_{-1} = \bar{Q} \left[1 + \frac{1}{3}\mathcal{A}^* - \frac{2}{9}\mathcal{A}^{*2} + \frac{8}{27}\mathcal{A}^{*3} - \frac{14}{27}\mathcal{A}^{*4} + \frac{256}{243}\mathcal{A}^{*5} - \frac{572}{243}\mathcal{A}^{*6} + \mathcal{O}(\mathcal{A}^{*7}) \right] . \quad (4.50)$$

4.6 The large charge expansion in the $O(N)$ model: NLO

The time is ripe to determine the leading quantum corrections Δ_0 to be added to the classical result (4.49). Since we will need to renormalize our results, we rewrite our expansion as

$$E_{\vec{Q}} R = \sum_{j=-1}^{\infty} g_0^j e_j(\mathcal{A}_0, d) = \sum_{j=-1}^{\infty} g^j \bar{e}_j(\mathcal{A}, d, RM) , \quad (4.51)$$

where e_j and \bar{e}_j are, respectively, the bare and renormalized coefficients of the large charge expansion.

In order to calculate e_0 , we have to expand the path integral (4.37) to the quadratic order as

$$\begin{aligned} \langle \psi_{\vec{Q}} | e^{-HT} | \psi_{\vec{Q}} \rangle &= e^{-\frac{e_{-1}(\mathcal{A}_0, d)T}{g_0 R}} \frac{\int \mathcal{D}\sigma \mathcal{D}\chi e^{-\hat{\mathcal{S}}^{(2)}}}{\int \mathcal{D}\varphi \mathcal{D}\bar{\varphi} e^{-\int_{-T/2}^{T/2} \sqrt{g} (g_{\mu\nu} \partial^\mu \bar{\varphi}_i \partial^\nu \varphi_i + m^2 \bar{\varphi}_i \varphi_i)}} \\ &= \tilde{\mathcal{N}} \exp \left\{ - \left[\frac{1}{g_0} e_{-1}(\mathcal{A}_0, d) + e_0(\mathcal{A}_0, d) \right] \frac{T}{R} \right\} , \end{aligned} \quad (4.52)$$

where $\hat{\mathcal{S}}^{(2)}$ is the modified action at the quadratic order in the fluctuation fields. In order to find $\hat{\mathcal{S}}^{(2)}$, we expand around the saddle point configuration (4.32) considering the ground state in (4.39). We parametrize the fluctuations as

$$\begin{cases} \chi_i = -i\mu t + \frac{1}{v} p_i(x) , & i = 1, \dots, \frac{N}{2} - 1 , \\ \chi_{N/2} = -i\mu t + \frac{1}{v} \pi(x) , \\ \sigma_i = s_i(x) , & i = 1, \dots, \frac{N}{2} - 1 , \\ \sigma_{N/2} = v + r(x) . \end{cases} , \quad (4.53)$$

Expanding the Lagrangian (4.38) to the quadratic order in the fluctuations, we arrive at

$$\begin{aligned} \mathcal{L}_2 &= \frac{1}{2} (\partial\pi)^2 + \frac{1}{2} (\partial r)^2 + (\mu^2 - m^2) r^2 - 2i\mu r \dot{\pi} \\ &\quad + \frac{1}{2} \partial s_i \partial s_i + \frac{1}{2} \partial p_i \partial p_i - 2i\mu s_i \dot{p}_i . \end{aligned} \quad (4.54)$$

The quadratic Lagrangian contains a "U(1) sector" given by π and r . To obtain their dispersion relations, we move to Fourier space and define the inverse propagator $\mathcal{P}^{-1}(p)$, with p the momentum,

as

$$S^{(2)} = \int \frac{d^d p}{(2\pi)^d} [r(-p) \ \pi(-p)] \mathcal{P}^{-1}(p) \begin{bmatrix} r(p) \\ \pi(p) \end{bmatrix}. \quad (4.55)$$

We have

$$\mathcal{P}^{-1}(p) = \begin{pmatrix} \frac{1}{2}(\omega^2 - p^2) - (\mu^2 - m^2) & i\omega\mu \\ -i\omega\mu & \frac{1}{2}(\omega^2 - p^2) \end{pmatrix}. \quad (4.56)$$

The dispersion relations are then obtained from $\det \mathcal{P}^{-1}(p) = 0$, and read

$$\omega_{\pm}(l) = \sqrt{J_{\ell}^2 + 3\mu^2 - m^2 \pm \sqrt{4J_{\ell}^2\mu^2 + (3\mu^2 - m^2)^2}}, \quad (4.57)$$

with

$$J_{\ell}^2 = \ell(\ell + d - 2)/R^2 = p^2. \quad (4.58)$$

are the eigenvalues of the Laplacian the sphere. Their multiplicity n_{ℓ} has been given in Eq.(3.61).

These modes can be identified as one relativistic (type I) Goldstone boson $\chi_{N/2}$ and one massive state $\sigma_{N/2}$ with mass $\sqrt{6\mu^2 - 2m^2}$. This is the fluctuation spectrum in the $O(2)$ case. Additionally, the non-abelian case also features $k - 1 = \frac{N}{2} - 1$ non-relativistic (type II) Goldstone bosons and $N/2 - 1$ massive states with mass 2μ (type III Goldstones)

$$\omega_{\pm\pm}(l) = \sqrt{J_{\ell}^2 + \mu^2} \pm \mu. \quad (4.59)$$

Notice that the gap of type III Goldstones is fixed by symmetry and does not receive radiative corrections [122].

The counting of massless Goldstone bosons satisfies the charged Goldstone theorem. In fact

$$1 + 2 \times \left(\frac{N}{2} - 1 \right) = N - 1 = \dim \left(U \left(\frac{N}{2} \right) / U \left(\frac{N}{2} - 1 \right) \right). \quad (4.60)$$

e_0 is determined by the fluctuation functional determinant which can be written in terms of the dispersion relations found above as

$$T \frac{e_0}{R} = \log \frac{\sqrt{\det \widehat{\mathcal{S}}^{(2)}}}{\det(-\partial_\tau^2 - \Delta_{S^{d-1}} + m^2)} = \frac{T}{2} \sum_{\ell=0}^{\infty} n_\ell \int \frac{d\omega}{2\pi} \sum_i g_i \log \frac{[\omega^2 + \omega_i^2(\ell)]}{[\omega^2 + \omega_0^2(\ell)]} \quad (4.61)$$

$$= \frac{T}{2} \sum_{\ell=0}^{\infty} n_\ell \left[\sum_i g_i(N) \omega_i(\ell) - N \omega_0(\ell) \right], \quad (4.62)$$

where $i = +, -, ++, --$ and the sum runs over all the dispersion relations of the spectrum, each counted with its multiplicity $g_i(N)$. $\omega_0^2(\ell) = J_\ell^2 + m^2$ is the free dispersion relation and satisfies $\omega_0(\ell)|_{d=4} = \frac{1+l}{R^2}$. We can compute the contribution of $\omega_0(\ell)$ by using dimensional regularization, where, for enough negative d , we have

$$\sum_{\ell=0}^{\infty} n_\ell = \sum_{\ell=0}^{\infty} n_\ell \ell = 0 \quad \Rightarrow \quad \sum_{\ell=0}^{\infty} n_\ell \omega_0(\ell) = 0. \quad (4.63)$$

Then our final expression for e_0 reads

$$e_0 = \frac{R}{2} \sum_{\ell=0}^{\infty} n_\ell \left[\omega_+(\ell) + \omega_-(\ell) + \left(\frac{N}{2} - 1 \right) (\omega_{++}(\ell) + \omega_{--}(\ell)) \right]. \quad (4.64)$$

It is instructive to analyze what happens to our computation if we do not fix all the $N/2$ charges Q_i but only $k < N/2$ out of them. It is easy to show that in such a case, the number of type II Goldstone bosons and massive particles with dispersion relation in Eq.(4.59) becomes $k-1$, whereas the spectrum is completed by $2 \times [(N/2-1) - (k-1)] = N-2k$ new massive "spectator" states with mass μ and dispersion relation

$$\omega_*(\ell) = \sqrt{J_\ell^2 + \mu^2}. \quad (4.65)$$

Accordingly, the expression for e_0 becomes

$$e_0 = \frac{R}{2} \sum_{\ell=0}^{\infty} n_\ell [\omega_+(\ell) + \omega_-(\ell) + (k-1)(\omega_{++}(\ell) + \omega_{--}(\ell)) + (N-2k)\omega_*]. \quad (4.66)$$

Since $\omega_{++}(\ell) + \omega_{--}(\ell) = 2\omega_*(\ell)$, e_0 does not depend on the number of charges we fix. This result is consistent with the scaling dimension not being sensitive to the charge configuration but only to

the sum of the charges.

The sum over ℓ in Eq.(4.64) diverges and needs regularization. This will be done in the next section, along with the renormalization procedure.

4.7 Regularization and renormalization

The renormalization is performed by using Eqs.(4.7) and (4.10) into Eq.(4.51) and expanding every term $g_0^j e_j(\bar{Q}g_0, d)$ in powers of g . This procedure mixes the bare orders of the expansion. In particular, we have

$$\frac{e_{-1}(\mathcal{A}, d)}{g_0} = \frac{e_{-1}(\mathcal{A}, d)}{g} + \sum_{j=0} g^j f_j(\mathcal{A}, d, RM). \quad (4.67)$$

Since f_0 is of the same order $\mathcal{O}(g^0) = \mathcal{O}(\bar{Q}^0)$ of e_0 in the renormalized large charge expansion, we have

$$\bar{e}_{-1}(\mathcal{A}, d) = e_{-1}(\mathcal{A}, d), \quad \bar{e}_0(\mathcal{A}, d, RM) = e_0(\mathcal{A}, d) + f_0(\mathcal{A}, d, RM), \quad (4.68)$$

We compute f_0 by expanding e_{-1} (which is obtained as Δ_{-1} in Eq.(4.46) but working in $d = 4 - \varepsilon$ instead that $d = 4$) in powers of g and retaining the term of order g_0 . We have

$$\begin{aligned} f_0(\mathcal{A}, d, RM) &= \frac{8+N}{16}(\mu^2 R^2 - 1)^2 \left(\frac{1}{\varepsilon} - \log(MR\sqrt{\pi}) - \frac{\gamma}{2} \right) \\ &+ \frac{8+N}{32}(\mu^2 R^2 - 1)(\mu^2 R^2 + 3) + \mathcal{O}(\varepsilon), \end{aligned} \quad (4.69)$$

where we expand in ε by taking the renormalized coupling fixed. γ is the Euler–Mascheroni constant. To compute Δ_0 , we have to consider the theory at the FP $g^* = g^*(\varepsilon)$ given by Eq.(4.11). Being the fixed point coupling expressed as a power series in ε , this step mixes again different orders of the expansion, now the renormalized ones. In particular, Δ_0 is given by \bar{e}_0 in $d = 4$ plus the expansion of the LO \bar{e}_{-1}/g to the first order in ε (for fixed coupling)

$$\begin{aligned} \Delta_0 &= \left\{ \bar{e}_0(\mathcal{A}, RM, 4) + \varepsilon \frac{\partial}{\partial \varepsilon} \left[\frac{1}{g} \bar{e}_{-1}(\mathcal{A}, RM, 4 - \varepsilon) \right]_{\varepsilon=0} \right\}_{g=g^*} \\ &= \left\{ \lim_{\varepsilon \rightarrow 0} \left[\frac{R}{2} \sum_{\ell=0}^{\infty} n_{\ell} \left[\boldsymbol{\omega}_+(\ell) + \boldsymbol{\omega}_-(\ell) + \left(\frac{N}{2} - 1 \right) (\boldsymbol{\omega}_{++}(\ell) + \boldsymbol{\omega}_{--}(\ell)) \right] \right] \right\}_{g=g^*} \end{aligned}$$

$$+ \frac{8+N}{16\epsilon} (\mu^2 R^2 - 1)^2 \Bigg] \Bigg\}_{g=g^*} , \quad (4.70)$$

where we take the $\epsilon \rightarrow 0$ limit by keeping the coupling fixed. Notice that at the FP the dependence on the renormalization scale M drops, as expected from conformal invariance. On the other hand, we are left with a $\frac{1}{\epsilon}$ term which diverges in the limit $\epsilon \rightarrow 0$ and must cancel after we regularize the sum over ℓ .

To perform the regularization, we first isolate the divergent part by performing an expansion of the summand around $\ell = \infty$

$$Rn_\ell \left[\omega_+(\ell) + \omega_-(\ell) + \left(\frac{N}{2} - 1 \right) (\omega_{++}(\ell) + \omega_{--}(\ell)) \right] \sim \sum_{n=1}^{\infty} c_n \ell^{d-n} . \quad (4.71)$$

In $d = 4$, the first five terms of the expansion diverge when $\ell \rightarrow \infty$. Their coefficients read

$$\begin{aligned} c_1 &= N + \mathcal{O}(\epsilon) , & c_2 &= 3N + \mathcal{O}(\epsilon) , \\ c_3 &= \frac{1}{2} [(N+2)\mu^2 R^2 + 5N - 2] + \mathcal{O}(\epsilon) , & c_4 &= \frac{1}{2} [(N+2)\mu^2 R^2 + N - 2] + \mathcal{O}(\epsilon) , \\ c_5 &= -\frac{(N+8)(\mu^2 R^2 - 1)^2}{8} + \frac{1}{240} (-45\mu^4(N+8)R^4 - 20\mu^2(N-7)R^2 \\ &\quad + 30\gamma(N+8)(\mu^2 R^2 - 1)^2 + 3N + 220) \epsilon + \mathcal{O}(\epsilon^2) . \end{aligned} \quad (4.72)$$

Then we can isolate the divergent part as²³

$$\begin{aligned} \frac{R}{2} \sum_{\ell=0}^{\infty} n_\ell \left[\omega_+(\ell) + \omega_-(\ell) + \left(\frac{N}{2} - 1 \right) (\omega_{++}(\ell) + \omega_{--}(\ell)) \right] &= \\ \frac{1}{2} \sum_{n=1}^5 c_n \sum_{\ell=1}^{\infty} \ell^{d-n} + \frac{1}{2} \sum_{\ell=1}^{\infty} \sigma(\ell) + \frac{R}{2} \omega_+(0) + \frac{R}{2} \left(\frac{N}{2} - 1 \right) \omega_{++}(0) , \end{aligned} \quad (4.73)$$

with²⁴

$$\sigma(\ell) = Rn_\ell \left[\omega_+(\ell) + \omega_-(\ell) + \left(\frac{N}{2} - 1 \right) (\omega_{++}(\ell) + \omega_{--}(\ell)) \right] - \sum_{n=1}^5 c_n \ell^{d-n}$$

²³ In writing this expression, we used that $\omega_-(0) = \omega_{--}(0) = 0$.

²⁴ Since $\sigma(\ell)$ is a convergent sum, we can evaluate it directly in $d = 4$.

$$\begin{aligned}
&= R(1+\ell)^2 \left[\boldsymbol{\omega}_+(\ell) + \boldsymbol{\omega}_-(\ell) + \left(\frac{N}{2} - 1 \right) (\boldsymbol{\omega}_{++}(\ell) + \boldsymbol{\omega}_{--}(\ell)) \right]_{d=4} - N \ell^3 - 3N \ell^2 \\
&+ \frac{1}{2} (2 - 5N - (2+N)R^2\mu^2) \ell + \frac{1}{2} (2 - N - (N+2)R^2\mu^2) + \frac{1}{8}(N+8) (R^2\mu^2 - 1)^2 \frac{1}{\ell} .
\end{aligned} \tag{4.74}$$

Finally, we zeta-regularize the divergent part by using that $\sum_{\ell=1}^{\infty} \ell^x = \zeta(-x)$ and $\zeta(1+\varepsilon) = \frac{1}{\varepsilon} + \gamma + \mathcal{O}(\varepsilon)$. We obtain

$$\frac{1}{2} \sum_{n=1}^5 c_n \sum_{\ell=1}^{\infty} \ell^{d-n} = -\frac{8+N}{16R\varepsilon} (\mu^2 R^2 - 1)^2 - \frac{3\mu^4(N+8)R^4 + 6\mu^2NR^2 + 7N - 24}{32R} . \tag{4.75}$$

The $1/\varepsilon$ term in the regularized contribution above cancels exactly the $1/\varepsilon$ term in f_0 . Hence we can now consistently take the limit $\varepsilon \rightarrow 0$ in Eq.(4.70), after which we are left with a finite result. Notice that, since the two $1/\varepsilon$ terms come from different orders of the bare expansion, their cancellation can be used as a non-trivial self-consistency check of the correctness of the calculations. This check can be particularly useful when dealing with more complicated theories such as the $U(N) \times U(M)$ model that we will investigate in Chap.6.

4.8 Results

After regularization and renormalization, we finally obtain our final result for Δ_0

$$\begin{aligned}
\Delta_0(\mathcal{A}^*) = & -\frac{15\mu^4R^4 + 6\mu^2R^2 - 5}{16} + \frac{1}{2} \sum_{\ell=1}^{\infty} \sigma(\ell) + \frac{\sqrt{3\mu^2R^2 - 1}}{\sqrt{2}} \\
& - \frac{1}{16} \left(\frac{N}{2} - 1 \right) [7 + R\mu (-16 + 6R\mu + 3R^3\mu^3)] ,
\end{aligned} \tag{4.76}$$

where $\sigma(\ell)$ is given by Eq.(4.74), and all the quantities are evaluated in $d = 4$. As a non-trivial test of our result, we now compare it with the known 2-loop perturbative result in Eq.(4.21). To this end, we use Eq.(4.48) to express Δ_0 as a function of \mathcal{A}^* , and we expand Δ_0 for small \mathcal{A}^* , where $\sigma(\ell)$ can be computed analytically

$$\Delta_0(\mathcal{A}^*) = -\left(\frac{5}{3} + \frac{N}{6}\right)\mathcal{A}^* + \left(\frac{1}{3} - \frac{N}{18}\right)\mathcal{A}^{*2} + \frac{1}{27}[N-36+28\zeta(3)+2N\zeta(3)]\mathcal{A}^{*3} + \mathcal{O}(\mathcal{A}^{*4}) . \quad (4.77)$$

The sum of the classical contribution (4.50) and the leading quantum correction (4.77) reads

$$\begin{aligned} \frac{\Delta_{-1}(\mathcal{A}^*)}{g^*} + \Delta_0(\mathcal{A}^*) &= \bar{Q} - \frac{\mathcal{A}^*}{6}(10+N-2\bar{Q}) + \frac{\mathcal{A}^{*2}}{18}(6-N-4\bar{Q}) \\ &\quad + \frac{\mathcal{A}^{*3}}{27}[N-36+8\bar{Q}+2(14+N)\zeta(3)] + \mathcal{O}(\bar{Q}\mathcal{A}^{*4}) , \end{aligned} \quad (4.78)$$

Finally, evaluating the above expression at the fixed point (4.11), we obtain

$$\Delta_{\bar{Q}} = \bar{Q} + \left(-\frac{\bar{Q}}{2} + \frac{\bar{Q}(\bar{Q}-1)}{8+N}\right)\varepsilon - \left[\frac{2}{(8+N)^2}\bar{Q}^3 + \frac{(N-22)(N+6)}{2(8+N)^3}\bar{Q}^2 + \mathcal{O}(\bar{Q})\right]\varepsilon^2 , \quad (4.79)$$

in agreement with the diagrammatic result (4.21).

At order $\mathcal{O}(\varepsilon^3)$ and $\mathcal{O}(\varepsilon^4)$, our semiclassical computation captures the leading and next to leading terms in the charge. However, we can determine also the remaining terms by asking that we reproduce the known results for the cases $\bar{Q} = 1$ (4.18), $\bar{Q} = 2$ (4.19), and $\bar{Q} = 4$ (4.20). In this way, we obtain the complete scaling dimension of the operators $T_{0,\bar{Q}}$ to order $\mathcal{O}(\varepsilon^4)$, which reads

$$\begin{aligned} \Delta_{\bar{Q}} = \bar{Q} - \frac{\bar{Q}}{2}\varepsilon + [c_{1,1}\bar{Q} + c_{1,2}\bar{Q}^2]\varepsilon + [c_{2,1}\bar{Q} + c_{2,2}\bar{Q}^2 + c_{2,3}\bar{Q}^3]\varepsilon^2 + [c_{3,1}\bar{Q} + c_{3,2}\bar{Q}^2 \\ + c_{3,3}\bar{Q}^3 + c_{3,4}\bar{Q}^4]\varepsilon^3 + [c_{4,1}\bar{Q} + c_{4,2}\bar{Q}^2 + c_{4,3}\bar{Q}^3 + c_{4,4}\bar{Q}^4 + c_{4,5}\bar{Q}^5]\varepsilon^4 + \mathcal{O}(\varepsilon^5) , \end{aligned} \quad (4.80)$$

where

$$\begin{aligned} c_{1,1} &= \frac{-1}{8+N} , & c_{1,1} &= \frac{1}{8+N} , & c_{2,1} &= -\frac{184+N(14-3N)}{4(8+N)^3} , \\ c_{2,2} &= -\frac{(N-22)(N+6)}{2(8+N)^3} , & c_{2,3} &= -\frac{2}{(8+N)^2} , \end{aligned}$$

$$\begin{aligned}
c_{3,1} &= \frac{-69504 + 3N[-5216 + N(184 + N(86 + N))] + 64(8 + N)(178 + N(37 + N))\zeta(3)}{16(N + 8)^5}, \\
c_{3,2} &= \frac{-N^4 - 57N^3 + 258N^2 - 24(N + 6)(N + 8)(N + 26)\zeta(3) + 8176N + 31008}{4(N + 8)^5}, \\
c_{3,3} &= \frac{-456 - 64N + N^2 + 2(8 + N)(14 + N)\zeta(3)}{(8 + N)^4}, \quad c_{3,4} = \frac{8}{(8 + N)^3}, \\
c_{4,1} &= \frac{1}{960(8 + N)^7} (45N^6 + 32\pi^4N^5 + 5820N^5 + 1952\pi^4N^4 + 322440N^4 + 40256\pi^4N^3 \\
&\quad + 1972440N^3 + 380416\pi^4N^2 - 16196640N^2 - 9600(N + 8)^2(N(25N + 418) + 1240)\zeta(5) \\
&\quad - 240(N + 8)(N(N(N(N + 40) + 1056) - 3496) - 100480) - 300096)\zeta(3) + 1699840\pi^4N \\
&\quad - 191091840N + 2916352\pi^4 - 494461440), \\
c_{4,2} &= -\frac{1}{80(N + 8)^7} (10N^6 + 4\pi^4N^5 + 915N^5 + 224\pi^4N^4 + 34120N^4 + 4464\pi^4N^3 + 86600N^3 \\
&\quad + 41600\pi^4N^2 - 3928440N^2 - 400(N + 8)^2(N(65N + 958) + 2496)\zeta(5) - 35161600N \\
&\quad - 20(N + 8)(N(N(N(N + 52) + 904) - 12224) - 181184) - 514112)\zeta(3) + 185344\pi^4N \\
&\quad + 319488\pi^4 - 87127680), \\
c_{4,3} &= \frac{1}{60(8 + N)^6} (\pi^4N^4 + 60N^4 + 38\pi^4N^3 + 4020N^3 + 528\pi^4N^2 - 88800N^2 - 1577280N \\
&\quad - 4200(N - 2)(N + 8)^2\zeta(5) - 60(N + 8)(N(N(3N - 44) - 1720) - 7464)\zeta(3) + 3200\pi^4N \\
&\quad + 7168\pi^4 - 5662560), \\
c_{4,4} &= \frac{-4N^2 - 5(N + 8)(N + 30)\zeta(5) - 2(N + 8)(6N + 65)\zeta(3) + 476N + 3344}{(8 + N)^5}, \\
c_{4,5} &= -\frac{42}{(8 + N)^4}. \tag{4.81}
\end{aligned}$$

As anticipated, the above result corrects the one in [148] demonstrating the power of the approach. Moreover, we can now predict the classical and quantum correction for the higher perturbative loops of the anomalous dimension. To help future checks we provide explicit results up to order g^* ²⁵.

$$\begin{aligned}
\text{5-loops:} & \left(\frac{256}{243} \bar{Q} + \frac{1}{243} [3(-800 + 7N) + 28\zeta(3)(28 + 3N) \right. \\
& \quad \left. + 40\zeta(5)(22 + N) + 14\zeta(7)(62 + N)] \right) (\mathcal{A}^*)^5, \tag{4.82}
\end{aligned}$$

²⁵After this work appeared, an independent 4-loop diagrammatic check of our results has been carried out in [151].

$$\begin{aligned}
\text{6-loops:} & \left(-\frac{572}{243}\bar{Q} + \frac{2}{279}[10191 - 64N - 2\zeta(3)(1327 + 160N) - 2\zeta(5)(1441 + 80N) \right. \\
& \left. - 70\zeta(7)(46 + N) - 21\zeta(9)(126 + N)] \right) (\mathcal{A}^*)^6. \tag{4.83}
\end{aligned}$$

It is instructive to study also the large \mathcal{A}^* limit of our results, which, according to Eq.(4.47), corresponds to the large chemical potential limit. When μ is large the massive particles decouple from the IR physics and can be integrated out. Furthermore, we can also neglect the type II Goldstone bosons since they are slow with respect to the phonon excitations $\chi_{N/2}$, which, in the large μ limit, propagate at the speed of sound $c_s = \frac{1}{\sqrt{d-1}}$. This can be seen by expanding their dispersion relation (4.57) for large μ

$$\omega_-^2(p) = \frac{1}{3}p^2 + \mathcal{O}(\mu^{-2}) . \tag{4.84}$$

In the large \mathcal{A} limit we can, therefore, describe the theory via a large charge EFT of phonons, as discussed in Sec.3.5 using RG arguments. In fact, the parameter which separate the two regimes is the chemical potential μ that controls the gap of the massive modes. We are then providing a microscopic description of the large charge EFT. Furthermore, since in the IR limit the $O(N)$ model has the same spectrum of the $U(1)$ model considered in Sec.3.5, (i.e. a single phonon mode whose universal properties are dictated by conformal symmetry), the effective action is again given by Eq.(3.56), and all the difference between the two models (i.e. the dependence on N) is contained in the non-perturbative Wilson coefficients c_i of the effective action. As a consequence, we expect the large \mathcal{A}^* limit of our result for $\Delta_{\bar{Q}}$ to take the form (3.58), which we propose again below

$$\Delta_{\bar{Q}} = \bar{Q}^{\frac{d}{d-1}} \left[\alpha_1 + \alpha_2 \bar{Q}^{\frac{-2}{d-1}} + \alpha_3 \bar{Q}^{\frac{-4}{d-1}} + \dots \right] + \bar{Q}^0 \left[\beta_0 + \beta_1 \bar{Q}^{\frac{-2}{d-1}} + \dots \right] + \dots . \tag{4.85}$$

The large \mathcal{A}^* expansion of Δ_{-1} reads

$$\bar{Q}\Delta_{-1} = \frac{3}{4g^*} \left[\frac{3}{4} \left(\frac{4g^*\bar{Q}}{3} \right)^{\frac{4}{3}} + \frac{1}{2} \left(\frac{4g^*\bar{Q}}{3} \right)^{\frac{2}{3}} + \mathcal{O}(1) \right] . \tag{4.86}$$

The large \mathcal{A} expansion of Δ_0 can be obtained as explained in [21], i.e. we approximate the sum over ℓ , evaluate Δ_0 numerically at large values of μ , and, finally, fit the results to the expected functional

form (3.58). As a result, we have

$$\Delta_0 = \left[\alpha + \frac{N+8}{48} \ln \left(\frac{4g^* \bar{Q}}{3} \right) \right] \left(\frac{4g^* \bar{Q}}{3} \right)^{\frac{4}{3}} + \left[\beta - \frac{N+8}{72} \ln \left(\frac{4g^* \bar{Q}}{3} \right) \right] \left(\frac{4g^* \bar{Q}}{3} \right)^{\frac{2}{3}} + \mathcal{O}(1), \quad (4.87)$$

where

$$\begin{aligned} \alpha &= -0.4046 - 0.0854N, \\ \beta &= -0.8218 - 0.0577N. \end{aligned} \quad (4.88)$$

The values of α and β do not appear in our publication [84], on which most of this chapter is based. Instead, they have been derived few months later by I. Jack and D. R. T. Jones in [151]²⁶. By combining Eqs.(4.86) and (4.87) and rewriting the result at the FP, we obtain

$$\begin{aligned} \Delta_{\bar{Q}} &= \frac{1}{\varepsilon} \left(\frac{4\varepsilon \bar{Q}}{N+8} \right)^{\frac{d}{d-1}} \left[\frac{3(N+8)}{16} + \varepsilon \left(\alpha + \frac{3(3N+14)}{16(N+8)} \right) + \mathcal{O}(\varepsilon^2) \right] \\ &\quad + \frac{1}{\varepsilon} \left(\frac{4\varepsilon \bar{Q}}{N+8} \right)^{\frac{d-2}{d-1}} \left[\frac{N+8}{8} + \varepsilon \left(\beta - \frac{3N+14}{8(N+8)} \right) + \mathcal{O}(\varepsilon^2) \right] + \mathcal{O}[(\varepsilon \bar{Q})^0], \end{aligned} \quad (4.89)$$

which agrees with the general form (3.58). Since the coefficients in (3.58) are combinations of the c_i Wilson coefficient of the EFT (3.56), Eq.(4.89) represents a first-principle calculation of the EFT coefficients at the leading order in the ε -expansion. Below, we compare our prediction (4.89) (with $\varepsilon = 1$) for the leading coefficient α_1 in Eq.(3.58) with the results obtained via the large N expansion (at LO in $1/N$ and $d = 3$) [137] and Monte Carlo simulations [11, 12, 130, 152]

	ε -expansion	$1/N$ -expansion	Monte Carlo	
$N = 2$	0.424	0.471	0.337	
$N = 3$	0.39	0.39	0.32	(4.90)
$N = 4$	0.368	0.333	0.301	
$N = 5$	0.35	0.30	0.29	

²⁶ However, the comparison with Monte Carlo and large N results is original and does not appear elsewhere.

The comparison is encouraging, despite the evident limitations of taking $\varepsilon = 1$, and motivates the computation of higher orders Δ_k of the large charge expansion. The first Wilson coefficient c_1 of the effective action (3.56) can be obtained from α_1 using Eq.(3.59).

4.9 How large is the charge?

It is crucial to know how large the charge has to be in order to have the $\frac{1}{\bar{Q}}$ expansion under control. In other words, at which value of \bar{Q} we expect to obtain good predictions for experiments? To partially answer this question, we conduct a heuristic analysis along the lines of [153], where the author studied the same issue in the context of the large number of flavor N_f expansion. Consider the scaling dimension at the FP for the $\varphi^{\bar{Q}}$ operators in the $U(1)$ theory in $4 - \varepsilon$ dimension

$$\Delta_{\bar{Q}} = \sum_{k=-1} \frac{1}{\bar{Q}^k} \Delta_k(\mathcal{A}) , \quad \mathcal{A} \equiv \bar{Q}\varepsilon . \quad (4.91)$$

Numerically, this expansion reads

$$\begin{aligned} \Delta_{\bar{Q}} = \bar{Q} \left[& \left(1 + 0.1\mathcal{A} - 0.02\mathcal{A}^2 + 0.008\mathcal{A}^3 - 0.0042\mathcal{A}^4 + 0.00256\mathcal{A}^5 + \dots \right) + \frac{1}{\bar{Q}} \left(-0.1\mathcal{A} \right. \right. \\ & + 0.08\mathcal{A}^2 - 0.01953\mathcal{A}^3 + 0.007697\mathcal{A}^4 - 0.003227\mathcal{A}^5 + \dots \left. \right) + \frac{1}{\bar{Q}^2} \left(-0.05\mathcal{A}^2 - 0.04175\mathcal{A}^3 \right. \\ & \left. \left. + 0.009723\mathcal{A}^4 + 0.00093\mathcal{A}^5 + \dots \right) + \frac{1}{\bar{Q}^3} \left(0.06279\mathcal{A}^3 + 0.06284\mathcal{A}^4 - 0.01067\mathcal{A}^5 + \dots \right) \right. \\ & \left. + \frac{1}{\bar{Q}^4} \left(-0.8858\mathcal{A}^4 - 0.246\mathcal{A}^5 + \dots \right) + \frac{1}{\bar{Q}^5} \left(0.268\mathcal{A}^5 + \dots \right) + \dots \right] . \end{aligned} \quad (4.92)$$

The terms up to order $\mathcal{O}(\mathcal{A}^4)$ follow from Eq.(4.80) for $N = 2$. The remaining terms have been computed in [21]. Following [153], we compare the leading terms in \mathcal{A} at each order in $\frac{1}{\bar{Q}}$, and we ask the k -th order to be strictly smaller than the $k - 1$ -th one for all $k \geq 6$ and \mathcal{A} as big as 5. The value $\mathcal{A} = 5$ marks the transition between perturbative and superfluid regimes where the expansion takes, respectively, the form of Eqs.(4.79) and (4.86)²⁷. We found out that quite large values of the charge $\bar{Q} \gtrsim 70$ are needed to control the expansion when $\mathcal{A} = 5$. If instead we just ask for the sum

²⁷ Note that a key difference between the case at hand and the large N_f expansion in gauge theories considered in [153], is that the latter has a finite radius convergence in the 't Hooft coupling, which is determined by the pole structure. Less is known about the pole structure of the large charge expansion, and we cannot naturally set an upper limit on \mathcal{A} . Thus, we instead ask to be in the perturbative regime, i.e. $\mathcal{A} \leq 5$. Notice that this is needed in order to consistently truncate every order of the expansion at the leading power of \mathcal{A} .

of all the subleading orders to be strictly smaller than the leading one, we obtain smaller values $\bar{Q} \gtrsim 6$. Of course, when $\mathcal{A} \ll 5$ both limits decrease accordingly.

Finally, notice that the large \bar{Q} perturbativity is intimately related to the suppression of the instanton contributions in the large \bar{Q} limit. In fact, they typically scale as $e^{-\frac{1}{\lambda}} = e^{-\frac{\bar{Q}}{\mathcal{A}}}$, and thus go exponentially to zero for $\bar{Q} \rightarrow \infty$ when \mathcal{A} is kept fixed. This is related to the slow (polynomial) growth of the number of Feynman diagrams which contribute to a given order of the $\frac{1}{\bar{Q}}$ expansion. This observation has been illustrated via a specific example in [154].

4.10 Cubic anisotropy

In this section, we continue the exploration of anisotropic perturbations in the $O(N)$ model by studying the spectrum of anomalous dimension in the $O(N)$ model with cubic anisotropy. The impact of the latter on the critical properties is controlled by $T_{0,4}$ [152]. In nature, this model appears in the description of critical cubic magnets [51], structural phase transitions in crystals [155], and the randomly dilute Ising model [156]. The action of the theory reads

$$\mathcal{S} = \int D^d x \left(\frac{(\partial \phi_i)^2}{2} + \frac{(4\pi)^2}{4!} V_{ijkl} \phi_i \phi_j \phi_k \phi_l \right) , \quad (4.93)$$

where

$$V_{ijkl} = \frac{g_1}{3} (\delta_{ij} \delta_{kl} + \delta_{il} \delta_{kj} + \delta_{ik} \delta_{jl}) + g_2 \delta_{ijkl} , \quad (4.94)$$

with

$$\delta_{ijkl} = \begin{cases} 1, & \text{when } i = j = k = l , \\ 0, & \text{otherwise .} \end{cases} \quad (4.95)$$

When $g_2 = 0$, we re-obtain the $O(N)$ action (4.6). On the other hand, the g_2 coupling breaks the $O(N)$ symmetry to the hypercubic group $H_N \subset O(N)$, realized as the symmetry group of an N -dimensional hypercube.

An RG analysis of the model reveals that, at the 1-loop level, it exhibits four FPs

$$(g_1^G, g_2^G) = (0, 0) , \quad (g_1^I, g_2^I) = \left(0, \frac{\epsilon}{3} \right) ,$$

$$(g_1^O, g_2^O) = \left(\frac{3\epsilon}{N+8}, 0 \right), \quad (g_1^C, g_2^C) = \left(\frac{\epsilon}{N}, \frac{(N-4)}{3N}\epsilon \right). \quad (4.96)$$

There is a Gaussian FP, an Ising-like FP (N decoupled Ising models), and an $O(N)$ -symmetric FP. The fourth one is the so-called *cubic fixed point* and is described by an H_N -invariant CFT.

Note that for $N = N_c = 4$ the cubic FP reduces to the $O(N)$ symmetric one, while, for $N \rightarrow \infty$, it coincides with the Ising one. When $N = 1$, there is only one coupling constant $g_1 + g_2$, and the cubic FP becomes non-interacting.

Moreover, when $N = 2$, the interaction term is invariant under a combined $\frac{\pi}{4}$ rotation of the fields [132],

$$\phi'_1 = \frac{\phi_1 + \phi_2}{\sqrt{2}}, \quad \phi'_2 = \frac{\phi_1 - \phi_2}{\sqrt{2}}, \quad (4.97)$$

and redefinition of the coupling constants

$$g'_1 = g_1 + \frac{3}{2}g_2, \quad g'_2 = -g_2. \quad (4.98)$$

This turns the cubic FP into the Ising one.

The limits described above will be used to test our results.

The value of N_c such that $O(N)$ and cubic FPs coincide, determines the stability of the cubic FP with important implication on the critical behaviour of cubic $N = 3$ magnets. In fact, the cubic critical regime is realized only when $N > N_c$. Otherwise, the critical system belongs to the Heisenberg ($O(3)$) universality class. Since $N_c \sim 3$, the existence of magnets in the cubic universality class has been discussed for a long time [132, 152, 157]. Recently, this issue has been settled, in favor of a stable cubic FP controlling the critical behaviour, via a bootstrap analysis in [158].

Present-day results on the H_N model include the beta function and some critical exponents at the 6-loops level in the ϵ -expansion [157, 159]. Recently, this theory has been also explored non-perturbatively via the conformal bootstrap method [158, 160–163]. Nevertheless, little is known about the operator content of the hypercubic model. The present section aims to fill this gap. To this end, we consider composite operators with arbitrarily large classical dimension n but no derivatives, and we compute the entire spectrum of 1-loop anomalous dimensions for such operators. Since the global symmetry group is discrete, we have to momentarily leave aside the large charge method discussed so far. Instead, it is well-known that 1-loop anomalous dimensions can be calculated by

solving a diagonalization problem involving only free-theory CFT data [52]. We explicitly illustrate this point by making use of a recently-developed method [164, 165] combining the EOM with the conformal constraints. The idea is to use the EOM inside the three-point function $\langle \square \phi_i S_n S_{n+1} \rangle$ to rewrite it as

$$\langle \square \phi_i S_n S_{n+1} \rangle = \frac{(4\pi)^2}{3!} \langle (g_1 \phi_i \phi^2 + g_2 \phi_i^3) S_n S_{n+1} \rangle , \quad (4.99)$$

where S_n is a composite operator with classical dimension (in $d=4$) n and scaling dimension

$$\Delta_{S_n} = n \left(1 - \frac{\epsilon}{2} \right) + \gamma_{S_n} \epsilon + \mathcal{O}(\epsilon^2) , \quad (4.100)$$

with γ_{S_n} defined as the coefficient of the 1-loop anomalous dimensions. As we saw in Chap.2, conformal symmetry fixes entirely the form of the three-point functions. Then Eq.(4.99) can be cast as an eigenvalues equation for γ_{S_n}

$$\gamma_{S_n} S_{i_1, i_2, \dots, i_n} = \frac{n(n-1)}{2} V_{j_1, j_2, (i_1, i_2) S_{i_3, \dots, i_n}, j_1, j_2} . \quad (4.101)$$

Here, V_{j_1, j_2, i_1, i_2} is the tensor defined in Eq.(4.94), while the tensors S are given by

$$S_{i_1, i_2, \dots, i_n} = \frac{1}{n!} \partial_{i_1} \partial_{i_2} \dots \partial_{i_n} S_n . \quad (4.102)$$

Finally, it is convenient to rewrite the eigenvalue equation as

$$\mathcal{D} S_n = \gamma_{S_n} S_n , \quad (4.103)$$

with

$$\mathcal{D} = \frac{1}{3N} \left(\frac{\phi^2 \partial^2}{2} + (\phi \cdot \partial)^2 - \phi \cdot \partial + \frac{N-4}{2} \sum_i \phi_i^2 \partial_i^2 \right) . \quad (4.104)$$

The next step is the explicit construction of the S_n operators.

4.10.1 Composite operators in the H_N model

Here, we construct composite operators with no derivatives and transforming according to the H_N irreducible representations. Our construction builds upon the results obtained in [166–168].

To work out the irreducible representations of H_N , we use that $H_N = S_N \ltimes \mathcal{Z}_2^N$, and we start by building the irreps of \mathcal{Z}_2^N . Labeling as $[1^2]$ and $[2]$ the two irreducible representations of \mathcal{Z}_2 , the irreps of \mathcal{Z}_2^N are given by

$$[2]^{\otimes \alpha} \otimes [1^2]^{\otimes \beta}, \quad \alpha + \beta = N. \quad (4.105)$$

Then we take the wreath product $S_N \ltimes \mathcal{Z}_2^N$ by splitting the symmetric group S_N into direct products $S_\alpha \times S_\beta$. Finally, we obtain the irreducible representations of H_N by multiplying these products with the corresponding irreps of \mathcal{Z}_2^N in Eq.(4.105) [169].

The main consequence of the above construction is that we can represent the irreducible representations of H_N as double-partitions of N , (α, β) which can be depicted as ordered pairs of Young tableau with, respectively, α and β boxes [168, 170]. The left (*right*) tableau represents α (β) objects, even (*odd*) under \mathcal{Z}_2 , and transforming according to S_α (S_β) under the action of the symmetric group.

For instance, the irreducible representations of \mathcal{Z}_2^3 are

$$[2]^{\otimes 3}, [2]^{\otimes 2} \otimes [1^2], [2] \otimes [1^2]^{\otimes 2}, [1^2]^{\otimes 3}. \quad (4.106)$$

Multiplying them, respectively, with the irreducible representations of \mathcal{S}_3 , $\mathcal{S}_2 \times \mathcal{S}_1$, $\mathcal{S}_1 \times \mathcal{S}_2$, and \mathcal{S}_3 , we obtain the ten irreducible representations of H_3

$$\begin{aligned} ([2]^{\otimes 3} \otimes \mathbf{S}_3) : & (\square \square \square, \emptyset), (\begin{array}{|c|c|}\hline \square & \square \\ \hline \end{array}, \emptyset), (\begin{array}{|c|}\hline \square \\ \hline \end{array}, \emptyset); \quad ([2]^{\otimes 2} \otimes [1^2] \otimes \mathbf{S}_2 \times \mathbf{S}_1) : (\square \square, \square), (\begin{array}{|c|c|}\hline \square & \square \\ \hline \end{array}, \square); \\ ([1^2]^{\otimes 3} \otimes \mathbf{S}_3) : & (\emptyset, \square \square \square), (\emptyset, \begin{array}{|c|c|}\hline \square & \square \\ \hline \end{array}), (\emptyset, \begin{array}{|c|}\hline \square \\ \hline \end{array}); \quad ([2] \otimes [1^2]^{\otimes 2} \otimes \mathbf{S}_1 \times \mathbf{S}_2) : (\square, \square \square), (\square, \begin{array}{|c|}\hline \square \\ \hline \end{array}), \end{aligned} \quad (4.107)$$

where " \emptyset " stays for the empty partition.

The dimension of the (α, β) representation is [170]

$$\dim(\alpha, \beta) = \binom{N}{\alpha} \times \dim(\alpha) \times \dim(\beta), \quad (4.108)$$

with $\dim(\alpha)$ ($\dim(\beta)$) the dimension of the corresponding irrep of S_α (S_β) which can be easily

obtained through the hook's rule.

The defining N -dimensional vector representation is

$$\phi_i = (N-1, 1) = \left(\underbrace{\square \square \dots \square}_{N-1}, \square i \right). \quad (4.109)$$

The decomposition of the tensor product of $(N-1, 1)$ with an arbitrary representation (α, β) is given by

$$(N-1, 1) \otimes (\alpha, \beta) = \sum_{\alpha^+, \beta^-} (\alpha^+, \beta^-) \oplus \sum_{\alpha^-, \beta^+} (\alpha^-, \beta^+), \quad (4.110)$$

where α^+ (α^-) is obtained by moving one box from β to α (α to β). The same procedure applies to β^+ and to β^- . For instance

$$\left(\underbrace{\square \square \dots}_{N-1}, \square \right) \otimes \left(\underbrace{\square \square \dots}_{N-1}, \square \right) = \left(\underbrace{\square \square \dots}_{N}, \emptyset \right) \oplus \left(\underbrace{\square \square \dots}_{N-2}, \emptyset \right) \oplus \left(\underbrace{\square \square \dots}_{N-2}, \square \square \right) \oplus \left(\underbrace{\square \square \dots}_{N-2}, \square \right). \quad (4.111)$$

To construct composite H_N operators with CSD n and no derivatives we start by listing the corresponding H_N -irreps, which are obtained by computing n times the tensor product of the defining representation (4.109) with itself.

The resulting bi-tableaux can be divided into two families. The members of the first family are those bi-tableaux which do not appear at smaller n . These representations correspond to a *unique* composite operator with CSD n , which is the MSD operator transforming in the given representation of H_N . Instead, in the second family fall all the bi-tableaux that already appeared at lower n . In such a case, it is possible to associate more than one operator with CSD n to the same irrep, and it will be, therefore, necessary to solve the mixing among them.

Consider a *unique* composite operator in the representation $(\alpha = N, \beta = 0)$. For instance

$$\left(\begin{array}{|c|c|c|} \hline & & \\ \hline & & \\ \hline & & \\ \hline \end{array} \dots \square, \emptyset \right). \quad (4.112)$$

We begin by filling the tableau with indices

$$\left(\begin{array}{|c|c|c|} \hline \mu_1 & \mu_2 & \dots & \mu_s \\ \hline i & j & & \\ \hline k & & & \\ \hline \end{array} \dots \square, \emptyset \right), \quad (4.113)$$

on which we impose the condition $i \neq j \neq k \neq \mu_1 \neq \mu_2 \neq \dots \neq \mu_s \dots$. In fact, since we are considering MSD operators, we cannot contract any pairs of indices.

We then write an indexed field raised to the *zeroth* power for every box in the first row; indexed fields raised to the *second* power to the boxes in the second row and so on, with increasing *even* powers of the fields for subsequent rows.

Finally, we impose the symmetry properties of the given tableau on the indices. For our example, this leads to ($n = 8$ in this case)

$$\begin{aligned} \left(\begin{array}{|c|c|c|} \hline \mu_1 & \mu_2 & \dots & \mu_s \\ \hline i & j & & \\ \hline k & & & \\ \hline \end{array}, \emptyset \right) &= (\phi_{[k}^4 \phi_i^2 \phi_{\mu_1]}^0) \cdot (\phi_{[j}^2 \phi_{\mu_2]}^0) \cdot \phi_{\mu_3}^0 \phi_{\mu_4}^0 \dots \phi_{\mu_s}^0 = \\ &= (\phi_k^4 \phi_i^2 + \phi_{\mu_1}^4 \phi_k^2 + \phi_i^4 \phi_{\mu_1}^2 - \phi_k^4 \phi_{\mu_1}^2 - \phi_i^4 \phi_k^2 - \phi_{\mu_1}^4 \phi_i^2) (\phi_j^2 - \phi_{\mu_2}^2) \quad i \neq j \neq k \neq \mu_1 \neq \mu_2. \end{aligned} \quad (4.114)$$

The same rules apply also to the right partition β , but now considering *odd* powers of the fields²⁸.

The most general Young diagram has k different "types" of columns (with a different number of boxes) that we label with the index i . Each type of column can occur with multiplicity p_i . Hence, we can write the *unique* operator corresponding to the most general bi-tableau as

$$H_{n, \{m_i\}, \{p_i\}} = \prod_{i=1}^k (\phi_{[\mu_1^i}^{m_i} \phi_{\mu_2^i]}^{m_i-2} \phi_{\mu_3^i]}^{m_i-4} \dots \phi_{\mu_{q_i}^i]}^M)^{p_i} \quad \mu_1^i \neq \mu_2^i \neq \dots \neq \mu_{q_i}^i, \quad (4.115)$$

where we labeled the highest power of the field in a given column by m_i and

$$M = \begin{cases} 0 & \text{if } m_i \text{ is even} \\ 1 & \text{if } m_i \text{ is odd.} \end{cases} \quad (4.116)$$

We now consider the second family of bi-tableaux, i.e. those which "reappeared" at the level n and correspond to non-MSD operators. In this case, we can build more than one operator with the same CSD and belonging to the same irrep. The guiding principle is that everything that can mix will do it. Then these operators can be found by writing the corresponding *unique* MSD operator

²⁸If a bi-tableau appears for the first time at a value of n too small to allow the construction of the operator here described, then the corresponding operator requires derivatives to be constructed.

by using the procedure described above and multiplying the result with the power of ϕ^2 needed to reach CSD n . For example, for $n = 6$, we have

$$\left(\underbrace{\begin{array}{|c|c|c|c|} \hline & & & \\ \hline & & & \\ \hline \end{array} \dots, \emptyset} _N \right) = (\phi^2)^2(\phi_i^2 - \phi_j^2), \quad i \neq j.$$

Then one has to "redistribute" the ϕ^2 factors through the rest of the tensor in all the possible ways as follows:

$$\left(\underbrace{\begin{array}{|c|c|c|c|} \hline & & & \\ \hline & & & \\ \hline \end{array} \dots, \emptyset} _N \right) = \begin{cases} (\phi^2)^2(\phi_i^2 - \phi_j^2) \\ (\phi^2)(\phi_i^4 - \phi_j^4) \quad i \neq j \\ (\phi_i^6 - \phi_j^6) \end{cases}$$

Eventually, we need to consider also the mixing between powers of ϕ^2 and the other H_N -scalars with the same CSD. These are given by products and powers of all the operators of the form

$$\sum_i \phi_i^2 = \phi^2, \sum_i \phi_i^4, \sum_i \phi_i^6, \dots, \sum_i \phi_i^n. \quad (4.117)$$

In our example, $(\phi^2)^2$ mixes with $\sum_i \phi_i^4$, and we have to add one more operator to our list, obtaining

$$\left(\underbrace{\begin{array}{|c|c|c|c|} \hline & & & \\ \hline & & & \\ \hline \end{array} \dots, \emptyset} _N \right) = \begin{cases} \sum_k \phi_k^4(\phi_i^2 - \phi_j^2) \\ (\phi^2)^2(\phi_i^2 - \phi_j^2) \quad i \neq j \\ (\phi^2)(\phi_i^4 - \phi_j^4) \\ (\phi_i^6 - \phi_j^6) \end{cases}$$

This procedure provides a basis of operators with the same CSD and symmetry properties. By acting on these operators with \mathcal{D} defined in Eq.(4.104), one obtains the mixing matrix that needs to be diagonalized in order to find the energy eigenstates, i.e. the operators with a definite scaling dimension.

4.10.2 Spectrum of anomalous dimensions in hypercubic theories

Using the above construction, one can build all the composite H_N operators with no derivatives. Here, we give explicit results for their anomalous dimensions to 1-loop. We check our results by considering the cases $N = 1, 2, 4, \infty$ previously discussed.

Since we are considering operators without derivatives, the $O(N)$ operators that we recover when $N = 4$ are again the $T_{p,\bar{Q}}$ introduced in Eq.(4.13), which have CSD $n = \bar{Q} + 2p$ and 1-loop anomalous dimensions given by [171, 172]

$$\gamma_{\bar{Q},p} = \frac{\bar{Q}(\bar{Q}-1) + p(N+6(p+\bar{Q})-4)}{N+8}. \quad (4.118)$$

Instead, in the Ising model, which is obtained for $N = 2$ and $N = \infty$, all the H_N representations collapse to the ϕ^n operators, whose 1-loop anomalous dimension reads

$$\gamma_n = \frac{n(n-1)}{6}. \quad (4.119)$$

In full analogy with (4.118) and (4.119), there is an infinite family of H_N composite operators whose 1-loop anomalous dimensions can be written in close form. These are the MSD operators. In fact, by plugging the family of operators defined in Eq.(4.115), $H_{n,\{m_i\},\{p_i\}}$, into the eigenvalue equation (4.103), we have

$$\gamma_{n,\{m_i\},\{p_i\}} = \frac{1}{6N} \left(2n(n-1) + (N-4) \sum_{i=1}^k p_i [m_i(m_i-1) + (m_i-2)(m_i-3) + \dots] \right). \quad (4.120)$$

For $N = 4$, Eq.(4.120) reduces to Eq.(4.118) with $p = 0$.

Let us proceed with a couple of examples. First, consider the family of bi-tableaux with one row, that is $k = 1$, $m_i = 1$, and $p_i = p = n$

$$(\underbrace{\square \square \square \square \dots}_{N-p}, \underbrace{\square \square \square \square \dots}_p). \quad (4.121)$$

The corresponding operators are

$$\phi_{\mu_1} \phi_{\mu_2} \dots \phi_{\mu_p} , \quad \mu_1 \neq \mu_2 \neq \dots \neq \mu_p . \quad (4.122)$$

Using Eqs.(4.108) and (4.120), one promptly obtains

$$\dim = \binom{N}{n} , \quad \gamma_n = \frac{n(n-1)}{3N} . \quad (4.123)$$

We now move to the family of bi-tableau with two rows, i.e. $k = 3$, $m_i = \{1, 2, 3\}$ and $p_i = \{p_1, p_2, p_3\}$. The first and second rows of the left (*right*) partition have, respectively, $N - p_1 - p_2 - p_3$ and p_2 (p_1 and p_3) boxes. We can write the related operators as

$$\underbrace{\phi_{\mu_1} \phi_{\mu_2} \dots \phi_{\mu_{p_1}}}_{p_1 \text{ terms}} \underbrace{(\phi_{\mu_{p_1+1}}^2 - \phi_{\mu_{p_1+2}}^2)(\phi_{\mu_{p_1+3}}^2 - \phi_{\mu_{p_1+4}}^2) \dots (\phi_{\mu_{p_1+2p_2-1}}^2 - \phi_{\mu_{p_1+2p_2}}^2)}_{p_2 \text{ terms}} \\ \times \underbrace{(\phi_{\mu_{p_1+2p_2+1}}^3 \phi_{\mu_{p_1+2p_2+2}} - \phi_{\mu_{p_1+2p_2+2}}^3 \phi_{\mu_{p_1+2p_2+1}}) \dots (\phi_{\mu_{q-1}}^3 \phi_{\mu_q} - \phi_{\mu_q}^3 \phi_{\mu_{q-1}})}_{p_3 \text{ terms}} , \quad \mu_1 \neq \mu_2 \neq \dots \neq \mu_q , \quad (4.124)$$

where

$$q = p_1 + 2p_2 + 2p_3 , \quad n = p_1 + 2p_2 + 4p_3 . \quad (4.125)$$

In this case, Eqs.(4.108) and (4.120) give

$$\dim = \binom{N}{p_2} \binom{N - p_2}{2p_3 + p_1} \binom{2p_3 + p_1}{p_3 + p_1} \frac{(N - p_1 - 2p_3 - 2p_2 + 1)(p_1 + 1)}{(N - p_1 - 2p_3 - p_2 + 1)(p_1 + p_3 + 1)} , \quad (4.126)$$

and

$$\gamma_{n, p_1, p_2} = \frac{4n(n-1) + (N-4)(3n-2p_2-3p_1)}{12N} . \quad (4.127)$$

We may now proceed by considering bi-tableaux with three rows, four rows, and so on. In short, Eq.(4.120) gives the anomalous dimension of all the MSD operators (i.e. all the operators which, for a given irreducible representation, have the minimal scaling dimension).

Moreover, the procedure presented here allows the computation of γ for *all* composite operators

with no derivatives, not only the MSD ones. Below, we present explicit results up to CSD $n = 5$. All the indices of the operators are understood to assume different values, e.g. when we write $\phi_i \phi_j$, we imply $i \neq j$.

For the case $n = 2$ we have

$$\begin{aligned} \dim(\underbrace{\square \square \square \dots}_{N-2}, \square \square) &= \binom{N}{2} & \phi_i \phi_j & \gamma = \frac{2}{3N} \\ \dim(\underbrace{\square \square \square \dots}_{N}, \emptyset) &= (N-1) & \phi_i^2 - \phi_j^2 & \gamma = \frac{N-2}{3N} \\ \dim(\underbrace{\square \square \square \dots}_{N}, \emptyset) &= 1 & \phi^2 & \gamma = \frac{2(N-1)}{3N}. \end{aligned}$$

These results have been already obtained in [163] via the conformal bootstrap method.

The 1-loop anomalous dimensions of the operators with CSD $n = 3$ are

$$\begin{aligned} \dim(\underbrace{\square \square \square \dots}_{N-3}, \square \square \square) &= \binom{N}{3} & \phi_i \phi_j \phi_k & \gamma = \frac{2}{N} \\ \dim(\underbrace{\square \square \square \dots}_{N-1}, \square) &= N(N-2) & \phi_i(\phi_j^2 - \phi_k^2) & \gamma = \frac{2+N}{3N} \\ \dim(\underbrace{\square \square \square \dots}_{N-1}, \square) &= N & \phi_i \phi^2 - 2\phi_i^3 & \gamma = \frac{2(N-1)}{3N} \\ \dim(\underbrace{\square \square \square \dots}_{N-1}, \square) &= N & \phi_i \phi^2 + \frac{N-4}{3} \phi_i^3 & \gamma = 1. \end{aligned}$$

To the best of our knowledge, the results above are new. When $N = 4$ we obtain the corresponding $O(N)$ results Eq.(4.118) with $p = 0$ and $\bar{Q} = 3$ for the first three operators and $p = \bar{Q} = 1$ for the last one. For $N = 2$ and $N = \infty$ only the last operator survives, and we obtain Eq.(4.119). Finally, for $N = 1$, all the operators vanish except the third one, for which we obtain the free theory result $\gamma = 0$.

For the operators with CSD $n = 4$, we have

$$\begin{aligned} \phi_i \phi_j \phi_k \phi_l & & \gamma = \frac{4}{N} \\ (\phi_i \phi_j^3 - \phi_j \phi_i^3) & & \gamma = 1 \\ (\phi_i^2 - \phi_j^2)(\phi_k^2 - \phi_l^2) & & \gamma = \frac{2(N+2)}{3N} \end{aligned}$$

$$\phi_i \phi_j (\phi_k^2 - \phi_l^2)$$

$$\gamma = \frac{N+8}{3N}$$

$$\frac{1}{12}(12 - N + \sqrt{N^2 + 24N - 48})(\phi_i \phi_j \phi^2) + \phi_i \phi_j^3 + \phi_j \phi_i^3 \quad \gamma = \frac{12 + 5N + \sqrt{N^2 + 24N - 48}}{6N}$$

$$\frac{1}{12}(12 - N - \sqrt{N^2 + 24N - 48})(\phi_i \phi_j \phi^2) + \phi_i \phi_j^3 + \phi_j \phi_i^3 \quad \gamma = \frac{12 + 5N - \sqrt{N^2 + 24N - 48}}{6N}$$

$$\frac{4-N}{2}(\phi_i^2 - \phi_j^2)\phi^2 + \phi_i^4 - \phi_j^4 \quad \gamma = 1$$

$$\frac{4}{3}(\phi_i^2 - \phi_j^2)\phi^2 + \phi_i^4 - \phi_j^4 \quad \gamma = \frac{2(3N-2)}{3N}$$

$$(\phi^2)^2 - 2 \sum_{i=1}^N \phi_i^4 \quad \gamma = \frac{4(N-1)}{3N}$$

$$(\phi^2)^2 + \frac{N-4}{3} \sum_{i=1}^N \phi_i^4 \quad \gamma = 2 .$$

These results confirm those obtained in [173]. Finally, for $n = 5$, we obtain

$$\phi_i \phi_j \phi_k \phi_l \phi_m \quad \gamma = \frac{20}{3N}$$

$$\phi_i (\phi_j^2 - \phi_k^2) (\phi_l^2 - \phi_m^2) \quad \gamma = \frac{2(N+6)}{3N}$$

$$\phi_i (\phi_j^3 \phi_k - \phi_k^3 \phi_j) \quad \gamma = \frac{3N+8}{3N}$$

$$\phi_i \phi_j \phi_k (\phi_l^2 - \phi_m^2) \quad \gamma = \frac{16+N}{3N}$$

$$\begin{pmatrix} \phi^2 \phi_i \phi_j \phi_k \\ \phi_i^3 \phi_j \phi_k + perm \end{pmatrix} \quad \gamma = \frac{30 + 5N \pm \sqrt{(46+N)(N-2)}}{6N}$$

$$\begin{aligned}
& \begin{pmatrix} \phi_i^2 \phi_i (\phi_j^2 - \phi_k^2) \\ \phi_i^3 (\phi_j^2 - \phi_k^2) \\ \phi_i (\phi_j^4 - \phi_k^4) \end{pmatrix} \quad \gamma = \frac{1}{3N} \begin{pmatrix} 3(N+6) & 3 & 6 \\ 2(N-4) & 4(N+1) & 0 \\ 4(N-4) & 0 & 2(3N-2) \end{pmatrix} \\
& \begin{pmatrix} \phi_i (\phi^2)^2 \\ \phi_i^5 \\ \phi_i^2 \phi_i^3 \\ \phi_i \sum_{j=1}^N \phi_j^4 \end{pmatrix} \quad \gamma = \frac{1}{3N} \begin{pmatrix} 4(N+5) & 0 & 3 & 6 \\ 0 & 10(N-2) & 6(N-4) & 4(N-4) \\ 4(N-4) & 10 & 5(N+2) & 4 \\ 4(N-4) & 0 & 0 & 2(3N-2) \end{pmatrix}.
\end{aligned}$$

The consistency checks for $N = 1, 2, 4, \infty$ are passed as in the $n = 3$ case. We are not aware of results for $n \geq 5$ in the literature.

We conclude this chapter with an intriguing feature of the spectrum of anomalous dimensions in the hypercubic model. Consider the sum of the 1-loop anomalous dimensions of order n operators, S_n , weighted by the dimensions of the corresponding H_N -irreps d_{S_n} , that is

$$W_n = \sum_{S_n} d_{S_n} \gamma_{S_n}, \quad (4.128)$$

where the sum runs over all the irreducible representations appearing at the level n . Clearly, the Gaussian limit requires $W_n \propto N - 1$. Moreover, the values of W_n show an intriguing pattern

$$\begin{aligned}
W_2 &= \frac{2}{3}(N-1), & W_3 &= \frac{2}{3}(N-1)(N+2), \\
W_4 &= \frac{1}{3}(N-1)(N+2)(N+3), & W_5 &= \frac{1}{9}(N-1)(N+2)(N+3)(N+4),
\end{aligned} \quad (4.129)$$

suggesting the existence of a general formula for W_n . After [85] was published, a general expression for W_n (or better, for a related quantity) has been derived from first principles in [174].

5 CHARGING A QUARTIC/CUBIC DUALITY

5.1 The $O(N)$ model in $4 < d < 6$

In the previous chapter, we investigated the $g(\phi_a\phi_a)^2$ $O(N)$ theory in $4 - \varepsilon$ dimensions. Instead, the goal of the present chapter is to extend our results above four dimensions. At first sight, this idea may sound weird as in $d > 4$ the quartic interaction becomes RG irrelevant, resulting in trivial IR physics. However, in the large N expansion, it can be shown that in the UV the model flows to an interacting FP, which makes the theory, at least at large N , non-perturbatively renormalizable [30].

The idea that a theory may be UV completed by the emergence of a nontrivial FP takes the name of *asymptotic safety* (AS) and has been firstly proposed long ago by S. Weinberg as a possible scenario for quantum gravity [81]. The existence of interacting UV FP in gravity is in general investigated through functional RG methods, which, over the course of the years, provided intriguing results supporting it [82, 175–178]. However, critiques to the AS program, or better to its actual practice, have sometimes been raised in the literature [179, 180]. Recently, the emergence of an interacting UV FP has been explored also in four-dimensional Standard model-like theories [35, 181]. In the light of the above, it is, therefore, of general interest to explore realizations of the AS scenario in non-gravity theories such as the one at hand²⁹.

In parallel, it has been pointed out that d -dimensional $O(N)$ CFTs can have a holographic description in terms of Vasiliev higher-spin theories in AdS_{d+1} [31, 183, 184]. In particular, the AdS_6 dual of the critical $d = 5$ quartic model (4.6) was explored in [32].

The scaling dimension of the $\phi_a\phi_a$ operator is $2 + \mathcal{O}(1/N)$, and thus it violates the unitarity bound (2.16) in $d > 6$. We will then focus on $4 < d < 6$, where the UV CFT might be unitary. In this range, the $O(N)$ model is usually investigated via the large N expansion, which is generated by performing a Hubbard-Stratonovich transformation, which turns the Lagrangian Eq.(4.6) in

$$S = \int d^d x \left(\frac{1}{2} (\partial\phi_a)^2 + \frac{1}{2} \sigma \phi_a \phi_a - \frac{3\sigma^2}{2g_0(4\pi)^2} \right), \quad (5.1)$$

where we introduced an auxiliary field σ that can be integrated out via its EOM $\sigma = \frac{(4\pi)^2 g_0}{6} \phi_i \phi_i$ to

²⁹ Interestingly, also Einstein gravity, when coupled to N matter fields, develops a UV interacting FP at large enough N in $2 < d < 4$ [182].

come back to the original action (4.6). It can be shown that at the critical point we can neglect the last term and we are left with the following action [185]

$$S_{\text{crit}} = \int d^d x \left(\frac{1}{2} (\partial \phi_a)^2 + \frac{1}{2\sqrt{N}} \sigma \phi_a \phi_a \right) , \quad (5.2)$$

where we have rescaled σ as $\sigma \rightarrow \frac{\sigma}{\sqrt{N}}$. The $1/N$ expansion is then obtained by integrating out the fields ϕ_a which appear quadratic in the action.

In [33], the authors conjectured an alternative UV-complete description of the quartic $O(N)$ model given by a theory with $N+1$ fields, $O(N)$ symmetry, and cubic potential, which is described by the Lagrangian

$$\mathcal{L} = \frac{1}{2} (\partial \phi_a)^2 + \frac{1}{2} (\partial \eta)^2 + \frac{g_0}{2} \eta (\phi_a)^2 + \frac{h_0}{6} \eta^3 , \quad (5.3)$$

where ϕ_a is again an $O(N)$ vector. This model is usually studied near its upper critical dimension, $d = 6$, where the infrared dynamics become free. In $d = 6 - \varepsilon$, the one-loop beta functions of the model read

$$\beta_1 = -\frac{\varepsilon}{2} g + \frac{(N-8)g^3 - 12g^2h + gh^2}{12(4\pi)^3} , \quad \beta_2 = -\frac{\varepsilon}{2} h + \frac{-4Ng^3 + Ng^2h - 3h^3}{4(4\pi)^3} , \quad (5.4)$$

and at LO in large N simplify as

$$\beta_1 = -\frac{\varepsilon}{2} g + \frac{Ng^3}{12(4\pi)^3} , \quad \beta_2 = -\frac{\varepsilon}{2} h + \frac{-4Ng^3 + Ng^2h}{4(4\pi)^3} . \quad (5.5)$$

The FPs have been computed at the four-loop level in [186]

$$g^* \equiv \sqrt{\frac{6\varepsilon(4\pi)^3}{N}} x , \quad h^* \equiv 6\sqrt{\frac{6\varepsilon(4\pi)^3}{N}} y , \quad (5.6)$$

where

$$\begin{aligned} x &= 1 + \frac{22}{N} + \frac{726}{N^2} - \frac{326180}{N^3} + \dots + \left(-\frac{155}{6N} - \frac{1705}{N^2} + \frac{912545}{N^3} + \dots \right) \varepsilon \\ &+ \left(\frac{1777}{144N} + \frac{29093/36 - 1170\zeta(3)}{N^2} + \dots \right) \varepsilon^2 + \mathcal{O}(\varepsilon^3) , \end{aligned} \quad (5.7)$$

$$y = 1 + \frac{162}{N} + \frac{68766}{N^2} + \frac{41224420}{N^3} + \dots + \left(-\frac{215}{2N} - \frac{86335}{N^2} - \frac{75722265}{N^3} + \dots \right) \varepsilon + \left(\frac{2781}{48N} + \frac{270911 - 157140\zeta(3)}{6N^2} + \dots \right) \varepsilon^2 + \mathcal{O}(\varepsilon^3). \quad (5.8)$$

The critical value of N above which this FP exists and gives rise to a unitary CFT is an interesting open question. From the four-loop beta functions, it can be derived that for $\varepsilon = 1$ we have $N_{\text{crit}} \approx 400$.

In proposing the equivalence of the critical quartic (4.6) and cubic (5.3) $O(N)$ theories, Ref. [33], showed that the scaling dimensions of the ϕ_a and η operators at the FP strikingly match those of the ϕ_a and σ field in the quartic $O(N)$ model. This analysis has been later extended to the three-loop level in [34]. Notice that the manifest instability of the cubic potential is reflected by the fact that in $4 + \varepsilon$ dimensions, the UV FP trivially obtained by analytically continuing Eq.(4.11) to negative ε and occurs at a negative value of g . However, the FP theory may be metastable, at least at large enough N [33].

The instability is realized by instantonic effects that, in the $O(N)$ quartic model, give rise to complex scaling dimensions. At large N , the imaginary parts are exponentially suppressed as $e^{-Nf(d)}$, where $f(d)$ is given by the free energy of a conformal scalar on S^{d-2} [187]

$$f(d) = \frac{1}{\sin(\pi d/2)\Gamma(d-1)} \int_0^1 dx x \sin(\pi x) \Gamma\left(\frac{d}{2} + x - 1\right) \Gamma\left(\frac{d}{2} - x - 1\right). \quad (5.9)$$

The function $f(d)$ is shown in Fig.10.

In [187], it was shown that in $6 - \varepsilon$ dimensions, the instantonic corrections to the scaling dimensions in the cubic and the quartic theory match, providing another non-trivial test of the duality. Notice that, in general, the cubic theory exhibits a larger universality class, and only by further fine-tuning the theory to a critical manifold it is possible to reach the universality class of the quartic model.

In this chapter, we use the large charge expansion to non-trivially test the equivalence between the two CFTs by computing the scaling dimensions for the whole family of charge \bar{Q} MSD $O(N)$ operators $T_{0,\bar{Q}}$ defined in Eq.(4.13) in the cubic model and comparing with the existing $O(N)$ lit-

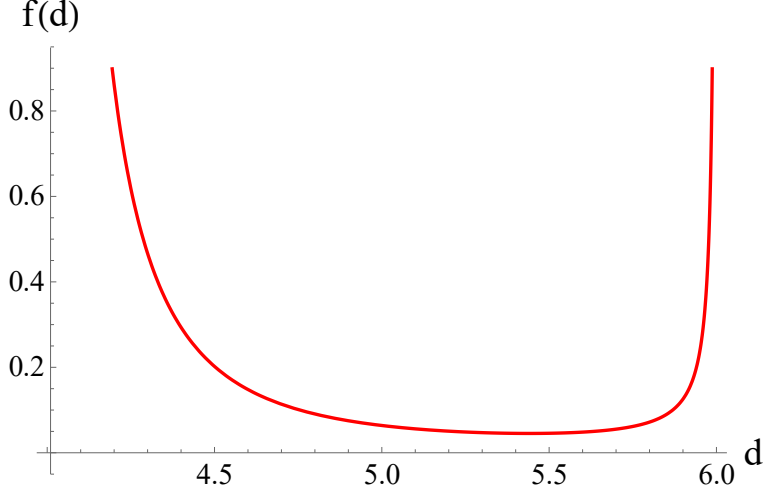


Figure 10: The instantonic function $f(d)$.

erature. The large charge expansion allows comparing terms at arbitrarily high perturbative orders providing non-trivial insights about the dual picture.

To this end, we begin by reviewing large N results regarding the critical $O(N)$ quartic model in $4 < d < 6$. $T_{0,1}$ is the fundamental ϕ_a field. Its scaling dimension in $6 - \varepsilon$ reads [186]

$$\tilde{\Delta}_\phi = 2 - \frac{\varepsilon}{2} + \left(\frac{1}{N} + \frac{44}{N^2} + \frac{1936}{N^3} + \dots \right) \varepsilon + \left(-\frac{11}{12N} - \frac{835}{6N^2} - \frac{16352}{N^3} + \dots \right) \varepsilon^2 + \mathcal{O}(\varepsilon^3) , \quad (5.10)$$

We use the "tilde"s to denote the scaling dimensions computed in the quartic theory.

The scaling dimension of the $T_{0,\bar{Q}}$ operators has been computed for arbitrary \bar{Q} at LO ($\frac{1}{N}$) in the large N expansion [188]

$$\tilde{\Delta}_{\bar{Q}} = \left(\frac{d}{2} - 1 \right) \bar{Q} - \frac{2^{d-3} d \sin\left(\frac{\pi d}{2}\right) \Gamma\left(\frac{d-1}{2}\right)}{\pi^{3/2} \Gamma\left(\frac{d}{2} + 1\right)} \frac{\bar{Q}(\bar{Q}-2) + \frac{4\bar{Q}}{d}}{N} + \mathcal{O}\left(\frac{1}{N^2}\right) , \quad (5.11)$$

and in $d = 6 - \varepsilon$ reads

$$\tilde{\Delta}_{\bar{Q}} = 2\bar{Q} - \frac{\varepsilon}{2}\bar{Q} + \frac{1}{N} \left[(-3\bar{Q}^2 + 4\bar{Q}) \varepsilon + \left(\frac{7}{4}\bar{Q}^2 - \frac{8}{3}\bar{Q} \right) \varepsilon^2 + \mathcal{O}(\varepsilon^3) \right] + \mathcal{O}\left(\frac{1}{N^2}\right) . \quad (5.12)$$

Furthermore, these operators have been recently studied to the leading order in the large charge expansion in [137] ($d = 3$) and [189] (in arbitrary d). In both cases, the scaling dimension of the

$T_{0,\bar{Q}}$ operators takes the form

$$\tilde{\Delta}_{\bar{Q}} = \sum_{k=-1} \frac{1}{N^k} \tilde{\Delta}_k(J) , \quad (5.13)$$

where $J = \bar{Q}/N$ is the 't Hooft coupling of the large charge semiclassical expansion. Here $1/N$, where N is taken to be large, has the role of the coupling constant of the theory. $\tilde{\Delta}_{-1}$ reads [189]

$$\tilde{\Delta}_{-1} = \left[f(c_\sigma) + J \sqrt{\left(\frac{d}{2} - 1 \right)^2 + c_\sigma} \right]_{c_\sigma=c_\sigma(J)} , \quad (5.14)$$

where $c_\sigma(J)$ solves

$$\frac{d}{dc_\sigma} \left[f(c_\sigma) + J \sqrt{\left(\frac{d}{2} - 1 \right)^2 + c_\sigma} \right] = 0 , \quad (5.15)$$

and $f(c_\sigma)$ is given by

$$f(c_\sigma) = -\frac{c_\sigma}{d-2} \int_0^\infty dt \frac{J_2(\sqrt{c_\sigma}t)}{t(2\cosh t - 2)^{\frac{d}{2}-1}} , \quad (5.16)$$

with J_2 the Bessel function of the first kind. The small J expansion of $\tilde{\Delta}_{-1}$ reads [189]

$$\tilde{\Delta}_{-1} = \left(\frac{d}{2} - 1 \right) J + h_2(d) J^2 + h_3(d) J^3 + \dots , \quad (5.17)$$

where

$$\begin{aligned} h_2(d) &= -\frac{2^{d-3} d \sin\left(\frac{\pi d}{2}\right) \Gamma\left(\frac{d-1}{2}\right)}{\pi^{3/2} \Gamma\left(\frac{d}{2}+1\right)} , \\ h_3(d) &= -\frac{(d-2)d^2 \Gamma(d-2)^2 \left(\pi^2 - 6\psi^{(1)}\left(\frac{d}{2}\right)\right)}{6\Gamma\left(2-\frac{d}{2}\right)^2 \Gamma\left(\frac{d}{2}-1\right)^4 \Gamma\left(\frac{d}{2}+1\right)^2} , \\ h_4(d) &= \dots \end{aligned} \quad (5.18)$$

In $d = 4 - \varepsilon$, Eq.(5.17) reproduces the leading N terms of our previous result (4.80). Instead, in $d = 6 - \varepsilon$, we have

$$N\tilde{\Delta}_{-1} = 2\bar{Q} - \frac{\varepsilon}{2}\bar{Q} + \bar{Q} \sum_j \left(\frac{\bar{Q}}{N} \right)^j (\alpha_j \varepsilon^j + \beta_j \varepsilon^{j+1} + \gamma_j \varepsilon^{j+2} + \dots) . \quad (5.19)$$

For later comparison with the scaling dimensions in the cubic model we list below the values of the first α_j and β_j coefficients

$$\begin{aligned} \alpha_1 &= -3, & \alpha_2 &= -45, & \alpha_3 &= -1350, & \alpha_4 &= -\frac{213597}{4}, & \alpha_5 &= -2457216 \\ \alpha_6 &= -\frac{995773905}{8}, & \alpha_7 &= -6739459200, & \alpha_8 &= -\frac{24526111620285}{64}. \end{aligned} \quad (5.20)$$

$$\begin{aligned} \beta_1 &= \frac{7}{4}, & \beta_2 &= \frac{3}{4}(48\zeta(3) + 31), & \beta_3 &= \frac{27}{2}(128\zeta(3) + 40\zeta(5) + 41), \\ \beta_4 &= \frac{81}{16}(18208\zeta(3) + 7168\zeta(5) + 1792\zeta(7) + 3117), \\ \beta_5 &= 648(8202\zeta(3) + 3510\zeta(5) + 1218\zeta(7) + 252\zeta(9) + 677) \\ \beta_6 &= \frac{2187}{32}(4727888\zeta(3) + 2109440\zeta(5) + 836864\zeta(7) + 256000\zeta(9) + 45056\zeta(11) + 110211). \end{aligned} \quad (5.21)$$

Finally, the large J expansion of $\tilde{\Delta}_{-1}$ in $d = 6 - \varepsilon$ dimensions reads [189]

$$N\tilde{\Delta}_{-1} \approx -e^{\pm i4\pi/5} \frac{5N}{3} (2\varepsilon)^{1/5} J^{6/5}, \quad (5.22)$$

while, in $d = 4 + \varepsilon$, we have

$$N\tilde{\Delta}_{-1} \approx -e^{\pm i\pi/3} \frac{3N}{2^{4/3}} \varepsilon^{1/3} J^{4/3}. \quad (5.23)$$

In both cases, the scaling dimension in the large J expansion is complex. In fact, in [189], it has been observed that in $4 < d < 6$, it exists a critical value of J , J_c , above which the scaling dimensions become complex. This happens when there are no real solutions to the saddle point equations. In [189], J_c has been evaluated numerically, with the result displayed in Fig.11. Intriguingly, $J_c(d)$ looks very similar to the instantonic function $f(d)$.

The first test of the equivalence of the large charge sector in the two descriptions has been carried out in [154], where the authors showed that exponentiation of the diagrams with the leading \bar{Q} -scaling at every loop order³⁰, leads to the same result in both models. This result is $\tilde{\Delta}_{\bar{Q}}$ at LO in all the expansion parameters: $1/\bar{Q}$, $1/N$, and ε .

In the next section, we will re-derive Eqs.(5.12) and (5.19) in the cubic model in $6 - \varepsilon$, signifi-

³⁰This exponentiation is analogous to that of the Kermit diagrams discussed in Sec.3.6.

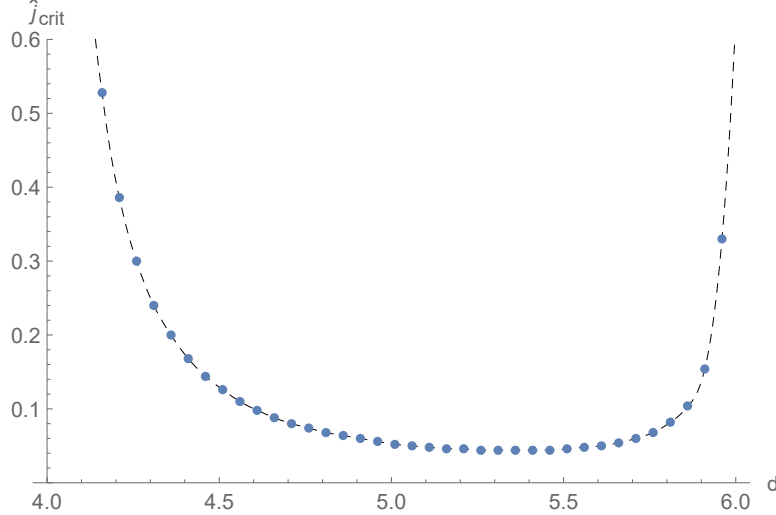


Figure 11: J_c as a function of d , for $4 < d < 6$. Note: reprinted from [189].

cantly extending previous tests of the duality.

5.2 Large charge expansion in the cubic model: LO

In order to compute the leading (classical) order in the semiclassical large charge expansion, we follow the procedure outlined in the previous chapter. Since this model shares the same $O(N)$ symmetry, most of the considerations made there still apply to the theory at hand. For instance, the $T_{0,\bar{Q}}$ operators are the MSD operators with total charge \bar{Q} , and, in the saddle-point expansion, their scaling dimension takes the form

$$\Delta_{\bar{Q}} = \sum_{k=-1} \frac{1}{\bar{Q}^k} \Delta_k(\mathcal{A}) , \quad \mathcal{A} = \bar{Q}\varepsilon . \quad (5.24)$$

We start by introducing $N/2$ complex fields as

$$\varphi_j = \phi_{2j-1} + i\phi_{2j} = \frac{1}{\sqrt{2}} \rho_j e^{i\chi_j} , \quad j = 1, \dots, N/2 , \quad (5.25)$$

and we map the theory to the cylinder. The cylinder Lagrangian reads

$$\mathcal{L}_{\text{cyl}} = (\partial \vec{\varphi})^2 + \frac{1}{2} \partial \eta \partial \eta + g_0 \eta \vec{\varphi}^2 + \frac{h_0}{6} \eta^3 + \frac{m^2}{2} \eta^2 + m^2 \vec{\varphi}^2$$

$$= \frac{1}{2} \partial \rho_i \partial \rho_i + \frac{1}{2} \rho_i \rho_i \partial \chi_i \partial \chi_i + \frac{1}{2} \partial \eta \partial \eta + \frac{g_0}{2} \eta (\rho_i \rho_i) + \frac{h_0}{6} \eta^3 + \frac{m^2}{2} \eta^2 + \frac{m^2}{2} \rho_i \rho_i , \quad (5.26)$$

where m is given by Eq.(2.31). The EOM are

$$(\partial^\mu \partial_\mu - \partial^\mu \chi_j \partial_\mu \chi_j + g_0 \eta + m^2) \rho_j = 0 , \quad (5.27)$$

$$\partial^\mu \partial_\mu \eta = \frac{g_0}{2} (\rho_i \rho_i) + \frac{h_0}{2} \eta^2 + m^2 \eta , \quad (5.28)$$

$$i \partial^\mu (\sigma_i \sigma_i \partial_\mu \chi_i) = 0 . \quad (5.29)$$

We look for a spatially homogeneous solution, which is given by

$$\begin{cases} \rho_i = A_i , \quad \chi_i = -i\mu t \quad i = 1, \dots, k , \\ \eta = v , \end{cases} \quad (5.30)$$

where $k \leq N/2$ is the number of charges we fix. As explained in the previous chapter, the value of k is irrelevant for the computation of the scaling dimension of the MSD operators as long as it is different from zero. Notice that, due to the interactions between φ and η , at equilibrium, we have a non-zero vev also for the latter field. The parameters A_i , v , and μ are fixed by the EOM and the expression for the Noether charge as

$$\mu^2 - m^2 = g_0 v , \quad \frac{g_0}{2} f^2 + \frac{h_0}{2} v^2 + m^2 v = 0 , \quad \frac{\bar{Q}}{\Omega_{d-1} R^{d-1}} = \mu f^2 , \quad (5.31)$$

where R is the radius of S^{d-1} , and we defined

$$f^2 \equiv \sum_{i=1}^{N/2} A_i^2 , \quad \bar{Q} \equiv \sum_{i=1}^{N/2} \bar{Q}_i , \quad (5.32)$$

with \bar{Q} the sum of the charges. From Eq.(5.31), we have

$$R\mu [(R\mu)^2 - 4] (8g_0 + h_0 [(R\mu)^2 - 4]) + \frac{\bar{Q}g_0^3}{\pi^3} = 0 , \quad (5.33)$$

which, once rewritten at the FP, implicitly defines the chemical potential as a function of the 't

Hooft coupling \mathcal{A} . The above equation can be solved numerically, or analytically for small/large values of \mathcal{A} . The former expansion reads

$$R\mu = 2 - \frac{g_0^2 \bar{Q}}{64\pi^3} - \frac{g_0^3 \bar{Q}^2 (3g_0 + 2h_0)}{16384\pi^6} - \frac{g_0^4 \bar{Q}^3 (2g_0^2 + 2g_0 h_0 + h_0^2)}{524288\pi^9} . \quad (5.34)$$

The classical energy is obtained by adding the usual charge-fixing boundary term, i.e. $H \rightarrow \hat{H} = H + \bar{Q}\mu$

$$E_{\text{class}} = -\frac{f^2 \mu^2}{2} + \frac{g_0 v f^2}{2} + \frac{h_0 v^3}{6} + \frac{m^2 f^2}{2} + \frac{m^2 v^2}{2} + \frac{\bar{Q}\mu}{V} . \quad (5.35)$$

Using Eq.(5.34) in the classical energy above and evaluating the result at the FP, we obtain the leading order Δ_{-1} of the large charge expansion. By expanding Δ_{-1} in the perturbative regime and plugging the FP value of the couplings (5.6), we obtain

$$\begin{aligned} \bar{Q}\Delta_{-1} = & 2\bar{Q} - \varepsilon \bar{Q}^2 \left(\frac{3}{N} + \mathcal{O} \left(\frac{1}{N^2} \right) \right) - \bar{Q}^3 \varepsilon^2 \left(\frac{45}{N^2} + \mathcal{O} \left(\frac{1}{N^3} \right) \right) - \bar{Q}^4 \varepsilon^3 \left(\frac{1350}{N^3} + \mathcal{O} \left(\frac{1}{N^4} \right) \right) \\ & - \bar{Q}^5 \varepsilon^4 \left(\frac{213597}{4N^4} + \mathcal{O} \left(\frac{1}{N^5} \right) \right) - \bar{Q}^6 \varepsilon^5 \left(\frac{2457216}{N^5} + \mathcal{O} \left(\frac{1}{N^6} \right) \right) \\ & - \bar{Q}^7 \varepsilon^6 \left(\frac{995773905}{8N^6} + \mathcal{O} \left(\frac{1}{N^7} \right) \right) - \bar{Q}^8 \varepsilon^7 \left(\frac{6739459200}{N^7} + \mathcal{O} \left(\frac{1}{N^8} \right) \right) \\ & - \bar{Q}^9 \varepsilon^8 \left(\frac{24526111620285}{64N^8} + \mathcal{O} \left(\frac{1}{N^9} \right) \right) + \mathcal{O}(\bar{Q}^{10} \varepsilon^9) . \end{aligned} \quad (5.36)$$

The above remarkably reproduces the α_j coefficients in Eq.(5.20) for the scaling dimension in the quartic $O(N)$ model. Notice that $\tilde{\Delta}_{-1}(J)$ in (5.19) and $\Delta_{-1}(\mathcal{A})$ in (5.36) are the leading order of two distinct expansions, which besides taking the charge to be large assume, large N and small ε , respectively. However, since at LO in the $1/N$ expansion the cubic FPs (5.6) are 1-loop exact (in the ε -expansion), all (and only) the terms scaling as $\bar{Q} \left(\frac{\bar{Q}\varepsilon}{N} \right)^j$ appear at the LO of both expansions. For this series of terms, we have³¹

$$\bar{Q}\Delta_{-1} = N\tilde{\Delta}_{-1} . \quad (5.37)$$

³¹In truth, at the moment, we explicitly checked the agreement only up to order $\mathcal{O}(\varepsilon^{10})$, i.e. α_{10} .

The expansion of Δ_{-1} for large 't Hooft coupling \mathcal{A} reads

$$\bar{Q}\Delta_{-1} = -e^{\pm\frac{4i\pi}{5}}(2\epsilon)^{\frac{1}{5}}\frac{5N}{3}J^{6/5} - e^{\pm\frac{2i\pi}{5}}\frac{5N}{6}(2\epsilon)^{-\frac{1}{5}}J^{4/5} + \frac{N}{9}(2\epsilon)^{-\frac{3}{5}}J^{2/5} - \frac{5N}{324\epsilon} + \mathcal{O}\left(J^{-\frac{2}{5}}\right), \quad (5.38)$$

where we rewrote the result in terms of J . The above matches the $O(N)$ result (5.22), confirming Eq.(5.37). Notice that Eq.(5.38) agrees with the expected form (3.58) of the large charge expansion in the large chemical potential limit obtained via the large charge EFT in Sec.3.5. As for the quartic model in $4 < d < 6$, we again observe that in this limit the scaling dimensions become complex signaling instability of the ground state of the theory. On the other hand, since every order of the small 't Hooft coupling expansions (5.19) and (5.36) is real, the appearance of complex anomalous dimensions implies the existence of non-analytic terms, i.e. the classical ground state shows some non-perturbative features.

5.3 Large charge expansion in the cubic model: NLO

The time is ripe to compute the leading quantum correction Δ_0 in the semiclassical expansion, which, as we saw in the previous chapter, is given by the functional determinant of the fluctuation around the classical solution (5.30). We start by noting that we have the same superfluid symmetry breaking pattern (4.43) discussed for the $O(N)$ model in Sec.4.3, whose obvious generalization in the case we fix only k over $N/2$ charges is

$$SO(d+1, 1) \times O(N) \rightarrow SO(d) \times D' \times O(N-2k) \times U(k-1), \quad (5.39)$$

and, according to the charged Goldstone theorem, we expect $2k-1$ massless modes (counting twice the type II Goldstones)³² i.e. one type I scalar plus one type II $U(k-1)$ -vector. Moreover, as shown in Chap.4, we can use an $O(N)$ rotation to assign all the charge to a single Cartan generator. For sake of simplicity, we then fix only one charge. Then, in the light of the discussion in Sec.4.6, we expect one relativistic Goldstone boson (the $U(1)$ phonon), two gapped modes, and $N-2$

³²Indeed, this is the dimension of the coset of the "spontaneous" part of the total symmetry breaking, which is $U(k) \rightarrow U(k-1)$.

"spectator" states, with gap μ and dispersion relation given by Eq.(4.65)

$$\omega_* = \sqrt{p^2 + \mu^2} . \quad (5.40)$$

For the remaining three d.o.f., we can expand the fluctuations as follows:

$$\begin{cases} \rho_1 = f + r(x) , \quad \chi_1 = -i\mu t + \pi(x) , \\ \eta = v + \tilde{\eta}(x) . \end{cases} \quad (5.41)$$

Then the quadratic Lagrangian for these three modes reads

$$\mathcal{L}^{(2)} = \frac{1}{2}(\partial r)^2 + \frac{1}{2}(\partial \tilde{\eta})^2 + \frac{1}{2}(\partial \pi)^2 - 2i\mu r \dot{\pi} + g_0 f \tilde{\eta} r + \frac{h_0}{2} v \tilde{\eta}^2 + \frac{m^2}{2} \tilde{\eta}^2 + \frac{m^2}{2} r^2 . \quad (5.42)$$

The dispersion relations can be computed as explained in Sec.(4.6), i.e. we go to momentum space and consider the inverse propagator $\mathcal{P}^{-1}(p)$

$$S^{(2)} = \int \frac{d^d p}{(2\pi)^d} [r(-p) \ \tilde{\eta}(-p) \ \pi(-p)] \mathcal{P}^{-1}(p) \begin{bmatrix} r(p) \\ \tilde{\eta}(p) \\ \pi(p) \end{bmatrix} , \quad (5.43)$$

with p the momentum. Then the dispersion relations are the positive energy solutions of $\det \mathcal{P}^{-1}(p) = 0$, where

$$\mathcal{P}^{-1}(p) = \begin{pmatrix} \frac{1}{2}(\omega^2 - p^2) & i\omega\mu & A \\ -i\omega\mu & \frac{1}{2}(\omega^2 - p^2) & 0 \\ A & 0 & \frac{1}{2}(\omega^2 - p^2) - B \end{pmatrix} , \quad (5.44)$$

with

$$A = \frac{1}{2} \sqrt{\frac{(m^2 - \mu^2)[2g_0 m^2 + h_0(\mu^2 - m^2)]}{g_0}} , \quad (5.45)$$

$$B = \frac{1}{2} \left(m^2 + \frac{h_0}{g_0} (\mu^2 - m^2) \right) . \quad (5.46)$$

It is easy to check that one of the dispersion relations describes a relativistic massless Goldstone boson which at large μ propagates at the speed of sound $\sqrt{\frac{1}{d-1}} = \frac{1}{\sqrt{5}}$.

Clearly, at large N the N spectator fields provide the leading N contribution to Δ_0 , which we denote as $\Delta_0^{(N)}$. Since our goal is to compare with large N results in the quartic model, we start by computing $\Delta_0^{(N)}$. First, we write the large charge expansion in its bare and renormalized forms

$$E_{\bar{Q}}^{(N)} R = \sum_{j=-1}^{\infty} \frac{1}{\bar{Q}^j} e_j^{(N)}(g_0, h_0, \bar{Q}, d) = \sum_{j=-1}^{\infty} \frac{1}{\bar{Q}^j} \bar{e}_j^{(N)}(g, h, \bar{Q}, d, RM) . \quad (5.47)$$

As shown in Chap.4, e_0 is given by

$$e_0(g_0, h_0, \bar{Q}, d) = \frac{R}{2} \sum_{\ell=0}^{\infty} n_{\ell} \sum_i \omega_i(p^2 = J_{\ell}) , \quad (5.48)$$

where the second sum runs over the dispersion relations of all the fluctuations. The expressions of the eigenvalues of the Laplacian on the sphere J_{ℓ} and their multiplicity n_{ℓ} have been given in Eqs.(4.58) and (3.61), respectively.

The renormalization is carried out at the LO order in $1/N$. From the beta functions Eq.(5.5), it is easy to derive the relation between bare and renormalized couplings at the 1-loop level

$$g_0 = M^{\varepsilon} \left(g + \frac{g^3 N}{1536 \pi^3 \varepsilon} \right) , \quad h_0 = M^{\varepsilon} \left(h + \frac{g^2 N (h - 4g)}{512 \pi^3 \varepsilon} \right) , \quad (5.49)$$

with M the sliding scale. Proceeding as in Sec.4.7, we have³³

$$\bar{e}_0^{(N)}(g, h, \bar{Q}, d, RM) = e_0^{(N)}(g, h, \bar{Q}, d) + f_0^{(N)}(g, h, \bar{Q}, d, RM) , \quad (5.50)$$

where

$$\begin{aligned} f_0^{(N)} &= \frac{N (\mu^2 R^2 - 4)^2 (\mu^2 R^2 - 2)}{384 R} \left(\frac{1}{\varepsilon} - \log(MR\sqrt{\pi}) \right) - \frac{N}{1536 R} \\ &\times \left((\mu^2 R^2 - 4) ((2\gamma - 3)\mu^4 R^4 - 12\gamma\mu^2 R^2 - 2\mu^2 R^2 + 16\gamma + 24) \right) + \mathcal{O}(\varepsilon) . \end{aligned} \quad (5.51)$$

with γ is the Euler–Mascheroni constant. Finally, we evaluate this expression at the FP. In order to include in $\Delta_0^{(N)}$ all the terms with the right scaling, we need to add the expansion of $\bar{Q}\bar{e}_{-1}$ to the leading order in ε . After this procedure, the term which depends on M drops and $\Delta_0^{(N)}$ depends

³³The dependence on charge and couplings is hidden in μ .

only on the combination $\mathcal{A} = \bar{Q}\varepsilon$. We have

$$\Delta_0^{(N)}(\mathcal{A}) = \left\{ \lim_{\varepsilon \rightarrow 0} \left[\frac{R}{2} \sum_{\ell=0}^{\infty} n_{\ell} N \omega_{*}(\ell) + \frac{N (\mu^2 R^2 - 4)^2 (\mu^2 R^2 - 2)}{384 R \varepsilon} \right] \right\}_{g,h=g^*(\varepsilon),h^*(\varepsilon)}. \quad (5.52)$$

The sum over ℓ can be regularized as done in Sec.4.7. In the regularization procedure, also the $\frac{1}{\varepsilon}$ pole in Eq.(5.52) cancels, providing an internal consistency check of our computation. The final result reads

$$\Delta_0^{(N)} = N \frac{25R^6\mu^6 - 130R^4\mu^4 - 640R^2\mu^2 + 2304R\mu - 1568}{4608} + \frac{N}{2} \sum_{\ell=1}^{\infty} \sigma^{(N)}(\ell), \quad (5.53)$$

where the sum over ℓ converges and $\sigma(\ell)$ is given by

$$\begin{aligned} \sigma^{(N)}(\ell) = & \frac{1}{192} (16(\ell+1)(\ell+2)^2(\ell+3) \sqrt{R^2\mu^2 + \ell(\ell+4)} - \frac{1}{\ell} [R^6\mu^6 + 32(R^2\mu^2 - 1) \\ & - 2(\ell(\ell+2) + 5)R^4\mu^4 + 8\ell(\ell+2)(\ell(\ell+4) + 5)R^2\mu^2 + 16\ell(\ell+2)^3(\ell(\ell+4) + 1)]) . \end{aligned} \quad (5.54)$$

For small 't Hooft couplings the sum over ℓ can be computed analytically, yielding

$$\Delta_0^{(N)} = -\bar{Q}\varepsilon \left[\frac{1}{2} + \frac{22}{N} + \frac{242}{N^2} + \mathcal{O}\left(\frac{1}{N^3}\right) \right] + (\bar{Q}\varepsilon)^2 \left[\frac{7}{4N} - \frac{1106}{N^2} + \mathcal{O}\left(\frac{1}{N^3}\right) \right] + \mathcal{O}((\bar{Q}\varepsilon)^3). \quad (5.55)$$

Let us compare the above with Eq.(5.12) for the scaling dimension in the quartic model. We have a $-\frac{\varepsilon}{2}\bar{Q}$ term which matches. Furthermore, also the coefficients of the term of order $\frac{\bar{Q}^2\varepsilon^2}{N}$ agree between the two formulas. Since these terms, being leading in $1/N$, do not receive other contributions, this constitutes another check of the duality, now at the NLO in the large charge expansion. The subleading term $-\frac{22\varepsilon}{N}\bar{Q}$ instead receives contributions from the remaining modes in the fluctuation spectrum. This contribution can be computed by means of the same procedure used for the spectator fields but with two crucial differences. First, now one cannot truncate the expression to the leading $1/N$ order. Second, being the dispersion relations more involved, the fluctuation determinant has to be regularized and evaluated numerically at fixed values of N , \bar{Q} , and ε . Then, in order to determine the coefficient of the term scaling as $\frac{\varepsilon}{N}\bar{Q}$, which is leading in ε , we considered small values of ε and performed a numerical fit. After summing the result to the

contribution of the spectator fields we obtained that such a coefficient is $+4$, again in agreement with Eq.(5.12). To summarize, we add $\bar{Q}\Delta_{-1}$ to Δ_0 and rewrite our findings as

$$\tilde{\Delta}_{\bar{Q}} = 2\bar{Q} - \frac{\varepsilon}{2}\bar{Q} + \frac{1}{N} \left[(-3\bar{Q}^2 + 4\bar{Q})\varepsilon + \left(\frac{7}{4}\bar{Q}^2 - \mathcal{O}(\bar{Q})\right)\varepsilon^2 + \mathcal{O}(\varepsilon^3)\right] + \mathcal{O}\left(\frac{1}{N^2}\right), \quad (5.56)$$

which matches Eq.(5.12), including the term $\frac{4\bar{Q}\varepsilon}{N}$, which is in the NLO of the large charge expansion in both models i.e. is contained in both Δ_0 and $\tilde{\Delta}_0$.

Notice now that all the terms scaling as $N\left(\frac{\varepsilon\bar{Q}}{N}\right)^j$ in Δ_0 can come only from the contribution of the spectator fields. These terms have exactly the right scaling to match the β_j coefficients in Eq.(5.21). We have

$$\begin{aligned} \tilde{\Delta}_{\bar{Q}} = & -\bar{Q}\varepsilon \left[\frac{1}{2} + \mathcal{O}\left(\frac{1}{N}\right) \right] + (\bar{Q}\varepsilon)^2 \left[\frac{7}{4N} + \mathcal{O}\left(\frac{1}{N^2}\right) \right] \\ & + (\bar{Q}\varepsilon)^3 \left[\frac{3}{4N^2} (48\zeta(3) + 31) + \mathcal{O}\left(\frac{1}{N^3}\right) \right] \\ & + (\bar{Q}\varepsilon)^4 \left[\frac{27}{2N^3} (128\zeta(3) + 40\zeta(5) + 41) + \mathcal{O}\left(\frac{1}{N^4}\right) \right] \\ & + (\bar{Q}\varepsilon)^5 \left[\frac{81}{16N^4} (18208\zeta(3) + 7168\zeta(5) + 1792\zeta(7) + 3117) + \mathcal{O}\left(\frac{1}{N^5}\right) \right] \\ & + (\bar{Q}\varepsilon)^6 \left[\frac{648}{N^5} (8202\zeta(3) + 3510\zeta(5) + 1218\zeta(7) + 252\zeta(9) + 677) + \mathcal{O}\left(\frac{1}{N^6}\right) \right] \\ & + (\bar{Q}\varepsilon)^7 \left[\frac{2187}{32N^6} (4727888\zeta(3) + 2109440\zeta(5) + 836864\zeta(7) + 256000\zeta(9) + 45056\zeta(11) \right. \\ & \quad \left. + 110211) + \mathcal{O}\left(\frac{1}{N^7}\right) \right] + \mathcal{O}((\bar{Q}\varepsilon)^8), \end{aligned} \quad (5.57)$$

in remarkable agreement with the values listed in Eq.(5.21) for the quartic model. Our findings provide a non-trivial check for the equivalence between the cubic and the quartic critical theories, showing at the same time the power of the large charge expansion.

We conclude this section with a simple observation. In $5d$, both the $O(N)$ and the cubic theory are non-perturbative but accessible by the large charge EFT considered in Sec.3.5. This opens the interesting possibility of non-perturbatively testing the duality in the large charge limit. To this end, notice that, as we saw in Sec.3.5, the form of the EFT action is dictated by symmetry arguments and thus is trivially the same in both models. In particular, as discussed in the previous chapter,

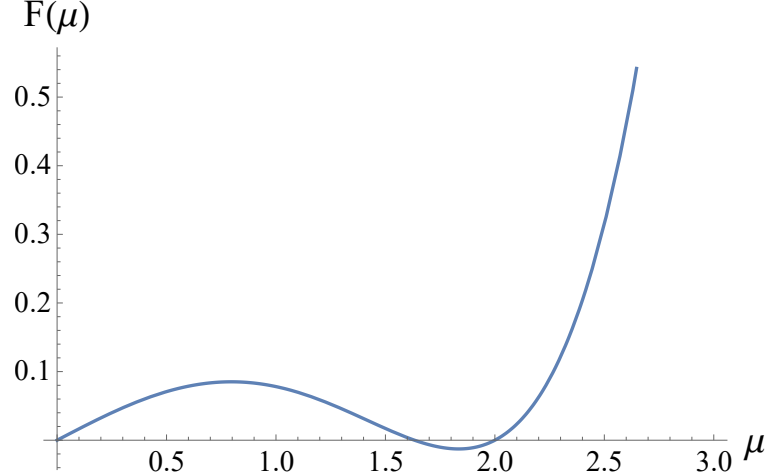


Figure 12: $F(\mu)$ as a function of μ .

the effective action is again given by Eq.(3.56), and eventual differences between the cubic and the quartic theory are contained in the Wilson coefficients. The scaling dimension thus takes the form of Eq.(3.58), that is

$$\Delta_{\bar{Q}} = a_1 \bar{Q}^{5/4} + a_2 \bar{Q}^{3/4} + a_3 \bar{Q}^{1/4} - 0.1079 + \mathcal{O}(\bar{Q}^{-1/4}) . \quad (5.58)$$

The a_i coefficients can be determined on the lattice. Notice the appearance of the universal \bar{Q}^0 term typical of the large charge expansion in an odd number of dimensions, which as discussed in Sec.3.5, comes from the zero-point energy of the phonon mode. For 5d $O(N)$ -invariant CFTs, this term has been originally computed in [131].

5.4 Complex anomalous dimensions

As in the $O(N)$ model, our results show the existence of a critical value of the charge above which the scaling dimensions are complex. The imaginary part arises in the chemical potential μ , which is given implicitly by Eq.(5.33). Let us fix $R = 1$ and rewrite Eq.(5.33) in terms of J . We have

$$F(\mu) = \frac{1}{192} \mu (3\mu^4 - 20\mu^2 + 32) = -J \varepsilon + \mathcal{O}(\varepsilon^2) . \quad (5.59)$$

The plot of $F(\mu)$ is given in Fig.12.

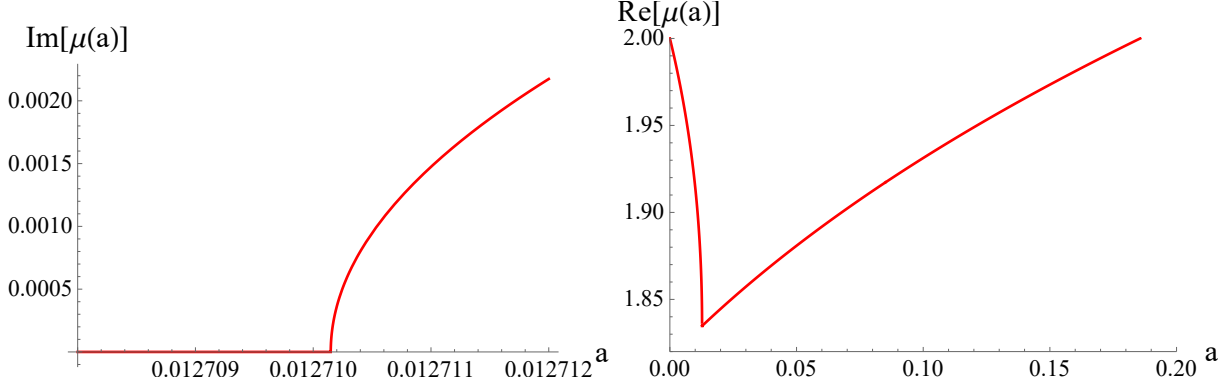


Figure 13: $\text{Im}(\mu)$ (left) and $\text{Re}(\mu)$ (right) as a function of $a = J\epsilon$. The imaginary part starts at $a_c = \frac{1}{90}(-9 + \sqrt{105})\sqrt{\frac{1}{30}(15 + \sqrt{105})}$.

Since by definition, we are interested in the region where $F(\mu)$ is negative, i.e. where $J\epsilon > 0$, we note that only a limited range of values of the product $J\epsilon \equiv a$ are allowed when the chemical potential is real. As in the $O(N)$ case, above J_c there are no real solutions to the saddle-point equations. In Fig.13 we show real and imaginary part of the chemical potential as a function of a . The imaginary part arises at the global minimum of $F(\mu)$. There the real part of the chemical potential has a spike and its first derivative diverges. This gives J_c to the leading order in the ϵ -expansion and in large N

$$J_c = \frac{1}{90\epsilon}(-9 + \sqrt{105})\sqrt{\frac{1}{30}(15 + \sqrt{105})}. \quad (5.60)$$

In Fig.14 we show the plot of J_c as a function of d . Notice that the difference with the numerical evaluation of $J_c(d)$ shown in Fig.11 and performed in [189], does not come from the FPs truncation but instead from terms with higher powers of ϵ , which are subleading in our large charge expansion (5.24) but not in the expansion (5.13).

For the sake of completeness, we study the $O(N)$ model in $4 - \epsilon$ with $\epsilon < 0$, which is obtained by continuing the results of the previous chapter to negative ϵ . First, we expand Eq.(4.49) for large values of μ , obtaining

$$\bar{Q}\Delta_{-1} = -e^{\pm i\pi/3} \frac{3N}{2^{4/3}} \epsilon^{1/3} J^{4/3}, \quad (5.61)$$

in agreement with Eq.(5.23). To study the imaginary part, we proceed as above and rewrite

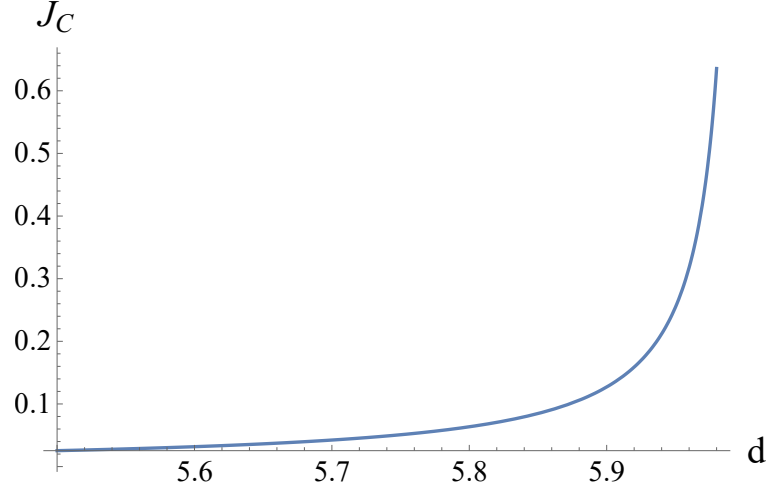


Figure 14: J_c as a function of the spacetime dimension d .

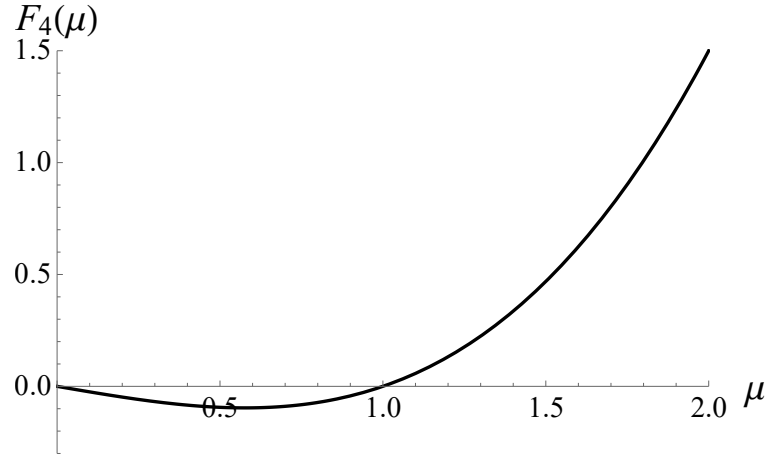


Figure 15: $F_4(\mu)$ as a function of μ .

Eq.(4.47) at the large N FP $g^* = \frac{3}{N}\varepsilon$ (setting $R = 1$) as

$$F_4(\mu) = \frac{1}{4}(\mu^3 - \mu) = J\varepsilon . \quad (5.62)$$

The plot of $F_4(\mu)$ is shown in Fig.15. We have two regimes which correspond to ε positive and negative. For positive ε , $F_4(\mu)$ is positive and monotonic and there are no complex anomalous dimensions, as expected. At negative ε , there is a minimum in $\mu = \frac{1}{\sqrt{3}}$. As before, J_c critical is

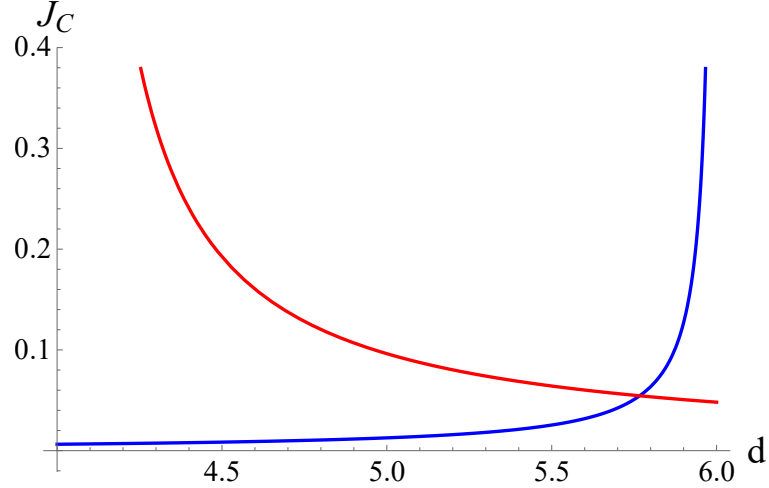


Figure 16: The leading behaviour of $J_c^{(tot)}$ near $d = 4$ (red curve) and $d = 6$ (blue curve).

given by

$$J_c = \frac{F_4\left(\frac{1}{\sqrt{3}}\right)}{\varepsilon} = -\frac{1}{6\sqrt{3}\varepsilon}, \quad (5.63)$$

that is where the square roots in (4.48) vanish.

In Fig. 16, we show the two tails we found for J_c around 6 and 4 dimensions. We observe that the qualitative behaviour is controlled by having the free theory on both sides.

6 CHARGING NON-ABELIAN HIGGS THEORIES

In the previous chapters, we saw that in $O(N)$ -symmetric theories, if the ground state is spatially homogeneous, then every charge configuration $\vec{Q} = \bar{Q}(q_1, q_2, \dots, q_{N/2})$ can be $O(N)$ -rotated to the simple configuration $\vec{Q} = \bar{Q}(1, 0, \dots, 0)$. Thus we effectively have only one charge \bar{Q} , and the charge configuration does not affect the computation of the scaling dimension of the MSD operators. Additionally, this fact almost trivializes the identification of the fixed-charge MSD operator when the theory is perturbative.

To allow for more variations in the charge configuration without having to consider non-homogeneous ground states, which lead to complicated saddle-point equations, in this chapter, we investigate the large charge expansion in the $U(N) \times U(M)$ CFT in $d = 4 - \varepsilon$ dimensions. As we shall see, the non-trivial structure of this model allows studying classical configurations with different values of the Cartan charges, corresponding to primary operators transforming in different irreducible representations. This opens the intriguing possibility of computing the scaling dimensions of MSD operators as explicit functions of their quantum numbers (i.e. of the charge configuration) and obtaining with a single computation the scaling dimension of a wide range of operators, pushing forward the frontiers of large charge methods.

On the other hand, as discussed in Sec. 4.1, given a charge configuration, we do not know, a priori, the exact form of the corresponding MSD operator. We will, therefore, develop a general operator-identification strategy based on the interplay between semiclassical methods and group theory constraints. Even though we focus on the $U(N) \times U(M)$ model, the ideas presented here can be easily generalized to other non-abelian theories.

In Euclidean spacetime, the Lagrangian of the theory reads

$$\mathcal{L} = \text{Tr}(\partial_\mu H^\dagger \partial^\mu H) + u_0 \text{Tr}(H^\dagger H)^2 + v_0 (\text{Tr} H^\dagger H)^2, \quad (6.1)$$

where H is an $N \times M$ complex matrix. For $N = M$ and $v_0 > 0$, this model describes the finite-temperature phase transition in massless QCD with N flavors [36, 135, 136], with H playing the role of the order parameter. In the last years, this model has also been studied in relation to asymptotically safe theories structurally similar to the Standard Model [35, 181, 190], of which it constitutes

the Higgs sector. In [61], the large charge regime of this model has been investigated in exactly four dimensions via the EFT approach introduced in Sec.3.5³⁴. Notice that, for $u = 0$, we recover the $O(2NM)$ theory studied in Chap.4. This fact will be used to non-trivially test our results.

We work in the \overline{MS} scheme. The couplings are renormalized as

$$u_0 M^{-\varepsilon} = u + \sum_{n=0}^{\infty} \frac{a_u^{(n)}(u, v)}{\varepsilon^n}, \quad v_0 M^{-\varepsilon} = v + \sum_{n=0}^{\infty} \frac{a_v^{(n)}(u, v)}{\varepsilon^n}. \quad (6.2)$$

The beta functions of the couplings are given by

$$\begin{aligned} \beta_u \equiv \frac{du}{d\log M} \Big|_{\varepsilon=0} &= -\varepsilon u + u \frac{\partial a_u^{(1)}}{\partial u} + v \frac{\partial a_u^{(1)}}{\partial v} - a_u^{(1)}, \\ \beta_v \equiv \frac{dv}{d\log M} \Big|_{\varepsilon=0} &= -\varepsilon v + u \frac{\partial a_v^{(1)}}{\partial u} + v \frac{\partial a_v^{(1)}}{\partial v} - a_v^{(1)}, \end{aligned} \quad (6.3)$$

and, at 1-loop, read [191]

$$\beta_u(u, v) = -\varepsilon u + \frac{1}{4\pi^2} (6uv + (N+M)u^2), \quad (6.4)$$

$$\beta_v(u, v) = -\varepsilon v + \frac{1}{4\pi^2} ((NM+4)v^2 + 2(N+M)uv + 3u^2). \quad (6.5)$$

At the 1-loop level, the model features four fixed points: a Gaussian FP ($u^* = v^* = 0$), an $O(2NM)$ FP ($u^* = 0$), and are other two FPs given by

$$u_{\pm}^* = 4\pi^2 \frac{A_{MN} \mp 3\sqrt{R_{MN}}}{D_{MN}} \varepsilon, \quad v_{\pm}^* = 4\pi^2 \frac{B_{MN} \pm (M+N)\sqrt{R_{MN}}}{2D_{MN}} \varepsilon, \quad (6.6)$$

where

$$\begin{aligned} A_{MN} &= NM^2 + MN^2 - 5N - 5M, & B_{MN} &= 36 - (M+N)^2, \\ R_{MN} &= 24 + M^2 + N^2 - 10MN, & D_{MN} &= (MN-8)(M+N)^2 + 108. \end{aligned} \quad (6.7)$$

The beta functions to five loops have been derived in [38], where the authors concluded that no stable FP, with both u^* and v^* real and different from zero, exists for $N = M$ and $d = 3$. This

³⁴In 4 dimensions the FP is obtained by introducing additional degrees of freedom.

suggests that the finite-temperature chiral phase transition in QCD is first-order. When $R_{MN} < 0$, the fixed points are complex, and thus, as discussed in Sec.2.6, we expect regions of the parameters space where the theory exhibits near-conformal "walking" dynamics. To elucidate the emergence of a near-conformal behaviour and its connection with complex CFTs, we take $N = M$ and consider the large N limit. To this end, we introduce the N -rescaled couplings $\alpha_h = \frac{uN}{(4\pi)^2}$ and $\alpha_v = \frac{vN^2}{(4\pi)^2}$, and consider their 1-loop beta function

$$\beta_{\alpha_v} = -\varepsilon\alpha_v + 4\alpha_v^2 \left(1 + \frac{4}{N^2}\right) + 16\alpha_v\alpha_h + 12\alpha_h^2, \quad (6.8)$$

$$\beta_{\alpha_h} = -\varepsilon\alpha_h + \frac{24}{N^2}\alpha_v\alpha_h + 8\alpha_h^2. \quad (6.9)$$

At infinite N , α_v does not influence the running of the α_h coupling which flows to an interacting fixed point in the infrared $\alpha_h^* = \varepsilon/8$. Substituting this value in the beta function for the double-trace operator, one notices that the double-trace beta function is positive and has a minimum near the origin, with the distance from the origin controlled by ε^2 . Hence, the running of α_v slows near this point, i.e. its running behaviour is replaced by a walking one. At the same time, the zeros of β_{α_v} occur at complex conjugate values of the α_v coupling $\alpha_v^* = -\frac{\varepsilon}{8}(1 \pm i\sqrt{2})$. One can also show that such behaviour persists at finite N .

Since complex CFTs are non-unitary, it is natural to wonder if large charge methods and the related CFT tools, such as Weyl maps and state-operator correspondence, can still be applied to them. In the affirmative case, this offers the attractive opportunity of studying non-conformal field theories via large charge methods by considering the associated complex CFTs and extrapolating the results to the theory with real couplings. Notice that, in general, such an extrapolation is straightforward and limited only by the knowledge of the value of the couplings at the FP. In fact, it is enough to use the latter to rewrite the obtained scaling dimensions as a power series in the couplings. Clearly, the resulting expression will be valid for *any* value of the coupling and not only at the FP. Together with the study of the charge configuration, exploring the large charge expansion in complex CFTs is our second main motivation for considering the $U(N) \times U(M)$ model.

The u coupling breaks the $O(2NM)$ symmetry to $U(M) \times U(N)$. It is, therefore, convenient to think about representations of this model as a decomposition of the $O(2NM)$ multiplets. In particular, the defining (vector) and the 2-index traceless symmetric representations of $O(2NM)$,

decompose as

$$\square_{O(2NM)} = \mathbf{2NM} = [N, \bar{M}] \oplus [\bar{N}, M], \quad (6.10)$$

$$\begin{aligned} \square\square_{O(2NM)} &= (1, \text{Adj}) \oplus (\text{Adj}, 1) \oplus (\text{Adj}, \text{Adj}) \oplus [(\square\square, \square\square^*) \oplus (\square, \square^*) \oplus c.c.], \\ 2N^2M^2 + NM - 1 &= \mathbf{N^2 - 1} \oplus \mathbf{M^2 - 1} \oplus \left(\mathbf{N^2 - 1}\right) \left(\mathbf{M^2 - 1}\right) \\ &\oplus \mathbf{2} \left(\frac{\mathbf{N(N+1)}}{2}\right) \left(\frac{\mathbf{M(M+1)}}{2}\right) \oplus \mathbf{2} \left(\frac{\mathbf{N(N-1)}}{2}\right) \left(\frac{\mathbf{M(M-1)}}{2}\right), \end{aligned} \quad (6.11)$$

where in the last line we explicitly show the dimension of the representations appearing in the decomposition. Little is known about composite operators in the $U(N) \times U(M)$ model. Thus, as the first step of our investigations, we compute the scaling dimensions of the MSD operators transforming according to the irreps appearing in the RHS of (6.11) for $N = M$ and to the first loop order. As discussed in Sec.(4.10), the 1-loop anomalous dimension can be obtained by means of an eigenvalue equation that follows directly from the EOM and conformal symmetry. The details of the computation are given in App.B, while the final results read

$$\begin{array}{cccc} \text{Rep.} & (\text{Adj}, 1) & (\text{Adj}, \text{Adj}) & (\square\square, \square\square^*) \\ \text{Oper.} & \text{Tr} [HT^aH^\dagger] & \text{Tr} [T^aHT^aH^\dagger] & \text{Tr} [K^iH\bar{K}^iH] & \text{Tr} [L^iH\bar{L}^iH] \\ \gamma_{\text{1-loop}} & \frac{v + Nu}{4\pi^2} & \frac{v}{4\pi^2} & \frac{v + u}{4\pi^2} & \frac{v - u}{4\pi^2} \end{array} \quad (6.12)$$

where the T^a are the generalized Gell-Mann matrices and $K^i(\bar{K}^i)$ and $L^i(\bar{L}^i)$ are the Clebsch-Gordan coefficients for the $SU(N)$ representations $\square\square$ ($\square\square^*$) and \square (\square^*), respectively [192]. The scaling dimensions for the operators transforming in the representations $(1, \text{Adj})$ and $(\text{Adj}, 1)$ are identical. Notice that for $u = 0$ all these operators have the same scaling dimensions, due to the enhanced $O(2N^2)$ symmetry. To the best of our knowledge, the results in Eq.(6.12) are new, except the scaling dimension of the bi-adjoint operator $\text{Tr} [T^aHT^aH^\dagger]$ which has been computed to

two-loops in [190] and reads

$$\Delta_{\text{Tr}[\text{T}^a \text{HT}^a \text{H}^\dagger]} = 2 - \varepsilon + \frac{v}{4\pi^2} + \frac{1}{64\pi^4} \left[(N^2 - 5) u^2 - 4Nuv - (N^2 + 5) v^2 \right]. \quad (6.13)$$

This result will be used as a check for our semiclassical computations.

6.1 Charging the system

The global symmetry of the model is

$$\mathcal{G} \equiv SU(N)_L \times SU(M)_R \times U(1)_A, \quad (6.14)$$

in which $U(1)_A$ is the universal phase rotation of the H field ³⁵. Under $SU(N)_L \times SU(M)_R$, the H and H^\dagger fields transform as

$$H \rightarrow LHR^\dagger, \quad H^\dagger \rightarrow RH^\dagger L^\dagger, \quad (6.15)$$

with $L \in SU(N)$ and $R \in SU(M)$.

We start, as usual, by Weyl mapping the theory to a cylinder of radius R , i.e. $\mathbb{R}^d \rightarrow \mathbb{R} \times S^{d-1}$.

The cylinder action is given by

$$\mathcal{S}_{cyl} = \int d^d x \sqrt{g} \left[\text{Tr}(\partial_\mu H^\dagger \partial^\mu H) + u_0 \text{Tr}(H^\dagger H)^2 + v_0 (\text{Tr} H^\dagger H)^2 + m^2 \text{Tr}(H^\dagger H) \right]. \quad (6.16)$$

where g denotes the metric determinant and m is given by Eq.(2.31).

As in the previous chapters, we look for a spatially homogeneous solution to the EOM that, if existing, is the solution with the smallest energy. We, therefore, consider the following homogeneous ansatz

$$H_0(\tau) = e^{2iM_E \tau} \bar{B}, \quad (6.17)$$

³⁵ It does not matter whether the universal $U(1)$ rotation acts from the left or the right. Therefore, precisely speaking, the global symmetry should be written as Eq. (6.14). Writing it as $U(N) \times U(M)$ is less rigorous but more convenient, see [38] for example.

with τ the cylinder time. M_E is an $N \times N$ diagonal matrix while \bar{B} is an $N \times M$ matrix of the form

$$\bar{B}_{N \times M} = \begin{pmatrix} B_{N \times N} & \mathbf{0}_{N \times (M-N)} \end{pmatrix}, \quad (6.18)$$

where B is an $N \times N$ diagonal matrix. The Noether charges associated with the Cartan generators are encoded in the following charge matrices

$$\mathcal{Q}_L = -V\dot{H}_0 H_0^\dagger, \quad \bar{\mathcal{Q}}_R = V H_0^\dagger \dot{H}_0, \quad (6.19)$$

with $V = R^{d-1} \Omega_{d-1}$ being the volume of S^{d-1} . Plugging in the ansatz Eq. (6.17), it is straightforward to show that

$$\mathcal{Q}_L = -2iVM_E B^\dagger B, \quad \bar{\mathcal{Q}}_R = 2iVM_E \begin{pmatrix} B^\dagger B & \mathbf{0}_{N \times (M-N)} \\ \mathbf{0}_{(M-N) \times N} & \mathbf{0}_{(M-N) \times (M-N)} \end{pmatrix}. \quad (6.20)$$

If we parametrize $\bar{\mathcal{Q}}_R$ as

$$\bar{\mathcal{Q}}_R = \begin{pmatrix} \mathcal{Q}_R & \mathbf{0}_{N \times (M-N)} \\ \mathbf{0}_{(M-N) \times N} & \mathbf{0}_{(M-N) \times (M-N)} \end{pmatrix}, \quad (6.21)$$

then from Eq. (6.20) we find the constraint

$$\mathcal{Q}_L + \mathcal{Q}_R = 0. \quad (6.22)$$

Since B is diagonal, \mathcal{Q}_L and \mathcal{Q}_R are diagonal too. From now on, we restrict our attention to the sector neutral under $U(1)_A$, which implies

$$\text{Tr} \mathcal{Q}_L = \text{Tr} \mathcal{Q}_R = 0. \quad (6.23)$$

To simplify the notation, in the following we will denote \mathcal{Q}_L simply as \mathcal{Q} , that is

$$\mathcal{Q} \equiv \mathcal{Q}_L = -\mathcal{Q}_R. \quad (6.24)$$

The Euler-Lagrange equations read

$$\partial_0^2 H + \nabla^2 H + 2u_0 H \left(H^\dagger H \right) + 2v_0 \text{Tr} \left(H^\dagger H \right) H + m^2 H = 0 , \quad (6.25)$$

and for our homogeneous ansatz Eq. (6.17), they reduce to:

$$2M_E^2 B = -u_0 B^\dagger B^2 - v_0 \text{Tr} \left(B^\dagger B \right) B - \frac{m^2}{2} B . \quad (6.26)$$

We label the diagonal entries of M_E as $M_{E,ii} = -i\mu_i$, and those of B as $B_{ii} = b_i$. The μ_i are a set of chemical potentials and should not be mistaken with the group-theoretical weight matrix μ used later in this chapter. Unlike the other models considered in this thesis, here we have multiple independent chemical potentials, whose relative importance is determined by charge configuration. The EOM can be rewritten in component form as

$$2\mu_i^2 = u_0 b_i^2 + v_0 \sum_{k=1}^N b_k^2 + \frac{m^2}{2} , \quad (6.27)$$

while the corresponding "charges" read

$$J_i \equiv (\mathcal{Q}_L)_{ii} = -2V b_i^2 \mu_i . \quad (6.28)$$

Then, unlike the $O(N)$ case, a spatially homogeneous ground state is compatible with every diagonal charge matrix \mathcal{Q} .

The classical energy E is given by evaluating the cylinder Lagrangian \mathcal{L}_{cyl} in (6.16) with an appropriate boundary term $-\sum_{i=1}^N \mu_i \frac{\partial \mathcal{L}_{\text{cyl}}}{\partial \mu_i}$, which implements the charge fixing. We obtain

$$\frac{E}{V} = \mathcal{L}_{\text{cyl}} - \sum_{i=1}^N \mu_i \frac{\partial \mathcal{L}_{\text{cyl}}}{\partial \mu_i} = 4 \sum_{i=1}^N b_i^2 \mu_i^2 + u_0 \sum_{i=1}^N b_i^4 + v_0 \left(\sum_{i=1}^N b_i^2 \right)^2 + m^2 \sum_{i=1}^N b_i^2 . \quad (6.29)$$

Before proceeding with the computation of the scaling dimensions, in the next section, we will perform a group-theoretical analysis of the $U(N) \times U(M)$ model apt at determining the relation between a given charge configuration and the associated MSD operators.

6.2 Fixed-charge operators in the $U(N) \times U(M)$ model

In this section, we study the identification of the irreducible representation associated with a given charge configuration from Lie algebraic considerations. To this end, we will introduce and prove several propositions about the group-theoretical properties of the MSD operators. We assume perturbativity and make use of the MCSD assumption introduced in Sec.4.1.

Proposition 1: Consider a fixed-charge operator \mathcal{O} with minimal CSD. We denote the CSD of \mathcal{O} by D . Furthermore, suppose \mathcal{O} belongs to some irreducible representation (Γ_L, Γ_R) of $SU(N)_L \times SU(M)_R$ in the $U(1)_A$ -neutral sector. Then Γ_L must appear in $(\mathbf{Adj}_L)^{D/2}$, with \mathbf{Adj}_L being the adjoint representation of $SU(N)_L$; Γ_R must appear in $(\mathbf{Adj}_R)^{D/2}$, with \mathbf{Adj}_R being the adjoint representation of $SU(M)_R$.

Proof of Proposition 1: Since we are considering a homogeneous ground state and MCSD, \mathcal{O} must be a Lorentz scalar with no derivatives. Then \mathcal{O} must be built out of the product of $D/2$ H fields and $D/2$ H^\dagger fields (so that \mathcal{O} is also neutral under $U(1)_A$). Now, under $SU(N)_L \times SU(M)_R$

$$H \sim (\mathbf{F}_L, \bar{\mathbf{F}}_R), \quad H^\dagger \sim (\bar{\mathbf{F}}_L, \mathbf{F}_R), \quad (6.30)$$

where \mathbf{F}_L and $\bar{\mathbf{F}}_L$ are the fundamental and anti-fundamental representations of $SU(N)_L$, respectively. The notation for representations of $SU(M)_R$ is self-explanatory. Therefore, \mathcal{O} must transform as an irreducible component inside the reducible representation

$$(\Gamma_{L0}, \Gamma_{R0}), \quad \Gamma_{L0} \equiv (\mathbf{F}_L \otimes \bar{\mathbf{F}}_L)^{D/2}, \quad \Gamma_{R0} \equiv (\mathbf{F}_R \otimes \bar{\mathbf{F}}_R)^{D/2}. \quad (6.31)$$

On the other hand, the tensor product $\mathbf{F}_L \otimes \bar{\mathbf{F}}_L$ decomposes as

$$\mathbf{F}_L \otimes \bar{\mathbf{F}}_L = \mathbf{1}_L \oplus \mathbf{Adj}_L, \quad \mathbf{F}_R \otimes \bar{\mathbf{F}}_R = \mathbf{1}_R \oplus \mathbf{Adj}_R, \quad (6.32)$$

and thus

$$\Gamma_{L0} = (\mathbf{1}_L \oplus \mathbf{Adj}_L)^{D/2}, \quad \Gamma_{R0} = (\mathbf{1}_R \oplus \mathbf{Adj}_R)^{D/2}. \quad (6.33)$$

All singlet components in $\mathbf{1}_L \oplus \mathbf{Adj}_L$ and $\mathbf{1}_R \oplus \mathbf{Adj}_R$ can be dropped because \mathcal{O} is an MCSD operator. In fact, if a singlet component contributes, then one would be able to construct another operator that corresponds to the same charge configuration with less number of H and H^\dagger fields, in contradiction to the MCSD requirement. Then proposition 1 follows.

Proposition 2: (Γ_L, Γ_R) must appear in the $U(1)_A$ -neutral sector of the decomposition of the D -index traceless fully symmetric tensor of $O(2NM)$ under the branching

$$O(2NM) \supset SU(NM) \times U(1)_A \supset SU(N)_L \times SU(M)_R \times U(1)_A . \quad (6.34)$$

Proposition 2 follows straightforwardly from the MCSD assumption.

6.2.1 The charge configuration

Our next step is to determine the precise correspondence between the charge matrices \mathcal{Q} and the weight of the irreducible representations of $U(N) \times U(M)$. By definition, they have to be equal up to a normalization factor which we now determine. The matrix \mathcal{Q} belongs to the special linear algebra $\text{sl}(N; \mathbb{C})$, which is the space of all the traceless $N \times N$ complex matrices. $\text{sl}(N; \mathbb{C})$ is the complexification of the real Lie algebra of the $SU(N)$ group [193]. The Cartan subalgebra \mathfrak{h} of $\text{sl}(N; \mathbb{C})$ can be characterized by

$$\mathfrak{h} = \left\{ \begin{pmatrix} \lambda_1 & & \\ & \ddots & \\ & & \lambda_N \end{pmatrix} \middle| \lambda_j \in \mathbb{C}, \lambda_1 + \dots + \lambda_N = 0 \right\} . \quad (6.35)$$

A weight is a linear functional on \mathfrak{h} . Nevertheless, it is convenient to identify linear functionals on \mathfrak{h} with elements of \mathfrak{h} itself, by virtue of an inner product on \mathfrak{h} . Suppose K and K' are two elements of \mathfrak{h} , we define their inner product by

$$\langle K, K' \rangle = \text{Tr}(K^* K') . \quad (6.36)$$

If ϕ is a linear functional on \mathfrak{h} , there is a unique element λ in \mathfrak{h} such that

$$\phi(K) = \langle \lambda, K \rangle \quad \forall K \in \mathfrak{h} . \quad (6.37)$$

Therefore, by virtue of the inner product defined in Eq. (6.36), a weight μ can be thought of as an element in \mathfrak{h} .

The charge configuration matrix \mathcal{Q} should be proportional to some weight μ of a representation of $\text{sl}(N; \mathbb{C})$. Let us now determine the precise correspondence, assuming $\mathcal{Q} = \mathcal{Q}_L$ is normalized as in Eq. (6.19). Suppose \mathcal{Q} can be decomposed as

$$\mathcal{Q} = \sum_{j=1}^{N-1} x_j \hat{h}_j , \quad (6.38)$$

with \hat{h}_j being a set of *orthonormal* basis elements of \mathfrak{h} , with the orthogonality defined through the inner product (6.36), and the normalization condition being

$$\text{Tr}(\hat{h}_j^2) = \frac{1}{2} , \quad j = 1, 2, \dots, N-1 . \quad (6.39)$$

For instance, the following element is normalized

$$\hat{h}_1 = \frac{1}{2}(E_{11} - E_{22}) , \quad (6.40)$$

where E_{ij} is an $N \times N$ matrix with a "1" in the (i, j) entry and "0" elsewhere. The normalization of basis elements is required as in Eq. (6.39) because, for example, one can compute the commutation relation

$$[\hat{h}_1, E_{12}] = E_{12} , \quad (6.41)$$

which implies a raising operator constructed with a single E_{12} will carry charge +1 corresponding to \hat{h}_1 . One may wish to make this argument more precisely by rewriting Eq. (6.41) as a commutation relation between the corresponding charge operator and the corresponding fixed-charge operator, computed with the help of canonical commutation relations of fundamental fields.

Then x_j in Eq. (6.38) gives the Cartan charge associated with \hat{h}_j , and can be computed as

$$x_j = 2\text{Tr}(\mathcal{Q}\hat{h}_j) . \quad (6.42)$$

On the other hand, for the weight μ , the Cartan charge associated with \hat{h}_j is given by

$$\mu(\hat{h}_j) = \langle \mu, \hat{h}_j \rangle = \text{Tr}(\mu^* \hat{h}_j) . \quad (6.43)$$

Here we use the same symbol μ for the weight as a linear functional and as an element in \mathfrak{h} . We will only be concerned with the case of real μ , and therefore the Cartan charge reads

$$\mu(\hat{h}_j) = \text{Tr}(\mu \hat{h}_j) . \quad (6.44)$$

Comparing Eq. (6.42) and Eq. (6.44), we conclude that the correspondence between \mathcal{Q} and μ is

$$\mathcal{Q} = \frac{1}{2}\mu . \quad (6.45)$$

This leads to the following proposition

Proposition 3: Suppose \mathcal{O} belongs to the irreducible representation (Γ_L, Γ_R) of $SU(N)_L \times SU(M)_R$ in the $U(1)_A$ -neutral sector. Then $2\mathcal{Q}$ must be a weight of Γ_L , and $-2\mathcal{Q}$ must be a weight of Γ_R .

Since the weights of Lie algebra representations sit on a discrete weight lattice, we then deduce from Eq. (6.45) that the charge configuration \mathcal{Q} is also quantized.

According to Proposition 1, the weights of our interest should belong to $(\mathbf{Adj}_L)^{D/2}$ when we consider the $SU(N)_L$ factor. The nonzero weights of \mathbf{Adj}_L are nonzero roots of $\text{sl}(N; \mathbb{C})$, which are given by [193]

$$\alpha_{jk} = e_j - e_k , \quad j \neq k , \quad j, k = 1, 2, \dots, N , \quad (6.46)$$

where e_j 's denote the standard basis elements of \mathbb{C}^N , that is

$$e_j = \{ \underbrace{0, \dots, 0}_{j-1}, 1, \underbrace{0, \dots, 0}_{N-j} \} , \quad (6.47)$$

for $j = 1, 2, \dots, N$. Note that in this representation of roots we have identified \mathfrak{h} with the subspace of \mathbb{C}^N consisting of vectors whose components sum to zero [193]. Since the weights of a tensor product representation are given by the sum of the weights of the component representations [194], we conclude that if μ is a weight of $(\mathbf{Adj}_L)^{D/2}$, then we can express it as

$$\mu = \sum_{p=1}^{D/2} s_p \alpha_{j_p k_p} , \quad \text{with } s_p = 1 \text{ or } 0 , \quad (6.48)$$

and for $p = 1, 2, \dots, D/2$, $\alpha_{j_p k_p} = e_{j_p} - e_{k_p}$ with $j_p \neq k_p$ is one of the weights in Eq. (6.46). From Eq. (6.48) we deduce that if we write $\mu = (\mu_1, \mu_2, \dots, \mu_N)$, then $\mu_i \in \mathbb{Z}$, $\forall i = 1, 2, \dots, N$, and then Eq. (6.45) tells us the diagonal entries of \mathcal{Q} must be integers or half-integers.

Given a vector $v \equiv (v_1, v_2, \dots, v_N) \in \mathbb{C}^N$, we define the A-length $A[v]$ of v as

$$A[v] \equiv \sum_{i=1}^N |v_i| . \quad (6.49)$$

The A-length satisfy the following triangle inequality

$$A[v + \rho] \leq A[v] + A[\rho] , \quad v, \rho \in \mathbb{C}^N . \quad (6.50)$$

In fact

$$A[v + \rho] = \sum_{i=1}^N |v_i + \rho_i| \leq \sum_{i=1}^N |v_i| + \sum_{i=1}^N |\rho_i| = A[v] + A[\rho] . \quad (6.51)$$

Also, the A-length has clearly a linearity property with respect to multiplication by a c-number. Then by using the triangle inequality (6.50) and the linearity property of the A-length, Eq. (6.48) yields

$$A[\mu] \leq \sum_{p=1}^{D/2} A[s_p \alpha_{j_p k_p}] = \sum_{p=1}^{D/2} |s_p| A[\alpha_{j_p k_p}] . \quad (6.52)$$

Now let us note that

$$|s_p| \leq 1 , \quad A[\alpha_{j_p k_p}] = 2 , \quad (6.53)$$

and thus

$$A[\mu] \leq 2 \times D/2 = D . \quad (6.54)$$

On the other hand, from Eq.(6.45), we have

$$A[\mathcal{Q}] = \frac{1}{2}A[\mu] , \quad (6.55)$$

then

$$D \geq 2A[\mathcal{Q}] , \quad (6.56)$$

and we arrive at the following proposition

Proposition 4 The classical dimension D of an operator carrying the charge configuration $\mathcal{Q} = \text{diag}\{Q_1, Q_2, \dots, Q_N\}$ satisfies the inequality

$$D \geq 2 \sum_{i=1}^{i=N} |Q_i| . \quad (6.57)$$

Eq.(6.57) relates the classical dimension of the operators with the charge configuration they carry.

6.2.2 Scaling dimension and operator construction

All the conclusions achieved so far are deduced without the explicit construction of the operators. Here, we illustrate how to construct the MSD operators and show that they satisfy Eq. (6.57) with the equality sign. To this end, we first consider building blocks with simple definite transformation properties under $SU(N)_L \times SU(M)_R \times U(1)_A$, and then we iterate them. Intuitively, we build the fixed-charge operators as a product of "unit-charge" blocks. For example, consider the block

$$\text{Tr}(\tau_L H \tau_R^\dagger H^\dagger) , \quad (6.58)$$

where τ_L is an $N \times N$ matrix in some root subspace of the $\text{sl}(N; \mathbb{C})$ Lie algebra, and τ_R is an $M \times M$ matrix related to τ_L in the following manner

$$\tau_R = \begin{pmatrix} \tau_L & \mathbf{0}_{N \times (M-N)} \\ \mathbf{0}_{(M-N) \times N} & \mathbf{0}_{(M-N) \times (M-N)} \end{pmatrix}. \quad (6.59)$$

The building block in Eq. (6.58) lives in the bi-adjoint representation of $SU(N)_L \times SU(M)_R$, i.e. $(\mathbf{Adj}_L, \mathbf{Adj}_R)$. It is constructed such that $\mathcal{Q}_L + \mathcal{Q}_R = 0$ is manifestly satisfied, with \mathcal{Q}_L corresponding to a weight of \mathbf{Adj}_L . The explicit form of τ_L is given by

$$\tau_L = E_{pq}, \quad (6.60)$$

for some $p, q = 1, 2, \dots, N$ and $p \neq q$. This follows from the commutation relation

$$[\hat{h}_j, E_{pq}] = \frac{1}{2}(\delta_{jp} - \delta_{jq} - \delta_{j+1,p} + \delta_{j+1,q})E_{pq}, \quad (6.61)$$

where $j = 1, 2, \dots, N-1$ and \hat{h}_j is defined by

$$\hat{h}_j \equiv \frac{1}{2}(E_{j,j} - E_{j+1,j+1}), \quad (6.62)$$

which satisfy the normalization condition $\text{Tr}(\hat{h}_j^2) = \frac{1}{2}$.

Let us identify the charge configuration associated with Eq. (6.58). Define a set of N linear functionals $\varepsilon_p, p = 1, \dots, N$ acting on \mathfrak{h} as follows:

$$\varepsilon_p(\hat{h}_j) = \frac{1}{2}(\delta_{jp} - \delta_{j+1,p}). \quad (6.63)$$

Then Eq. (6.61) can be written as

$$[\hat{h}_j, E_{pq}] = \{\varepsilon_p(\hat{h}_j) - \varepsilon_q(\hat{h}_j)\}E_{pq}, \quad (6.64)$$

which means E_{pq} corresponds to the root $\varepsilon_p - \varepsilon_q$, which when mapped into \mathfrak{h} using the inner product

Eq. (6.36) gives α_{pq} defined in Eq. (6.46)³⁶. This α_{pq} corresponds to the weight of \mathbf{Adj}_L associated with Eq. (6.58) and the related charge configuration is simply $\frac{1}{2}\alpha_{pq}$, according to Eq. (6.45).

To build operators in more general charge configuration, we may consider

$$\mathrm{Tr}\left[\Pi_j(\tau_{Lj}H\tau_{Rj}^\dagger H^\dagger)^{y_j}\right]. \quad (6.65)$$

Here $y_j > 0$ is a positive integer, and τ_{Lj} is an $N \times N$ matrix with the explicit form given by $\tau_{Lj} = E_{p(j)q(j)}$ for some $p, q = 1, 2, \dots, N$ that depend on j . The way that Eq. (6.65) is constructed implies that its charge configuration \mathcal{Q} is simply the appropriate linear combination of the charge configuration \mathcal{Q}_j of its corresponding building blocks

$$\mathcal{Q} = \sum_j y_j \mathcal{Q}_j, \quad (6.66)$$

where

$$\mathcal{Q}_j = \frac{1}{2} \alpha_{p(j)q(j)}. \quad (6.67)$$

We can now reverse the logic and ask, for a given \mathcal{Q} , how one may choose τ_{Lj} and y_j in order to construct a MCSD operator in the form of Eq. (6.65). To this end, we may rewrite Eq. (6.66) as

$$2\mathcal{Q} = \sum_j y_j \alpha_{p(j)q(j)}. \quad (6.68)$$

Note that $2\mathcal{Q} \in \mathbb{C}^N$, with all entries being integers and the sum of all entries is zero. We also have $\alpha_{p(j)q(j)} \in \mathbb{C}^N$, which for a given j has only two nonzero entries, filled by $+1$ and -1 respectively. MCSD requires the minimization of $\sum_j y_j$ for a given \mathcal{Q} . We can rewrite Eq. (6.68) as

$$2\mathcal{Q} - \sum_j y_j \alpha_{p(j)q(j)} = 0, \quad (6.69)$$

where now the LHS indicates a process in which we subtract $\alpha_{p(j)q(j)}$'s from the given \mathbb{C}^N vector $2\mathcal{Q}$. Suppose each time we are only allowed to subtract one $\alpha_{p(j)q(j)}$, which we call an *elementary*

³⁶This can be deduced from the results in Appendix G of the textbook by J. F. Cornwell [194].

subtraction. (For a given j we, therefore, eventually subtract it y_j times). Hence the sum $\sum_j y_j$ equals the total number of times we need to perform such elementary subtractions to make the resulting \mathbb{C}^N vector vanish. Then $\sum_j y_j$ is minimized when, during the subtraction process, each entry of the \mathbb{C}^N vector changes in a *monotonic* manner (or remains unchanged). For example, we take $2\mathcal{Q} = (2, -1, -1)$. The following subtraction process is monotonic

$$(2, -1, -1) \rightarrow (1, 0, -1) \rightarrow (0, 0, 0) , \quad (6.70)$$

while the following subtraction is not monotonic

$$(2, -1, -1) \rightarrow (1, 0, -1) \rightarrow (1, -1, 0) \rightarrow (0, 0, 0) . \quad (6.71)$$

This simple example shows the general fact that non-monotonic subtractions increase the total number of times we need to subtract the vector to zero. Monotonic subtraction can always be realized, by subtracting from the positive entry with the largest absolute value and the negative entry with the largest absolute value each time. In such a case, the total number of times we need to perform elementary subtractions is simply $A[2\mathcal{Q}]/2 = A[\mathcal{Q}]$, that is

$$A[\mathcal{Q}] = \sum_j y_j . \quad (6.72)$$

On the other hand, the CSD D of the operator in Eq. (6.65) is

$$D = 2 \sum_j y_j . \quad (6.73)$$

Therefore, we conclude that the fixed-charge \mathcal{Q} operators with the MCSD satisfy

$$D = 2A[\mathcal{Q}] , \quad (6.74)$$

saturating our previous finding Eq. (6.57), which we derived without constructing the operators.

Notice that the method does not guarantee that the MCSD operator is unique. In fact, one may redistribute the trace operation (i.e. splitting one trace into multiple traces), change the order of

matrix products for different $\tau_{Lj}H\tau_{Rj}^\dagger H^\dagger$ factors, or change the root basis, to obtain more operators associated with the same charge configuration. Even if we impose the MCSD requirement, there can be multiple solutions. It is also not known whether the above method based on the $\tau_{Lj}H\tau_{Rj}^\dagger H^\dagger$ building blocks with appropriate application of the trace operation covers all fixed-charge MCSD operators.

Nevertheless, for a special type of charge configuration, there is a unique answer, and we know the above way of explicit construction must lead to the unique answer. This charge configuration is

$$\mathcal{Q}_J = \text{diag} \{ -J, J, 0, \dots, 0 \} , \quad (6.75)$$

with J integer or half-integer. This charge configuration corresponds to the highest weight in the tensor product of \mathbf{Adj}_L , which is, in turn, the sum of the highest weight of \mathbf{Adj}_L . The uniqueness results from the fact that the highest weight of a representation is always simple. This representation has Dynkin label

$$\Gamma_J = (2J, 0, \dots, 0, 2J) . \quad (6.76)$$

For $J = 1/2$ the MSD operator lives in the bi-adjoint representation (Adj , Adj). For $N = M$, its 2-loop scaling dimension is given by Eq.(6.13).

The above discussion paves the way for a general identification of the irreducible representations associated to a given charge configuration. Within the MCSD assumption, the MCSD can be determined by virtue of Proposition 4 from the given charge matrix \mathcal{Q} . Then the candidate irreducible representations must satisfy the requirements of Proposition 1-3.

For a given charge configuration, we are, therefore, left with a (reduced by the above analysis) list of candidates for the MSD operator. To further narrow down the list to a single operator, we need to add to the group-theoretical constraints the actual computation of the scaling dimensions in the large charge expansion. The complete strategy can be schematized as follows:

1. Fix the CSD. Then, list all the charge configurations which satisfy Eq.(6.74).
2. For each charge configuration list all the irreps satisfying propositions 1-3 that contain it, and compute the ground state energy to NLO in the large charge expansion.
3. If for different charge configurations, we obtain different ground state energies, then the

corresponding MSD operators are distinct. This basic observation allows pinning down the correspondence between charge configuration and MSD operators.

This procedure will be discussed in the next two sections.

6.3 Semiclassical expansion and results

Having introduced the necessary group-theoretical results, we proceed with the semiclassical calculation of the scaling dimensions in the large charge expansion.

To this end, we start by considering a 2-parameters family of charge configurations

$$\mathcal{Q}_{J,s} = \text{diag}(\underbrace{J, J, \dots, J}_{s}, \underbrace{-J, -J, \dots, -J}_{s}, \underbrace{0, 0, \dots, 0}_{N-2s}). \quad (6.77)$$

For $N = M$ and varying s , this charge configuration interpolates between the ones considered in [86] ($s = 1$; given in Eq.(6.75)) and [61] ($s = N/2$). From Eq.(6.74) we have that the CSD of the corresponding operator is $\bar{Q} = 4sJ$. Notice that, since $J \geq 1/2$, this implies that the results obtained in [61] for the case $M = N$, $s = N/2$ make sense only when $\bar{Q} \geq N$ and not for arbitrary values of \bar{Q} and N .

At fixed CSD we can access the anomalous dimension of operators transforming in various irreducible representations by varying the parameters s and J .

The classical energy for this charge configuration can be easily computed along the lines of Chap.4. By parameterizing the M_E and B matrices as follow

$$\mu_i = \begin{cases} \mu & i = 1, \dots, s, \\ -\mu & i = s + 1, \dots, 2s, \\ 0 & i = 2s + 1, \dots, N, \end{cases} \quad b_i = \begin{cases} b & i = 1, \dots, 2s, \\ 0 & i = 2s + 1, \dots, N, \end{cases} \quad (6.78)$$

the charge constraint (6.28) and EOM (6.27) become

$$J = 2V\mu b^2, \quad 2\mu^2 = (u_0 + 2sv_0)b^2 + \frac{m^2}{2}. \quad (6.79)$$

We work with N -rescaled (renormalized³⁷) 't Hooft couplings, which we define as

$$\mathcal{A}_h = J \frac{uN}{(4\pi)^2}, \quad \mathcal{A}_v = J \frac{2svN}{(4\pi)^2}. \quad (6.80)$$

Then the above equations imply

$$2\frac{\mu}{m} = \frac{3^{\frac{1}{3}} + x^{\frac{2}{3}}}{3^{\frac{2}{3}}x^{\frac{1}{3}}}, \quad x = \frac{72}{N}(\mathcal{A}_h + \mathcal{A}_v) + \sqrt{-3 + \left(\frac{72}{N}(\mathcal{A}_h + \mathcal{A}_v)\right)^2}, \quad (6.81)$$

and our semiclassical expansion takes the form

$$\Delta_{\mathcal{O}_{J,s}} = \sum_{k=-1} \frac{1}{J^k} \Delta_k(\mathcal{A}_h^*, \mathcal{A}_v^*, s). \quad (6.82)$$

The leading order in the semiclassical expansion follows straightforwardly from the results above by setting $d = 4$ and $\mathcal{A}_{h,v} = \mathcal{A}_{h,v}^*$, where the star denotes the value of the couplings at the FP. We have

$$\Delta_{-1}(\mathcal{A}_h^*, \mathcal{A}_v^*, s) = \frac{sN}{144(\mathcal{A}_h^* + \mathcal{A}_v^*)} \frac{1}{x^{*\frac{4}{3}}} \left(\sqrt[3]{3}x^{*8/3} - 3x^{*4/3} + 6\sqrt[3]{3}x^{*2/3} + 2\sqrt[3]{3}x^{*2} + 3^{5/3} \right). \quad (6.83)$$

The expansion for small $\mathcal{A}_{h,v}^*$ reads

$$\begin{aligned} J\Delta_{-1}(\mathcal{A}_h^*, \mathcal{A}_v^*, s) = \bar{Q} \left[1 + 4 \left(\frac{\mathcal{A}_h^* + \mathcal{A}_v^*}{N} \right) - 32 \left(\frac{\mathcal{A}_h^* + \mathcal{A}_v^*}{N} \right)^2 \right. \\ \left. + 512 \left(\frac{\mathcal{A}_h^* + \mathcal{A}_v^*}{N} \right)^3 + \mathcal{O} \left(\frac{\mathcal{A}_h^* + \mathcal{A}_v^*}{N} \right)^4 \right]. \end{aligned} \quad (6.84)$$

We checked that for $\mathcal{A}_h = 0$, Eq.(6.83) reduces to the classical energy of the $O(2NM)$ model (4.49).

Before proceeding with the computation of Δ_0 , it is useful to study the induced symmetry breaking pattern. As in the $O(N)$ case, it can be seen as a two-step process: an explicit symmetry breaking induced by the charge-fixing term followed by an SSB induced by the classical ground state. The explicit breaking can, in general, be deduced by adding the charge-fixing boundary term

³⁷At the classical level, bare and renormalized coupling are equal.

$-\sum_{i=1}^N \mu_i \frac{\partial \mathcal{L}_{\text{cyl}}}{\partial \mu_i}$ to the Lagrangian and check which symmetries it preserves.

We have

$$SU(N)_L \times SU(M)_R \times U(1)_A \xrightarrow{\text{explicit}} C(R)_L \times SU(M)_R \times U(1)_A , \quad (6.85)$$

where $C(R)_L$ is the $SU(N)_L$ subgroup commuting with $P_1 = \text{diag}(\underbrace{1, 1, \dots, 1}_s, \underbrace{-1, -1, \dots, -1}_s, \underbrace{0, 0, \dots, 0}_{N-2s})$ and it is explicitly given by

$$C(R)_L = SU(s)_{Lu} \times SU(s)_{Ld} \times SU(N-2s)_{Ld} \times U(1)_{L3} \times U(1)_{L5} , \quad (6.86)$$

where $SU(s)_{Lu}$ and $SU(s)_{Ld}$ are rotations in the first and second upper $s \times s$ blocks of $SU(N)_L$ while $SU(N-2s)_{Ld}$ rotates the lower $N-2s \times N-2s$ block. Finally $U(1)_{L3}$ and $U(1)_{L5}$ are generated, respectively, by P_1 and $P_2 = \text{diag}(\underbrace{1, 1, \dots, 1}_{2s}, \underbrace{0, 0, \dots, 0}_{N-2s})$ and act on the left factor.

The spontaneous symmetry breaking is determined by the vacuum configuration, which is proportional to the P_2 matrix defined above. We have

$$\begin{aligned} C(R)_L \times SU(M)_R \times U(1)_A &\xrightarrow{\text{SSB}} & SU(s)_{Lu} \times SU(s)_{Ld} \times SU(N-2s)_{Ld} \times U(1)_{D3} \\ && \times U(1)_{D5} \times SU(M-2s)_{Rd} \times U(1)_{A6} . \end{aligned} \quad (6.87)$$

Here, $U(1)_{D3,5}$ are the diagonal subgroup of $U(1)_{L3,5} \times U(1)_{R3,5}$ where $U(1)_{R3,5}$ are the counterparts of $U(1)_{L3,5}$ acting on the right factor. Finally, $SU(M-2s)_{Rd}$ is defined as the $SU(M-2s)$ rotation in the lower $M-2s \times M-2s$ block of $SU(M)_R$. To define $U(1)_{A6}$, we first introduce $U(1)_{L6}$ which is generated by $\text{diag}(\underbrace{0, 0, \dots, 0}_{2s}, \underbrace{1, 1, \dots, 1}_{N-2s})$ and acts on the left, and $U(1)_{R6}$ which is generated by $\text{diag}(\underbrace{0, 0, \dots, 0}_{2s}, \underbrace{1, 1, \dots, 1}_{M-2s})$ and acts on the right. $U(1)_{A6}$ is then defined as the axial part of $U(1)_{L6}$ and $U(1)_{R6}$. Note the diagonal part of $U(1)_{L6}$ and $U(1)_{R6}$ is not independent from $U(1)_{D5}$ and is thus not counted.

The total number of broken generators of the SSB is

$$M^2 - 1 - [(M-2s)^2 - 1] = 4s(M-s) . \quad (6.88)$$

In order to determine the NLO of the large charge expansion, we parametrize the fluctuations

as

$$H(\tau, \mathbf{x}) = e^{2iM_E\tau}(\bar{B} + \phi(\tau, \mathbf{x})), \quad (6.89)$$

where $\phi(\tau, \mathbf{x})$ is a $N \times M$ matrix. The Lagrangian at the quadratic order in the fluctuations reads

$$\begin{aligned} \mathcal{L}^{(2)} = & \sum_{i=1}^N \sum_{j=1}^M \partial_\mu \phi_{ij} \partial^\mu \phi_{ij}^* - 2\mu \left[\sum_{i=1}^s \sum_{j=1}^M ((\partial_0 \phi_{ij}) \phi_{ij}^* - \phi_{ij} \partial_0 \phi_{ij}^*) - \sum_{i=s+1}^{2s} \sum_{j=1}^M ((\partial_0 \phi_{ij}) \phi_{ij}^* - \phi_{ij} \partial_0 \phi_{ij}^*) \right] \\ & + 2u_0 b^2 \sum_{i=1}^N \sum_{j=1}^{2s} \phi_{ij}^* \phi_{ij} + u_0 b^2 \sum_{i=1}^{2s} \sum_{j=1}^{2s} (\phi_{ij} \phi_{ji} + \phi_{ij}^* \phi_{ji}^*) + v_0 b^2 \left[\sum_{i=1}^{2s} (\phi_{ii} + \phi_{ii}^*) \right]^2 \\ & + (4sv_0 b^2 + m^2) \sum_{i=2s+1}^N \sum_{j=1}^M \phi_{ij} \phi_{ij}^*. \end{aligned} \quad (6.90)$$

It is useful to write ϕ in a block form as

$$\phi = \begin{pmatrix} \phi_{2s \times 2s}^{(11)} & \phi_{2s \times (M-2s)}^{(12)} \\ \phi_{(N-2s) \times 2s}^{(21)} & \phi_{(N-2s) \times (M-2s)}^{(22)} \end{pmatrix}. \quad (6.91)$$

The blocks decouple and we can decompose $\mathcal{L}^{(2)}$ as $\mathcal{L}^{(2)} = \mathcal{L}_{(11)}^{(2)} + \mathcal{L}_{(12)}^{(2)} + \mathcal{L}_{(21)}^{(2)} + \mathcal{L}_{(22)}^{(2)}$. The dispersion relations of the fluctuations appearing in the various blocks can be computed from the inverse propagator as explained in Sec.(4.6). The result reads

$$\begin{aligned} \omega_1 &= \sqrt{J_\ell^2 + 4\mu^2} & 4s(N-2s) \text{ d.o.f.} \\ \omega_2 &= \sqrt{J_\ell^2 + m_2^2} & 2(N-2s)(M-2s) \text{ d.o.f.} \\ \omega_{3,4} &= \sqrt{J_\ell^2 + 4\mu^2} \mp 2\mu & 2s(2M-3s) \text{ d.o.f.} \\ \omega_{5,6} &= \sqrt{J_\ell^2 + 4\mu^2 + m_1^2} \pm 2\mu & 2s^2 \text{ d.o.f.} \\ \omega_{7,8} &= \frac{1}{\sqrt{2}} \sqrt{2J_\ell^2 + m_1^2 + 16\mu^2 \pm \sqrt{(2J_\ell^2 + m_1^2 + 16\mu^2)^2 - 4J_\ell^2 (J_\ell^2 + m_1^2)}} & 4s^2 - 2 \text{ d.o.f.} \\ \omega_{9,10} &= \frac{1}{\sqrt{2}} \sqrt{2J_\ell^2 + m_0^2 + 16\mu^2 \pm \sqrt{(2J_\ell^2 + m_0^2 + 16\mu^2)^2 - 4J_\ell^2 (J_\ell^2 + m_0^2)}} & 2 \text{ d.o.f.}, \end{aligned} \quad (6.92)$$

where

$$m_0^2 = 8\mu^2 - 2m^2, \quad m_1^2 = (8\mu^2 - 2m^2) \frac{u_0}{u_0 + 2sv_0}, \quad m_2^2 = 4sv_0b^2 + m^2. \quad (6.93)$$

ω_3 describes type II Goldstone bosons while ω_8 and ω_{10} correspond to relativistic type I Goldstone bosons. The remaining dispersion relations describe gapped modes. It's easy to check that the number of real d.o.f. sums to $2NM$ while the counting of Goldstone modes with respect to the number of broken generators is

$$2 \times s(2M - 3s) + 2s^2 - 1 + 1 = 4s(M - s), \quad (6.94)$$

which agrees with Eq.(6.88), as dictated by the charged Goldstone theorem of Sec.(3.4). Proceeding as in Sec.4.6, it is easy to show that the (bare) NLO of the semiclassical expansion is given by

$$e_0 = \frac{R}{2} \sum_{\ell=0}^{\infty} n_{\ell} \sum_i g_i(M, N, s) \omega_i(\ell). \quad (6.95)$$

where ω_i are the dispersion relations in Eq.(6.92) and $g_i(M, N, s)$ is the number of the corresponding degrees of freedom. Regularization and renormalization are performed as outlined in Sec.(4.7), yielding

$$\begin{aligned} \Delta_0(\mathcal{A}_h^*, \mathcal{A}_v^*, s) = & \rho(x^*, M, N, s, \mathcal{A}_h^*, \mathcal{A}_v^*) + \frac{1}{2} \sum_{\ell=0}^{\infty} \left[R(1+\ell)^2 \left(\sum_i g_i(M, N, s) \omega_i(\ell, x^*, \mathcal{A}_h^*, \mathcal{A}_v^*) \right)_{d=4} \right. \\ & \left. + \sigma(\ell, x^*, M, N, s, \mathcal{A}_h^*, \mathcal{A}_v^*) \right], \end{aligned} \quad (6.96)$$

where x^* has been defined in Eq.(6.81) while $\rho(x^*, M, N, s, \mathcal{A}_h^*, \mathcal{A}_v^*)$ and $\sigma(\ell, x^*, M, N, s, \mathcal{A}_h^*, \mathcal{A}_v^*)$ are given in App.C.

We checked the cancellation of the divergent $1/\epsilon$ terms between Δ_{-1} and Δ_0 as explained in Sec.(4.7). For $\mathcal{A}_h = 0$ the result reduces to its counterpart in the $O(2NM)$ model (4.76).

The perturbative expansion of Δ_0 for small 't' Hooft couplings reads

$$\Delta_0 = -\frac{4}{N(\mathcal{A}_h^* + \mathcal{A}_v^*)} [2s\mathcal{A}_h^{*2}(M + N + 7s) + \mathcal{A}_h^*\mathcal{A}_v^*(2s(2(M + N) + s) + 7) + (MN + 5)\mathcal{A}_v^{*2}]$$

$$\begin{aligned}
& -\frac{16}{N^2} [2s\mathcal{A}_h^{*2}(M+N-s) + 4\mathcal{A}_h^*\mathcal{A}_v^*(s(M+N-2s)-1) + (MN-3)\mathcal{A}_v^{*2}] \\
& + \frac{128}{N^3} [2\mathcal{A}_h^{*2}\mathcal{A}_v^* (6\zeta(3)(s(M+N+5s)+2) + 3Ms + 3Ns - 28s^2 - 13) \\
& + \mathcal{A}_h^*\mathcal{A}_v^{*2} (12\zeta(3)(s(M+N)+3) + MN + 4Ms + 4Ns - 24s^2 - 44) \\
& + 2s\mathcal{A}_h^{*3} (2\zeta(3)(M+N+18s) + M+N-16s) + \mathcal{A}_v^{*3} (2\zeta(3)(MN+7) + MN-18)] \\
& + \mathcal{O}(\mathcal{A}_{v,h}^{*4}) . \tag{6.97}
\end{aligned}$$

The presence of the couplings at the denominator in the perturbative expansion above is a somewhat surprising feature of our results which, at first sight, can look suspicious. Nevertheless, one has to remind oneself that the above expression is strictly valid *only* at the FPs, so one should look at the conformal dimension Δ as a function of ε and not as a function of the couplings. On the other hand, from the above results, we can also extract the full 1-loop scaling dimension, which we can rewrite as a power series in the couplings

$$\begin{aligned}
\Delta_{\bar{Q},s}^{1-loop} &= \bar{Q} \left(1 - \frac{\varepsilon}{2}\right) + \frac{4}{N} (A_h^* (\bar{Q} - 2s^2) + (\bar{Q} - 1)A_v^*) \\
&= \bar{Q} \left(1 - \frac{\varepsilon}{2}\right) + \frac{\bar{Q}(\bar{Q} - 2s^2)}{(4\pi)^2 s} u^* + \frac{2\bar{Q}(\bar{Q} - 1)}{(4\pi)^2} v^* , \tag{6.98}
\end{aligned}$$

and depends neither on N nor M when rewritten in terms of the original couplings u and v . Notice that the result above is obviously valid for arbitrary values of the couplings and not only at the FP. This is the case also when there are no FPs for real couplings, and thus the CFT is complex. In other words, Eq.(6.98) shows how large charge methods can be used to investigate also non-conformal theory via the associated complex CFT, as anticipated at the beginning of this chapter.

Notice that, in deriving Eqs.(6.83) and (6.96), we implicitly assumed the validity of the operator-state correspondence and the Weyl invariance of the theory. On the other hand, these features are not guaranteed in non-unitary CFT [104–106]. Then, in order to validate our approach, we consider the special case $N = M$ and $s = 1$ and $\bar{Q} = 2$, where, according to Eq.(6.76), we expect to reproduce the anomalous dimension of the bi-adjoint operator $\text{Tr} [T^a H T^a H^\dagger]$. We have

$$\Delta_{\bar{Q}=2,s=1}^{1-loop} = 2 - \varepsilon + \frac{v}{4\pi^2} , \tag{6.99}$$

in agreement with Eq.(6.13). It should be added that the known examples of CFT without Weyl invariance [104–106], such as some higher-derivative scalar theories, are structurally very different from the $U(N) \times U(M)$ model considered here.

Since $\Delta_{\text{Tr}[\text{T}^a \text{H} \text{T}^a \text{H}^\dagger]}$ is known to the two-loop level for $N = M$, we are now in the position to "boost" perturbation theory, as done for the $O(N)$ model in Sec.4.8. In fact, by combining Eq.(6.13) with our semiclassical results, we can obtain the 2-loop scaling dimension for the whole family of $SU(N) \times SU(N)$ operators $\mathcal{O}_J = \text{Tr}[(E_{21} H E_{12} H^\dagger)^{\bar{Q}/2}]$ where E_{pq} has been introduced in Eq(6.60) . These operators have CSD $\bar{Q} = 4J$ and live in the irreducible representations (Γ_J, Γ_J) of $SU(N) \times SU(N)$ with Γ_J defined through its Dynkin label (6.76). We have

$$\begin{aligned} \Delta_{(\Gamma_J, \Gamma_J)}^{\text{2-loop}} = & \left(\frac{d}{2} - 1 \right) \bar{Q} + \frac{\bar{Q}(\bar{Q}-2)u}{16\pi^2} + \frac{\bar{Q}(\bar{Q}-1)v}{8\pi^2} + \bar{Q} \left(\frac{u^2(N^2+4N-3)}{128\pi^4} + \frac{uv(3N-2)}{32\pi^4} \right. \\ & \left. + \frac{v^2(3N^2-1)}{128\pi^4} \right) + \bar{Q}^2 \left(\frac{u^2(1-2N)}{128\pi^4} + \frac{uv(3-2N)}{32\pi^4} + \frac{v^2(3-N^2)}{64\pi^4} \right) - \frac{(u+2v)^2}{128\pi^4} \bar{Q}^3. \end{aligned} \quad (6.100)$$

We emphasize again that the above expression is valid for every value of the renormalized couplings and not only at the FP ones.

As clear from Eq.(6.98), for the considered family of charge configurations, there is no scaling dimension degeneracy in the perturbative regime and thus the corresponding operators live in different irreducible representations. These are accessed by varying s at fixed CSD \bar{Q} . In the next section, we will analyze some concrete examples by setting $\bar{Q} = 2, 4, 8$. To this end, we need to consider one more charge configuration given by

$$\mathcal{Q}_J = \text{diag}\{-2J, J, J, 0, \dots, 0\}. \quad (6.101)$$

The M_E and B matrices can be parametrized as

$$M_E = -i\text{diag}\{\mu_1, \mu_2, \mu_2, 0, \dots, 0\}, \quad B = \text{diag}\{b_1, b_2, b_2, 0, \dots, 0\}. \quad (6.102)$$

Then the EOM and the charge constraints read

$$\begin{aligned} J &= V\mu_1 b_1^2, & 2\mu_1^2 &= u_0 b_1^2 + v_0 (b_1^2 + 2b_2^2) + \frac{m^2}{2}, \\ J &= -2V\mu_2 b_2^2, & 2\mu_2^2 &= u_0 b_2^2 + v_0 (b_1^2 + 2b_2^2) + \frac{m^2}{2}. \end{aligned} \quad (6.103)$$

The physical solution is

$$\mu_1 = \frac{2J\mu_2 m^3 v_0}{\mathcal{C}}, \quad b_1 = \sqrt{\frac{\mathcal{C}}{4\pi^2 \mu_2 v_0}}, \quad b_2 = \sqrt{-\frac{Jm^3}{4\pi^2 \mu_2}}, \quad (6.104)$$

where $\mathcal{C} = Jm^3(u_0 + 2v_0) + 8\pi^2\mu_2^3 - 2\pi^2\mu_2 m^2$ and μ_2 solves the following equation

$$-\frac{16J^3\mu_2^2 m^9 v_0^3}{\mathcal{C}^3} + \frac{Jm^3 \left(-\frac{2Jm^3 v_0^2}{\mathcal{C}} + u_0 + v_0 \right)}{2\pi^2 \mu_2} + \frac{Jm^5 v_0}{\mathcal{C}} = 0. \quad (6.105)$$

We choose the solution of the above equation such that it reproduces the $O(2NM)$ limit when $u_0 = 0$. The perturbative expansion of this solution reads

$$\begin{aligned} \mu_2 &= -\frac{m}{2} - \frac{Jm(u_0 + 4v_0)}{4\pi^2} + \frac{J^2 m (3u_0^2 + 28u_0 v_0 + 48v_0^2)}{16\pi^4} \\ &+ \frac{J^3 (-4mu_0^3 - 67mu_0^2 v_0 - 240mu_0 v_0^2 - 256mv_0^3)}{16\pi^6} + \mathcal{O}(J^4). \end{aligned} \quad (6.106)$$

This solution is valid when $\mathcal{C} < 0$. It is easy to show that this condition is always satisfied at small values of the couplings. The leading contribution in the semiclassical approximation is given by the classical energy (6.29) evaluated on this solution

$$\begin{aligned} J\Delta_{-1} &= \bar{Q} \left[1 + \frac{\bar{Q}(3u^* + 8v^*)}{64\pi^2} - \frac{\bar{Q}^2 (5u^{*2} + 24u^* v^* + 32v^{*2})}{1024\pi^4} \right. \\ &\quad \left. + \frac{\bar{Q}^3 (9u^{*3} + 59u^{*2} v^* + 144u^* v^{*2} + 128v^{*3})}{8192\pi^6} + \mathcal{O}(\bar{Q}^4) \right], \end{aligned} \quad (6.107)$$

where we set the couplings to their FP values and $\bar{Q} = 8J$ is the CSD, as expected from Eq.(6.74). We checked that we recover the $O(2NM)$ case when $u = 0$. To find the fluctuation spectrum, we

expand around the classical trajectory as in Eq.(6.89). The dispersion relations read

$$\begin{aligned}
\tilde{\omega}_1 &= \sqrt{J_\ell^2 + 4\mu_1^2} \quad 2(N-3) \text{ d.o.f.} \\
\tilde{\omega}_2 &= \sqrt{J_\ell^2 + 4\mu_2^2} \quad 4(N-3) \text{ d.o.f.} \\
\tilde{\omega}_{3,4} &= \sqrt{J_\ell^2 + 4\mu_1^2} \pm 2\mu_1 \quad 2 \times (M-3) \text{ d.o.f.} \\
\tilde{\omega}_{5,6} &= \sqrt{J_\ell^2 + 4\mu_2^2} \pm 2\mu_2 \quad 2 \times 2(M-3) \text{ d.o.f.} \\
\tilde{\omega}_7 &= \sqrt{J_\ell^2 + m_3^2} \quad 2(N-3)(M-3) \text{ d.o.f.} \\
\tilde{\omega}_{8,9} &= \sqrt{J_\ell^2 + 2ub_2^2 + 8\mu_2^2 \pm \sqrt{(J_\ell^2 + 2ub_2^2 + 8\mu_2^2)^2 - J_\ell^2 (J_\ell^2 + 4ub_2^2)}} \quad 2 \times 3 \text{ d.o.f.} \\
\tilde{\omega}_{10,11,12,13} &: (J_\ell^2 - \omega^2 \pm 2\omega(\mu_1 - \mu_2)) [J_\ell^2 - \omega^2 \pm 2\omega(\mu_1 - \mu_2) + 2u(b_1^2 + b_2^2)] \\
&\pm 4u\omega(b_1^2 - b_2^2)(\mu_1 + \mu_2) - 4\omega^2(\mu_1 + \mu_2)^2 = 0 \quad 2 \times 4 \text{ d.o.f.} \\
\tilde{\omega}_{14,15,16,17} &: \det \mathcal{D}_A(\omega, J_\ell^2) = 0 \quad 4 \text{ d.o.f.} ,
\end{aligned}$$

where $m_3^2 = 2v_0(b_1^2 + 2b_2^2) + m^2$ and

$$\mathcal{D}_A = \begin{pmatrix} \omega^2 - J_\ell^2 + z_{00} & -\frac{4}{3}i(\mu_1 + 2\mu_2)\omega & z_{02} & -\frac{4}{3}\sqrt{2}i(\mu_1 - \mu_2)\omega \\ \frac{4}{3}i(\mu_1 + 2\mu_2)\omega & \omega^2 - J_\ell^2 & \frac{4}{3}\sqrt{2}i(\mu_1 - \mu_2)\omega & 0 \\ z_{02} & -\frac{4}{3}\sqrt{2}i(\mu_1 - \mu_2)\omega & \omega^2 - J_\ell^2 + z_{22} & -\frac{4}{3}i(2\mu_1 + \mu_2)\omega \\ \frac{4}{3}\sqrt{2}i(\mu_1 - \mu_2)\omega & 0 & \frac{4}{3}i(2\mu_1 + \mu_2)\omega & \omega^2 - J_\ell^2 \end{pmatrix} , \quad (6.108)$$

with

$$\begin{aligned}
z_{00} &= -\frac{4}{3} [(u_0 + v_0)b_1^2 + 4v_0b_1b_2 + 2(u_0 + 2v_0)b_2^2] , \\
z_{02} &= -\frac{4}{3}\sqrt{2}(b_1 - b_2)[(u_0 + v_0)b_1 + (u_0 + 2v_0)b_2] , \\
z_{22} &= -\frac{2}{3} [4(u_0 + v_0)b_1^2 - 8v_0b_1b_2 + 2(u_0 + 2v_0)b_2^2] .
\end{aligned} \quad (6.109)$$

Although not obvious, for $u = 0$, we recover the fluctuation spectrum of the $O(2NM)$ model discussed in Chap.4 when $k = 3M$ charges have been fixed. In particular, one of the last four d.o.f. reduces to the $U(1)$ phonon with dispersion relation Eq.(4.57).

We weren't able to find an analytical expression for Δ_0 in this case. Instead, we computed it numerically at fixed values of parameters and as a function of ε . The results are given in the next section.

6.4 On how to identify the fixed-charge operators

In this section, we focus on identifying the fixed charge operators associated with a certain charge configuration. In particular, we propose a practical identification strategy which we outline by performing a series of examples of increasing complexity. Since the MCSD assumption can be violated at large coupling, the procedure is valid only when the anomalous dimensions of the operators involved are small, i.e. in the perturbative regime. Since in weakly-coupled theories it is easy to find the explicit form of the MSD operator once its irreducible representation is known, we focus on identifying the latter. We first list the conclusions below before conducting a more detailed discussion.

- The representation of the MSD operators can be uniquely determined when a charge configuration is chosen. This conclusion is based on the three conditions summarized in Propositions 1 – 3 in Sec.6.2.
- To determine the representation of the fixed charge operators, both group theory and the actual semiclassical computations of the scaling dimensions should be implemented.

We start our analysis by considering operators with CSD $\bar{Q} = 2$; Eq.(6.74) implies that we can build only one $N \times N$ charge matrix

$$\mathcal{Q}_{L,1/2} = \text{diag} \{ -1/2, 1/2, 0, \dots, 0 \} . \quad (6.110)$$

This charge configuration is of the special type considered in Eq.(6.75). We can then immediately identify the MSD operator as $\text{Tr} [T^a H T^b H^\dagger]$ which sits in the bi-adjoint representation $(\text{Adj}, \text{Adj}) = (N^2 - 1, M^2 - 1)$. The underlying reason is that, at the level of operators with $\bar{Q} = 2$

fields, only this representation contains the weight (6.110). Its scaling dimension has been computed in the previous section, being a special case ($s = 1, J = 1/2$) of the charge configuration (6.77).

The simplest nontrivial example is obtained by fixing $N = M = 3$ and considering operators with CSD $\bar{Q} = 4$. Proposition 1 says that the fixed charge operators belong to the irreducible representations (Γ_L, Γ_R) of $SU(N)_L \times SU(N)_R$ where $\Gamma_L = \Gamma_R = (\text{Adj})^{\bar{Q}/2}$. Thus, in the case at hand, the operators live in the decomposition of the tensor product $\text{Adj} \otimes \text{Adj} = \mathbf{8} \otimes \mathbf{8}$. We have

$$\mathbf{8} \otimes \mathbf{8} = \mathbf{1} \oplus 2(\mathbf{8}) \oplus \mathbf{10} \oplus \overline{\mathbf{10}} \oplus \mathbf{27}. \quad (6.111)$$

To construct all the relevant charge configurations, we impose the following three requirements:

1. The charge matrix is diagonal and traceless i.e. $\text{tr} \mathcal{Q} = 0$;
2. The diagonal elements of the charge configuration matrix can only be integer or half-integer (Proposition 3);
3. The sum of the absolute value of the diagonal elements is equal to $\bar{Q}/2 = 2$ (Proposition 4).

By following the above three constraints, we can only construct two different charge matrices:

$$\mathcal{Q}_{3A}^{(4)} = \begin{pmatrix} 1 & 0 & 0 \\ 0 & -1 & 0 \\ 0 & 0 & 0 \end{pmatrix}, \quad \mathcal{Q}_{3B}^{(4)} = \begin{pmatrix} 1 & 0 & 0 \\ 0 & -1/2 & 0 \\ 0 & 0 & -1/2 \end{pmatrix}. \quad (6.112)$$

In Sec.6.2, we showed that the weight and the charge matrix are related as $\mu = 2\mathcal{Q}$ (Eq.(6.45)).

The nonzero roots of $SU(3)$ are

$$\alpha_1 = \begin{pmatrix} 1 & 0 & 0 \\ 0 & -1 & 0 \\ 0 & 0 & 0 \end{pmatrix}, \quad \alpha_2 = \begin{pmatrix} 0 & 0 & 0 \\ 0 & 1 & 0 \\ 0 & 0 & -1 \end{pmatrix}, \quad \alpha_3 = \alpha_1 + \alpha_2, \quad (6.113)$$

and $-\alpha_1, -\alpha_2, -\alpha_3$. We, therefore, obtain $\mu_{3A}^{(4)} = 2\alpha_1$ and $\mu_{3B}^{(4)} = 2\alpha_1 + \alpha_2$. By using the Cartan

matrix of the $SU(3)$ algebra

$$A_{SU(3)} = \begin{pmatrix} 2 & -1 \\ -1 & 2 \end{pmatrix}, \quad (6.114)$$

we obtain

$$\alpha_1 = 2w_1 - w_2, \quad \alpha_2 = -w_1 + 2w_2, \quad (6.115)$$

where w_1 and w_2 are the fundamental weights of $SU(3)$. Then we can decompose the weights $\mu_{3A}^{(4)}, \mu_{3B}^{(4)}$ as

$$\begin{aligned} \mu_{3A}^{(4)} &= 4w_1 - 2w_2 = (4, -2), \\ \mu_{3B}^{(4)} &= 3w_1 = (3, 0). \end{aligned} \quad (6.116)$$

The next step is to determine which representations contain the above weights. By inspecting the weight diagrams³⁸ of the irreducible representation appearing in the RHS of (6.111), we see that $(4, -2)$ only appears in $\mathbf{27}$ while $(3, 0)$ appears in both $\mathbf{27}$ and $\mathbf{10}$. Thus, we can set the following correspondence

$$\mathcal{Q}_{3A}^{(4)} : (\mathbf{27}, \mathbf{27}), \quad \mathcal{Q}_{3B}^{(4)} : \begin{cases} (\mathbf{27}, \mathbf{27}) \\ (\mathbf{10}, \overline{\mathbf{10}}) \end{cases}, \quad (6.117)$$

where we have already excluded asymmetric representations such as $(\mathbf{27}, \overline{\mathbf{10}})$ since they do not appear in the decomposition of the four indices traceless symmetric $O(2NM)$ tensor (Proposition 2). Notice that $\mathcal{Q}_{3A}^{(4)}$ is again of the type (6.75) and, indeed, it can be directly uniquely associated with $(\mathbf{27}, \mathbf{27})$.

Using group-theoretical arguments, we arrived at (6.117). To further disentangle the representations, we employ the semiclassical results obtained in the previous section. In fact, if the scaling dimensions stemming from the two charge configurations are different functions of ε we have that $\mathcal{Q}_{3B}^{(4)}$ corresponds to $(\mathbf{10}, \overline{\mathbf{10}})$. The scaling dimension of $\mathcal{Q}_{3A}^{(4)}$ at NLO in the large charge expansion has been calculated analytically ($s = J = 1, N = M = 3$ case of Eq.(6.77)) while $\mathcal{Q}_{3B}^{(4)}$ corresponds to the $J = 1/2, N = M = 3$ case of Eq.(6.101), and thus the associated scaling dimension has been evaluated numerically at fixed values of ε .

The results for the scaling dimensions at NLO in the large charge expansion are shown in

³⁸The weight diagrams are easily obtained with the help of the Mathematica package LieART [195, 196].

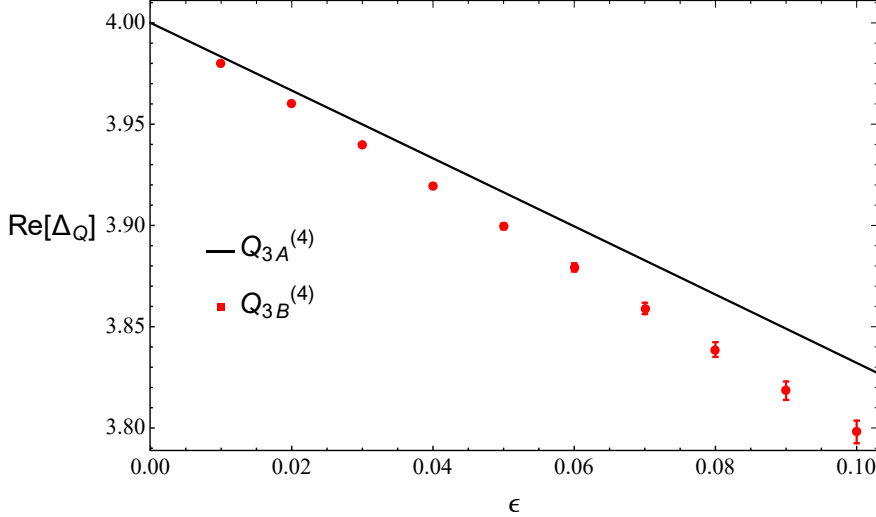


Figure 17: The results for the real part of the scaling dimension at the fixed point for the $U(3) \times U(3)$ operators with CSD $\bar{Q} = 4$, carrying the charges $\mathcal{Q}_{3A}^{(4)}$ (black line) and $\mathcal{Q}_{3B}^{(4)}$ (red dots) as a function of ε . The error bars encode the numerical error in evaluating Δ_0 for $\mathcal{Q}_{3B}^{(4)}$.

Fig. 17, where the black line and red dots denote, respectively, the cases $\mathcal{Q}_{3A}^{(4)}$ and $\mathcal{Q}_{3B}^{(4)}$. The error bar on the red dots takes into account all the potential numerical errors³⁹. Clearly, the two scaling dimensions are different functions of ε , and thus we can unequivocally associate representations and charges as

$$\mathcal{Q}_{3A}^{(4)} : (\mathbf{27}, \mathbf{27}), \quad \mathcal{Q}_{3B}^{(4)} : (\mathbf{10}, \overline{\mathbf{10}}) . \quad (6.118)$$

Notice that the scaling dimension corresponding to $\mathcal{Q}_{3B}^{(4)}$ is smaller than the one associated with $\mathcal{Q}_{3A}^{(4)}$, consistently with the MSD criteria selecting the fixed-charge operators.

As a third example, we keep $\bar{Q} = 4$ and we set $N = M = 4$. We can now build three independent charge matrices

³⁹The main source of error comes from performing a numerical Taylor expansion in ε of the one-loop functional determinant during the renormalization procedure. We estimate the numerical error as the difference of the scaling dimensions of $\mathcal{Q}_{3B}^{(4)}$ with the one of $\mathcal{Q}_{3A}^{(4)}$ in the limiting case of $u \rightarrow 0$. As we know, in this case, the scaling dimensions for $\mathcal{Q}_{3B}^{(4)}$ and $\mathcal{Q}_{3A}^{(4)}$ should be equal and coincide with the $O(18)$ result.

$$\begin{aligned}
\mathcal{Q}_{4A}^{(4)} &= \begin{pmatrix} 1 & 0 & 0 & 0 \\ 0 & -1 & 0 & 0 \\ 0 & 0 & 0 & 0 \\ 0 & 0 & 0 & 0 \end{pmatrix}, & \mathcal{Q}_{4B}^{(4)} &= \begin{pmatrix} 1 & 0 & 0 & 0 \\ 0 & -1/2 & 0 & 0 \\ 0 & 0 & -1/2 & 0 \\ 0 & 0 & 0 & 0 \end{pmatrix}, \\
\mathcal{Q}_{4C}^{(4)} &= \begin{pmatrix} 1/2 & 0 & 0 & 0 \\ 0 & -1/2 & 0 & 0 \\ 0 & 0 & 1/2 & 0 \\ 0 & 0 & 0 & -1/2 \end{pmatrix}.
\end{aligned} \tag{6.119}$$

To connect this example with our semiclassical calculations, we note that Eq.(6.77) encompasses $\mathcal{Q}_{4A}^{(4)}$ ($s = J = 1, N = M = 4$) and $\mathcal{Q}_{4C}^{(4)}$ ($s = 2, J = 1/2, N = M = 4$) while Eq.(6.101) reduces to $\mathcal{Q}_{4B}^{(4)}$ when $J = 1/2$ and $N = M = 4$. By denoting the three fundamental weights of $SU(4)$ as W_1 , W_2 , and W_3 , we can express the weights associated with the above charge matrices as

$$\begin{aligned}
\mu_{4A}^{(4)} &= 4W_1 - 2W_2 = (4, -2, 0), \\
\mu_{4B}^{(4)} &= 3W_1 - W_3 = (3, 0, -1), \\
\mu_{4C}^{(4)} &= 2W_1 - 2W_2 + 2W_3 = (2, -2, 2).
\end{aligned} \tag{6.120}$$

The tensor product of two adjoint representations of $SU(4)$ decomposes as

$$\mathbf{15} \otimes \mathbf{15} = \mathbf{1} \oplus 2(\mathbf{15}) \oplus \mathbf{20}' \oplus \mathbf{45} \oplus \overline{\mathbf{45}} \oplus \mathbf{84}. \tag{6.121}$$

Inspecting the weight diagram of the above representations, we obtain the correspondence summarized below:

$$\mathcal{Q}_{4A}^{(4)} : (\mathbf{84}, \mathbf{84}), \quad \mathcal{Q}_{4B}^{(4)} : \begin{cases} (\mathbf{84}, \mathbf{84}) \\ (\mathbf{45}, \overline{\mathbf{45}}) \end{cases}, \quad \mathcal{Q}_{4C}^{(4)} : \begin{cases} (\mathbf{84}, \mathbf{84}) \\ (\mathbf{45}, \overline{\mathbf{45}}) \\ (\mathbf{20}', \mathbf{20}') \end{cases}. \quad (6.122)$$

Again there is one charge matrix, $\mathcal{Q}_{4A}^{(4)}$, which is of the type considered in (6.75) and thus corresponds to a unique representation, $(\mathbf{84}, \mathbf{84})$. Then one can proceed by computing the scaling dimensions associated with $\mathcal{Q}_{4A}^{(4)}$ and $\mathcal{Q}_{4B}^{(4)}$ in the semiclassical expansion. If they are different then $\mathcal{Q}_{4B}^{(4)}$ corresponds to $(\mathbf{45}, \overline{\mathbf{45}})$, and we can proceed by computing the scaling dimension corresponding to $\mathcal{Q}_{4C}^{(4)}$. If the latter is also different from the previous ones, then we can further conclude that the operator with scaling dimension $\Delta_{\mathcal{Q}_{4C}^{(4)}}$ is in the $(\mathbf{20}', \mathbf{20}')$ representation. This is the case, as can be seen from the results for the real⁴⁰ and imaginary part of the scaling dimensions at NLO, which are shown in Figs. 18 and 19, respectively. Due to the numerical error, in this case, it is necessary to look also at the imaginary part to disentangle the results. If the results for $\Delta_{\mathcal{Q}_{4A}^{(4)}}$ were the same, we wouldn't have been able to identify the representation associated with $\mathcal{Q}_{4B}^{(4)}$, and would have been necessary to determine higher orders of the large charge expansion to check whether they broke the degeneracy or not. However, we could always deduce the irrep related to $\mathcal{Q}_{4C}^{(4)}$ as $(\mathbf{20}', \mathbf{20}')$ ⁴¹.

In conclusion, we have

$$\mathcal{Q}_{4A}^{(4)} : (\mathbf{84}, \mathbf{84}), \quad \mathcal{Q}_{4B}^{(4)} : (\mathbf{45}, \overline{\mathbf{45}}), \quad \mathcal{Q}_{4C}^{(4)} : (\mathbf{20}', \mathbf{20}'). \quad (6.123)$$

As the last example, we keep $N = M = 4$ and consider $\bar{Q} = 8$. The fourth tensor power of the adjoint representation decomposes as

⁴⁰ From Fig. 18, one may infer that $Re[\Delta_{\mathcal{Q}_{4B}^{(4)}}] > Re[\Delta_{\mathcal{Q}_{4A}^{(4)}}]$, in apparent violation of the MSD criteria. This apparent puzzle can be solved by taking into account the numerical errors plus the fact that the comparison of the magnitude of the scaling dimensions at small ϵ should in principle be performed in the expansion of conventional perturbation theory rather than in the semiclassical expansion. The difference between the two expansion is of order $\mathcal{O}(\bar{Q}\epsilon^2)$, but prefactors may magnify it and invert the scaling dimension hierarchy. By making use of the full 2-loop result of [86, 190], we estimated a difference between 0.04% and 0.5% for $\Delta_{\mathcal{Q}_{4B}^{(4)}}$ at $\epsilon = 0.1$. However, the difference in $\Delta_{\mathcal{Q}_{4B}^{(4)}}$ for the same value of epsilon may be much larger.

⁴¹ If $Re[\Delta_{\mathcal{Q}_{4A}^{(4)}}] = Re[\Delta_{\mathcal{Q}_{4B}^{(4)}}]$, it follows that $Re[\Delta_{(\mathbf{45}, \overline{\mathbf{45}})}] \geq Re[\Delta_{(\mathbf{84}, \mathbf{84})}]$, but since $Re[\Delta_{\mathcal{Q}_{4C}^{(4)}}] < Re[\Delta_{(\mathbf{84}, \mathbf{84})}]$, then $Re[\Delta_{\mathcal{Q}_{4C}^{(4)}}] = Re[\Delta_{(\mathbf{20}', \mathbf{20}')}]$

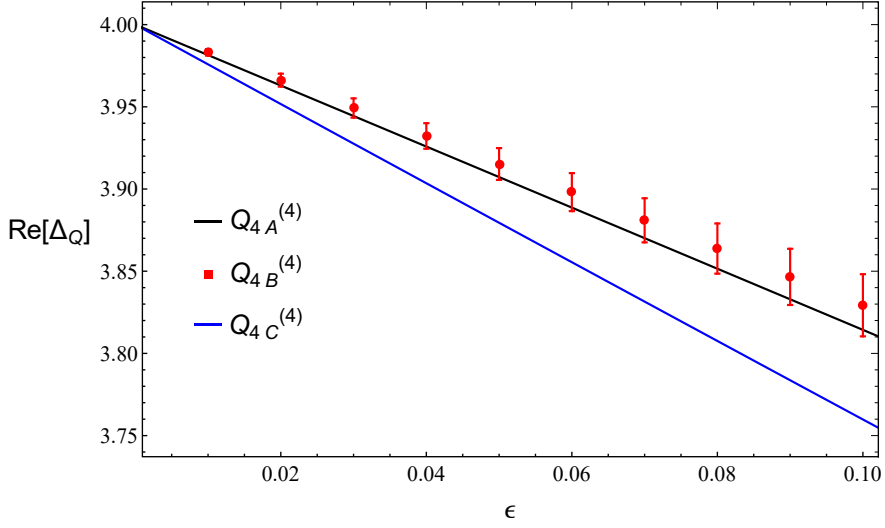


Figure 18: The results for the real part of scaling dimension for the $U(4) \times U(4)$ operators with CSD $\bar{Q} = 4$, carrying the charges $Q_{4A}^{(4)}$ (black line), $Q_{4B}^{(4)}$ (red dots) and $Q_{4C}^{(4)}$ (blue lines) as a function of ϵ . The error bars encode the numerical error in evaluating Δ_0 for $Q_{4B}^{(4)}$.

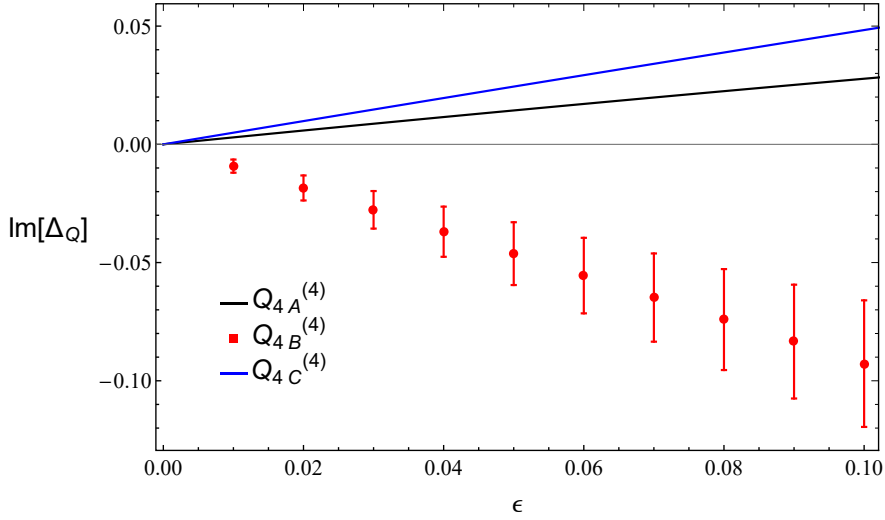


Figure 19: The imaginary part of the scaling dimension for the $U(4) \times U(4)$ operators with CSD $\bar{Q} = 4$, carrying the charges $Q_{4A}^{(4)}$ (black line), $Q_{4B}^{(4)}$ (red dots) and $Q_{4C}^{(4)}$ (blue lines) at the fixed point values as a function of ϵ . The error bars encode the numerical error in evaluating Δ_0 for $Q_{4B}^{(4)}$.

$$\begin{aligned}
\mathbf{15}^{\otimes 4} = & 9(\mathbf{1}) \oplus 43(\mathbf{15}) \oplus 30(\mathbf{20}') \oplus 9(\mathbf{35}) \oplus 9(\overline{\mathbf{35}}) \oplus 39(\mathbf{45}) \oplus 39(\overline{\mathbf{45}}) \oplus 42(\mathbf{84}) \oplus 4(\mathbf{105}) \\
& \oplus 39(\mathbf{175}) \oplus 3(\mathbf{189}) \oplus 3(\overline{\mathbf{189}}) \oplus 24(\mathbf{256}) \oplus 24(\overline{\mathbf{256}}) \oplus 6(\mathbf{280}) \oplus 6(\overline{\mathbf{280}}) \oplus 12(\mathbf{300}') \\
& \oplus 2(\mathbf{360}') \oplus 2(\overline{\mathbf{360}'}) \oplus 9(\mathbf{729}) \oplus (\mathbf{825}) \oplus 3(\mathbf{875}) \oplus 3(\overline{\mathbf{875}}) .
\end{aligned} \tag{6.124}$$

We can build seven charge matrices

$$\begin{aligned}
\mathcal{Q}_{4A}^{(8)} &= \text{diag}\{2, -2, 0, 0, \dots, 0\} , & \mathcal{Q}_{4B}^{(8)} &= \text{diag}\{-2, 1, 1, 0, \dots, 0\} , \\
\mathcal{Q}_{4C}^{(8)} &= \text{diag}\{1, -1, 1, -1, 0, \dots, 0\} , & \mathcal{Q}_{4D}^{(8)} &= \text{diag}\{2, -3/2, -1/2, 0, \dots, 0\} , \\
\mathcal{Q}_{4E}^{(8)} &= \text{diag}\{2, -1, -1/2, -1/2, 0, \dots, 0\} , & \mathcal{Q}_{4F}^{(8)} &= \text{diag}\{3/2, 1/2, -3/2, -1/2, 0, \dots, 0\} , \\
\mathcal{Q}_{4G}^{(8)} &= \text{diag}\{3/2, 1/2, -1, -1, 0, \dots, 0\} .
\end{aligned} \tag{6.125}$$

The corresponding weights, expressed in the fundamental weight basis, read

$$\begin{aligned}
\mu_{4A}^{(8)} &= (8, -4, 0) , & \mu_{4B}^{(8)} &= (6, 0, -2) , & \mu_{4C}^{(8)} &= (4, -4, 4) , & \mu_{4D}^{(8)} &= (7, 2, -1) , \\
\mu_{4E}^{(8)} &= (6, -1, 0) , & \mu_{4F}^{(8)} &= (2, 4, -2) , & \mu_{4G}^{(8)} &= (2, 3, 0) .
\end{aligned} \tag{6.126}$$

By analyzing the weight diagrams and checking the decomposition of the $O(2NM)$ traceless symmetric tensor of rank $Q = 8$, we obtain the correspondence below

$$\begin{aligned}
\mathcal{Q}_{4A}^{(8)} : & (\mathbf{825}, \mathbf{825}) , \quad \mathcal{Q}_{4D}^{(8)} : \begin{cases} (\mathbf{825}, \mathbf{825}) \\ (\mathbf{875}, \overline{\mathbf{875}}) \end{cases} , \quad \mathcal{Q}_{4B}^{(8)} : \begin{cases} (\mathbf{825}, \mathbf{825}) \\ (\mathbf{875}, \overline{\mathbf{875}}) \\ (\mathbf{360}', \overline{\mathbf{360}'}) \end{cases} , \quad \mathcal{Q}_{4F}^{(8)} : \begin{cases} (\mathbf{825}, \mathbf{825}) \\ (\mathbf{875}, \overline{\mathbf{875}}) \\ (\mathbf{729}, \mathbf{729}) \end{cases} , \\
\mathcal{Q}_{4E}^{(8)} : & \begin{cases} (\mathbf{825}, \mathbf{825}) \\ (\mathbf{875}, \overline{\mathbf{875}}) \\ (\mathbf{360}', \overline{\mathbf{360}'}) \\ (\mathbf{189}, \overline{\mathbf{189}}) \end{cases} , \quad \mathcal{Q}_{4G}^{(8)} : \begin{cases} (\mathbf{825}, \mathbf{825}) \\ (\mathbf{875}, \overline{\mathbf{875}}) \\ (\mathbf{729}, \mathbf{729}) \\ (\mathbf{360}', \overline{\mathbf{360}'}) \\ (\mathbf{280}, \overline{\mathbf{280}}) \end{cases} , \quad \mathcal{Q}_{4C}^{(8)} : \begin{cases} (\mathbf{825}, \mathbf{825}) \\ (\mathbf{875}, \overline{\mathbf{875}}) \\ (\mathbf{729}, \mathbf{729}) \\ (\mathbf{360}', \overline{\mathbf{360}'}) \\ (\mathbf{280}, \overline{\mathbf{280}}) \\ (\mathbf{105}, \mathbf{105}) \end{cases} .
\end{aligned} \tag{6.127}$$

If all the corresponding semiclassical computations give different functions of ε as result, then we can uniquely identify all the irreps where the fixed charge operators sit. These are the representations outlined in red above. To be more precise, to allow a complete identification it is not needed that all the scaling dimensions differ; for example, the results for $\mathcal{Q}_{4B}^{(4)}$ and $\mathcal{Q}_{4F}^{(4)}$ or for $\mathcal{Q}_{4E}^{(4)}$ and $\mathcal{Q}_{4F}^{(4)}$ can be equal.

To summarize, a general identification procedure consists in inspecting the weight diagrams of the various representations in order to obtain correspondences as Eq.(6.127) and then looking if the corresponding scaling dimensions are degenerate or not, following a sort of "identification chain" that starts from "highest weight" charge matrices of the form (6.75) for which there is only one candidate for the corresponding irrep. In the second step, the choice will be between this irrep and one new candidate, and so on. We analyzed many other examples and our findings strongly suggest that this identification procedure can always be implemented, and fails only in presence of particular degeneracies in the semiclassical results.

7 CONCLUSIONS

Every approach which can complement, extend, or even transcend ordinary diagrammatic methods is of great importance, especially in the light of the growing interest in the large-order behavior of perturbation theory (an area of research which takes the name of *resurgence theory* [197–200]), and of the relevance of multi-legged amplitudes for the next generation of high-energy physics experiments [44, 201–203]. Furthermore, the search for a classification of critical phenomena [51, 173, 204–207] demands novel methods able to shed light on the general properties of the spectrum of anomalous dimensions in conformal theories.

In this thesis, we explored the recently-developed large charge approach to QFT and, in particular, to CFT. After having reviewed the basics of CFTs at large charge in the first two chapters, we focused on the application of large charge methods in weakly-coupled non-abelian theories.

In Chap.4, we studied the $O(N)$ critical model in $d = 4 - \varepsilon$ dimensions. After having analyzed in detail the charge fixing procedure and the resulting symmetry breaking pattern, we determined the scaling dimensions of traceless symmetric composite operators to the next-to-leading order in the large charge expansion. These operators correspond to spatially homogeneous ground states when the theory is mapped to a cylinder. Interestingly, every order of the large charge expansion resums terms up to arbitrarily high orders in the ε -expansion. This allowed us to combine our results with the known diagrammatic literature to obtain the scaling dimensions to $\mathcal{O}(\varepsilon^4)$ in the ε -expansion as well as provide predictions for higher-order terms. This investigation paves the way for the first-principle study of the large charge expansion in non-abelian theories. Subsequently, we analyzed the $\varepsilon \rightarrow 1$ limit of our results, exploring the connection with previous EFT studies of the strongly-coupled three-dimensional $O(N)$ CFT. An obvious extension of our investigations is the study of non-homogeneous ground states, which are related to operators transforming in the antisymmetric and mixed-symmetry $O(N)$ representations. Also, computing the NNLO of the large charge expansion is strongly motivated by the possibility of comparison with the non-perturbative large charge EFT and Monte Carlo simulations.

In the last part of the chapter, we continued studying the anisotropic perturbations of the $O(N)$ model, focusing on the critical theory with cubic anisotropy. The latter is in general induced by the crystal structure of $O(3)$ magnets and, being RG relevant, drives them to a universality class

distinct from the Heisenberg one [158]. Leaving momentarily aside the large charge expansion, we unveiled the operator content of the model and derived the full 1-loop spectrum of anomalous dimensions for composite operators without derivatives and showed that it follows an interesting pattern. A natural direction is to consider other subgroups of $O(N)$, such as the hypertetrahedral symmetry group $H_{\text{tetrahedral}} \simeq \mathcal{S}_{N+1} \otimes \mathcal{Z}_2$. This line of research is also motivated by the recent results on the classification of scalar CFTs [173, 174, 207, 208].

In $4 < d < 6$, the $O(N)$ theory exhibits a UV fixed point non-perturbatively realizing the asymptotic safety scenario often considered in the quantum gravity literature. In Chap.5 we studied its proposed UV completion in terms of the WF IR fixed point of the cubic model, which, in $6 - \varepsilon$ dimension, is perturbative. We determined the scaling dimensions of a family of fixed-charge operators to NLO in the large charge expansion in the cubic model, finding complete agreement with previous calculations in the $O(N)$ model, hence providing non-trivial support to the conjectured duality between the two critical theories. It would be clearly interesting to compute the NLO in the large N -large charge expansion of the $O(N)$ model in various d . Furthermore, the appearance of complex anomalous dimensions above a critical value of the charge is a curious phenomenon related to the instability of the theory and its large charge states, which deserves further investigation.

In Chap.6, we explored the role of the charge configuration in the large charge expansion. Our findings show that by controlling the charge configuration, it is possible to efficiently calculate the scaling dimension of a multitude of composite operators going beyond traditional diagrammatical computations. We outlined our computational strategy, which merges large charge methods and group-theoretical considerations, by deriving many new results for the scaling dimensions of composite operators in the $U(N) \times U(M)$ CFT in $d = 4 - \varepsilon$ dimensions. For a wide range of N and M , the CFT occurs at complex values of the couplings defining a non-unitary complex CFT related to near-conformal dynamics. Starting from this observation, we illustrated how large charge methods can be successfully employed to compute renormalization group functions in theories without fixed points by considering the associated complex CFTs. It would be worth pursuing the study of the large charge expansion in near-conformal QFTs, for instance, using the semiclassical methods described here to obtain a microscopic description of the model considered in [209], where the near-conformal dynamics is guaranteed by adding a dilaton to the large charge $U(1)$ EFT in $d = 4$.

The field of the large charge expansion is relatively young and continuously growing. We think

that we are only at the beginning of the journey. For example, recently began the exploration of the convergence and resurgent properties of the expansion [210, 211] with the final ambitious goal of extending the validity of large charge methods to any value of the charge, including the small ones. Also, the first steps towards an efficient computation of the OPE coefficients, have been recently made [78]. Another noteworthy line of research is the study of the holographic duals of large charge CFTs [212–215]. For instance, there are indications that the large charge sector of the $U(1)$ three-dimensional scalar CFT extensively discussed in this thesis can be identified with AdS boson star solutions of the Einstein-Maxwell theory in four dimensions [213, 214]. In particular, it would be interesting to investigate the AdS_6 holographic description [32] of the 5-dimensional $O(N)$ model considered in Chap.5.

One of the most important future challenges of the field is, in our opinion, to efficiently apply the ideas underlying large charge methods to non-conformal theories and the computation of dynamical quantities such as cross-sections and decay rates. This would likely provide a breakthrough in our understanding of high-energy multi-particle production processes in the Standard Model. In fact, since the 90s, analogous semiclassical methods have been invoked in the literature for computing the multi-particle production amplitudes in QFT [216–218]. Unfortunately, after the first pioneering results, establishing the potential power of the approach, formidable technical obstacles, in this case not tamed by conformal invariance, almost arrested the progress. The large charge approach to CFT considered here, confirms (via an explicit realization) that, when dealing with multi-legged amplitudes in perturbative theories, saddle-point methods around a non-trivial trajectory provide a well-defined perturbative expansion even when the ordinary loop-expansion breaks down, motivating and paving the way for future investigations.

Another interesting possible extension of the ideas presented here is the study of large charge operators in fermionic CFTs, such as the infrared Banks-Zaks fixed point of $SU(N)$ gauge theories [1]. Intuitively, we expect their large charge sectors to be related to some *superconducting-like phase*, with potential applications in QCD [219–221].

Bibliography

- [1] T. Banks and A. Zaks, “On the Phase Structure of Vector-Like Gauge Theories with Massless Fermions,” *Nucl. Phys. B* **196** (1982), 189-204 doi:10.1016/0550-3213(82)90035-9
- [2] K. G. Wilson and M. E. Fisher, “Critical exponents in 3.99 dimensions,” *Phys. Rev. Lett.* **28** (1972), 240-243 doi:10.1103/PhysRevLett.28.240
- [3] K. G. Wilson, “Quantum field theory models in less than four-dimensions,” *Phys. Rev. D* **7** (1973), 2911-2926 doi:10.1103/PhysRevD.7.2911
- [4] A. M. Polyakov, “Nonhamiltonian approach to conformal quantum field theory,” *Zh. Eksp. Teor. Fiz.* **66** (1974), 23-42
- [5] R. Rattazzi, V. S. Rychkov, E. Tonni and A. Vichi, “Bounding scalar operator dimensions in 4D CFT,” *JHEP* **12** (2008), 031 doi:10.1088/1126-6708/2008/12/031 [arXiv:0807.0004 [hep-th]].
- [6] S. El-Showk, M. F. Paulos, D. Poland, S. Rychkov, D. Simmons-Duffin and A. Vichi, “Solving the 3D Ising Model with the Conformal Bootstrap,” *Phys. Rev. D* **86** (2012), 025022 doi:10.1103/PhysRevD.86.025022 [arXiv:1203.6064 [hep-th]].
- [7] J. M. Maldacena, “The Large N limit of superconformal field theories and supergravity,” *Adv. Theor. Math. Phys.* **2** (1998), 231-252 doi:10.1023/A:1026654312961 [arXiv:hep-th/9711200 [hep-th]].
- [8] E. Witten, “Anti-de Sitter space and holography,” *Adv. Theor. Math. Phys.* **2** (1998), 253-291 doi:10.4310/ATMP.1998.v2.n2.a2 [arXiv:hep-th/9802150 [hep-th]].
- [9] A. A. Belavin, A. M. Polyakov and A. B. Zamolodchikov, “Infinite Conformal Symmetry in Two-Dimensional Quantum Field Theory,” *Nucl. Phys. B* **241** (1984), 333-380 doi:10.1016/0550-3213(84)90052-X
- [10] S. Hellerman, D. Orlando, S. Reffert and M. Watanabe, “On the CFT Operator Spectrum at Large Global Charge,” *JHEP* **12** (2015), 071 doi:10.1007/JHEP12(2015)071 [arXiv:1505.01537 [hep-th]].

- [11] L. Alvarez-Gaume, O. Loukas, D. Orlando and S. Reffert, “Compensating strong coupling with large charge,” *JHEP* **1704**, 059 (2017) doi:10.1007/JHEP04(2017)059 [arXiv:1610.04495 [hep-th]].
- [12] D. Banerjee, S. Chandrasekharan and D. Orlando, “Conformal dimensions via large charge expansion,” *Phys. Rev. Lett.* **120** (2018) no.6, 061603 doi:10.1103/PhysRevLett.120.061603 [arXiv:1707.00711 [hep-lat]].
- [13] O. Loukas, D. Orlando and S. Reffert, “Matrix models at large charge,” *JHEP* **10** (2017), 085 doi:10.1007/JHEP10(2017)085 [arXiv:1707.00710 [hep-th]].
- [14] O. Loukas, “A matrix CFT at multiple large charges,” *JHEP* **06** (2018), 164 doi:10.1007/JHEP06(2018)164 [arXiv:1711.07990 [hep-th]].
- [15] G. Cuomo, L. V. Delacretaz and U. Mehta, “Large Charge Sector of 3d Parity-Violating CFTs,” [arXiv:2102.05046 [hep-th]].
- [16] M. Watanabe, “Chern-Simons-Matter Theories at Large Global Charge,” [arXiv:1904.09815 [hep-th]].
- [17] S. Hellerman and S. Maeda, “On the Large R -charge Expansion in $\mathcal{N} = 2$ Superconformal Field Theories,” *JHEP* **12** (2017), 135 doi:10.1007/JHEP12(2017)135 [arXiv:1710.07336 [hep-th]].
- [18] S. Hellerman and D. Orlando, “Large R-charge EFT correlators in N=2 SQCD,” [arXiv:2103.05642 [hep-th]].
- [19] M. Beccaria, “On the large R-charge $\mathcal{N} = 2$ chiral correlators and the Toda equation,” *JHEP* **02** (2019), 009 doi:10.1007/JHEP02(2019)009 [arXiv:1809.06280 [hep-th]].
- [20] G. ’t Hooft, “A Planar Diagram Theory for Strong Interactions,” *Nucl. Phys. B* **72** (1974), 461 doi:10.1016/0550-3213(74)90154-0
- [21] G. Badel, G. Cuomo, A. Monin and R. Rattazzi, “The Epsilon Expansion Meets Semiclassics,” *JHEP* **11** (2019), 110 doi:10.1007/JHEP11(2019)110 [arXiv:1909.01269 [hep-th]].

- [22] G. Arias-Tamargo, D. Rodriguez-Gomez and J. Russo, “The large charge limit of scalar field theories and the Wilson-Fisher fixed point at $\epsilon = 0$,” *JHEP* **10** (2019), 201 doi:10.1007/JHEP10(2019)201 [arXiv:1908.11347 [hep-th]].
- [23] G. Arias-Tamargo, D. Rodriguez-Gomez and J. G. Russo, “Correlation functions in scalar field theory at large charge,” *JHEP* **01** (2020), 171 doi:10.1007/JHEP01(2020)171 [arXiv:1912.01623 [hep-th]].
- [24] M. Watanabe, “Accessing Large Global Charge via the ϵ -Expansion,” [arXiv:1909.01337 [hep-th]].
- [25] F. J. Wegner, “Critical Exponents in Isotropic Spin Systems,” *Phys. Rev. B* **6** (1972), 1891-1893 doi:10.1103/PhysRevB.6.1891
- [26] M. E. Fisher and D. R. Nelson, “Spin Flop, Supersolids, and Bicritical and Tetracritical Points,” *Phys. Rev. Lett.* **32** (1974), 1350-1353 doi:10.1103/PhysRevLett.32.1350
- [27] P. Calabrese, A. Pelissetto and E. Vicari, “Critical structure factors of bilinear fields in $O(N)$ vector models,” *Phys. Rev. E* **65** (2002), 046115 doi:10.1103/PhysRevE.65.046115 [arXiv:cond-mat/0111160 [cond-mat.stat-mech]].
- [28] S. Weinberg, “Critical Phenomena for Field Theorists,” doi:10.1007/978-1-4684-0931-4_1
- [29] M. Niedermaier and M. Reuter, “The Asymptotic Safety Scenario in Quantum Gravity,” *Living Rev. Rel.* **9** (2006), 5-173 doi:10.12942/lrr-2006-5
- [30] G. Parisi, “The Theory of Nonrenormalizable Interactions. 1. The Large N Expansion,” *Nucl. Phys. B* **100** (1975), 368-388 doi:10.1016/0550-3213(75)90624-0
- [31] I. R. Klebanov and A. M. Polyakov, “AdS dual of the critical $O(N)$ vector model,” *Phys. Lett. B* **550** (2002), 213-219 doi:10.1016/S0370-2693(02)02980-5 [arXiv:hep-th/0210114 [hep-th]].
- [32] S. Giombi, I. R. Klebanov and B. R. Safdi, “Higher Spin AdS_{d+1}/CFT_d at One Loop,” *Phys. Rev. D* **89** (2014) no.8, 084004 doi:10.1103/PhysRevD.89.084004 [arXiv:1401.0825 [hep-th]].

- [33] L. Fei, S. Giombi and I. R. Klebanov, “Critical $O(N)$ models in $6 - \epsilon$ dimensions,” Phys. Rev. D **90** (2014) no.2, 025018 doi:10.1103/PhysRevD.90.025018 [arXiv:1404.1094 [hep-th]].
- [34] L. Fei, S. Giombi, I. R. Klebanov and G. Tarnopolsky, “Three loop analysis of the critical $O(N)$ models in $6 - \epsilon$ dimensions,” Phys. Rev. D **91** (2015) no.4, 045011 doi:10.1103/PhysRevD.91.045011 [arXiv:1411.1099 [hep-th]].
- [35] D. F. Litim and F. Sannino, “Asymptotic safety guaranteed,” JHEP **12** (2014), 178 doi:10.1007/JHEP12(2014)178 [arXiv:1406.2337 [hep-th]].
- [36] A. Butti, A. Pelissetto and E. Vicari, “On the nature of the finite temperature transition in QCD,” JHEP **08** (2003), 029 doi:10.1088/1126-6708/2003/08/029 [arXiv:hep-ph/0307036 [hep-ph]].
- [37] F. Sannino and K. Tuominen, “Spontaneous symmetry breaking in gauge theories via Bose-Einstein condensation,” Phys. Rev. D **68** (2003), 016007 doi:10.1103/PhysRevD.68.016007 [arXiv:hep-ph/0303167 [hep-ph]].
- [38] P. Calabrese and P. Parruccini, “Five loop epsilon expansion for $U(n) \times U(m)$ models: Finite temperature phase transition in light QCD,” JHEP **05** (2004), 018 doi:10.1088/1126-6708/2004/05/018 [arXiv:hep-ph/0403140 [hep-ph]].
- [39] D. B. Kaplan, J. W. Lee, D. T. Son and M. A. Stephanov, “Conformality Lost,” Phys. Rev. D **80** (2009), 125005 doi:10.1103/PhysRevD.80.125005 [arXiv:0905.4752 [hep-th]].
- [40] V. Gorbenko, S. Rychkov and B. Zan, “Walking, Weak first-order transitions, and Complex CFTs,” JHEP **10** (2018), 108 doi:10.1007/JHEP10(2018)108 [arXiv:1807.11512 [hep-th]].
- [41] G. Gabrielse, D. Hanneke, T. Kinoshita, M. Nio and B. C. Odom, “New Determination of the Fine Structure Constant from the Electron g Value and QED,” Phys. Rev. Lett. **97** (2006), 030802 [erratum: Phys. Rev. Lett. **99** (2007), 039902] doi:10.1103/PhysRevLett.97.030802
- [42] H. Goldberg, “Breakdown of perturbation theory at tree level in theories with scalars,” Phys. Lett. B **246** (1990), 445-450 doi:10.1016/0370-2693(90)90628-J

- [43] V. A. Rubakov, “Nonperturbative aspects of multiparticle production,” [arXiv:hep-ph/9511236 [hep-ph]].
- [44] C. Degrande, V. V. Khoze and O. Mattelaer, “Multi-Higgs production in gluon fusion at 100 TeV,” Phys. Rev. D **94** (2016), 085031 doi:10.1103/PhysRevD.94.085031 [arXiv:1605.06372 [hep-ph]].
- [45] M. L. Mangano, G. Zanderighi, J. A. Aguilar-Saavedra, S. Alekhin, S. Badger, C. W. Bauer, T. Becher, V. Bertone, M. Bonvini and S. Boselli, *et al.* “Physics at a 100 TeV pp Collider: Standard Model Processes,” doi:10.23731/CYRM-2017-003.1 [arXiv:1607.01831 [hep-ph]].
- [46] A. Abada *et al.* [FCC], “FCC-hh: The Hadron Collider: Future Circular Collider Conceptual Design Report Volume 3,” Eur. Phys. J. ST **228** (2019) no.4, 755-1107 doi:10.1140/epjst/e2019-900087-0
- [47] A. Abada *et al.* [FCC], “FCC Physics Opportunities: Future Circular Collider Conceptual Design Report Volume 1,” Eur. Phys. J. C **79** (2019) no.6, 474 doi:10.1140/epjc/s10052-019-6904-3
- [48] P. A. M. Dirac, “Quantum mechanics of many-electron systems,” Proceedings of the Royal Society of London. Series A, Vol. 123, No. 792 (1929).
- [49] O. Antipin, M. Gillioz, J. Krog, E. Mølgaard and F. Sannino, “Standard Model Vacuum Stability and Weyl Consistency Conditions,” JHEP **08** (2013), 034 doi:10.1007/JHEP08(2013)034 [arXiv:1306.3234 [hep-ph]].
- [50] M. Shaposhnikov and C. Wetterich, “Asymptotic safety of gravity and the Higgs boson mass,” Phys. Lett. B **683** (2010), 196-200 doi:10.1016/j.physletb.2009.12.022 [arXiv:0912.0208 [hep-th]].
- [51] A. Pelissetto and E. Vicari, “Critical phenomena and renormalization group theory,” Phys. Rept. **368** (2002), 549-727 doi:10.1016/S0370-1573(02)00219-3 [arXiv:cond-mat/0012164 [cond-mat]].
- [52] J. L. Cardy, “Scaling and renormalization in statistical physics,” (Cambridge Lecture Notes in Physics). Cambridge University Press. (1996) doi:10.1017/CBO9781316036440

[53] J. Polchinski, “String theory. Vol. 1: An introduction to the bosonic string,” doi:10.1017/CBO9780511816079

[54] M. Campostrini, M. Hasenbusch, A. Pelissetto, P. Rossi and E. Vicari, “Critical exponents and equation of state of the three-dimensional Heisenberg universality class,” *Phys. Rev. B* **65** (2002), 144520 doi:10.1103/PhysRevB.65.144520 [arXiv:cond-mat/0110336 [cond-mat]].

[55] M. Campostrini, M. Hasenbusch, A. Pelissetto and E. Vicari, “The Critical exponents of the superfluid transition in He-4,” *Phys. Rev. B* **74** (2006), 144506 doi:10.1103/PhysRevB.74.144506 [arXiv:cond-mat/0605083 [cond-mat]].

[56] W. Witczak-Krempa, E. Sorensen and S. Sachdev, “The dynamics of quantum criticality via Quantum Monte Carlo and holography,” *Nature Phys.* **10** (2014), 361 doi:10.1038/nphys2913 [arXiv:1309.2941 [cond-mat.str-el]].

[57] S. S. Gubser, I. R. Klebanov and A. M. Polyakov, “Gauge theory correlators from noncritical string theory,” *Phys. Lett. B* **428** (1998), 105-114 doi:10.1016/S0370-2693(98)00377-3 [arXiv:hep-th/9802109 [hep-th]].

[58] H. Casini and M. Huerta, “On the RG running of the entanglement entropy of a circle,” *Phys. Rev. D* **85** (2012), 125016 doi:10.1103/PhysRevD.85.125016 [arXiv:1202.5650 [hep-th]].

[59] S. Hellerman and I. Swanson, “String Theory of the Regge Intercept,” *Phys. Rev. Lett.* **114** (2015) no.11, 111601 doi:10.1103/PhysRevLett.114.111601 [arXiv:1312.0999 [hep-th]].

[60] M. Baker and R. Steinke, “Semiclassical quantization of effective string theory and Regge trajectories,” *Phys. Rev. D* **65** (2002), 094042 doi:10.1103/PhysRevD.65.094042 [arXiv:hep-th/0201169 [hep-th]].

[61] D. Orlando, S. Reffert and F. Sannino, “A safe CFT at large charge,” *JHEP* **1908**, 164 (2019) doi:10.1007/JHEP08(2019)164 [arXiv:1905.00026 [hep-th]].

[62] D. Orlando, S. Reffert and F. Sannino, “Charging the Conformal Window,” [arXiv:2003.08396 [hep-th]].

[63] A. De La Fuente, “The large charge expansion at large N ,” *JHEP* **08** (2018), 041 doi:10.1007/JHEP08(2018)041 [arXiv:1805.00501 [hep-th]].

[64] S. Favrod, D. Orlando and S. Reffert, “The large-charge expansion for Schrödinger systems,” *JHEP* **12** (2018), 052 doi:10.1007/JHEP12(2018)052 [arXiv:1809.06371 [hep-th]].

[65] S. M. Kravec and S. Pal, “Nonrelativistic Conformal Field Theories in the Large Charge Sector,” *JHEP* **02** (2019), 008 doi:10.1007/JHEP02(2019)008 [arXiv:1809.08188 [hep-th]].

[66] L. À. Gaumé, D. Orlando and S. Reffert, “Selected Topics in the Large Quantum Number Expansion,” [arXiv:2008.03308 [hep-th]].

[67] A. Palanques-Mestre and P. Pascual, “The $1/N_f$ Expansion of the γ and Beta Functions in {QED},” *Commun. Math. Phys.* **95** (1984), 277 doi:10.1007/BF01212398

[68] M. Beneke and V. M. Braun, “Heavy quark effective theory beyond perturbation theory: Renormalons, the pole mass and the residual mass term,” *Nucl. Phys. B* **426** (1994), 301-343 doi:10.1016/0550-3213(94)90314-X [arXiv:hep-ph/9402364 [hep-ph]].

[69] J. A. Gracey, “The QCD Beta function at $\mathcal{O}(1/N_f)$,” *Phys. Lett. B* **373** (1996), 178-184 doi:10.1016/0370-2693(96)00105-0 [arXiv:hep-ph/9602214 [hep-ph]].

[70] O. Antipin, N. A. Dondi, F. Sannino, A. E. Thomsen and Z. W. Wang, “Gauge-Yukawa theories: Beta functions at large N_f ,” *Phys. Rev. D* **98** (2018) no.1, 016003 doi:10.1103/PhysRevD.98.016003 [arXiv:1803.09770 [hep-ph]].

[71] G. ’t Hooft, “A Two-Dimensional Model for Mesons,” *Nucl. Phys. B* **75** (1974), 461-470 doi:10.1016/0550-3213(74)90088-1

[72] E. Witten, “Baryons in the $1/n$ Expansion,” *Nucl. Phys. B* **160** (1979), 57-115 doi:10.1016/0550-3213(79)90232-3

[73] J. C. Le Guillou and J. Zinn-Justin, 1990, Current Physics - Sources and Comments, Vol. 7, Large-order Behaviour of perturbation theory (North-Holland, Amsterdam, 1990)

[74] M. Beneke, “Renormalons,” *Phys. Rept.* **317** (1999), 1-142 doi:10.1016/S0370-1573(98)00130-6 [arXiv:hep-ph/9807443 [hep-ph]].

[75] I. Aniceto, G. Basar and R. Schiappa, “A Primer on Resurgent Transseries and Their Asymptotics,” *Phys. Rept.* **809** (2019), 1-135 doi:10.1016/j.physrep.2019.02.003 [arXiv:1802.10441 [hep-th]].

[76] G. Badel, G. Cuomo, A. Monin and R. Rattazzi, “Feynman diagrams and the large charge expansion in $3 - \varepsilon$ dimensions,” *Phys. Lett. B* **802** (2020), 135202 doi:10.1016/j.physletb.2020.135202 [arXiv:1911.08505 [hep-th]].

[77] A. Monin, D. Pirtskhalava, R. Rattazzi and F. K. Seibold, “Semiclassics, Goldstone Bosons and CFT data,” *JHEP* **06** (2017), 011 doi:10.1007/JHEP06(2017)011 [arXiv:1611.02912 [hep-th]].

[78] G. Cuomo, “The OPE meets semiclassics,” [arXiv:2103.01331 [hep-th]].

[79] Z. Komargodski and A. Zhiboedov, “Convexity and Liberation at Large Spin,” *JHEP* **11** (2013), 140 doi:10.1007/JHEP11(2013)140 [arXiv:1212.4103 [hep-th]].

[80] B. Basso and G. P. Korchemsky, “Anomalous dimensions of high-spin operators beyond the leading order,” *Nucl. Phys. B* **775** (2007), 1-30 doi:10.1016/j.nuclphysb.2007.03.044 [arXiv:hep-th/0612247 [hep-th]].

[81] S. Weinberg, “Ultraviolet divergences in quantum theories of gravitation,”

[82] M. Reuter, “Nonperturbative evolution equation for quantum gravity,” *Phys. Rev. D* **57** (1998), 971-985 doi:10.1103/PhysRevD.57.971 [arXiv:hep-th/9605030 [hep-th]].

[83] R. Mann, J. Meffe, F. Sannino, T. Steele, Z. W. Wang and C. Zhang, “Asymptotically Safe Standard Model via Vectorlike Fermions,” *Phys. Rev. Lett.* **119** (2017) no.26, 261802 doi:10.1103/PhysRevLett.119.261802 [arXiv:1707.02942 [hep-ph]].

[84] O. Antipin, J. Bersini, F. Sannino, Z. W. Wang and C. Zhang, “Charging the $O(N)$ model,” *Phys. Rev. D* **102** (2020) no.4, 045011 doi:10.1103/PhysRevD.102.045011 [arXiv:2003.13121 [hep-th]].

[85] O. Antipin and J. Bersini, “Spectrum of anomalous dimensions in hypercubic theories,” *Phys. Rev. D* **100** (2019) no.6, 065008 doi:10.1103/PhysRevD.100.065008 [arXiv:1903.04950 [hep-th]].

[86] O. Antipin, J. Bersini, F. Sannino, Z. W. Wang and C. Zhang, “Charging non-Abelian Higgs theories,” *Phys. Rev. D* **102** (2020) no.12, 125033 doi:10.1103/PhysRevD.102.125033 [arXiv:2006.10078 [hep-th]].

[87] O. Antipin, J. Bersini, F. Sannino, Z. W. Wang and C. Zhang, “Untangling scaling dimensions of fixed charge operators in Higgs Theories,” [arXiv:2102.04390 [hep-th]].

[88] P. Di Francesco, P. Mathieu, D. Senechal “Conformal field theory,” Springer, New York, USA (1997) doi:10.1007/978-1-4612-2256-9

[89] S. Rychkov, “EPFL Lectures on Conformal Field Theory in $D \geq 3$ Dimensions,” doi:10.1007/978-3-319-43626-5 [arXiv:1601.05000 [hep-th]].

[90] D. Simmons-Duffin, “The Conformal Bootstrap,” doi:10.1142/9789813149441_0001 [arXiv:1602.07982 [hep-th]].

[91] Y. Nakayama, “Scale invariance vs conformal invariance,” *Phys. Rept.* **569** (2015), 1-93 doi:10.1016/j.physrep.2014.12.003 [arXiv:1302.0884 [hep-th]].

[92] A. Dymarsky, Z. Komargodski, A. Schwimmer and S. Theisen, “On Scale and Conformal Invariance in Four Dimensions,” *JHEP* **10** (2015), 171 doi:10.1007/JHEP10(2015)171 [arXiv:1309.2921 [hep-th]].

[93] L. Cornalba, M. S. Costa and J. Penedones, “Deep Inelastic Scattering in Conformal QCD,” *JHEP* **03** (2010), 133 doi:10.1007/JHEP03(2010)133 [arXiv:0911.0043 [hep-th]].

[94] S. Weinberg, “Six-dimensional Methods for Four-dimensional Conformal Field Theories,” *Phys. Rev. D* **82** (2010), 045031 doi:10.1103/PhysRevD.82.045031 [arXiv:1006.3480 [hep-th]].

[95] G. Mack and A. Salam, “Finite component field representations of the conformal group,” *Annals Phys.* **53** (1969), 174-202 doi:10.1016/0003-4916(69)90278-4

[96] G. Mack, “All unitary ray representations of the conformal group $SU(2,2)$ with positive energy,” *Commun. Math. Phys.* **55** (1977), 1 doi:10.1007/BF01613145

[97] S. Minwalla, “Restrictions imposed by superconformal invariance on quantum field theories,” *Adv. Theor. Math. Phys.* **2** (1998), 783-851 doi:10.4310/ATMP.1998.v2.n4.a4 [arXiv:hep-th/9712074 [hep-th]].

[98] J. L. Cardy, “Conformal invariance and universality in finite-size scaling,” *J. Phys. A* **17** (1984), L385-L387

[99] J. Cardy, “Universal amplitudes in finite-size scaling: generalisation to arbitrary dimensionality,” *J. Phys. A* **18** (1985) no.13, L757-L760 doi:10.1088/0305-4470/18/13/005

[100] A. M. Polyakov, “Conformal symmetry of critical fluctuations,” *JETP Lett.* **12** (1970), 381-383

[101] G. Mack, “Convergence of Operator Product Expansions on the Vacuum in Conformal Invariant Quantum Field Theory,” *Commun. Math. Phys.* **53** (1977), 155 doi:10.1007/BF01609130

[102] S. Ferrara, A. F. Grillo and R. Gatto, “Tensor representations of conformal algebra and conformally covariant operator product expansion,” *Annals Phys.* **76** (1973), 161-188 doi:10.1016/0003-4916(73)90446-6

[103] D. Poland, S. Rychkov and A. Vichi, “The Conformal Bootstrap: Theory, Numerical Techniques, and Applications,” *Rev. Mod. Phys.* **91** (2019), 015002 doi:10.1103/RevModPhys.91.015002 [arXiv:1805.04405 [hep-th]].

[104] A. Iorio, L. O’Raifeartaigh, I. Sachs and C. Wiesendanger, “Weyl gauging and conformal invariance,” *Nucl. Phys. B* **495** (1997), 433-450 doi:10.1016/S0550-3213(97)00190-9 [arXiv:hep-th/9607110 [hep-th]].

[105] K. Farnsworth, M. A. Luty and V. Prilepsina, “Weyl versus Conformal Invariance in Quantum Field Theory,” *JHEP* **10** (2017), 170 doi:10.1007/JHEP10(2017)170 [arXiv:1702.07079 [hep-th]].

[106] G. K. Karananas and A. Monin, “Weyl vs. Conformal,” *Phys. Lett. B* **757** (2016), 257-260 doi:10.1016/j.physletb.2016.04.001 [arXiv:1510.08042 [hep-th]].

[107] L. S. Brown and J. C. Collins, “Dimensional Renormalization of Scalar Field Theory in Curved Space-time,” *Annals Phys.* **130** (1980), 215 doi:10.1016/0003-4916(80)90232-8

[108] R. Guida and N. Magnoli, “All order IR finite expansion for short distance behavior of massless theories perturbed by a relevant operator,” *Nucl. Phys. B* **471** (1996), 361-388 doi:10.1016/0550-3213(96)00175-7 [arXiv:hep-th/9511209 [hep-th]].

[109] A. Amoretti and N. Magnoli, “Conformal perturbation theory,” *Phys. Rev. D* **96** (2017) no.4, 045016 doi:10.1103/PhysRevD.96.045016 [arXiv:1705.03502 [hep-th]].

[110] V. Gorbenko, S. Rychkov and B. Zan, “Walking, Weak first-order transitions, and Complex CFTs II. Two-dimensional Potts model at $Q > 4$,” *SciPost Phys.* **5** (2018) no.5, 050 doi:10.21468/SciPostPhys.5.5.050 [arXiv:1808.04380 [hep-th]].

[111] B. Holdom, “Raising the Sideways Scale,” *Phys. Rev. D* **24** (1981) 1441. doi:10.1103/PhysRevD.24.1441

[112] B. Holdom, “Raising Condensates Beyond the Ladder,” *Phys. Lett. B* **213** (1988) 365-369. doi:10.1016/0370-2693(88)91776-5

[113] F. Sannino and K. Tuominen, “Orientifold theory dynamics and symmetry breaking,” *Phys. Rev. D* **71** (2005), 051901 doi:10.1103/PhysRevD.71.051901 [arXiv:hep-ph/0405209 [hep-ph]].

[114] A. G. Cohen and H. Georgi, “Walking Beyond the Rainbow,” *Nucl. Phys. B* **314** (1989), 7-24 doi:10.1016/0550-3213(89)90109-0

[115] J. L. Cardy, M. Nauenberg and D. J. Scalapino, “Scaling Theory of the Potts Model Multicritical Point,” *Phys. Rev. B* **22** (1980), 2560-2568 doi:10.1103/PhysRevB.22.2560

[116] C. Wang, A. Nahum, M. A. Metlitski, C. Xu and T. Senthil, “Deconfined quantum critical points: symmetries and dualities,” *Phys. Rev. X* **7** (2017) no.3, 031051 doi:10.1103/PhysRevX.7.031051 [arXiv:1703.02426 [cond-mat.str-el]].

[117] L. Landau and E. Lifshitz, Quantum Mechanics, Course of Theoretical Physics. Butterworth-Heinemann, 3 ed., 1977.

[118] A. Nicolis, R. Penco, F. Piazza and R. Rattazzi, “Zoology of condensed matter: Framids, ordinary stuff, extra-ordinary stuff,” *JHEP* **06** (2015), 155 doi:10.1007/JHEP06(2015)155 [arXiv:1501.03845 [hep-th]].

[119] D. T. Son, “Low-energy quantum effective action for relativistic superfluids,” [arXiv:hep-ph/0204199 [hep-ph]].

[120] J. Goldstone, A. Salam and S. Weinberg, “Broken Symmetries,” *Phys. Rev.* **127** (1962), 965-970 doi:10.1103/PhysRev.127.965

[121] H. B. Nielsen and S. Chadha, “On How to Count Goldstone Bosons,” *Nucl. Phys. B* **105** (1976) 445. doi:10.1016/0550-3213(76)90025-0

[122] T. Brauner, “Spontaneous Symmetry Breaking and Nambu-Goldstone Bosons in Quantum Many-Body Systems,” *Symmetry* **2** (2010), 609-657 doi:10.3390/sym2020609 [arXiv:1001.5212 [hep-th]].

[123] T. Schäfer, D. T. Son, M. A. Stephanov, D. Toublan and J. J. M. Verbaarschot, “Kaon condensation and Goldstone’s theorem,” *Phys. Lett. B* **522** (2001), 67-75 doi:10.1016/S0370-2693(01)01265-5 [arXiv:hep-ph/0108210 [hep-ph]].

[124] H. Watanabe and H. Murayama, “Effective Lagrangian for Nonrelativistic Systems,” *Phys. Rev. X* **4** (2014) no.3, 031057 doi:10.1103/PhysRevX.4.031057 [arXiv:1402.7066 [hep-th]].

[125] H. Watanabe and H. Murayama, “Unified Description of Nambu-Goldstone Bosons without Lorentz Invariance,” *Phys. Rev. Lett.* **108** (2012), 251602 doi:10.1103/PhysRevLett.108.251602 [arXiv:1203.0609 [hep-th]].

[126] H. Leutwyler, “Nonrelativistic effective Lagrangians,” *Phys. Rev. D* **49** (1994), 3033-3043 doi:10.1103/PhysRevD.49.3033 [arXiv:hep-ph/9311264 [hep-ph]].

[127] H. Leutwyler, “On the foundations of chiral perturbation theory,” *Annals Phys.* **235** (1994), 165-203 doi:10.1006/aphy.1994.1094 [arXiv:hep-ph/9311274 [hep-ph]].

[128] A. Nicolis and F. Piazza, “Implications of Relativity on Nonrelativistic Goldstone Theorems: Gapped Excitations at Finite Charge Density,” *Phys. Rev. Lett.* **110** (2013) no.1, 011602 doi:10.1103/PhysRevLett.110.011602 [arXiv:1204.1570 [hep-th]].

[129] H. Watanabe, T. Brauner and H. Murayama, “Massive Nambu-Goldstone Bosons,” *Phys. Rev. Lett.* **111** (2013) no.2, 021601 doi:10.1103/PhysRevLett.111.021601 [arXiv:1303.1527 [hep-th]].

[130] D. Banerjee, S. Chandrasekharan, D. Orlando and S. Reffert, “Conformal dimensions in the large charge sectors at the O(4) Wilson-Fisher fixed point,” *Phys. Rev. Lett.* **123** (2019) no.5, 051603 doi:10.1103/PhysRevLett.123.051603 [arXiv:1902.09542 [hep-lat]].

[131] G. Cuomo, “A note on the large charge expansion in 4d CFT,” *Phys. Lett. B* **812** (2021), 136014 doi:10.1016/j.physletb.2020.136014 [arXiv:2010.00407 [hep-th]].

[132] H. Kleinert and V. Schulte-Frohlinde, “Critical Properties of ϕ^4 -Theories”, (World Scientific, Singapore, 2001).

[133] D. Z. Freedman, K. Johnson and J. I. Latorre, “Differential regularization and renormalization: A New method of calculation in quantum field theory,” *Nucl. Phys. B* **371**, 353 (1992). doi:10.1016/0550-3213(92)90240-C

[134] S. C. Zhang, “A Unified Theory Based on SO(5) Symmetry of Superconductivity and Anti-ferromagnetism,” *Science* **275**, 1089-1097 (1997), DOI: 10.1126/science.275.5303.1089

[135] F. Wilczek, “Application of the renormalization group to a second order QCD phase transition,” *Int. J. Mod. Phys. A* **7** (1992), 3911-3925 doi:10.1142/S0217751X92001757

[136] R. D. Pisarski and F. Wilczek, “Remarks on the Chiral Phase Transition in Chromodynamics,” *Phys. Rev. D* **29** (1984), 338-341 doi:10.1103/PhysRevD.29.338

[137] L. Alvarez-Gaume, D. Orlando and S. Reffert, “Large charge at large N,” *JHEP* **12** (2019), 142 doi:10.1007/JHEP12(2019)142 [arXiv:1909.02571 [hep-th]].

[138] M. V. Kompaniets and E. Panzer, “Minimally subtracted six loop renormalization of $O(n)$ -symmetric ϕ^4 theory and critical exponents,” Phys. Rev. D **96** (2017) no.3, 036016 doi:10.1103/PhysRevD.96.036016 [arXiv:1705.06483 [hep-th]].

[139] J. D. Brock, A. Aharony, R. J. Birgeneau, K. W. Evans-Lutterodt, J. D. Litster, P. M. Horn, G. B. Stephenson, and A. R. Tajbakhsh, “Orientational and positional order in a tilted hexatic liquid-crystal phase,” Phys. Rev. Lett. 57, 98 (1985).

[140] A. Aharony, R. J. Birgeneau, J. D. Brock, and J. D. Litster, “Multicriticality in Hexatic Liquid Crystals,” Phys. Rev. Lett. 57, 1012 (1986).

[141] A. Aharony, in *Phase Transitions and Critical Phenomena*, edited by C. Domb and J. Lebowitz (Academic Press, New York, 1976), Vol. 6, p. 357.

[142] M.E. Fisher and D.R. Nelson, “Spin Flop, Supersolids, and Bicritical and Tetracritical Points,” Phys. Rev. Lett. 32, 1350 (1974).

[143] D.R. Nelson, J.M. Kosterlitz, and M.E. Fisher, “Renormalization-Group Analysis of Bicritical and Tetracritical Points,” Phys. Rev. Lett. 33, 13 (1974).

[144] P. Calabrese, A. Pelissetto and E. Vicari, “Multicritical phenomena in $O(n(1)) + O(n(2))$ symmetric theories,” Phys. Rev. B **67** (2003), 054505 doi:10.1103/PhysRevB.67.054505 [arXiv:cond-mat/0209580 [cond-mat]].

[145] D. V. Batkovich, K. G. Chetyrkin and M. V. Kompaniets, “Six loop analytical calculation of the field anomalous dimension and the critical exponent η in $O(n)$ -symmetric ϕ^4 model,” Nucl. Phys. B **906** (2016), 147-167 doi:10.1016/j.nuclphysb.2016.03.009 [arXiv:1601.01960 [hep-th]].

[146] M. Kompaniets and K. J. Wiese, “Fractal dimension of critical curves in the $O(n)$ -symmetric ϕ^4 model and crossover exponent at 6-loop order: Loop-erased random walks, self-avoiding walks, Ising, XY, and Heisenberg models,” Phys. Rev. E **101** (2020) no.1, 012104 doi:10.1103/PhysRevE.101.012104 [arXiv:1908.07502 [cond-mat.stat-mech]].

[147] S. K. Kehrein, “The Spectrum of critical exponents in phi**2 in two-dimensions theory in $D = (4-\epsilon)$ -dimensions: Resolution of degeneracies and hierarchical structures,” Nucl. Phys. B **453** (1995) 777 doi:10.1016/0550-3213(95)00375-3 [hep-th/9507044].

[148] D. J. Wallace and R. K. P. Zia, “Harmonic perturbations of generalized Heisenberg spin systems,” J. Phys. C: Solid State Phys. 8 839 (1975) 10.1088/0022-3719/8/6/014.

[149] S. Hellerman, N. Kobayashi, S. Maeda and M. Watanabe, “A Note on Inhomogeneous Ground States at Large Global Charge,” JHEP **10** (2019), 038 doi:10.1007/JHEP10(2019)038 [arXiv:1705.05825 [hep-th]].

[150] S. Hellerman, N. Kobayashi, S. Maeda and M. Watanabe, “Observables in Inhomogeneous Ground States at Large Global Charge,” [arXiv:1804.06495 [hep-th]].

[151] I. Jack and D. R. T. Jones, “Anomalous dimensions at large charge in $d=4$ $O(N)$ theory,” [arXiv:2101.09820 [hep-th]].

[152] M. Hasenbusch and E. Vicari, “Anisotropic perturbations in three-dimensional $O(N)$ -symmetric vector models,” Phys. Rev. B. **84** (2011) no.12, doi:10.1103/physrevb.84.125136

[153] B. Holdom, “Large N flavor beta-functions: a recap,” Phys. Lett. B **694** (2011), 74-79 doi:10.1016/j.physletb.2010.09.037 [arXiv:1006.2119 [hep-ph]].

[154] G. Arias-Tamargo, D. Rodriguez-Gomez and J. G. Russo, “On the UV completion of the $O(N)$ model in $6 - \epsilon$ dimensions: a stable large-charge sector,” [arXiv:2003.13772 [hep-th]].

[155] A. Aharony, (1973), Critical Behavior of Anisotropic Cubic Systems, Phys. Rev. B8, 4270

[156] M. Tissier, D. Mouhanna, J. Vidal, B. Delamotte, “Randomly dilute Ising model: A non-perturbative approach” Phys. Rev. B 65, 140402 (2002) doi:10.1103/PhysRevB.65.140402 [arXiv:cond-mat/0109176v3 [cond-mat.stat-mech]].

[157] J. M. Carmona, A. Pelissetto and E. Vicari, “The N component Ginzburg-Landau Hamiltonian with cubic anisotropy: A Six loop study,” Phys. Rev. B **61** (2000) 15136 doi:10.1103/PhysRevB.61.15136 [cond-mat/9912115].

[158] S. M. Chester, W. Landry, J. Liu, D. Poland, D. Simmons-Duffin, N. Su and A. Vichi, “Bootstrapping Heisenberg Magnets and their Cubic Instability,” [arXiv:2011.14647 [hep-th]].

[159] L. T. Adzhemyan, E. V. Ivanova, M. V. Kompaniets, A. Kudlis and A. I. Sokolov, “Six-loop ϵ expansion study of three-dimensional n -vector model with cubic anisotropy,” Nucl. Phys. B **940** (2019) 332 doi:10.1016/j.nuclphysb.2019.02.001 [arXiv:1901.02754 [cond-mat.stat-mech]].

[160] A. Stergiou, “Bootstrapping hypercubic and hypertetrahedral theories in three dimensions,” JHEP **1805** (2018) 035 doi:10.1007/JHEP05(2018)035 [arXiv:1801.07127 [hep-th]].

[161] S. R. Kousvos and A. Stergiou, “Bootstrapping Mixed Correlators in Three-Dimensional Cubic Theories,” [arXiv:1810.10015 [hep-th]].

[162] S. R. Kousvos and A. Stergiou, “Bootstrapping Mixed Correlators in Three-Dimensional Cubic Theories II,” [arXiv:1911.00522 [hep-th]].

[163] P. Dey, A. Kaviraj and A. Sinha, “Mellin space bootstrap for global symmetry,” JHEP **1707** (2017) 019 doi:10.1007/JHEP07(2017)019 [arXiv:1612.05032 [hep-th]].

[164] S. Rychkov and Z. M. Tan, “The ϵ -expansion from conformal field theory,” J. Phys. A **48** (2015) no.29, 29FT01 doi:10.1088/1751-8113/48/29/29FT01 [arXiv:1505.00963 [hep-th]].

[165] A. Codello, M. Safari, G. P. Vacca and O. Zanusso, “Leading order CFT analysis of multi-scalar theories in $d > 2$,” arXiv:1809.05071 [hep-th].

[166] M. Baake, “Structure and representations of the hyperoctahedral group”, J. Math. Phys. 25, 3171 (1984).

[167] M. Hamermesh, “Group Theory and its Applications to Physical Problems”, Dover Publications (1989).

[168] G. James, A. Kerber, The Representation Theory of the Symmetric Group, Encyclopedia of Mathematics and its Applications, 16. Addison-Wesley Publishing Co., Reading, Mass., 1981.

[169] K. Balasubramanian, (2016), Character tables of n- dimensional hyperoctahedral groups and their applications, Molecular Physics, 114(10):1-15.

[170] R. Orellana, *Contemporary Math.* **376**, (2005), 345-357.

[171] H. Osborn and D. E. Twigg, “Reparameterisation Invariance and RG equations: Extension of the Local Potential Approximation,” *J. Phys. A* **42** (2009) 195401 doi:10.1088/1751-8113/42/19/195401 [arXiv:0901.0450 [hep-th]].

[172] S. K. Kehrein and F. Wegner, “The Structure of the spectrum of anomalous dimensions in the N vector model in (4- ϵ)-dimensions,” *Nucl. Phys. B* **424** (1994) 521 doi:10.1016/0550-3213(94)90406-5 [hep-th/9405123].

[173] H. Osborn and A. Stergiou, “Seeking fixed points in multiple coupling scalar theories in the ϵ expansion,” *JHEP* **1805** (2018) 051 [arXiv:1707.06165 [hep-th]].

[174] M. Hogervorst and C. Toldo, “Bounds on multiscalar CFTs in the epsilon expansion,” [arXiv:2010.16222 [hep-th]].

[175] D. Dou and R. Percacci, “The running gravitational couplings,” *Class. Quant. Grav.* **15** (1998), 3449-3468 doi:10.1088/0264-9381/15/11/011 [arXiv:hep-th/9707239 [hep-th]].

[176] O. Lauscher and M. Reuter, “Ultraviolet fixed point and generalized flow equation of quantum gravity,” *Phys. Rev. D* **65** (2002), 025013 doi:10.1103/PhysRevD.65.025013 [arXiv:hep-th/0108040 [hep-th]].

[177] R. Percacci and D. Perini, “Asymptotic safety of gravity coupled to matter,” *Phys. Rev. D* **68** (2003), 044018 doi:10.1103/PhysRevD.68.044018 [arXiv:hep-th/0304222 [hep-th]].

[178] D. F. Litim, “Fixed points of quantum gravity,” *Phys. Rev. Lett.* **92** (2004), 201301 doi:10.1103/PhysRevLett.92.201301 [arXiv:hep-th/0312114 [hep-th]].

[179] M. M. Anber and J. F. Donoghue, “On the running of the gravitational constant,” *Phys. Rev. D* **85** (2012), 104016 doi:10.1103/PhysRevD.85.104016 [arXiv:1111.2875 [hep-th]].

[180] J. F. Donoghue, “A Critique of the Asymptotic Safety Program,” *Front. in Phys.* **8** (2020), 56 doi:10.3389/fphy.2020.00056 [arXiv:1911.02967 [hep-th]].

[181] D. F. Litim, M. Mojaza and F. Sannino, “Vacuum stability of asymptotically safe gauge-Yukawa theories,” *JHEP* **01** (2016), 081 doi:10.1007/JHEP01(2016)081 [arXiv:1501.03061 [hep-th]].

[182] L. Smolin, “A Fixed Point for Quantum Gravity,” *Nucl. Phys. B* **208** (1982), 439-466 doi:10.1016/0550-3213(82)90230-9

[183] E. S. Fradkin and M. A. Vasiliev, “On the Gravitational Interaction of Massless Higher Spin Fields,” *Phys. Lett. B* **189** (1987), 89-95 doi:10.1016/0370-2693(87)91275-5

[184] S. Giombi and X. Yin, “The Higher Spin/Vector Model Duality,” *J. Phys. A* **46** (2013), 214003 doi:10.1088/1751-8113/46/21/214003 [arXiv:1208.4036 [hep-th]].

[185] S. Giombi, “Higher Spin - CFT Duality,” doi:10.1142/9789813149441_0003 [arXiv:1607.02967 [hep-th]].

[186] J. A. Gracey, “Four loop renormalization of ϕ^3 theory in six dimensions,” *Phys. Rev. D* **92** (2015) no.2, 025012 doi:10.1103/PhysRevD.92.025012 [arXiv:1506.03357 [hep-th]].

[187] S. Giombi, R. Huang, I. R. Klebanov, S. S. Pufu and G. Tarnopolsky, “The $O(N)$ Model in $4 < d < 6$: Instantons and complex CFTs,” *Phys. Rev. D* **101** (2020) no.4, 045013 doi:10.1103/PhysRevD.101.045013 [arXiv:1910.02462 [hep-th]].

[188] K. Lang and W. Ruhl, “The Critical $O(N)$ sigma model at dimensions $2 < d < 4$: Fusion coefficients and anomalous dimensions,” *Nucl. Phys. B* **400** (1993), 597-623 doi:10.1016/0550-3213(93)90417-N

[189] S. Giombi and J. Hyman, “On the Large Charge Sector in the Critical $O(N)$ Model at Large N ,” [arXiv:2011.11622 [hep-th]].

[190] O. Antipin, E. Mølgaard and F. Sannino, “Higgs Critical Exponents and Conformal Bootstrap in Four Dimensions,” *JHEP* **06** (2015), 030 doi:10.1007/JHEP06(2015)030.

[191] R. Pisarski and D. Stein, “Critical Behavior of Linear ϕ^4 Models With $G \times G'$ Symmetry,” *Phys. Rev. B* **23** (1981), 3549-3552 doi:10.1103/PhysRevB.23.3549

[192] T. Han, I. Lewis and T. McElmurry, “QCD Corrections to Scalar Diquark Production at Hadron Colliders,” *JHEP* **01** (2010), 123 doi:10.1007/JHEP01(2010)123 [arXiv:0909.2666 [hep-ph]].

[193] B. C. Hall, “Lie Groups, Lie Algebras, and Representations”, (Springer, Second Edition, 2015).

[194] J. F. Cornwell, “Group Theory in Physics, Vol. 2”, (Academic Press, 1984).

[195] R. Feger and T. W. Kephart, “LieART—A Mathematica application for Lie algebras and representation theory,” *Comput. Phys. Commun.* **192** (2015), 166-195 doi:10.1016/j.cpc.2014.12.023 [arXiv:1206.6379 [math-ph]].

[196] R. Feger, T. W. Kephart and R. J. Saskowski, “LieART 2.0 – A Mathematica application for Lie Algebras and Representation Theory,” *Comput. Phys. Commun.* **257** (2020), 107490 doi:10.1016/j.cpc.2020.107490 [arXiv:1912.10969 [hep-th]].

[197] I. Aniceto, R. Schiappa and M. Vonk, “The Resurgence of Instantons in String Theory,” *Commun. Num. Theor. Phys.* **6** (2012), 339-496 doi:10.4310/CNTP.2012.v6.n2.a3 [arXiv:1106.5922 [hep-th]].

[198] D. Dorigoni, “An Introduction to Resurgence, Trans-Series and Alien Calculus,” *Annals Phys.* **409** (2019), 167914 doi:10.1016/j.aop.2019.167914 [arXiv:1411.3585 [hep-th]].

[199] G. V. Dunne and M. Unsal, “Resurgence and Trans-series in Quantum Field Theory: The CP(N-1) Model,” *JHEP* **11** (2012), 170 doi:10.1007/JHEP11(2012)170 [arXiv:1210.2423 [hep-th]].

[200] J. Bersini, A. Maiezza and J. C. Vasquez, “Resurgence of the renormalization group equation,” *Annals Phys.* **415** (2020), 168126 doi:10.1016/j.aop.2020.168126 [arXiv:1910.14507 [hep-th]].

[201] J. M. Cornwall, “On the High-energy Behavior of Weakly Coupled Gauge Theories,” *Phys. Lett. B* **243** (1990), 271-278 doi:10.1016/0370-2693(90)90850-6

[202] E. N. Argyres, R. H. P. Kleiss and C. G. Papadopoulos, “Amplitude estimates for multi - Higgs production at high-energies,” *Nucl. Phys. B* **391** (1993), 42-56 doi:10.1016/0550-3213(93)90140-K

[203] M. Dine, H. H. Patel and J. F. Ulbricht, “Behavior of Cross Sections for Large Numbers of Particles,” [arXiv:2002.12449 [hep-ph]].

[204] F. Kos, D. Poland, D. Simmons-Duffin and A. Vichi, “Precision Islands in the Ising and $O(N)$ Models,” *JHEP* **08** (2016), 036 doi:10.1007/JHEP08(2016)036 [arXiv:1603.04436 [hep-th]].

[205] R. Rattazzi, S. Rychkov and A. Vichi, “Central Charge Bounds in 4D Conformal Field Theory,” *Phys. Rev. D* **83** (2011), 046011 doi:10.1103/PhysRevD.83.046011.

[206] D. D. Dietrich and F. Sannino, “Conformal window of $SU(N)$ gauge theories with fermions in higher dimensional representations,” *Phys. Rev. D* **75** (2007), 085018 doi:10.1103/PhysRevD.75.085018 [arXiv:hep-ph/0611341 [hep-ph]].

[207] A. Codello, M. Safari, G. P. Vacca and O. Zanusso, “Critical models with $N \leq 4$ scalars in $d = 4 - \varepsilon$,” *Phys. Rev. D* **102** (2020) no.6, 065017 doi:10.1103/PhysRevD.102.065017 [arXiv:2008.04077 [hep-th]].

[208] S. Rychkov and A. Stergiou, “General Properties of Multiscalar RG Flows in $d = 4 - \varepsilon$,” *SciPost Phys.* **6** (2019) no.1, 008 doi:10.21468/SciPostPhys.6.1.008 [arXiv:1810.10541 [hep-th]].

[209] D. Orlando, S. Reffert and F. Sannino, “Near-Conformal Dynamics at Large Charge,” *Phys. Rev. D* **101** (2020) no.6, 065018 doi:10.1103/PhysRevD.101.065018 [arXiv:1909.08642 [hep-th]].

[210] N. Dondi, I. Kalogerakis, D. Orlando and S. Reffert, “Resurgence of the large-charge expansion,” [arXiv:2102.12488 [hep-th]].

[211] S. Hellerman, “On the exponentially small corrections to $\mathcal{N} = 2$ superconformal correlators at large R-charge,” [arXiv:2103.09312 [hep-th]].

[212] O. Loukas, D. Orlando, S. Reffert and D. Sarkar, “An AdS/EFT correspondence at large charge,” *Nucl. Phys. B* **934** (2018), 437-458 doi:10.1016/j.nuclphysb.2018.07.020 [arXiv:1804.04151 [hep-th]].

[213] A. de la Fuente and J. Zosso, “The large charge expansion and AdS/CFT,” *JHEP* **06** (2020), 178 doi:10.1007/JHEP06(2020)178 [arXiv:2005.06169 [hep-th]].

[214] H. S. Liu, H. Lu and Y. Pang, “Revisiting the AdS Boson Stars: the Mass-Charge Relations,” *Phys. Rev. D* **102** (2020) no.12, 126008 doi:10.1103/PhysRevD.102.126008.

[215] S. F. Guo, H. S. Liu, H. Lü and Y. Pang, “Large-Charge Limit of AdS Boson Stars with Mixed Boundary Conditions,” [arXiv:2101.00017 [hep-th]].

[216] M. V. Libanov, V. A. Rubakov and S. V. Troitsky, “Multiparticle processes and semiclassical analysis in bosonic field theories,” *Phys. Part. Nucl.* **28** (1997), 217-240 doi:10.1134/1.953038

[217] V. V. Khoze and J. Reiness, “Review of the semiclassical formalism for multiparticle production at high energies,” *Phys. Rept.* **822** (2019), 1-52 doi:10.1016/j.physrep.2019.06.004 [arXiv:1810.01722 [hep-ph]].

[218] D. T. Son, “Semiclassical approach for multiparticle production in scalar theories,” *Nucl. Phys. B* **477** (1996), 378-406 doi:10.1016/0550-3213(96)00386-0 [arXiv:hep-ph/9505338 [hep-ph]].

[219] D. T. Son, “Superconductivity by long range color magnetic interaction in high density quark matter,” *Phys. Rev. D* **59** (1999), 094019 doi:10.1103/PhysRevD.59.094019 [arXiv:hep-ph/9812287 [hep-ph]].

[220] M. G. Alford, A. Schmitt, K. Rajagopal and T. Schäfer, “Color superconductivity in dense quark matter,” *Rev. Mod. Phys.* **80** (2008), 1455-1515 doi:10.1103/RevModPhys.80.1455 [arXiv:0709.4635 [hep-ph]].

[221] D. T. Son and M. A. Stephanov, “QCD at finite isospin density,” *Phys. Rev. Lett.* **86** (2001), 592-595 doi:10.1103/PhysRevLett.86.592 [arXiv:hep-ph/0005225 [hep-ph]].

[222] A. J. Paterson, “Coleman-Weinberg Symmetry Breaking in the Chiral $SU(N) \times SU(N)$ Linear Sigma Model,” Nucl. Phys. B **190** (1981), 188-204 doi:10.1016/0550-3213(81)90489-2

Appendix A Proof of the *charged Goldstone theorem*

In this appendix, we present a partial proof of the charged Goldstone theorem stated in Sec.3.4. We refer the reader to the original papers [121, 125, 128, 129] for details and examples. We start by defining the matrix

$$M_{ia} \equiv \langle 0 | \phi_i(0), Q_a(t) | 0 \rangle , \quad (\text{A.1})$$

which we rewrite as

$$M_{ia} = \int d^3x \langle 0 | \phi_i(0) j_a^0(\vec{x}, t) | 0 \rangle - \text{c.c.} = \int d^3x \langle 0 | \phi_i(0) e^{i\mu Q t} j_a^0 e^{-i(Ht - P \cdot \vec{x})} | 0 \rangle - \text{c.c.} , \quad (\text{A.2})$$

where we used assumption (3) (time evolution of the operators), and we take j_a^0 and ϕ_i to be Hermitian. Then we use the completeness relation to rewrite the integrand above as

$$\begin{aligned} \langle 0 | \phi_i(0) e^{i\mu Q t} j_a^0 e^{-i(Ht - P \cdot \vec{x})} | 0 \rangle &= \sum_{n_k} e^{i\vec{k} \cdot \vec{x}} \langle 0 | \phi_i(0) e^{i\mu Q t} j_a^0 e^{-i\mu Q t} e^{-i\tilde{H} t} | n_k \rangle \\ &\quad \times \langle n_k | \phi_i(0) e^{i\mu Q t} j_a^0 e^{-i\mu Q t} e^{-i\tilde{H} t} | 0 \rangle , \end{aligned} \quad (\text{A.3})$$

with $|n_k\rangle$ a momentum eigenstate of the n -th particle species, which is also an eigenstate of \tilde{H} with eigenvalue E_k . After performing the integral over the space in (A.2), only the zero momentum states survive, and thus we have

$$M_{ia} = \sum_{n_k} e^{-iE_k t} \langle 0 | e^{i\mu Q t} j_a^0 e^{-i\mu Q t} | n_k \rangle \langle n_k | \phi_i | 0 \rangle - \text{c.c.} \Big|_{\mathbf{k} \rightarrow \mathbf{0}} . \quad (\text{A.4})$$

Consider first the case where Q_a commutes with the fixed charge Q . Then

$$M_{ia} = \sum_{n=1}^l e^{-iE_k t} \langle 0 | \phi_i | n_k \rangle \langle n_k | j_a^0 | 0 \rangle - \text{c.c.} \Big|_{\mathbf{k} \rightarrow \mathbf{0}} . \quad (\text{A.5})$$

The rank of M_{ia} equals the number of broken generators m by definition. Let us see which intermediate states can contribute to M_{ia} when $[Q_a, Q] = 0$. Charge conservation and relativistic invariance⁴² imply that $\frac{d}{dt} M_{ia} = 0$. Then the Fourier transform of M_{ia} has the following general

⁴²In particular, we use that space-like separated local operators commute.

form

$$\mathcal{F}[M_{ia}] = k^0 \delta(k^2) a(k_0) + (k^2 - k^{02}) b(k^2, k^0) + \delta(k^0) c(k^2) + \lambda \delta^d(k) , \quad (\text{A.6})$$

for arbitrary a, b, c , and λ .

The third term does not contribute. In fact, these intermediate states have $k^0 = 0$ for any \mathbf{k} completely breaking translation invariance violating assumption (2). Also, in relativistic theories, the fourth term has to be zero since it violates microcausality. In fact, M_{ia} would receive a contribution for all the positions in space. The remaining two terms imply massless states. Then the only states which contribute to M_{ia} have energy which goes to 0 as $\mathbf{k} \rightarrow 0$. These are massless Goldstone bosons. We denote their number as l .

Consider then the following matrix

$$v_{ia} = \sum_{n=1}^l \langle 0 | \phi_i | n_0 \rangle \langle n_0 | j_a^0 | 0 \rangle , \quad (\text{A.7})$$

such that

$$M_{ia} = 2 \text{Im}(v_{ia}) . \quad (\text{A.8})$$

Then $\text{Im}(v_{ia})$ has rank m . In order to calculate $\text{rank}(v_{ia}) = p$, we use that its columns are a linear combination of the following l vectors

$$A_n = \begin{pmatrix} \langle 0 | \phi_1 | n_0 \rangle \\ \vdots \\ \langle 0 | \phi_m | n_0 \rangle \end{pmatrix} , \quad n = 1, \dots, l . \quad (\text{A.9})$$

Then $\text{rank}(v_{ia}) \leq l$. Moreover, let us introduce also

$$v_a = \sum_{n=1}^l A_n \gamma_{an} , \quad \gamma_{an} = \langle n_0 | j_a^0 | 0 \rangle , \quad (\text{A.10})$$

so that we have

$$\text{Im}(v_a) = \sum_{n=1}^l \text{Re}(A_n) \text{Im}(\gamma_{an}) + \sum_{n=1}^l \text{Im}(A_n) \text{Re}(\gamma_{an}) . \quad (\text{A.11})$$

The above implies that the column of v_{ia} is a linear combination of the $2l$ column of $\text{Im}(A_n)$ and $\text{Re}(A_n)$. Then, since $\text{rank}(\text{Im}(v)) = m$, we have $l \geq m/2$.

The next step is to prove that at least one type II Goldstone exists. Since $p \leq l$, there are $m - p$ linear relations

$$\sum_{a=1}^m c_a^\alpha v_a = 0, \quad \alpha = 1, \dots, m-p, \quad (\text{A.12})$$

where not all the c_a^α vanish. Moreover,

$$\sum_{a=1}^m (c_a^\alpha)^* v_a \neq 0, \quad (\text{A.13})$$

otherwise $\text{rank}(\text{Im}(v)) < m$, violating the assumptions. Consider now the following commutator

$$N_i^\alpha = \langle 0 | [\phi_i, c_a^\alpha Q_a] | 0 \rangle, \quad (\text{A.14})$$

where a sum over $a = 1, \dots, m$ is implied. Its Fourier transform $\mathcal{F}(N_i^\alpha)$ can be written as

$$\mathcal{F}(N_i^\alpha) = -2\pi \sum_{n=1}^l \delta(k^0 + E_{-k}) \sum_{a=1}^m c_a^\alpha \langle 0 | j_a^0 | n_{-k} \rangle \langle n_{-k} | \phi_i | 0 \rangle \Big|_{\mathbf{k}=0}. \quad (\text{A.15})$$

Since the energies are positive $\mathcal{F}(N_i^\alpha)$ is non-zero only if $k^0 < 0$, i.e. on a hypersurface of the k -space that is tangent to the $k^0 = 0$ plane from below. Furthermore, $\mathcal{F}(N_i^\alpha)$ must be analytic in \mathbf{k} to preserve microcausality. Then, for $\mathbf{k} \rightarrow 0$, the hypersurface has to be of the form $E_k \sim k^{2s}$ with n integer. This is a type II Goldstone boson.

The counting of the massless Goldstones with respect to the number of broken generators follows from the fact that we cannot find a set of non-zero constants β_α such that

$$\sum_{\alpha=1}^{m-p} \beta_\alpha \sum_{a=1}^m C_a^{\alpha*} v_a. \quad (\text{A.16})$$

In fact, otherwise, we would have

$$\sum_{a=1}^m \text{Im}(v_a) \sum_{\alpha=1}^{m-p} (\beta_\alpha C_a^{\alpha*} + \beta_\alpha^* C_a^\alpha), \quad (\text{A.17})$$

which contradict $\text{rank}(\text{Im}(\nu)) = m$. Then we can build $(m - p)$ linearly independent vectors ρ^α

$$\rho_i^\alpha = \sum_{a=1}^m C_a^{\alpha*} (\nu_a)_i = \sum_{n=1}^l \langle 0 | \phi_i | n_0 \rangle \langle n_0 | \sum_{a=1}^m C_a^{\alpha*} j_a^0 | 0 \rangle , \quad (\text{A.18})$$

and we must have at least $m - p$ independent states (type II Goldstone bosons) which couple to the $m - p$ currents $C_a^{\alpha*} j_a^0$. If we count the type II bosons twice, we have

$$n_I + 2n_{II} = l - (m - p) + 2(m - p) = l + m - p \geq m . \quad (\text{A.19})$$

proving the inequality. We do not present the proof of the equality sign, which can be found in [125].

We now return to Eq.(A.4) and consider instead the case where $[Q_a, Q] \neq 0$. The commutators are

$$[Q_a, j_b^0(x)] = i f_{ab}^c j_c^0(x) , \quad (\text{A.20})$$

with f_{ab}^c the structure constants of \mathcal{G} . Using the commutator above, we can rewrite Eq.(A.4) as

$$e^{i\mu Q t} j_a^0 e^{-i\mu Q t} = (e^{-f_1 \mu t})_a^b j_b^0 , \quad (\text{A.21})$$

which can be derived by expanding the exponentials on the LHS. Here, f_1 is a real matrix whose entries are $(f_1)_a^b = f_{1a}^b$. It is real because we are considering direct products of Lie groups.

$$M_{ia} = \sum_n e^{-iE_k t} (e^{-f_1 \mu t})_a^b \langle 0 | j_b^0 | n_k \rangle \langle n_k | \phi_i | 0 \rangle - \text{c.c.} \Big|_{\mathbf{k} \rightarrow 0} . \quad (\text{A.22})$$

Assumption (4) implies that f_{ab}^c is totally antisymmetric. Then the non-zero eigenvalues of f_{1a}^b are pure imaginary and occur in complex conjugate pairs $(+iq_a, -iq_a)$. We can then find a basis where f_{1a}^b is real and block-diagonal, with the blocks being

$$\begin{pmatrix} 0 & +q_a \\ -q_a & 0 \end{pmatrix} . \quad (\text{A.23})$$

If j_a^0 corresponds to a vanishing eigenvalue of f_1 , then it commutes with Q , and, as discussed

above, we have a massless Goldstone boson. Otherwise, the exponential in (A.22) mixes its matrix elements with its block-partner. The mixing has frequency μq_a and generates the mass of the type III modes. In fact, by rewriting j_a^0 as $j_a^0 = \hat{j}_a^0 + \hat{j}_a^{0\dagger}$, with, \hat{j}_a^0 and $\hat{j}_a^{0\dagger}$ an Hermitian-conjugate pair of generators diagonalizing f_1 , we have

$$M_{ia} = \sum_n e^{-i(E_k - \mu q_a)t} \langle 0 | \hat{j}_a^0 | n_k \rangle \langle n_k | \phi_i | 0 \rangle + e^{-i(E_k + \mu q_a)t} \langle 0 | \hat{j}_a^{0\dagger} | n_k \rangle \langle n_k | \phi_i | 0 \rangle - \text{c.c.} \Big|_{\mathbf{k} \rightarrow 0}. \quad (\text{A.24})$$

Again, the states which contribute to M_{ia} are those satisfying $M_{ia} \neq 0$ and $\frac{d}{dt} M_{ia} = 0$, as dictated by charge conservation. By comparing the expression above with Eq.(A.5), we immediately see that now we have contributions from gapped modes, with mass

$$E_a(0) = \mu q_a. \quad (\text{A.25})$$

These are the type III Goldstone bosons. The proof of the part of the theorem concerning their counting is not given here and can be found in the original publication [129].

Appendix B One-loop computation in the $U(N) \times U(N)$ Higgs model

In this appendix, we derive the 1-loop anomalous dimensions of the $U(N) \times U(N)$ operators with classical dimension $\bar{Q} = 2$ appearing in the decomposition (6.11) of the 2-index traceless symmetric $O(2N^2)$ tensor. We write the H matrix as

$$H = \sum_{A=0}^{N^2-1} (\sigma_A + i\phi_A) T^A , \quad (\text{B.1})$$

where T^A are the generalized Gell-Mann matrices, extended to include $T_0 = \frac{1}{\sqrt{2N}} \mathbb{1}$ and normalized as $\text{Tr}(T^A T^B) = \frac{1}{2} \delta_{AB}$. Introducing $(\chi_{A1}, \chi_{A2}) = (\sigma_A, \phi_A)$, the vertices read [222]

$$4! u \text{Tr}[HH^\dagger HH^\dagger] = u U_{AiBjCkDl} \chi_{Ai} \chi_{Bj} \chi_{Ck} \chi_{Dl} ,$$

$$U_{AiBjCkDl} = 8 [(S_{ABCD} + S_{BADC}) N_{ijkl} + (S_{ABDC} + S_{BACD}) N_{ijlk} + (S_{ADBC} + S_{DABC}) N_{iljk}] . \quad (\text{B.2})$$

$$4! v (\text{Tr}[HH^\dagger])^2 = v V_{AiBjCkDl} \chi_{Ai} \chi_{Bj} \chi_{Ck} \chi_{Dl} ,$$

$$V_{AiBjCkDl} = 2 [\delta_{AB} \delta_{CD} \delta_{ij} \delta_{kl} + \delta_{AC} \delta_{BD} \delta_{ik} \delta_{jl} + \delta_{AD} \delta_{BC} \delta_{il} \delta_{jk}] , \quad (\text{B.3})$$

where $S_{ABCD} = \text{Tr}[T^A T^B T^C T^D]$ and $N_{ijkl} = N_{ij} N_{kl} + N_{ji} N_{lk}$ with

$$N = \frac{1}{2} \begin{pmatrix} 1 & -i \\ i & 1 \end{pmatrix} . \quad (\text{B.4})$$

We write the composite operators $O_{\bar{Q}}$ as $O_{\bar{Q}} = P_{A_1, i_1, A_2, i_2, \dots, A_{\bar{Q}}, i_{\bar{Q}}} \chi_{A_1, i_1} \chi_{A_2, i_2} \dots \chi_{A_{\bar{Q}}, i_{\bar{Q}}}$. Here \bar{Q} is both its CSD and its number of pair of indices. The 1-loop anomalous dimension $\gamma_{O_{\bar{Q}}}$ is determined by the following eigenvalue equation

$$\begin{aligned} \gamma_{O_{\bar{Q}}} P_{A_1, i_1, A_2, i_2, \dots, A_{\bar{Q}}, i_{\bar{Q}}} &= \frac{\bar{Q}(\bar{Q}-1)}{2(4\pi)^2} \left(u U_{B_1, j_1, B_2, j_2, (A_1, i_1, A_2, i_2) P_{A_3, i_3, \dots, A_{\bar{Q}}, i_{\bar{Q}}}, B_1, j_1, B_2, j_2} \right. \\ &\quad \left. + v V_{B_1, j_1, B_2, j_2, (A_1, i_1, A_2, i_2) P_{A_3, i_3, \dots, A_{\bar{Q}}, i_{\bar{Q}}}, B_1, j_1, B_2, j_2} \right) , \end{aligned} \quad (\text{B.5})$$

where the tensors $P_{A_1, i_1, A_2, i_2, \dots, A_Q, i_Q}$ have to be totally symmetric under interchanges of pairs of indices of the form $(A_\alpha i_\alpha) \leftrightarrow (A_\beta, i_\beta)$. The symmetrizations on the RHS of Eq.(B.5) is understood in the same way. The derivation of Eq.(B.5) is analogous to the one of Eq.(4.101) for the hypercubic model. Notice the appearance of the usual $\frac{Q(Q-1)}{2}$ combinatorial factor typical of quartic potentials. In diagrammatic terms, it stems from choosing the two legs (on \bar{Q}) of the operator insertion which enter the quartic vertex.

Specializing on the case $\bar{Q} = 2$, Eq.(B.5) becomes

$$\gamma_0 P_{AiBj} = \frac{1}{(4\pi)^2} (u U_{AiBjCkDl} + v V_{AiBjCkDl}) P_{CkDl} . \quad (\text{B.6})$$

For the (Adj, 1) operator, we have

$$Tr[HT_E H^\dagger] = Tr[T_A T_E T_B] \delta_{ij} \chi_{Ai} \chi_{Bj} \implies P_{AiBj} = Tr[T_A T_E T_B] \delta_{ij} , \quad (\text{B.7})$$

where the index E runs solely from 1 to $N^2 - 1$. Using (B.6), we obtain

$$\gamma_{Tr[HT_E H^\dagger]} = \frac{v + Nu}{4\pi^2} . \quad (\text{B.8})$$

For the bi-adjoint operator $Tr[T_E H T_E H^\dagger]$, we can use $T_{\alpha\beta}^E T_{\rho\sigma}^E = \frac{1}{2} (\delta_{\alpha\sigma} \delta_{\beta\rho} - \frac{1}{N} \delta_{\alpha\beta} \delta_{\rho\sigma})$ to perform the sum over E (which again does not include T_0). We have

$$Tr[T_E H T_E H^\dagger] = \frac{1}{2} \left(Tr H Tr H^\dagger - \frac{1}{N} Tr[HH^\dagger] \right) = \frac{1}{4} \delta_{ij} \left(N \delta_{A0} \delta_{B0} - \frac{1}{N} \delta_{AB} \right) \chi_{Ai} \chi_{Bj} , \quad (\text{B.9})$$

and thus

$$\gamma_{Tr[T_E H T_E H^\dagger]} = \frac{v}{4\pi^2} . \quad (\text{B.10})$$

We write the operators transforming in the anti/symmetric irreps as $\text{Tr} [K^i H \bar{K}^i H]$ and $\text{Tr} [L^i H \bar{L}^i H]$, where $K^i (\bar{K}^i)$ and $L^i (\bar{L}^i)$ are the Clebsch-Gordan coefficients for the $SU(N)$ representations $\square \square$ ($\square \square^*$) and $\square \square$ ($\square \square^*$), respectively. $K_i, \bar{K}_i, L_i, \bar{L}_i$ satisfy the completeness relations [192]

$$\begin{aligned} K_i^{\alpha\beta} \bar{K}_{\rho\sigma}^i &= \frac{1}{2}(\delta_{\alpha\sigma}\delta_{\beta\rho} + \delta_{\alpha\rho}\delta_{\beta\sigma}) , \\ L_i^{\alpha\beta} \bar{L}_{\rho\sigma}^i &= \frac{1}{2}(\delta_{\alpha\sigma}\delta_{\beta\rho} - \delta_{\alpha\rho}\delta_{\beta\sigma}) . \end{aligned} \quad (\text{B.11})$$

We have

$$\text{Tr} [K^i H \bar{K}^i H] = \frac{1}{2} R_{ij} (N \delta_{A0} \delta_{B0} + \delta_{AB}) \chi_{AI} \chi_{Bj} , \quad (\text{B.12})$$

$$\text{Tr} [L^i H \bar{L}^i H] = \frac{1}{2} R_{ij} (N \delta_{A0} \delta_{B0} - \delta_{AB}) \chi_{AI} \chi_{Bj} , \quad (\text{B.13})$$

where R is a symmetric and traceless matrix given by

$$R = \begin{pmatrix} 1 & i \\ i & -1 \end{pmatrix} . \quad (\text{B.14})$$

Plugging the above tensors in the eigenvalue equation (B.6), we obtain

$$\gamma_{\text{Tr}[K^i H \bar{K}^i H]} = \frac{v+u}{4\pi^2} , \quad (\text{B.15})$$

$$\gamma_{\text{Tr}[L^i H \bar{L}^i H]} = \frac{v-u}{4\pi^2} , \quad (\text{B.16})$$

where we used that $R_{ij} N_{ijkl} = R_{ij} N_{ijlk} = 0$ and $R_{ij} N_{iljk} = R_{kl}$.

Appendix C The functions $\rho(\mathcal{A}_h^*, \mathcal{A}_v^*)$ and $\sigma(\ell, \mathcal{A}_h^*, \mathcal{A}_v^*)$

Here, we provide explicit expression for the functions appearing in Eq.(6.96). Recalling that $x^* = \frac{72}{N}(\mathcal{A}_h^* + \mathcal{A}_v^*) + \sqrt{-3 + (\frac{72}{N}(\mathcal{A}_h^* + \mathcal{A}_v^*))^2}$, we have

$$\begin{aligned}
\rho(x^*, M, N, s, \mathcal{A}_h^*, \mathcal{A}_v^*) &= \frac{1}{144x^{*4/3}(\mathcal{A}_h^* + \mathcal{A}_v^*)^2} \left[-2\mathcal{A}_h^*\mathcal{A}_v^* \left(2M \left(102Nx^{*4/3} + 24\sqrt[3]{3}Nx^{*2/3} \right. \right. \right. \\
&\quad \left. \left. \left. + 8\sqrt[3]{3}Nx^{*2} + s \left(16\sqrt[3]{3}x^{*8/3} + 291x^{*4/3} + 216\sqrt[3]{3}x^{*2/3} + 72\sqrt[3]{3}x^{*2} + 48\sqrt[3]{3} \right) \right) \right. \\
&\quad \left. \left. + 2Ns \left(16\sqrt[3]{3}x^{*8/3} + 291x^{*4/3} + 216\sqrt[3]{3}x^{*2/3} + 72\sqrt[3]{3}x^{*2} + 48\sqrt[3]{3} \right) + 48\sqrt[3]{3}x^{*8/3} \right. \\
&\quad \left. \left. + 753x^{*4/3} + 552\sqrt[3]{3}x^{*2/3} + 184\sqrt[3]{3}x^{*2} + 144\sqrt[3]{3} \right) + \mathcal{A}_h^{*2} \left(-2M \left(72Nx^{*4/3} + s \left(16\sqrt[3]{3}x^{*8/3} \right. \right. \right. \right. \\
&\quad \left. \left. \left. \left. + 351x^{*4/3} + 264\sqrt[3]{3}x^{*2/3} + 88\sqrt[3]{3}x^{*2} + 48\sqrt[3]{3} \right) \right) - 2s \left(N \left(16\sqrt[3]{3}x^{*8/3} + 351x^{*4/3} \right. \right. \right. \\
&\quad \left. \left. \left. + 264\sqrt[3]{3}x^{*2/3} + 88\sqrt[3]{3}x^{*2} + 48\sqrt[3]{3} \right) + 6s \left(16\sqrt[3]{3}x^{*8/3} + 231x^{*4/3} + 168\sqrt[3]{3}x^{*2/3} \right. \right. \right. \\
&\quad \left. \left. \left. + 56\sqrt[3]{3}x^{*2} + 48\sqrt[3]{3} \right) \right) - \mathcal{A}_v^{*2} \left(MN \left(16\sqrt[3]{3}x^{*8/3} + 495x^{*4/3} + 264\sqrt[3]{3}x^{*2/3} + 88\sqrt[3]{3}x^{*2} \right. \right. \right. \\
&\quad \left. \left. \left. + 48\sqrt[3]{3} \right) + 4 \left(16\sqrt[3]{3}x^{*8/3} + 261x^{*4/3} + 192\sqrt[3]{3}x^{*2/3} + 64\sqrt[3]{3}x^{*2} + 48\sqrt[3]{3} \right) \right) \right] \\
&\quad + (M - 2s)(N - 2s) \sqrt{\frac{\mathcal{A}_h^* + \frac{4(x^{*2/3} + \sqrt[3]{3})^2 \mathcal{A}_v^*}{3\sqrt[3]{3}x^{*2/3}}}{\mathcal{A}_h^* + \mathcal{A}_v^*}} + \frac{s^2}{3} \sqrt{\frac{1}{x^{*2/3}(\mathcal{A}_h^* + \mathcal{A}_v^*)}} \left(6 \left(2\sqrt[3]{3}x^{*4/3} \right. \right. \\
&\quad \left. \left. + 9x^{*2/3} + 6\sqrt[3]{3} \right) \mathcal{A}_h^* + 4 \left(\sqrt[3]{3}x^{*4/3} + 6x^{*2/3} + 3\sqrt[3]{3} \right) \mathcal{A}_v^* \right)^{1/2} + \frac{2s^2 - 1}{2} \left(-\frac{1}{9x^{*4/6}(\mathcal{A}_h^* + \mathcal{A}_v^*)} \right. \\
&\quad \times \left[3 \left(4\sqrt[3]{3}x^{*4/3} + 21x^{*2/3} + 12\sqrt[3]{3} \right) \mathcal{A}_h^* + 8 \left(\sqrt[3]{3}x^{*4/3} + 6x^{*2/3} + 3\sqrt[3]{3} \right) \mathcal{A}_v^* \right] \\
&\quad + \left(\frac{4(x^{*2/3} + \sqrt[3]{3})^2}{3\sqrt[3]{3}x^{*2/3}} - 1 \right) \mathcal{A}_h^* + \frac{8(x^{*2/3} + \sqrt[3]{3})^2}{3\sqrt[3]{3}x^{*2/3}} \right)^{1/2} + \frac{4s(x^{*2/3} + \sqrt[3]{3})(M - N)}{3^{2/3}\sqrt[3]{x^*}} \\
&\quad + \frac{2s^2 - 1}{2} \left(\frac{3 \left(4\sqrt[3]{3}x^{*4/3} + 21x^{*2/3} + 12\sqrt[3]{3} \right) \mathcal{A}_h^* + 8 \left(\sqrt[3]{3}x^{*4/3} + 6x^{*2/3} + 3\sqrt[3]{3} \right) \mathcal{A}_v^*}{9x^{*4/6}(\mathcal{A}_h^* + \mathcal{A}_v^*)} \right. \\
&\quad + \left(\frac{4(x^{*2/3} + \sqrt[3]{3})^2}{3\sqrt[3]{3}x^{*2/3}} - 1 \right) \mathcal{A}_h^* + \frac{8(x^{*2/3} + \sqrt[3]{3})^2}{3\sqrt[3]{3}x^{*2/3}} \right)^{1/2} + \frac{8s(x^{*2/3} + \sqrt[3]{3})(N - 2s)}{3^{2/3}\sqrt[3]{x^*}}
\end{aligned}$$

$$+\frac{2s^2 \left(x^{*2/3}+\sqrt[3]{3}\right)}{3^{2/3} \sqrt[3]{x^*}} , \quad (C.1)$$

and

$$\begin{aligned} \sigma(\ell, x^*, M, N, s, \mathcal{A}_h^*, \mathcal{A}_v^*) = & -2\ell^3 MN - 6\ell^2 MN + \frac{\left(4 \sqrt[3]{3} x^{*4/3} + 15x^{*2/3} + 12\sqrt[3]{3}\right)^2}{324\ell x^{*4/3} (\mathcal{A}_h^* + \mathcal{A}_v^*)^2} \left(2s\mathcal{A}_h^{*2}\right. \\ & \times (M + N + 6s) + 2\mathcal{A}_h^* \mathcal{A}_v^* (2Ms + 2Ns + 3) + (MN + 4)\mathcal{A}_v^{*2} \Big) + \frac{\ell}{9x^{*2/3}(\mathcal{A}_h^* + \mathcal{A}_v^*)} \\ & \times \left[\mathcal{A}_h^* \left(54MNx^{*2/3} + Ms \left(8 \sqrt[3]{3} x^{*4/3} + 30x^{*2/3} + 24\sqrt[3]{3}\right) + 2Ns \left(4 \sqrt[3]{3} x^{*4/3} + 15x^{*2/3} + 12\sqrt[3]{3}\right)\right) \right. \\ & \left. + \mathcal{A}_v^* \left(MN \left(4 \sqrt[3]{3} x^{*4/3} + 69x^{*2/3} + 12\sqrt[3]{3}\right) + 4 \sqrt[3]{3} x^{*4/3} + 15x^{*2/3} + 12\sqrt[3]{3}\right) \right] \\ & - \frac{1}{9x^{*2/3}(\mathcal{A}_h^* + \mathcal{A}_v^*)} \left[-2\mathcal{A}_h^* \left(9MNx^{*2/3} + Ms \left(4 \sqrt[3]{3} x^{*4/3} + 15x^{*2/3} + 12\sqrt[3]{3}\right) + Ns \left(4 \sqrt[3]{3} x^{*4/3} + 15x^{*2/3} + 12\sqrt[3]{3}\right)\right) \right. \\ & \left. - \mathcal{A}_v^* \left(MN \left(4 \sqrt[3]{3} x^{*4/3} + 33x^{*2/3} + 12\sqrt[3]{3}\right) + 4 \sqrt[3]{3} x^{*4/3} + 15x^{*2/3} + 12\sqrt[3]{3}\right) \right] . \end{aligned} \quad (C.2)$$

On the author

Jahmall Bersini is a Ph.D. student in theoretical physics at the University of Zagreb (Faculty of Science), and, since November 2018, he is employed as a research assistant at the Institute Ruđer Bošković, Zagreb. He graduated in theoretical physics at the University of Torino (Italy) with a final mark of 110/110 cum laude and thesis: *Galaxy phenomenology from dark matter-baryon interactions*. His research interests concern strongly-interacting theories, CFT, resurgence theory, and non-perturbative aspects of QCD.

Publications list

Scientific Papers

- O. Antipin, J. Bersini, F. Sannino, Z. W. Wang and C. Zhang, “Untangling scaling dimensions of fixed charge operators in Higgs Theories,” arXiv:2102.04390 [hep-th]. *Manuscript submitted for publication in Journal of High Energy Physics (JHEP)*.
- O. Antipin, J. Bersini, F. Sannino, Z. W. Wang and C. Zhang, “Charging non-Abelian Higgs theories,” Phys. Rev. D 102 (2020) no.12, 125033, doi:10.1103/PhysRevD.102.125033, arXiv: 2006.10078 [hep-th].
- O. Antipin, J. Bersini, F. Sannino, Z. W. Wang, and C. Zhang, “Charging the O(N) model,” Phys. Rev. D 102 (2020) no.4, 045011, doi:10.1103/PhysRevD.102.045011, arXiv:2003.13121 [hep-th].
- J. Bersini, A. Maiezza, and J. C. Vasquez, “Resurgence of the renormalization group equation,” Annals Phys. 415 (2020), 168126, doi:10.1016/j.aop.2020.168126, arXiv:1910.14507 [hep-th].
- O. Antipin and J. Bersini, “Spectrum of anomalous dimensions in hypercubic theories,” Phys. Rev. D 100 (2019) no.6, 065008, doi:10.1103/PhysRevD.100.065008, arXiv:1903.04950 [hep-th].

Conference Proceedings

- J. Bersini, “Spectrum of anomalous dimensions in hypercubic theories,” PoS CORFU2019 (2020), 092, doi:10.22323/1.376.0092.